Supplementary Information for

Ether Solvent-induced Chirality Inversion of Helical Poly(quinoxaline-2,3-diyl)s Containing L-Lactic Acid Derived Side Chains

Yuuya Nagata,[†] Takuma Kuroda,[†] Keisuke Takagi,[†] and Michinori Suginome[*,†,‡]

[†]*Department of Synthetic Chemistry and Biological Chemistry, Graduate School of Engineering, Kyoto University, Katsura, Nishikyo-ku, Kyoto 615-8510 Japan, and* [‡]*CREST, Japan Science and Technology Agency (JST), Katsura, Nishikyo-ku, Kyoto 615-8510, Japan*

E-mail: suginome@sbchem.kyoto-u.ac.jp

Contents

[*]To whom correspondence should be addressed
[†]Department of Synthetic Chemistry and Biological Chemistry, Graduate School of Engineering, Kyoto University
[‡]JST, CREST

1 NMR Spectra of New Compounds

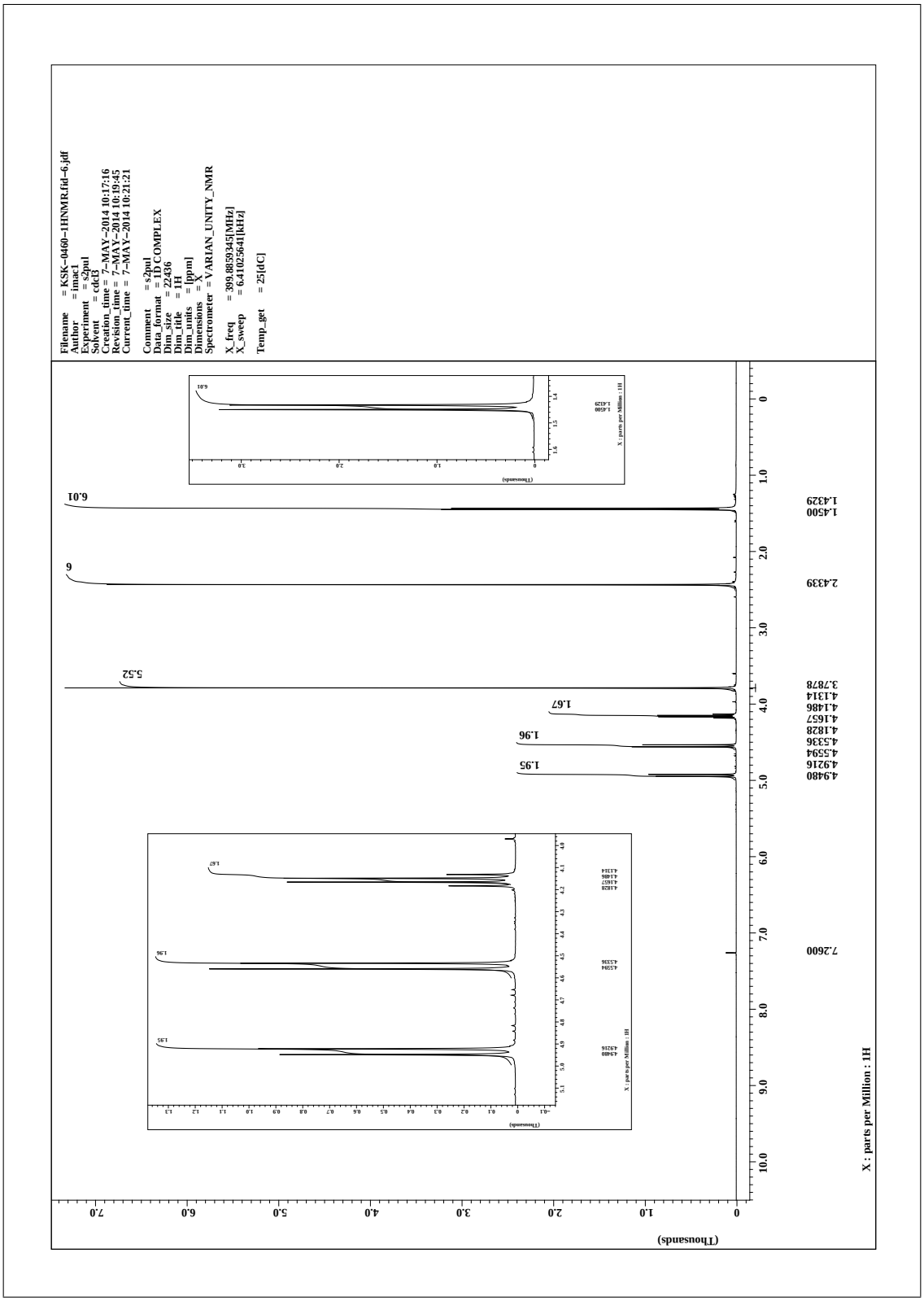

Figure S3. ^{1}H NMR spectrum of **M1-NO_2** in $CDCl_3$.

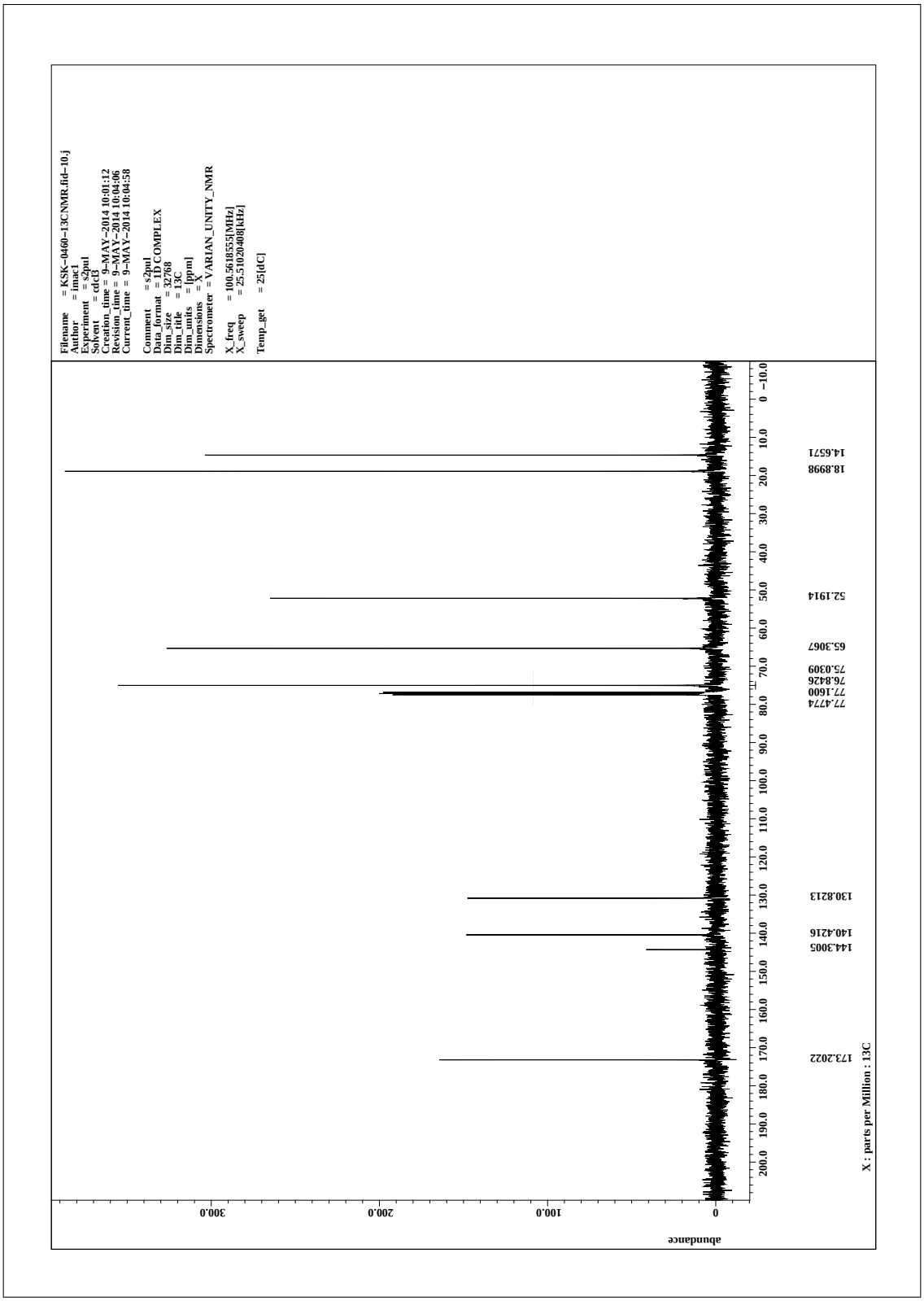

Figure S4. ^{13}C NMR spectrum of **M1-NO_2** in $CDCl_3$.

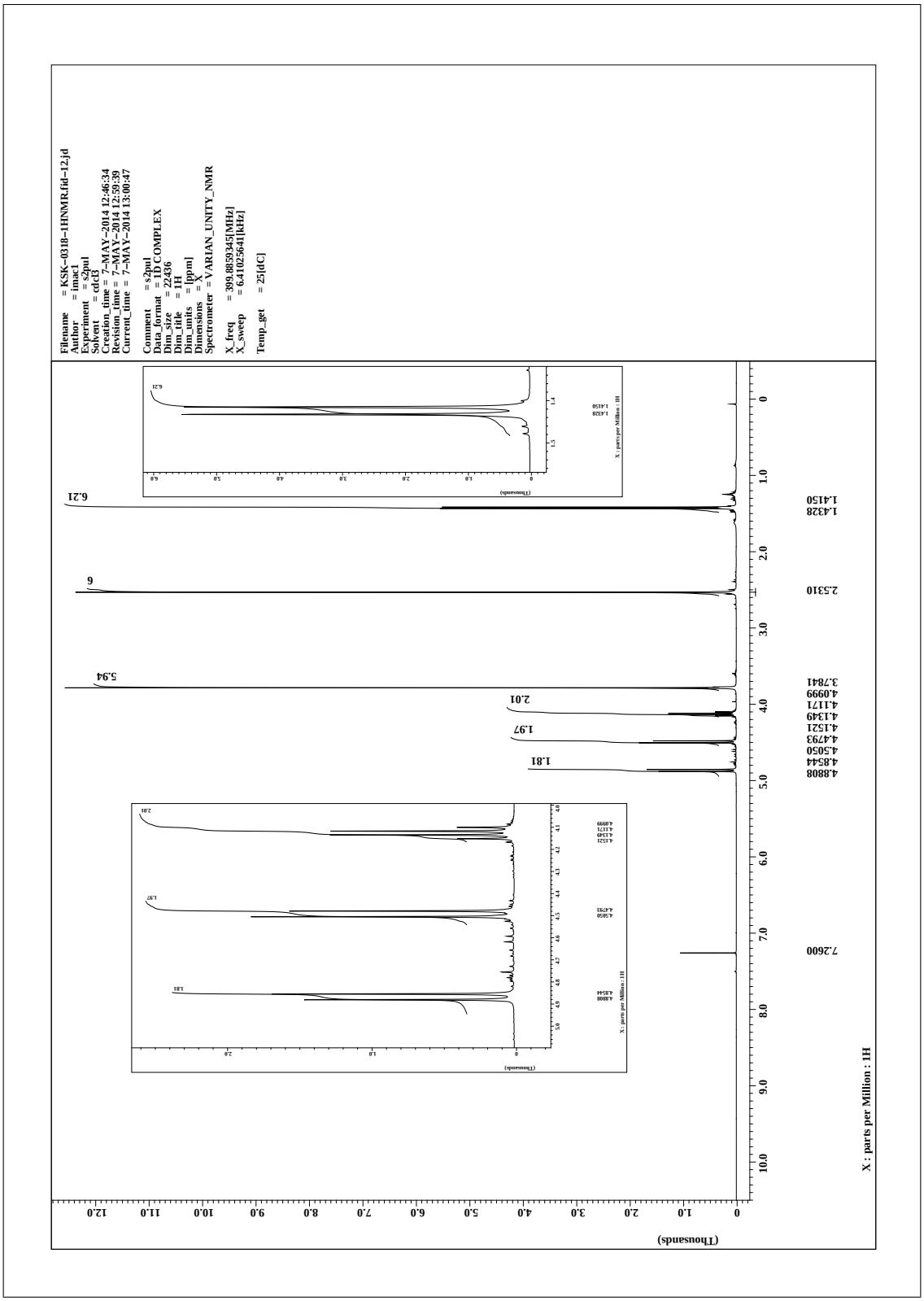

Figure S5. ^{1}H NMR spectrum of **M1-NC** in C_6D_6.

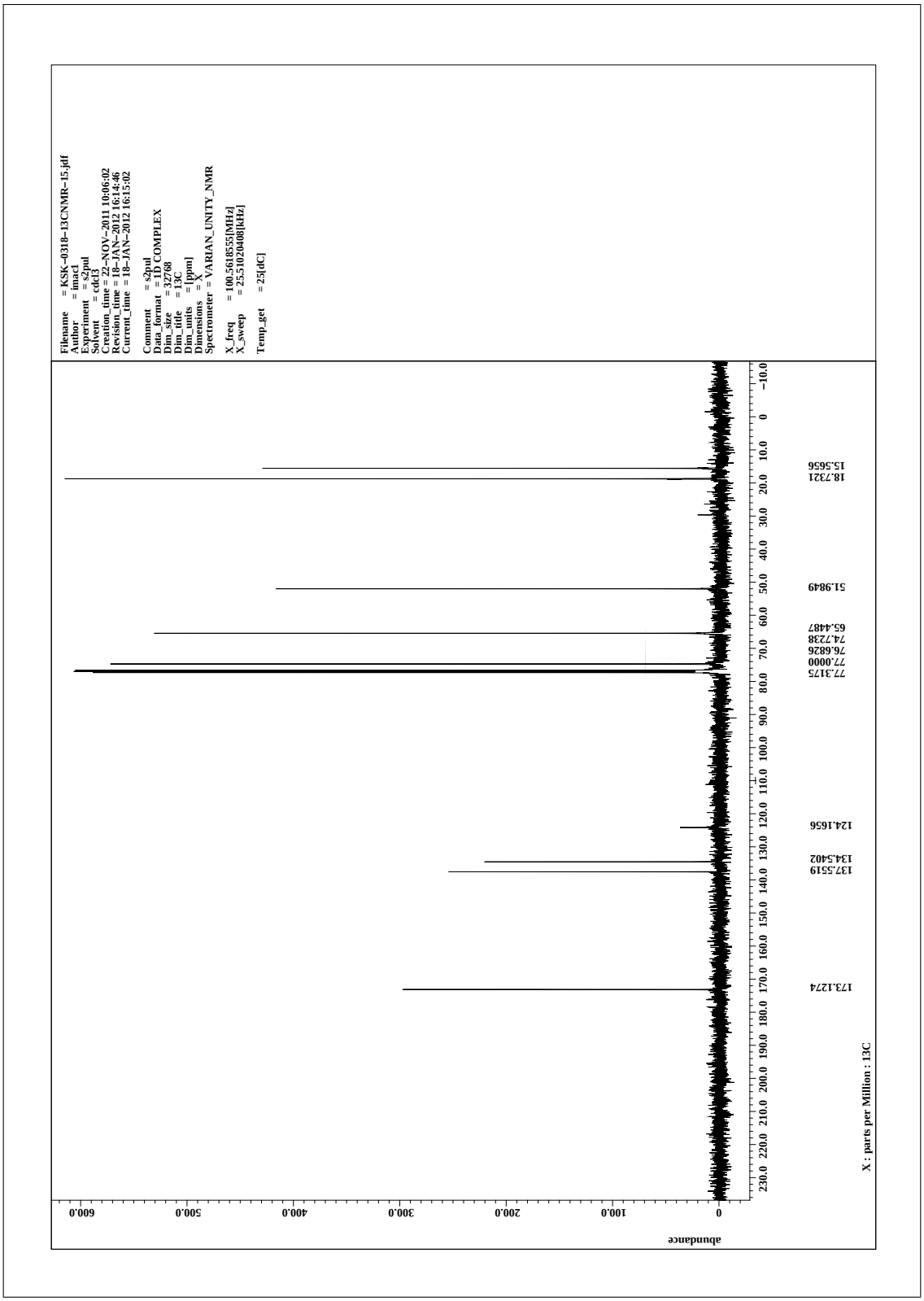

Figure S6. ^{13}C NMR spectrum of **M1-NC** in C_6D_6.

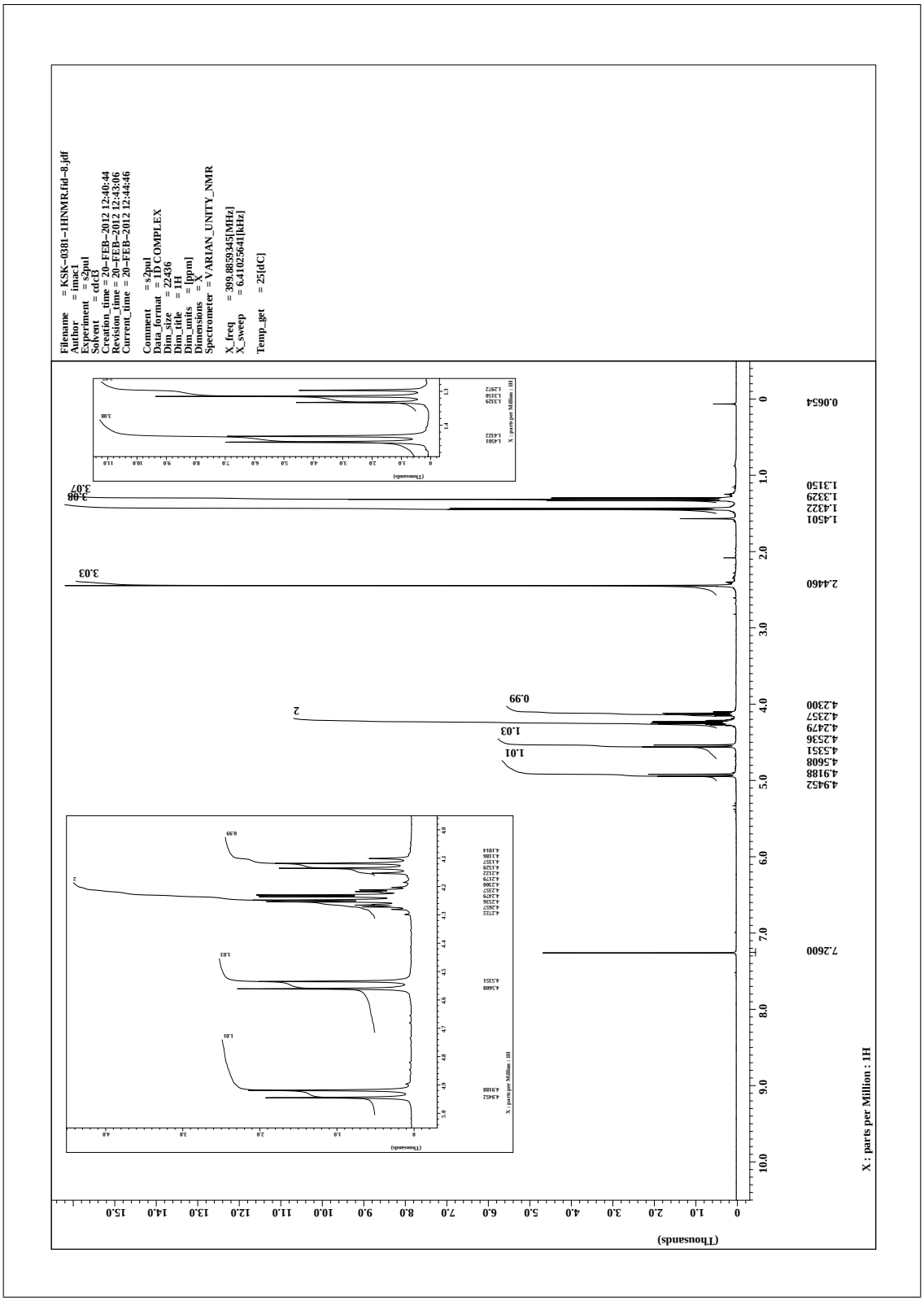

Figure S7. ^{1}H NMR spectrum of **M2-NO$_2$** in $CDCl_3$.

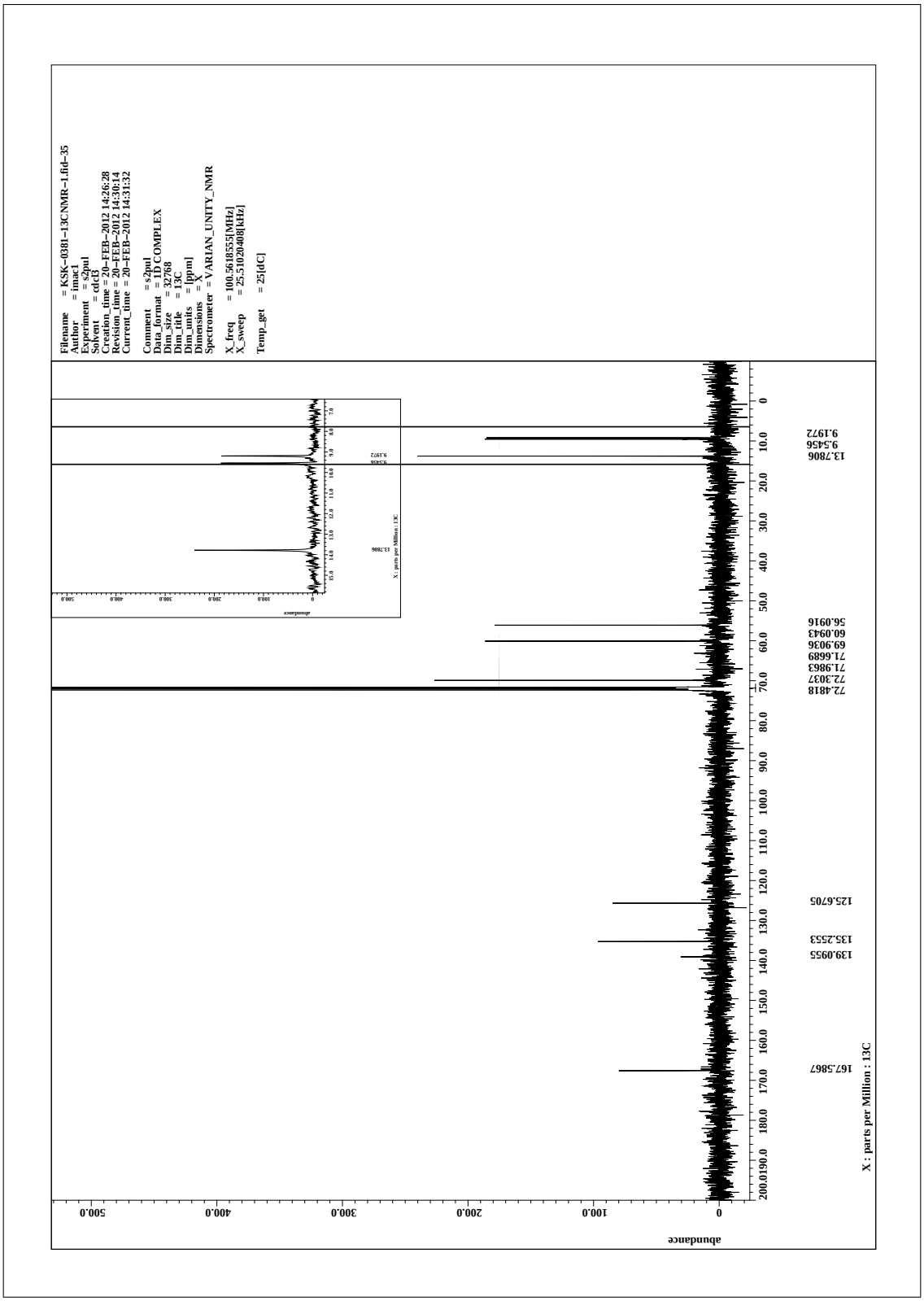

Figure S8. ^{13}C NMR spectrum of **M2-NO_2** in $CDCl_3$.

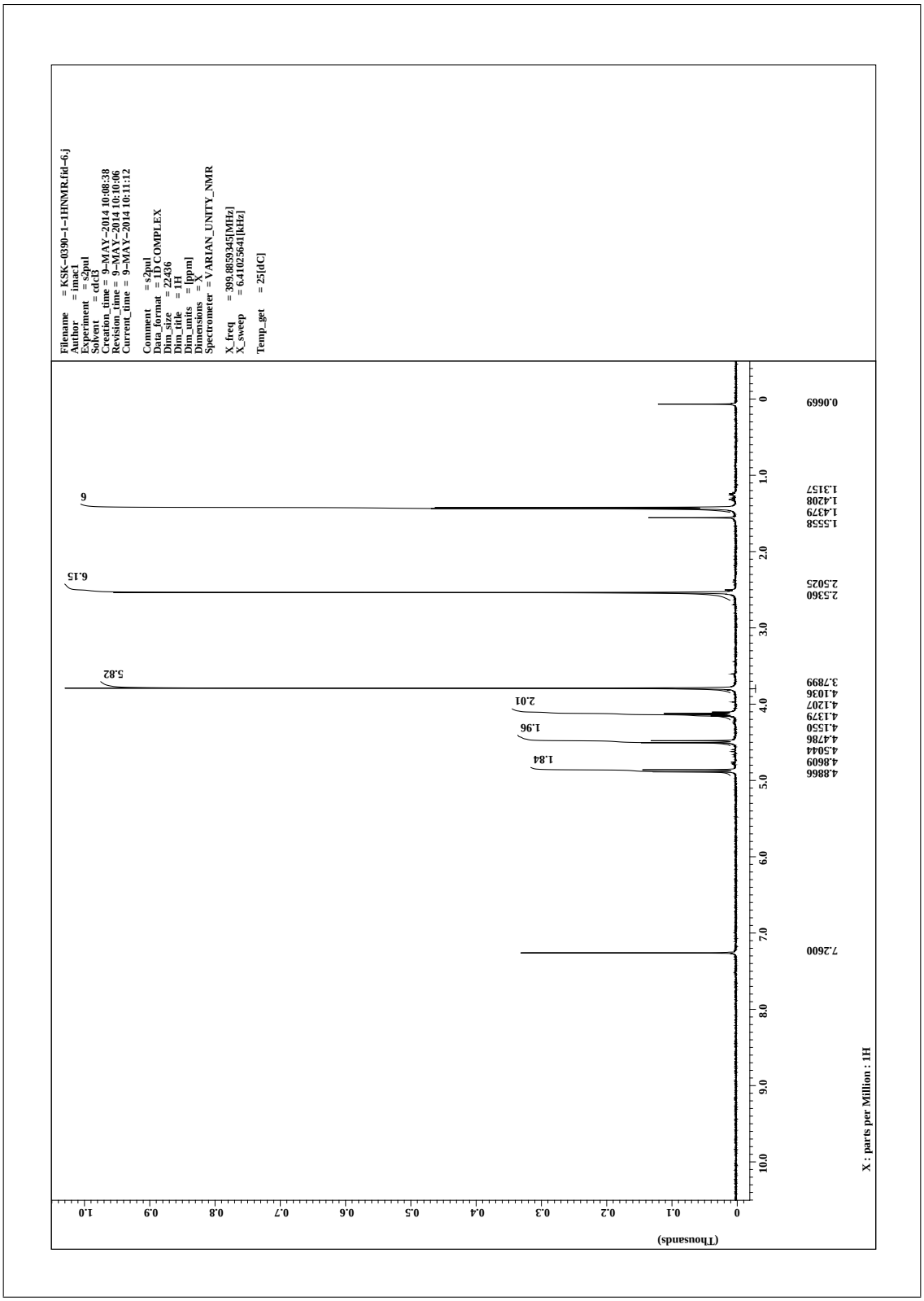

Figure S9. ^{1}H NMR spectrum of **M2-NC** in C_6D_6.

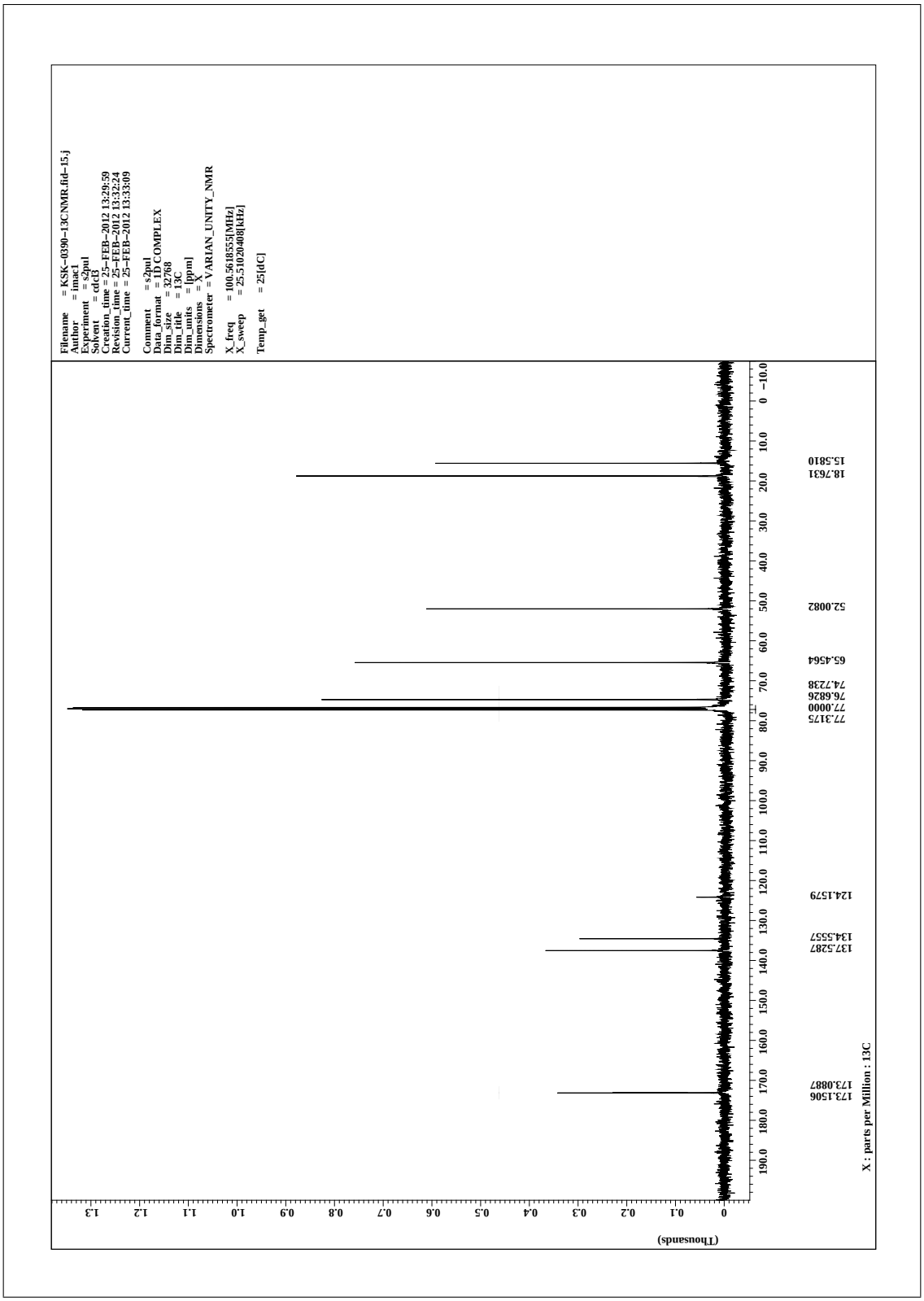

Figure S10. ^{13}C NMR spectrum of **M2-NC** in C_6D_6.

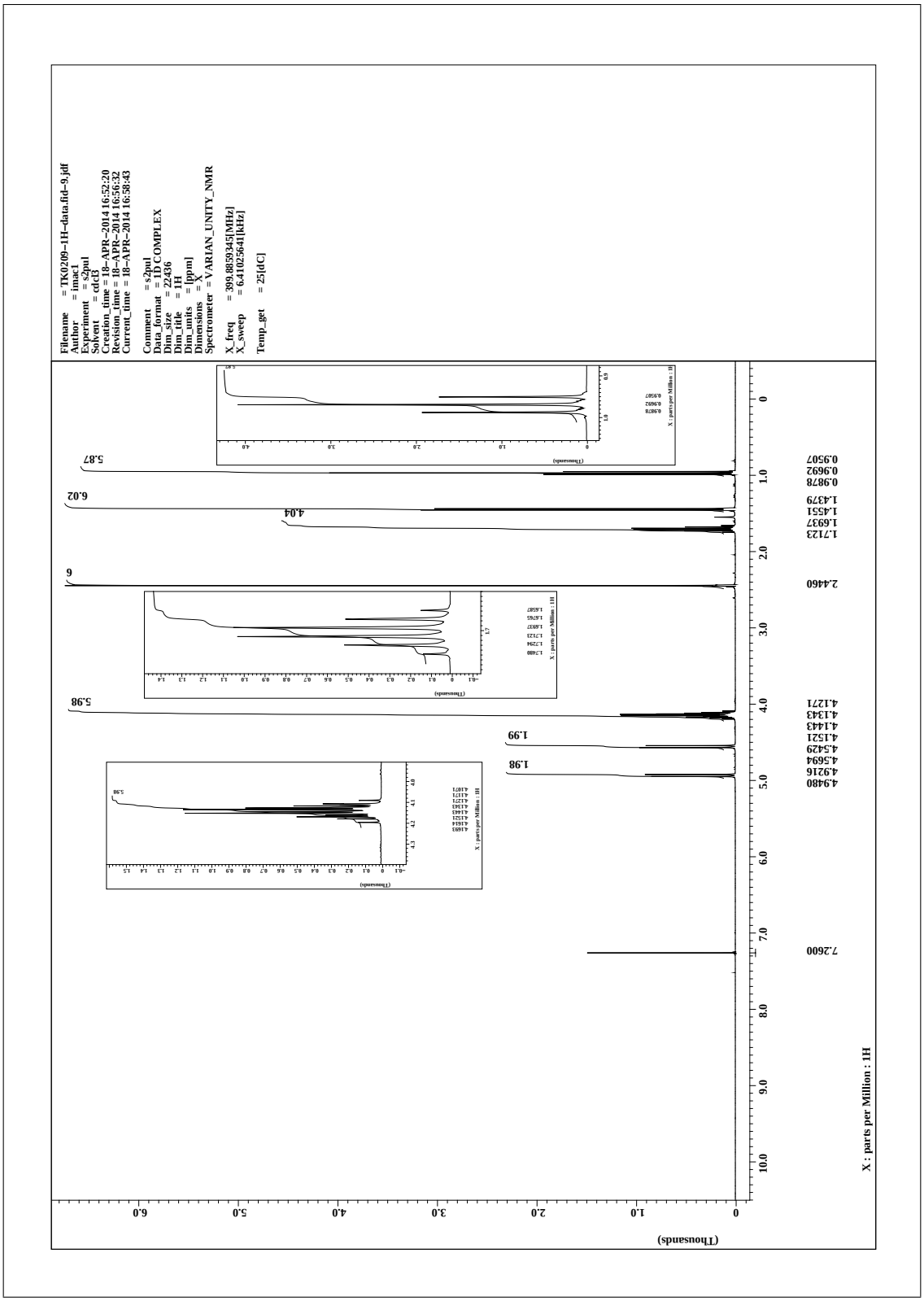

Figure S11. ^{1}H NMR spectrum of **M3-NO$_2$** in $CDCl_3$.

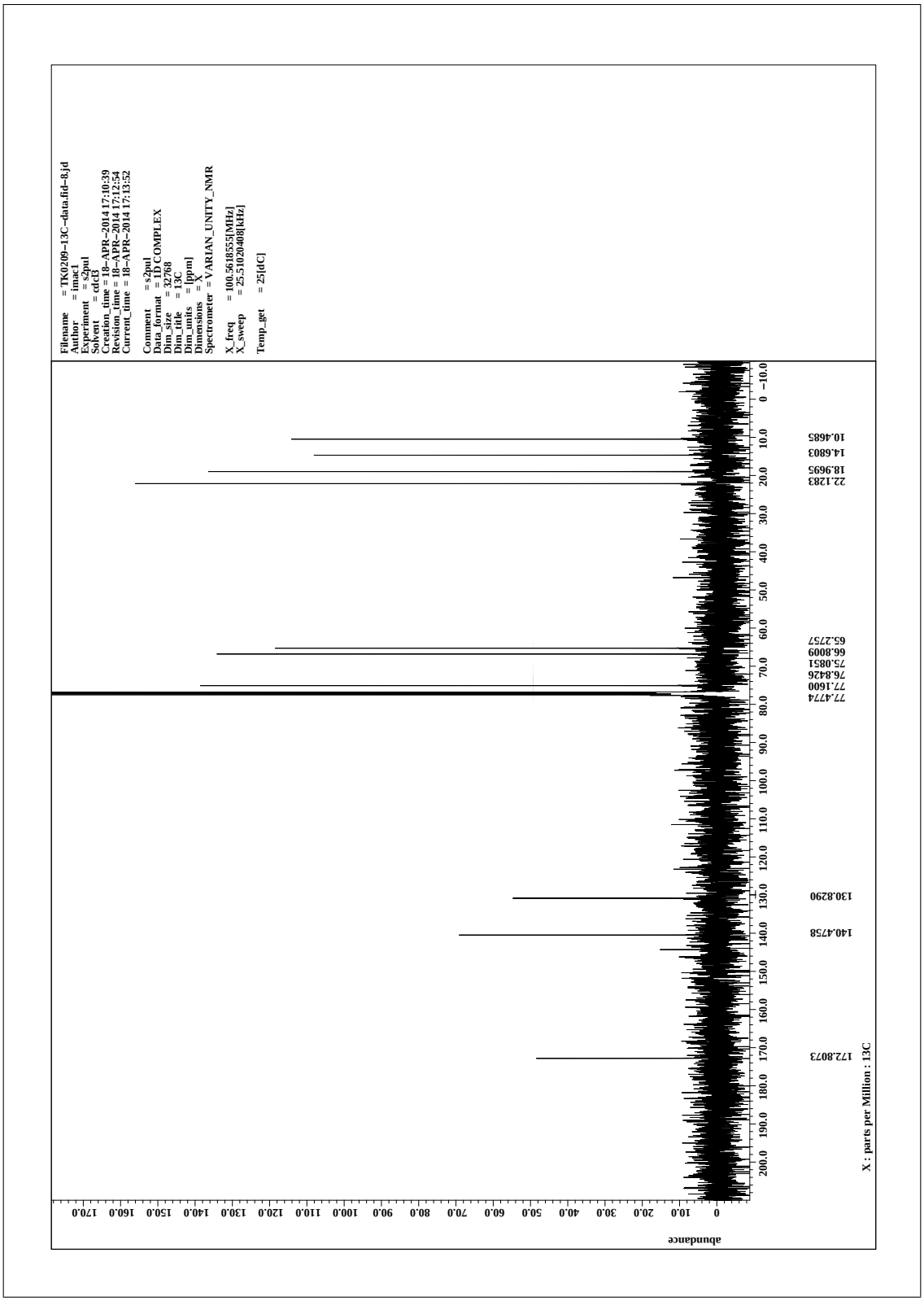

Figure S12. ^{13}C NMR spectrum of **M3-NO_2** in $CDCl_3$.

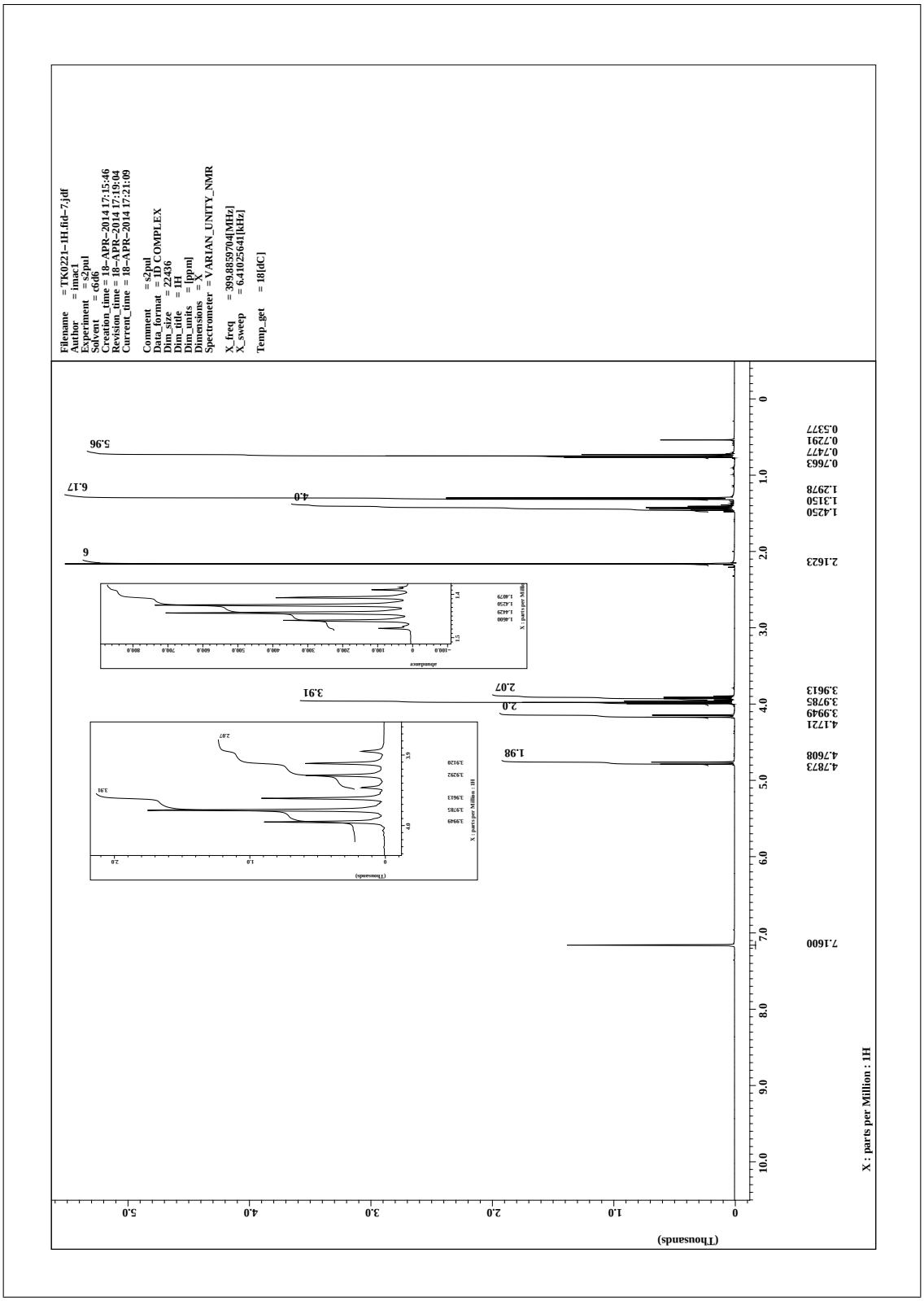

Figure S13. ^{1}H NMR spectrum of **M3-NC** in C_6D_6.

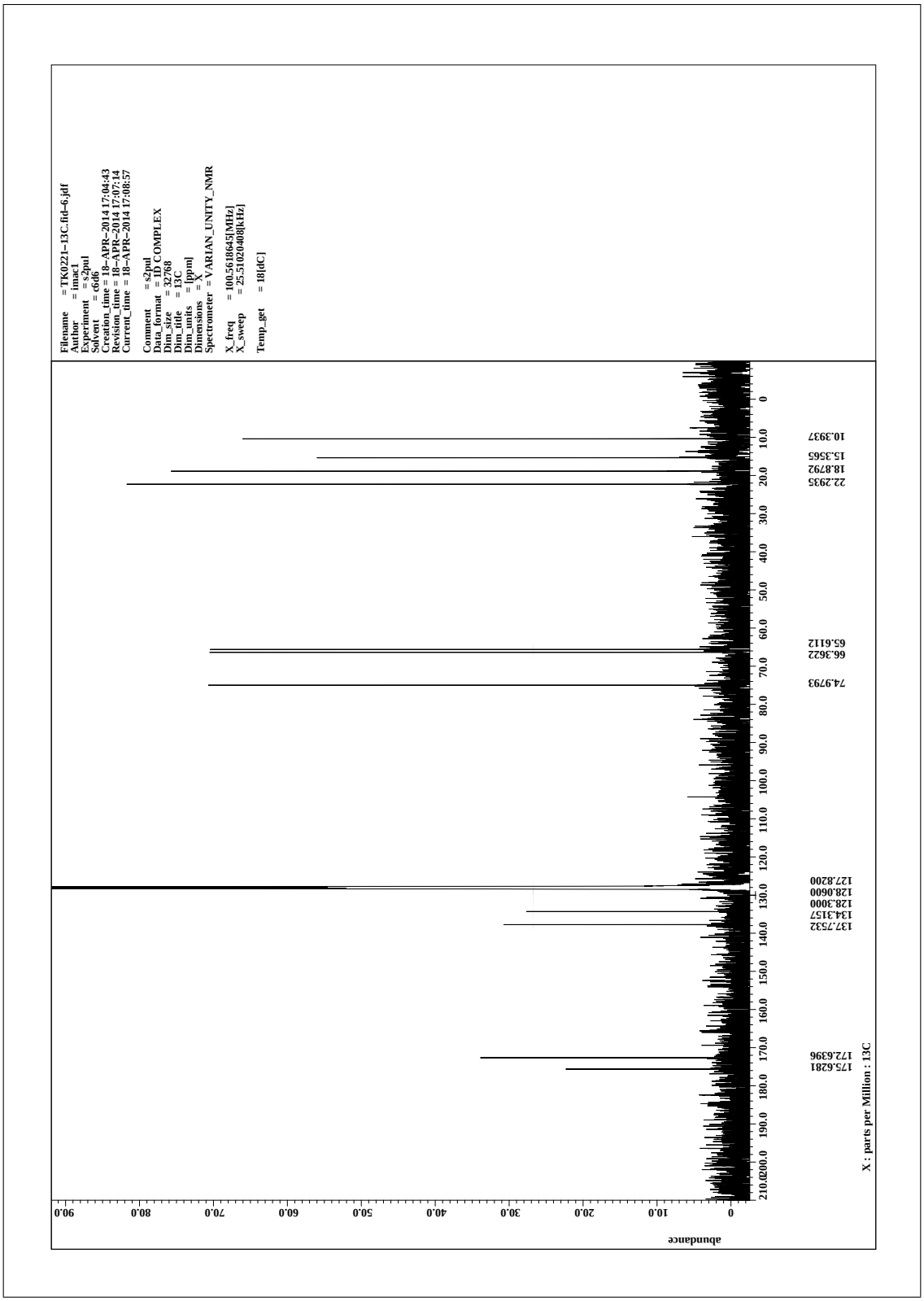

Figure S14. ^{13}C NMR spectrum of **M3-NC** in C_6D_6.

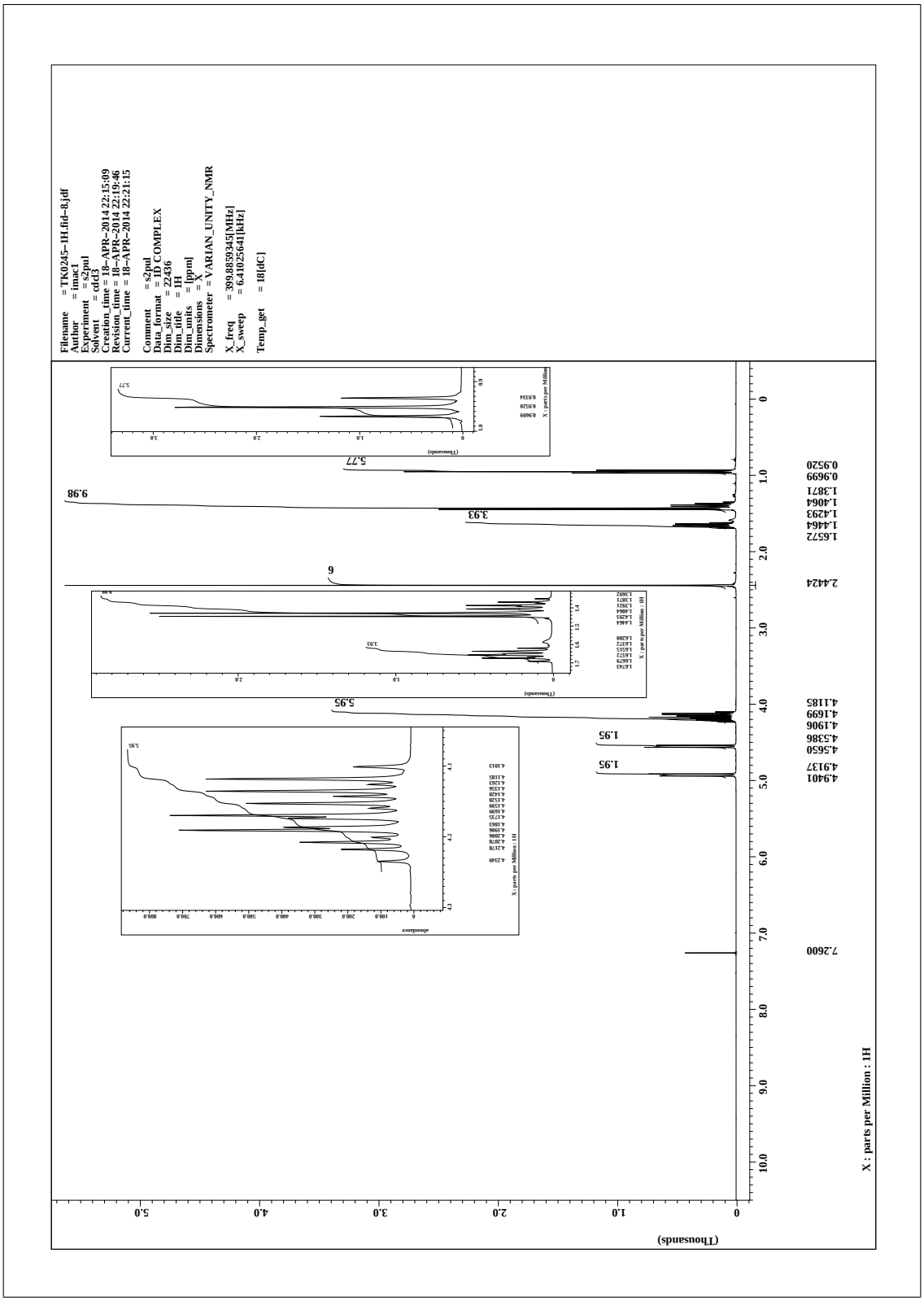

Figure S15. ^{1}H NMR spectrum of **M4-NO$_2$** in $CDCl_3$.

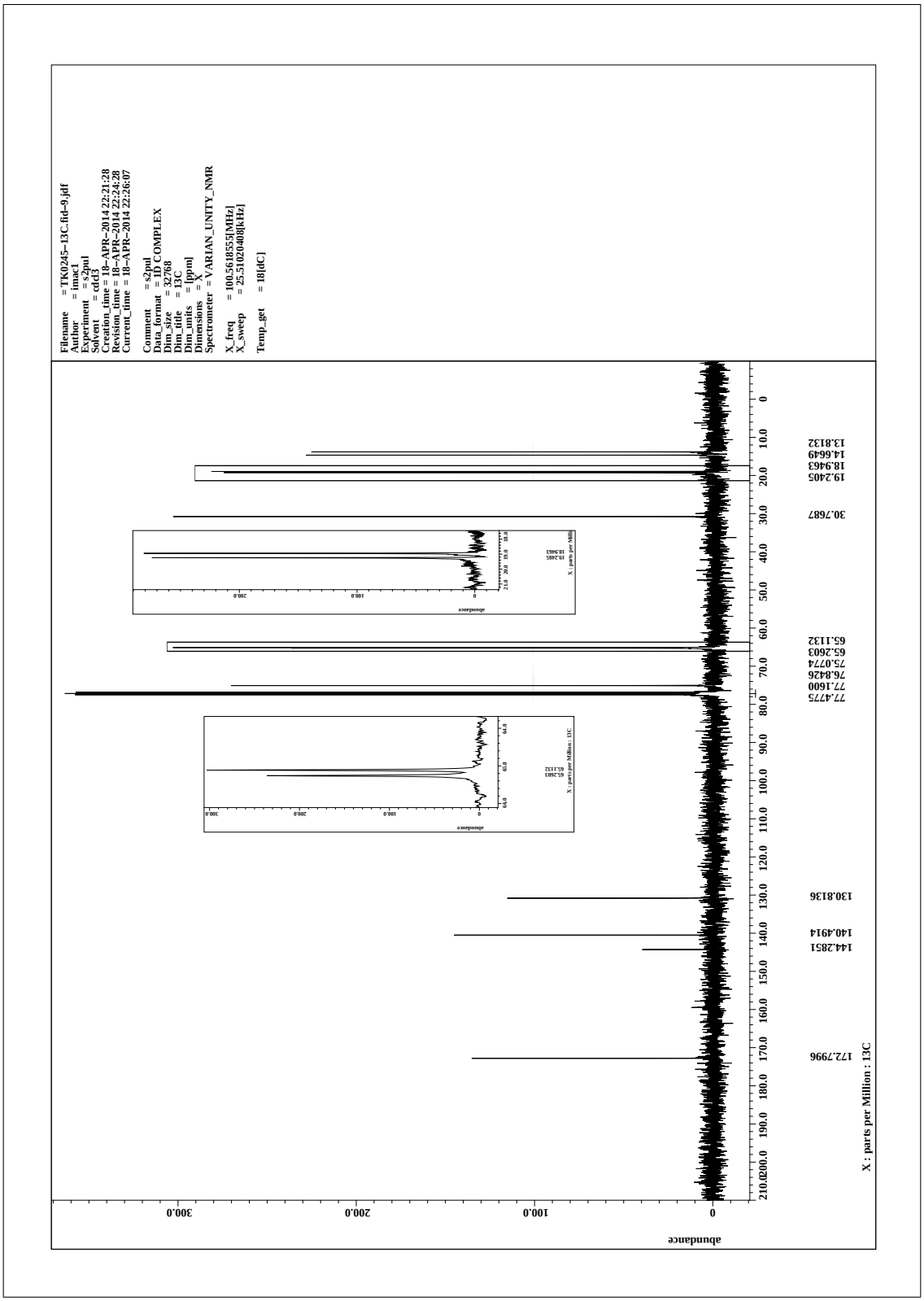

Figure S16. ^{13}C NMR spectrum of **M4-NO_2** in $CDCl_3$.

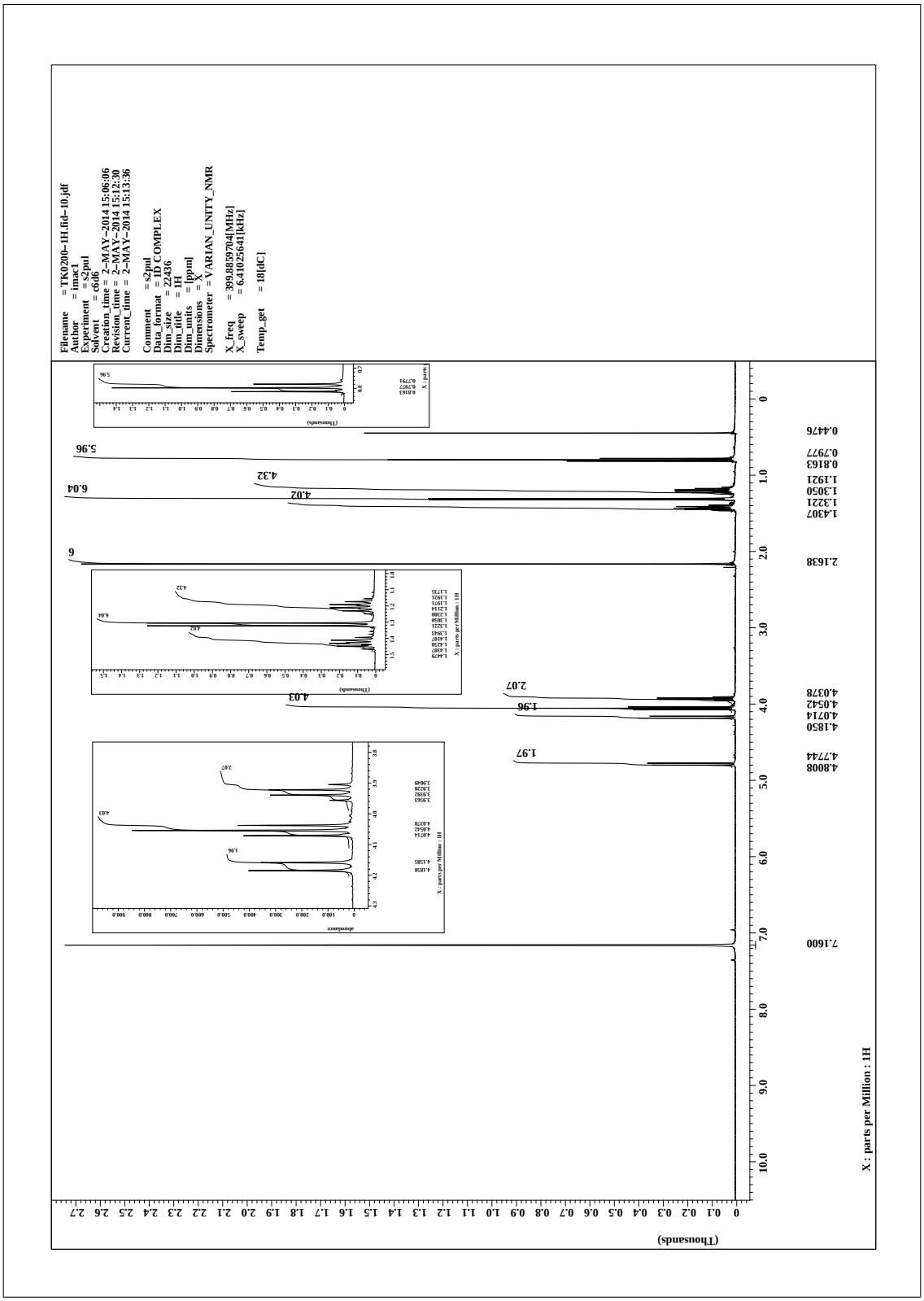

Figure S17. ^{1}H NMR spectrum of **M4-NC** in C_6D_6.

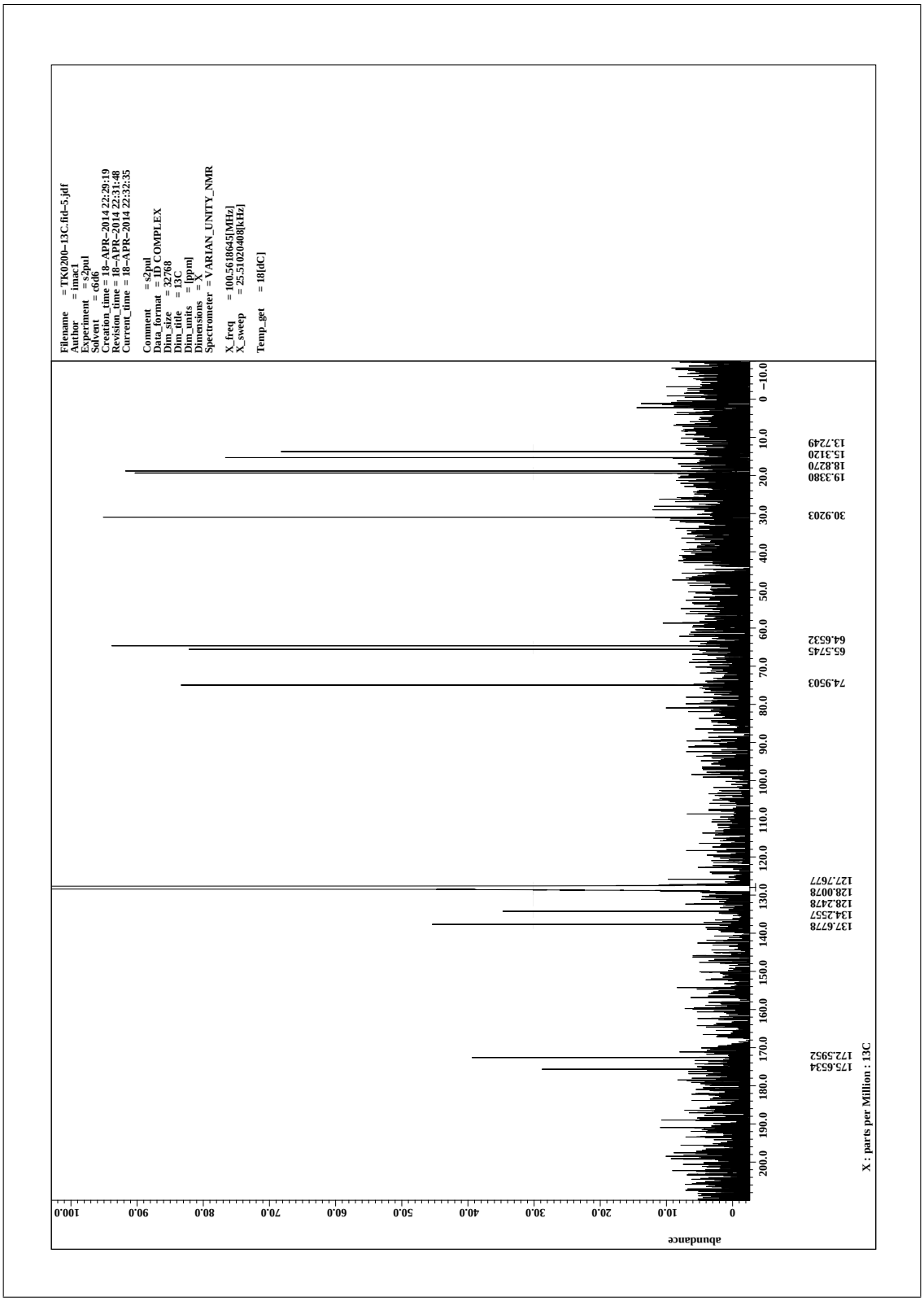

Figure S18. ^{13}C NMR spectrum of **M4-NC** in C_6D_6.

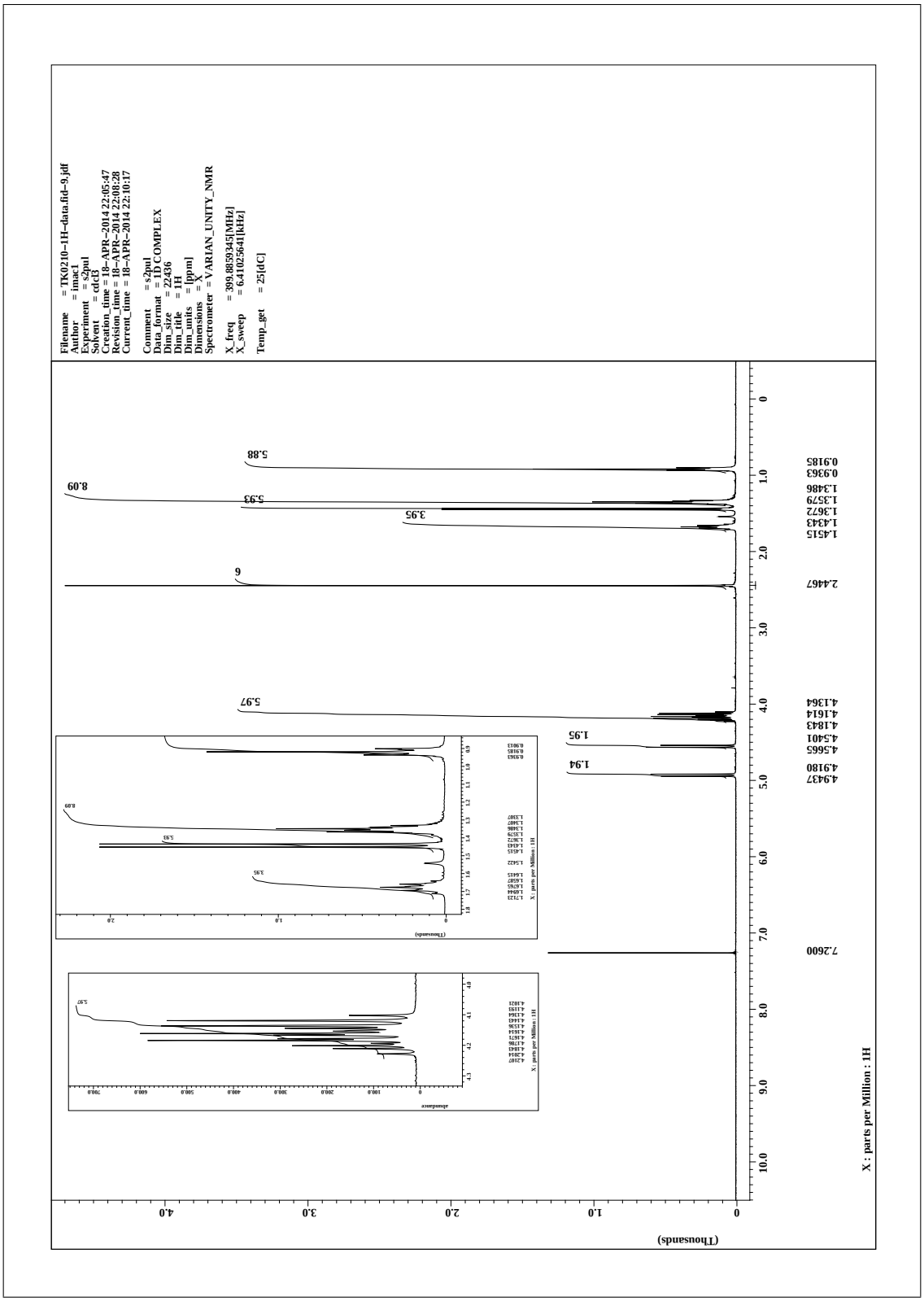

Figure S19. ^{1}H NMR spectrum of **M5-NO$_2$** in $CDCl_3$.

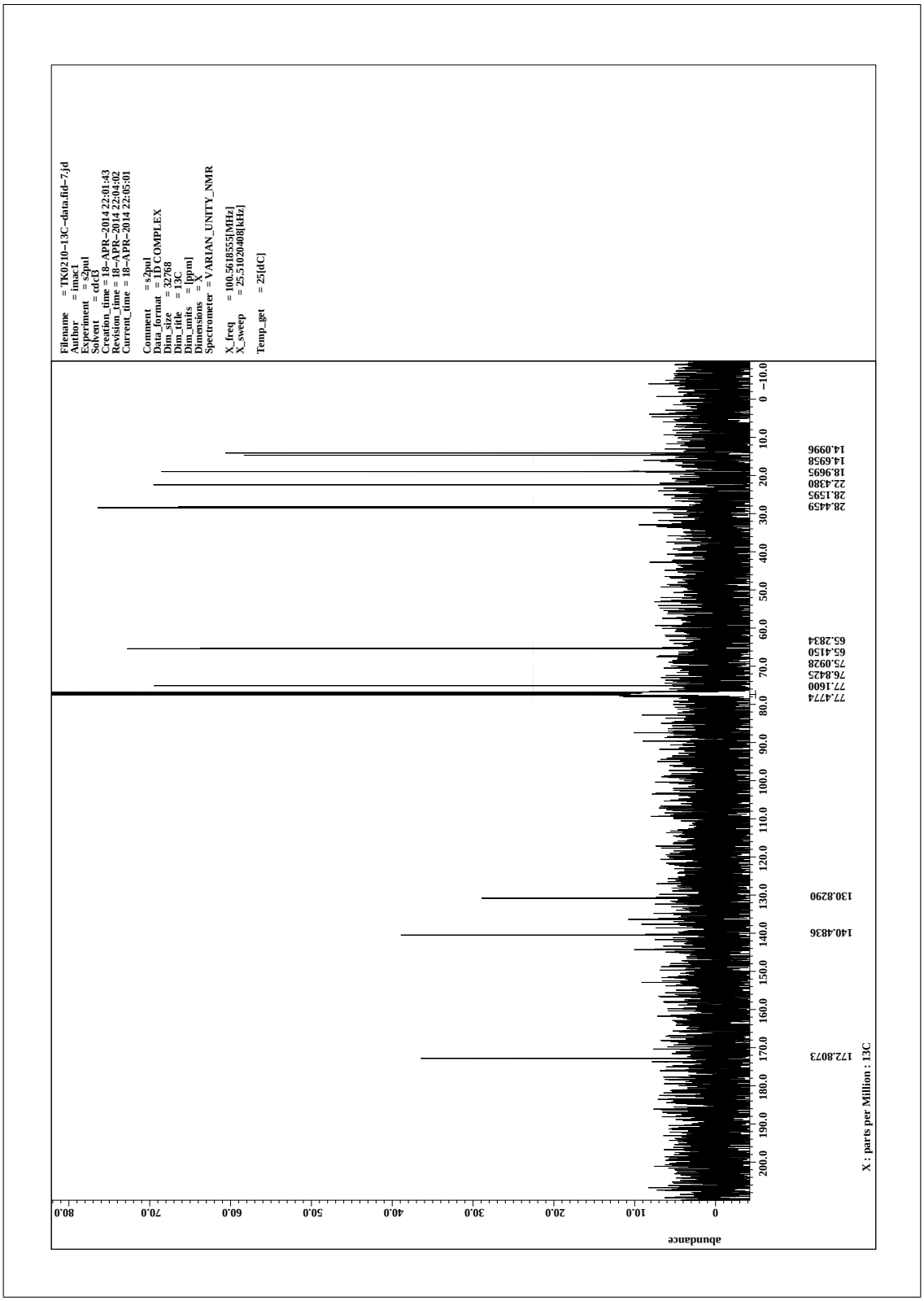

Figure S20. ^{13}C NMR spectrum of **M5-NO_2** in $CDCl_3$.

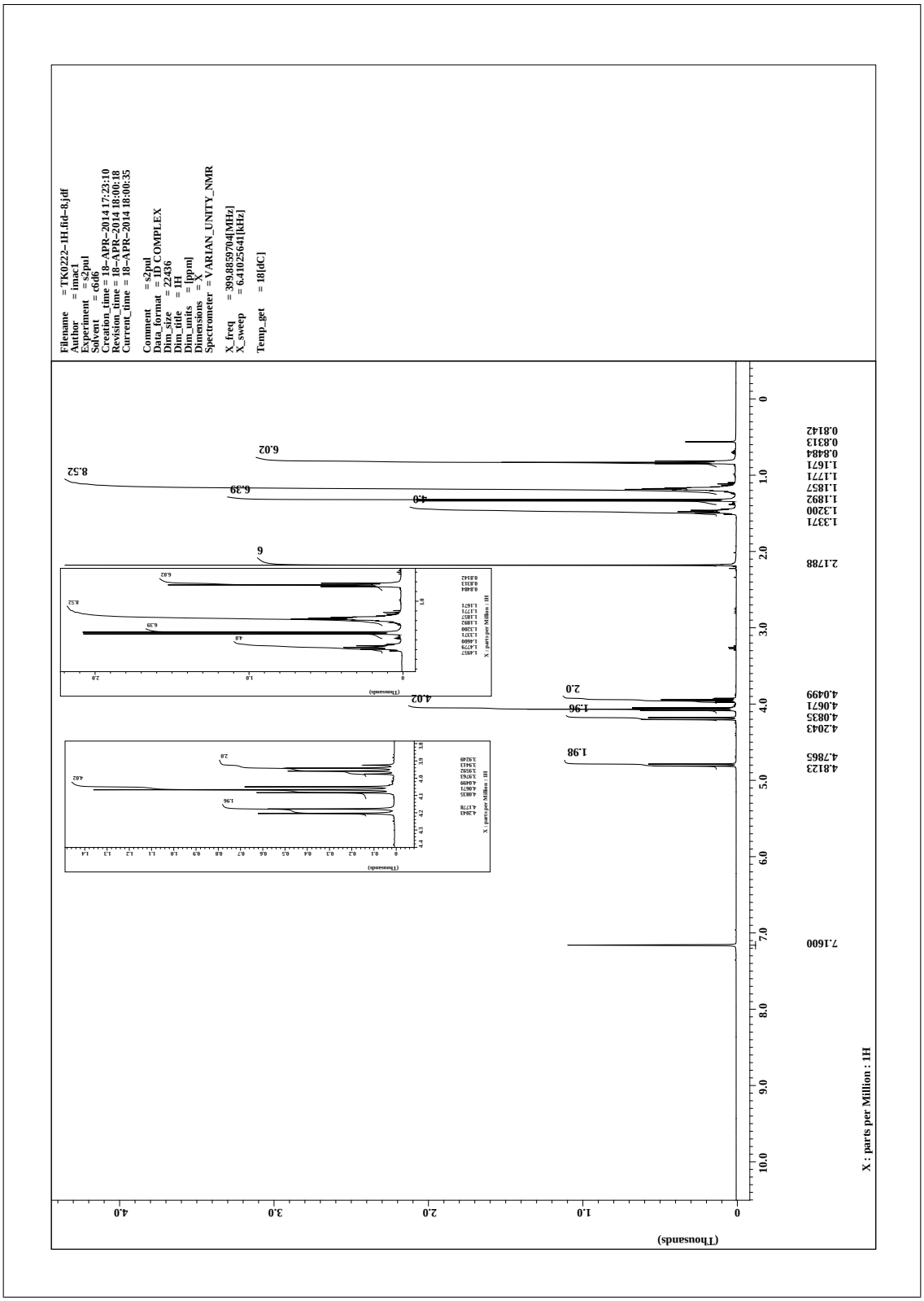

Figure S21. ^{1}H NMR spectrum of **M5-NC** in C_6D_6.

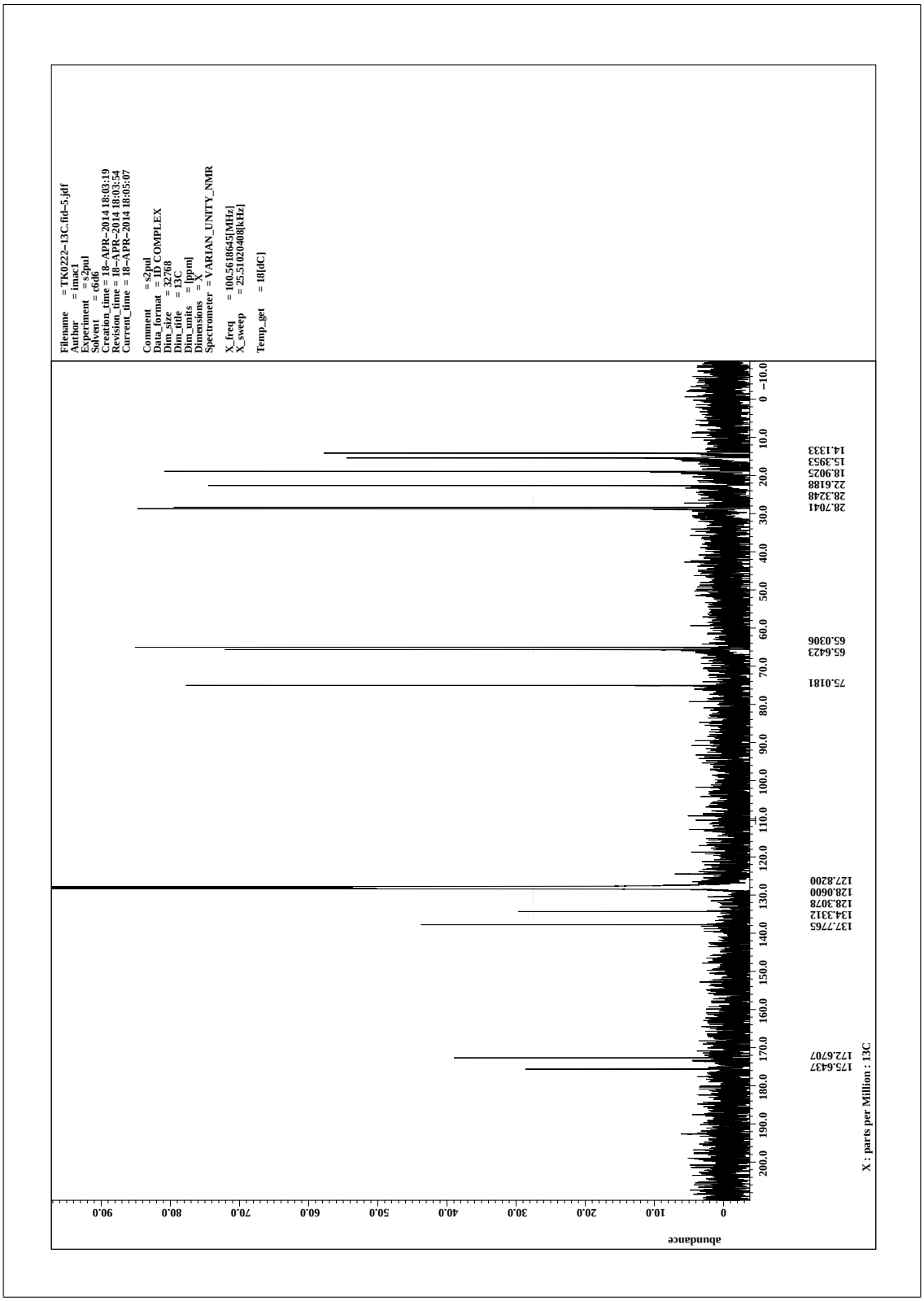

Figure S22. ^{13}C NMR spectrum of **M5-NC** in C_6D_6.

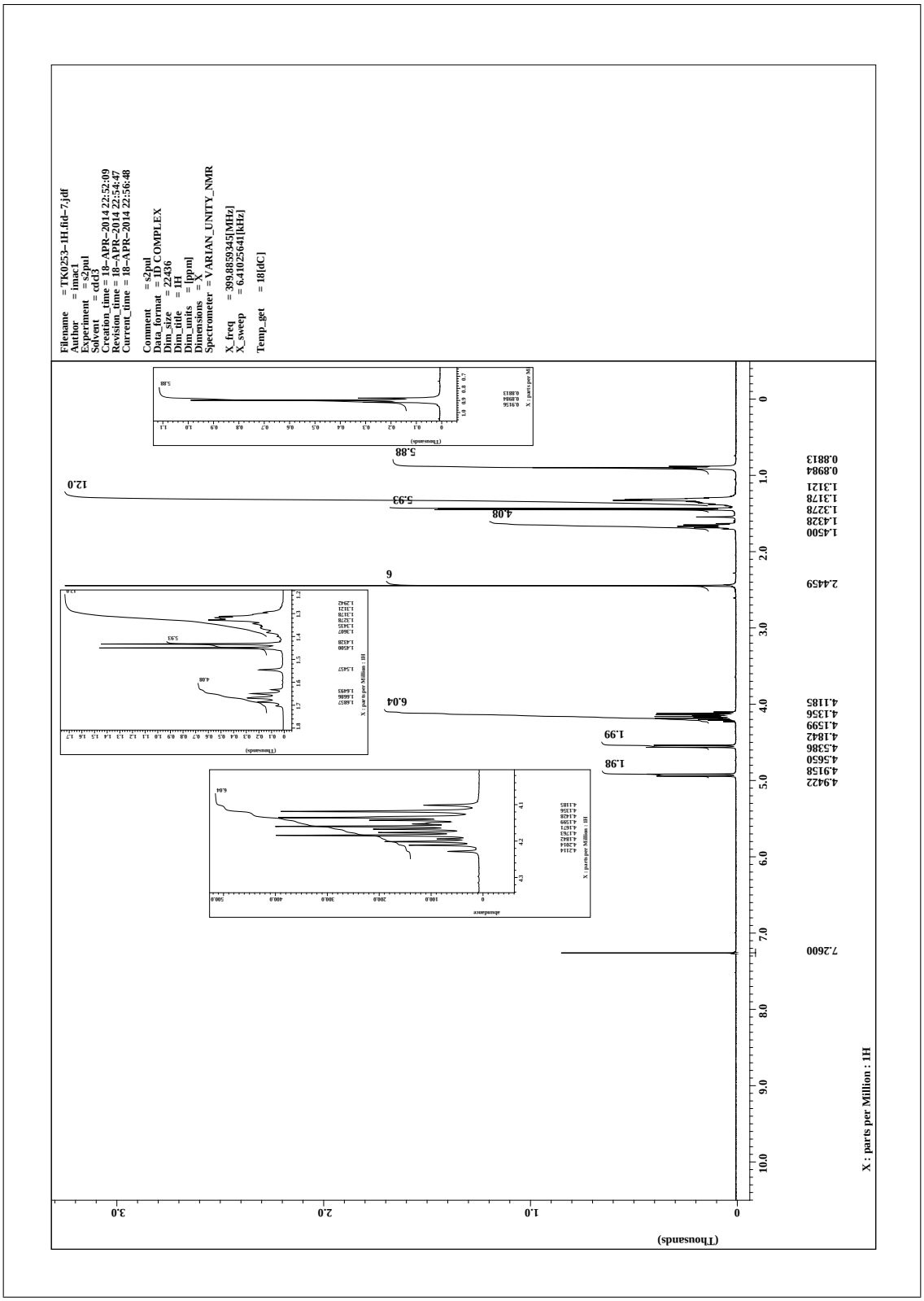

Figure S23. ^{1}H NMR spectrum of **M6-NO$_2$** in $CDCl_3$.

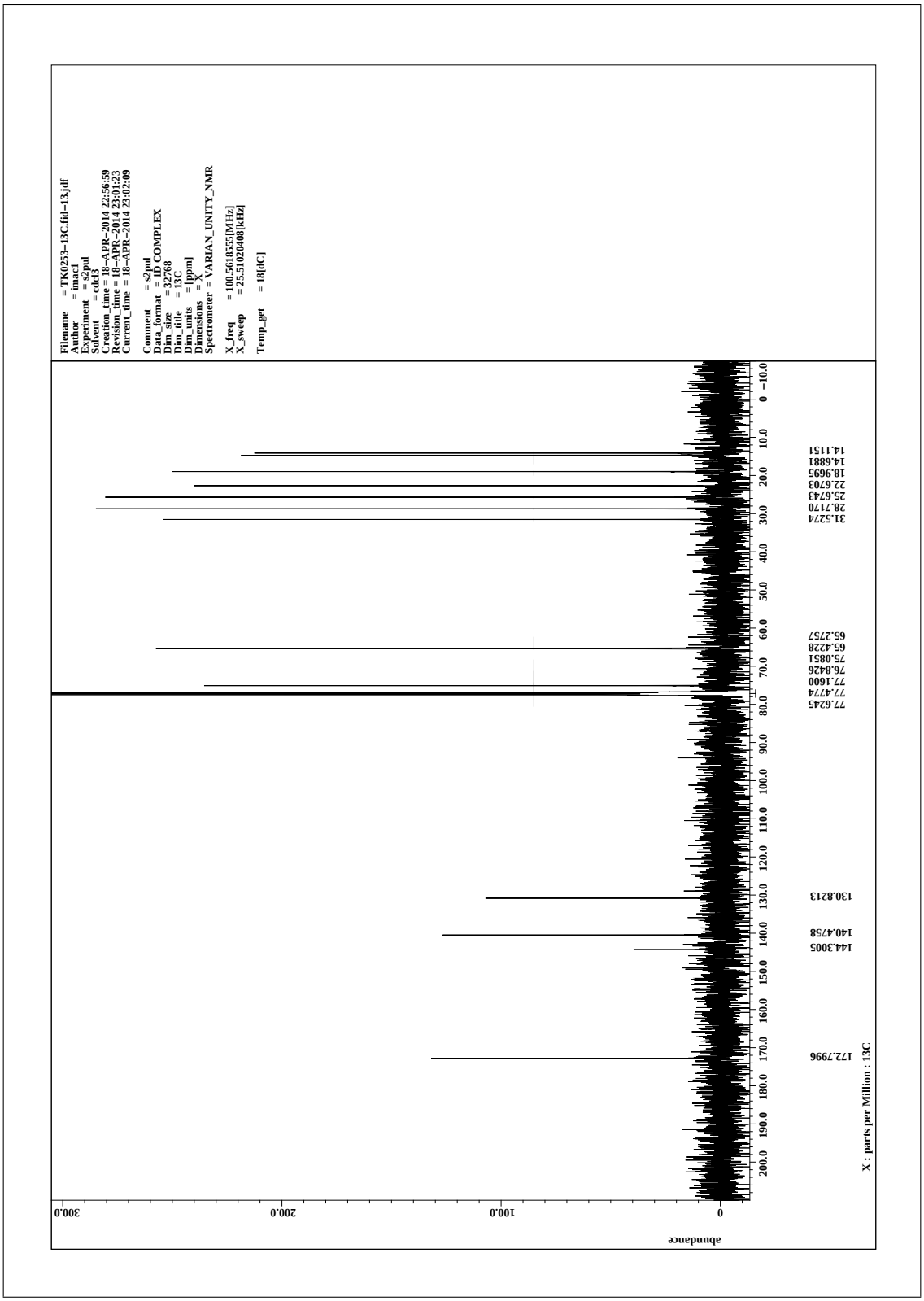

Figure S24. ^{13}C NMR spectrum of **M6-NO_2** in $CDCl_3$.

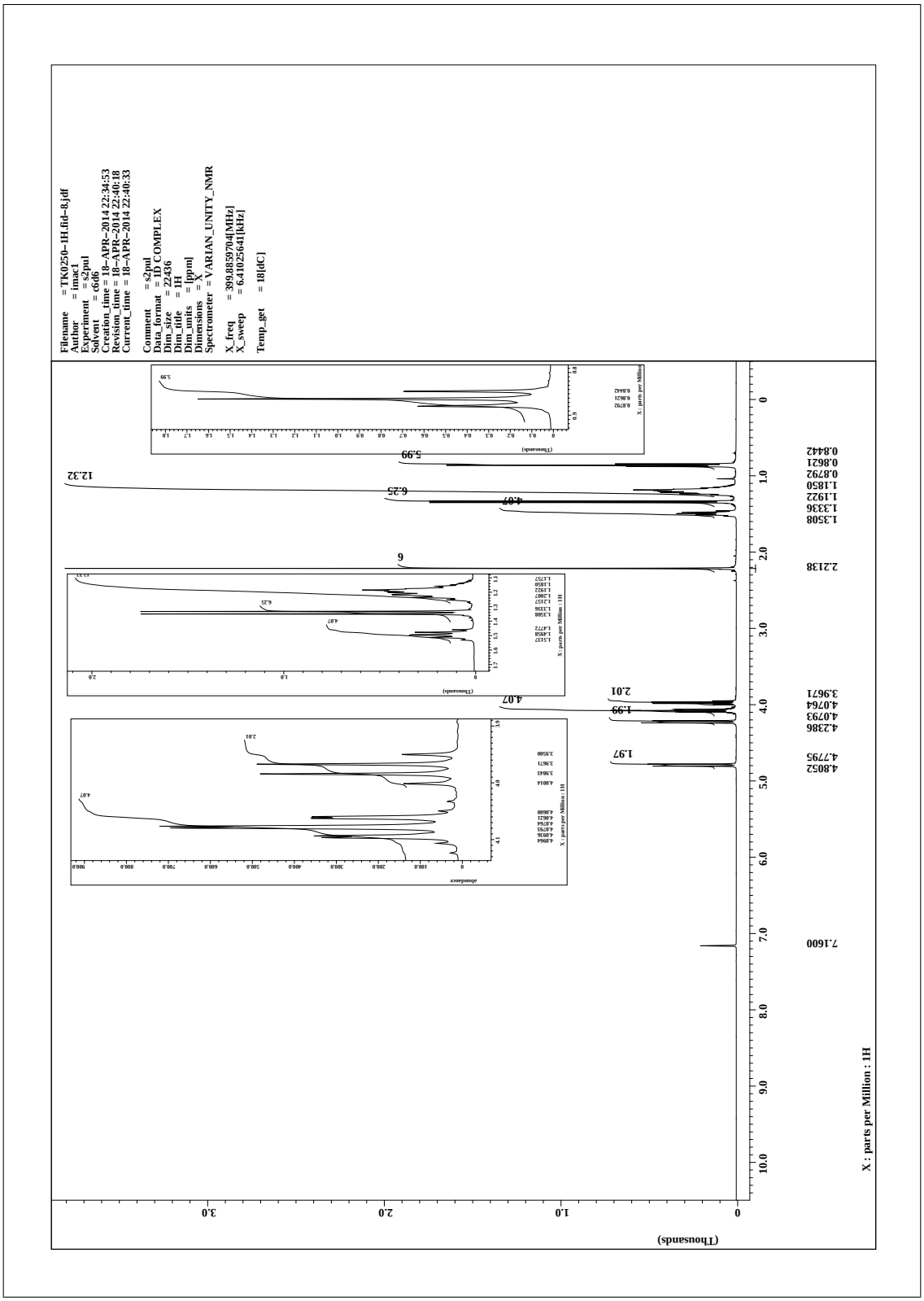

Figure S25. ^{1}H NMR spectrum of **M6-NC** in C_6D_6.

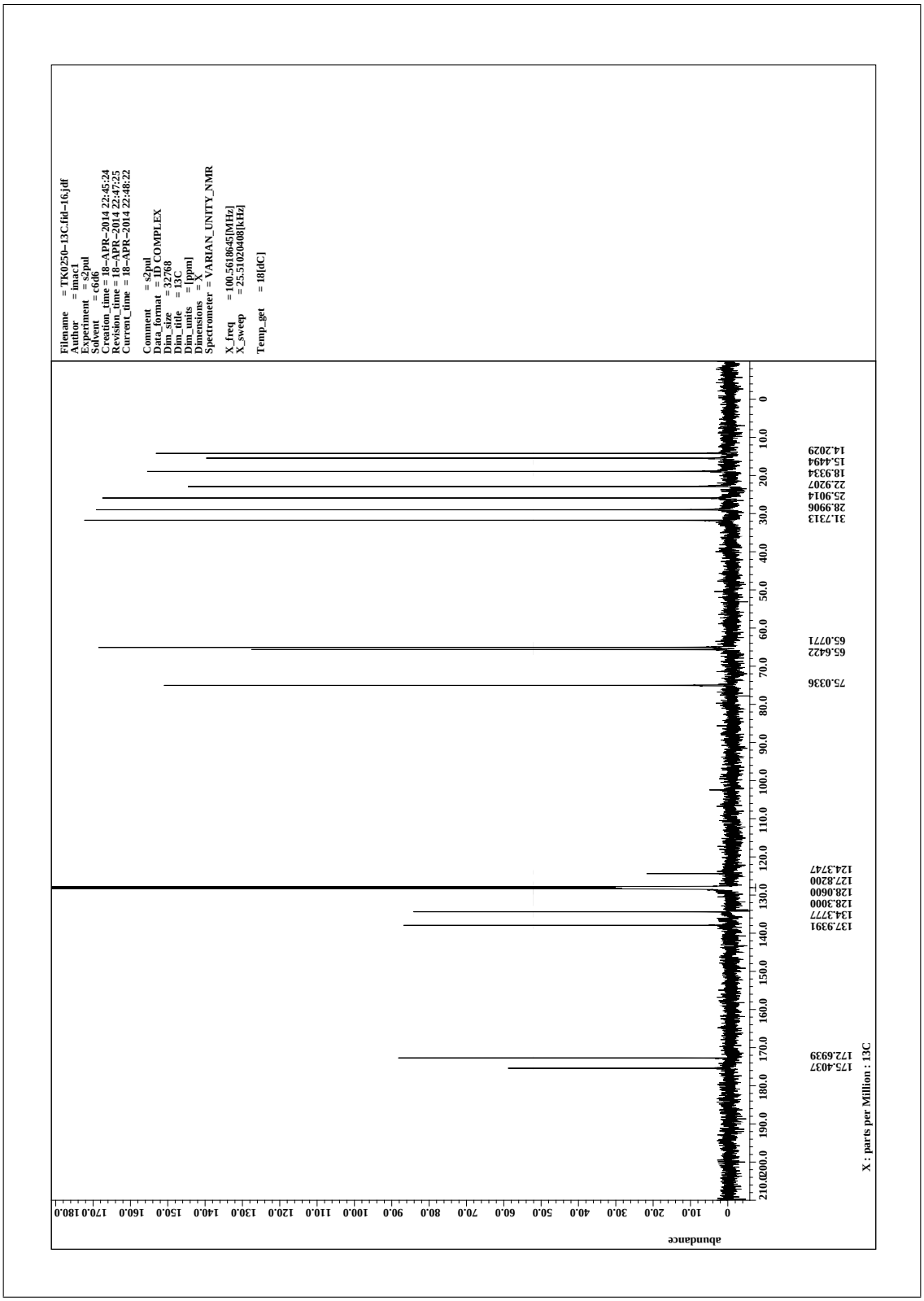

Figure S26. ^{13}C NMR spectrum of **M6-NC** in C_6D_6.

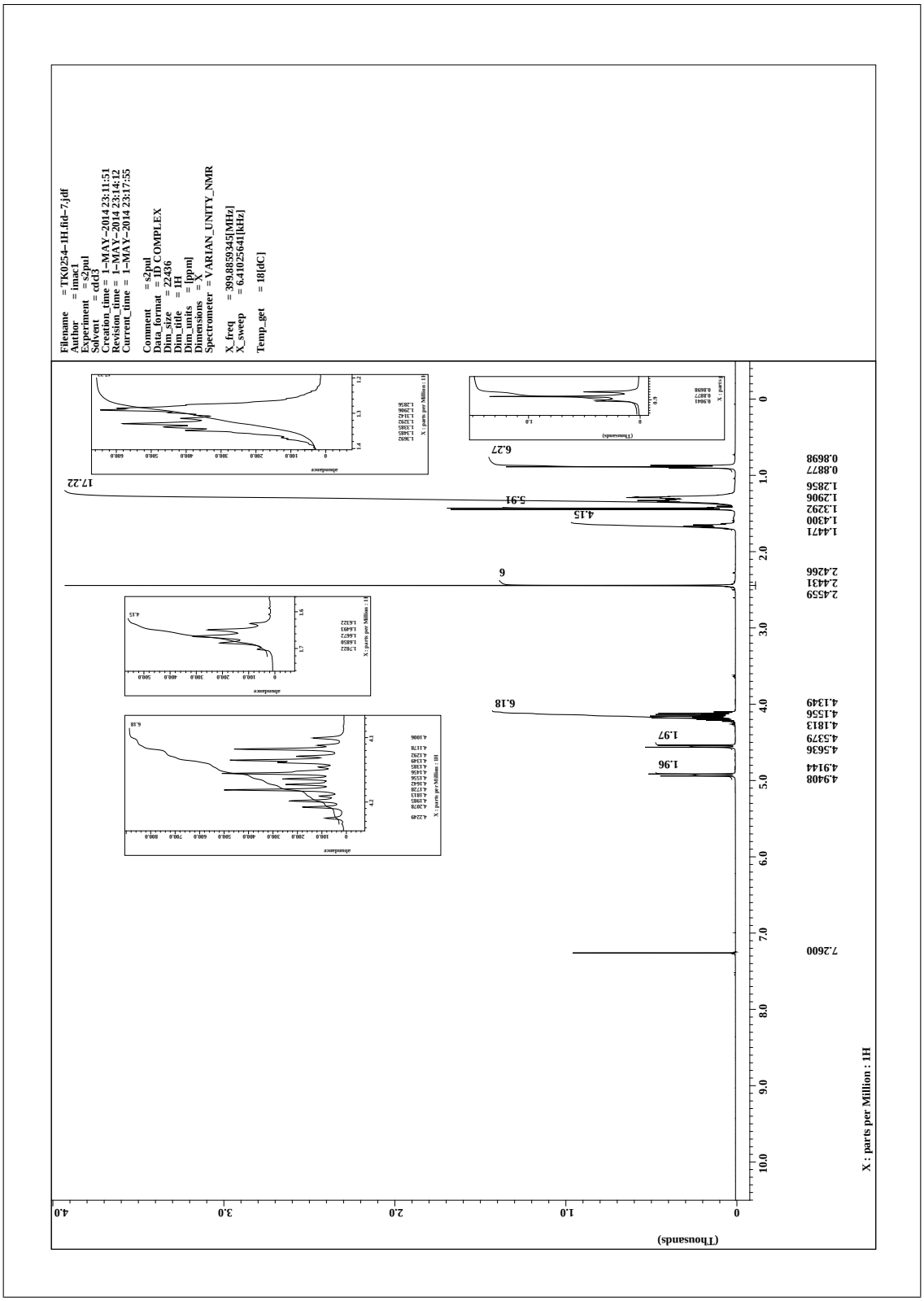

Figure S27. ^{1}H NMR spectrum of **M7-NO$_2$** in $CDCl_3$.

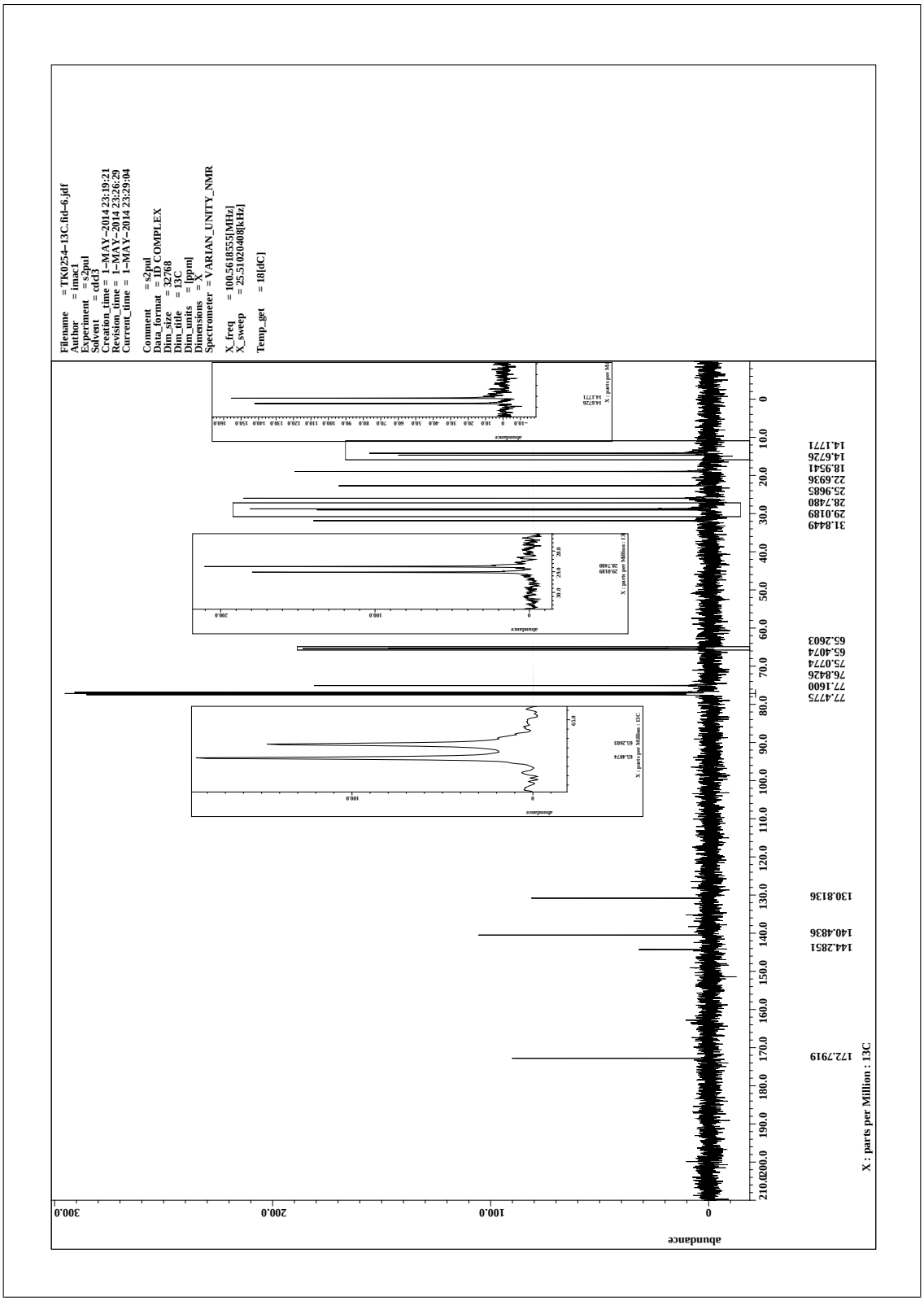

Figure S28. ^{13}C NMR spectrum of **M7-NO_2** in $CDCl_3$.

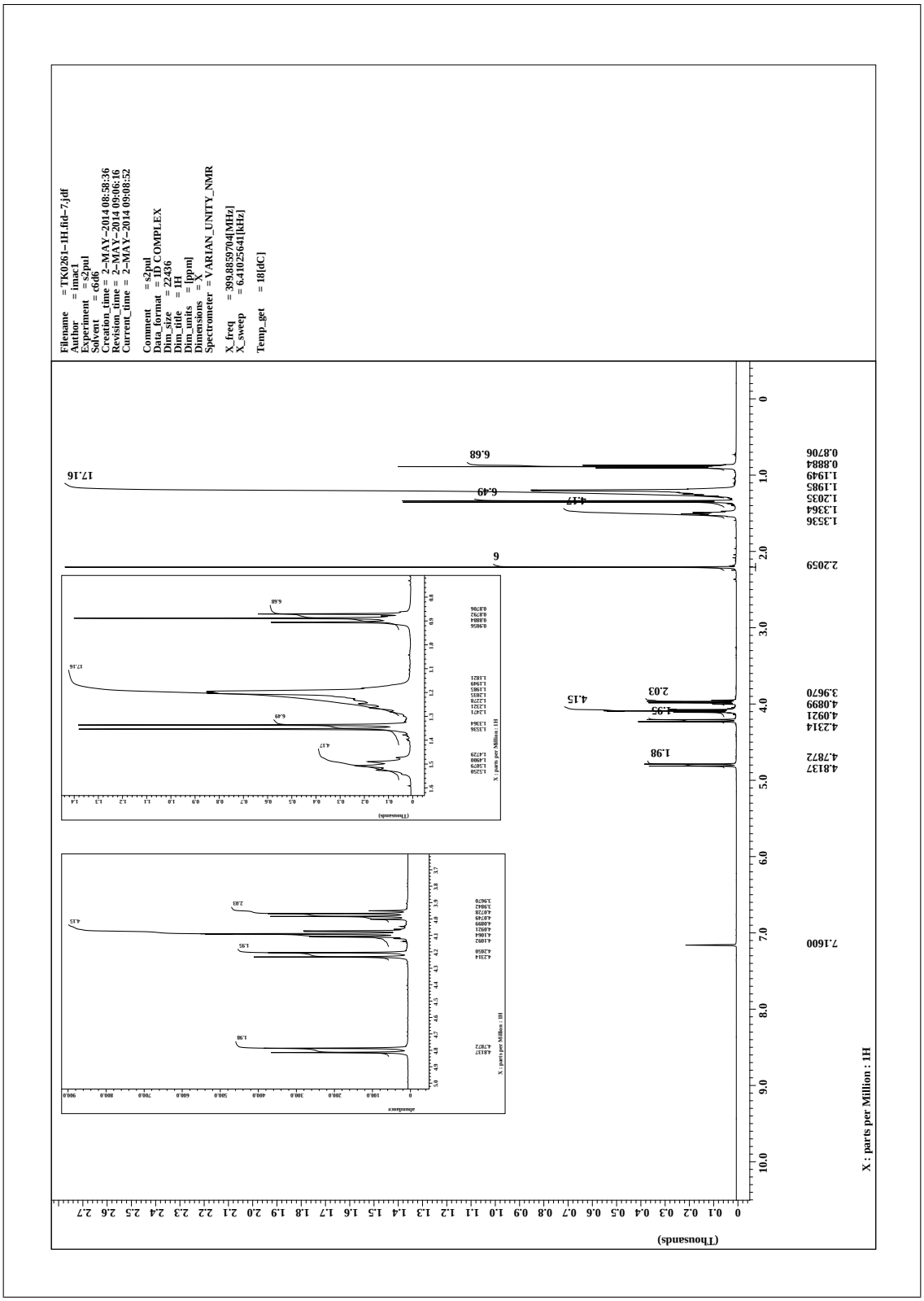

Figure S29. ^{1}H NMR spectrum of **M7-NC** in C_6D_6.

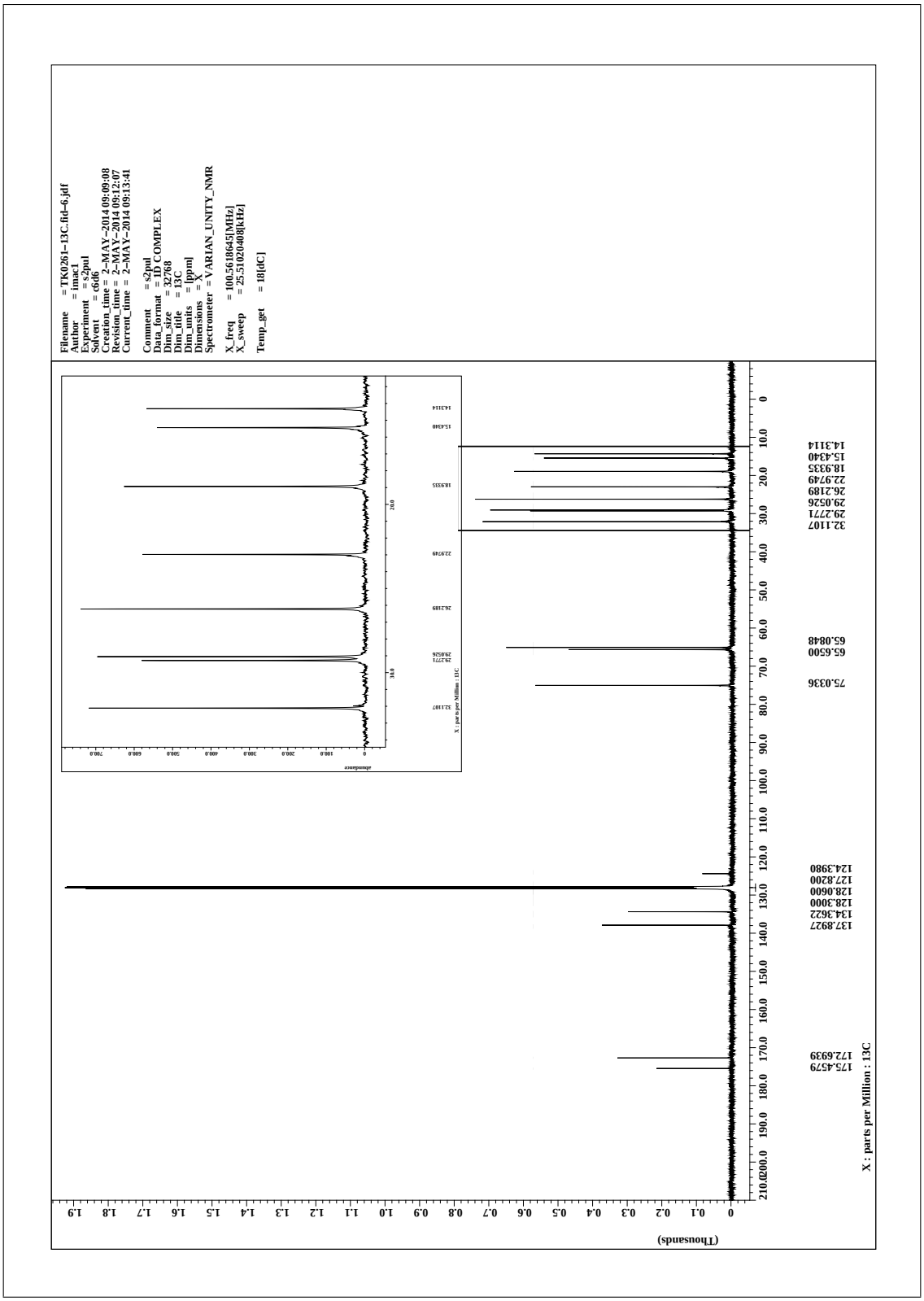

Figure S30. ^{13}C NMR spectrum of **M7-NC** in C_6D_6.

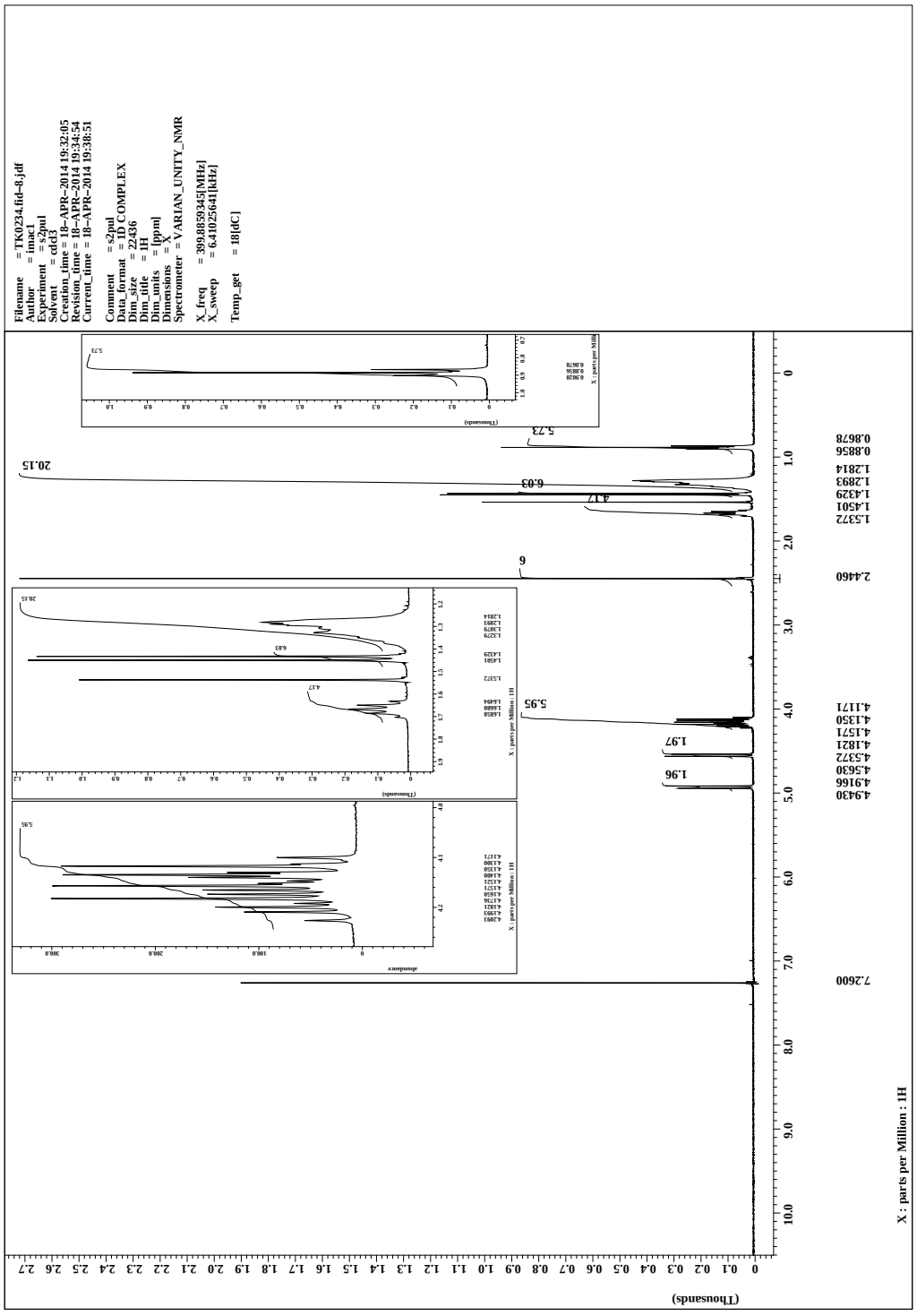

Figure S31. ^{1}H NMR spectrum of **M8-NO$_2$** in $CDCl_3$.

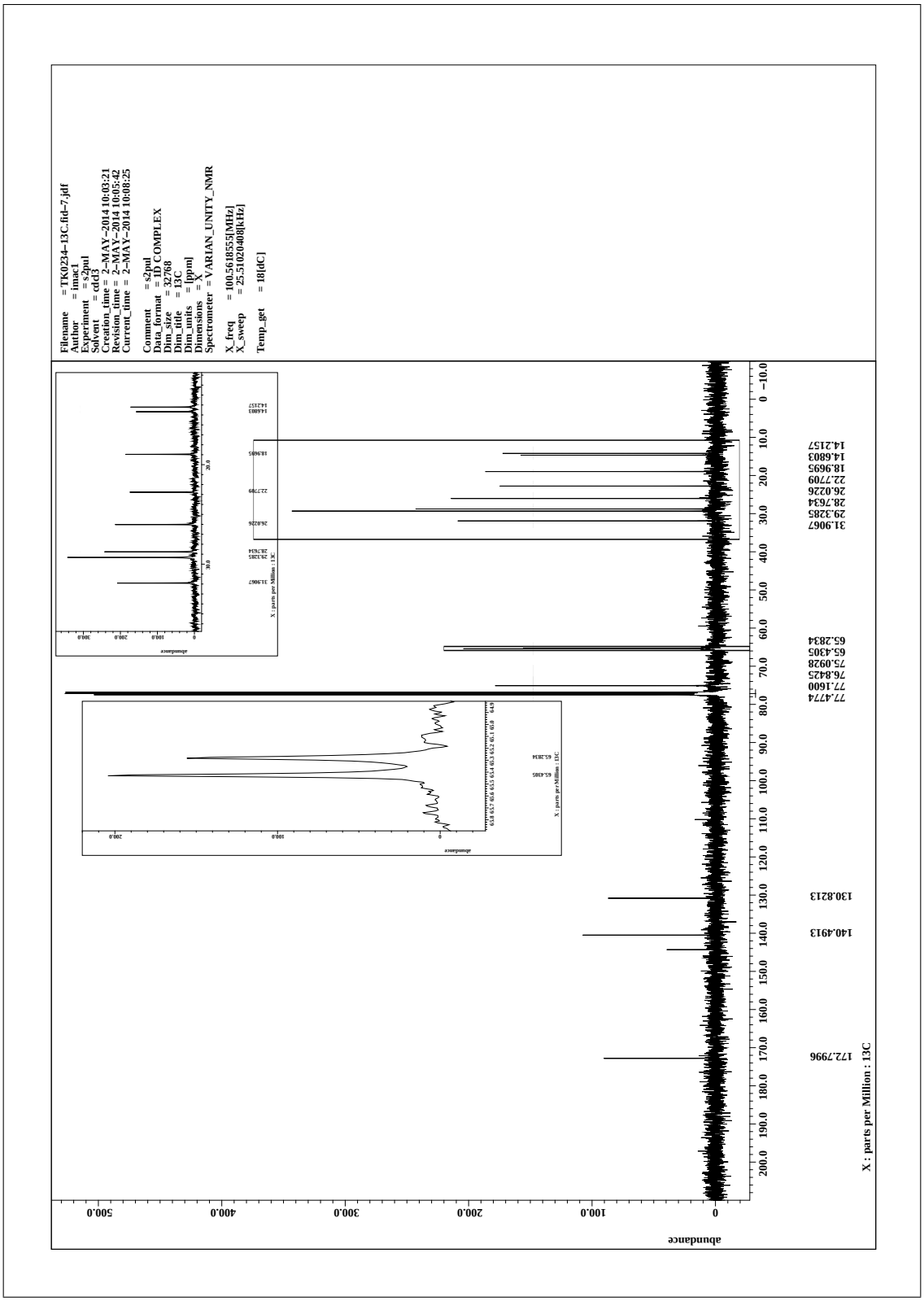

Figure S32. ^{13}C NMR spectrum of **M8-NO_2** in $CDCl_3$.

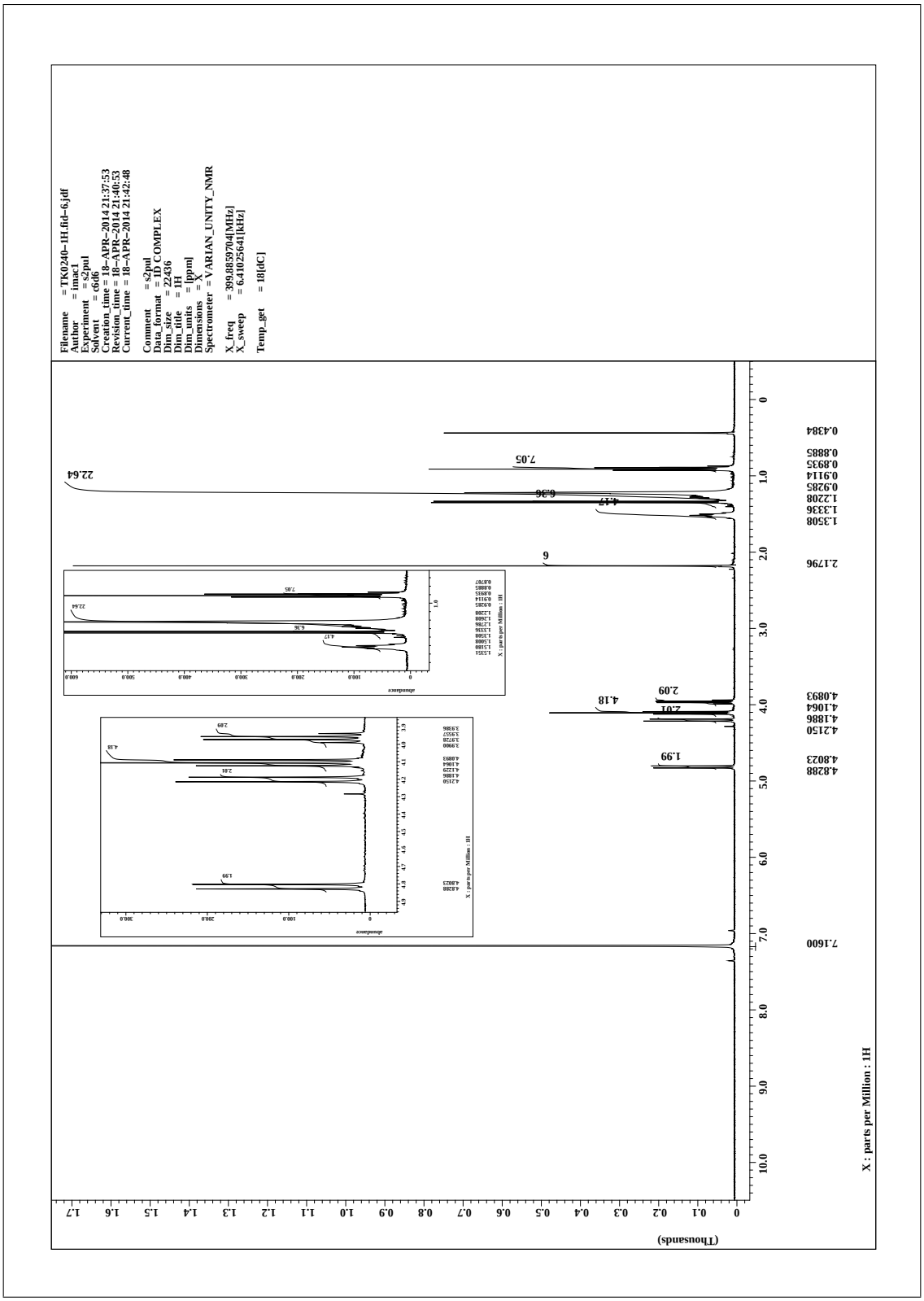

Figure S33. ^{1}H NMR spectrum of **M8-NC** in C_6D_6.

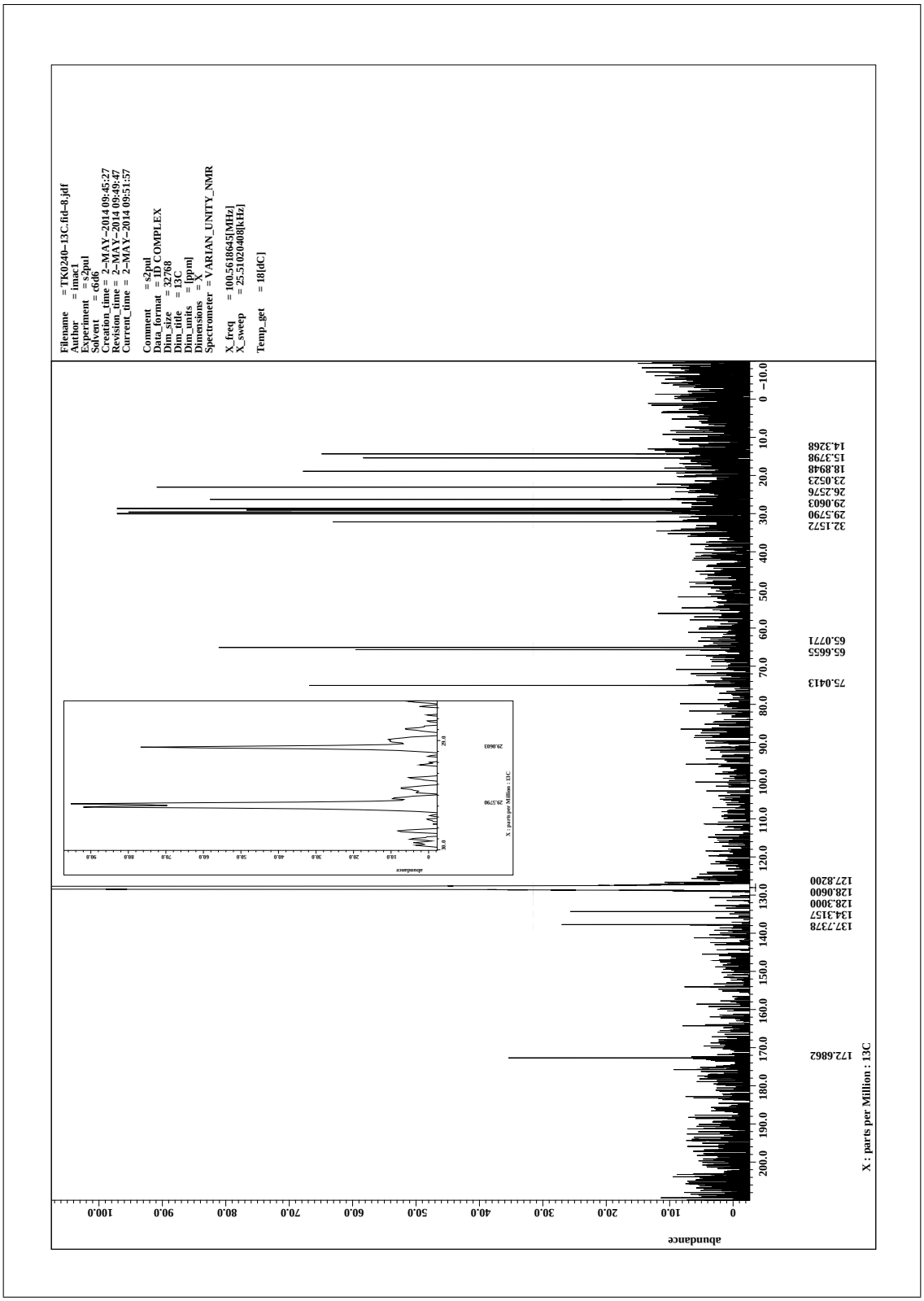

Figure S34. ^{13}C NMR spectrum of **M8-NC** in C_6D_6.

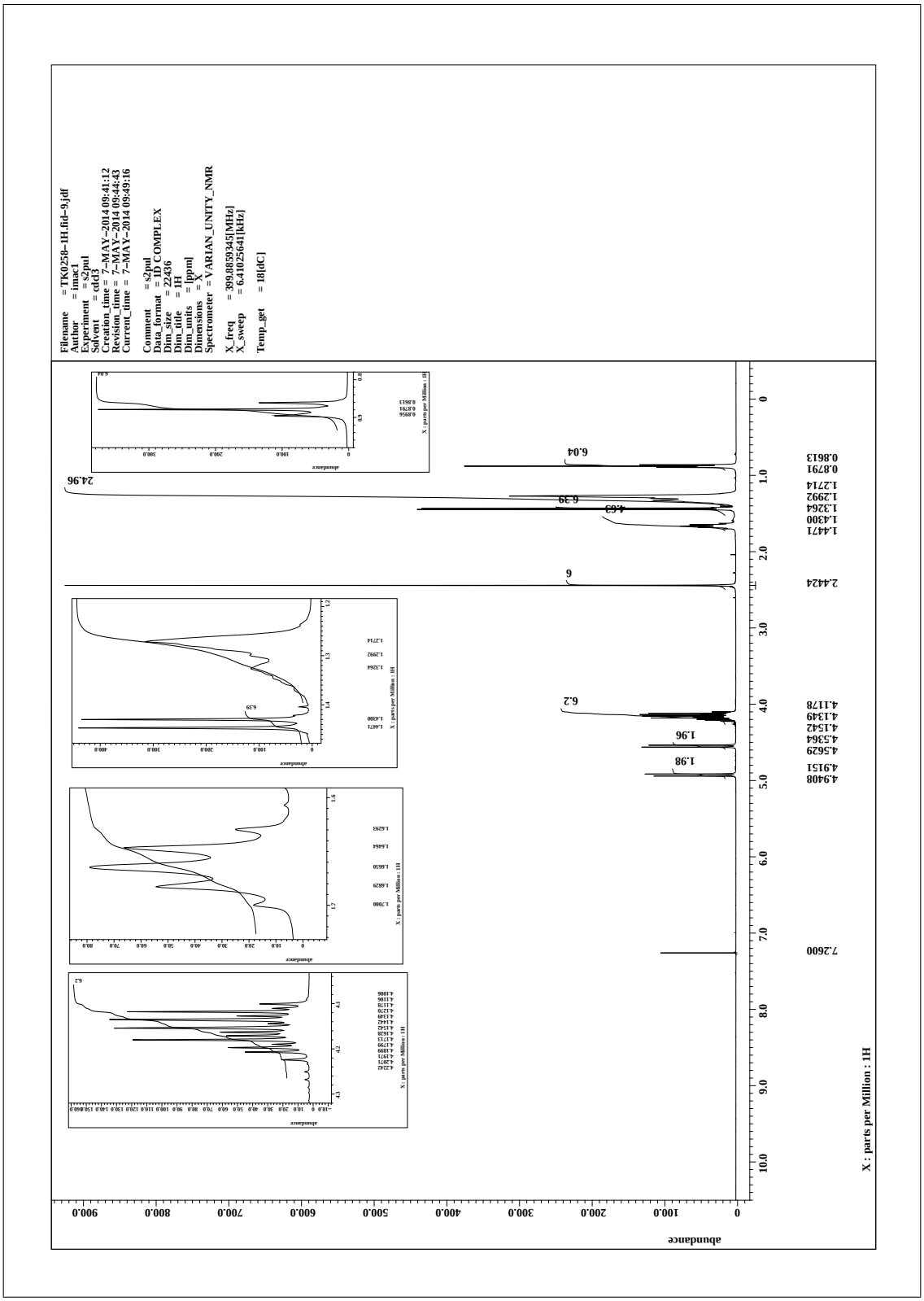

Figure S35. ^{1}H NMR spectrum of **M9-NO$_2$** in $CDCl_3$.

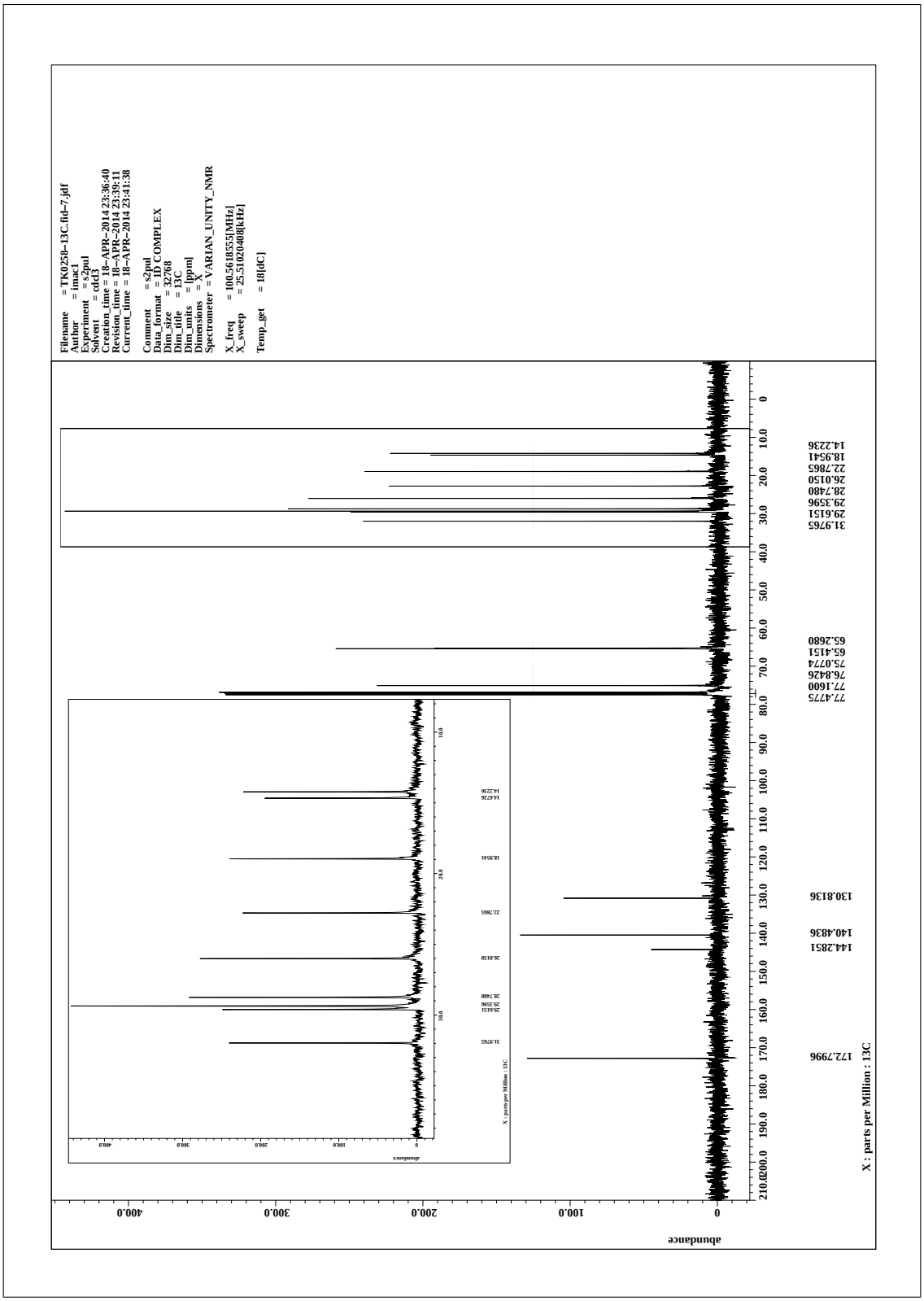

Figure S36. ^{13}C NMR spectrum of **M9-NO_2** in $CDCl_3$.

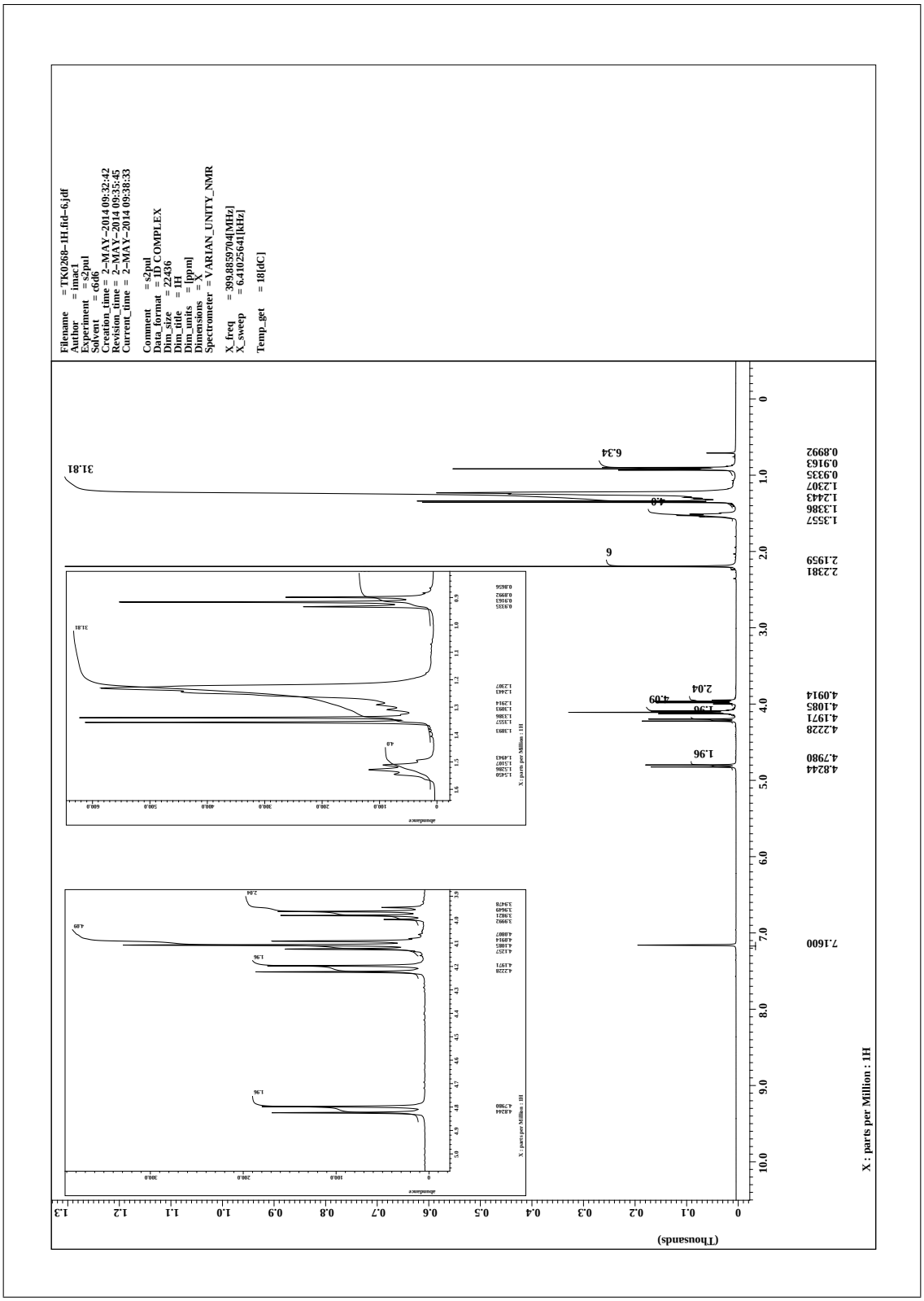

Figure S37. ^{1}H NMR spectrum of **M9-NC** in C_6D_6.

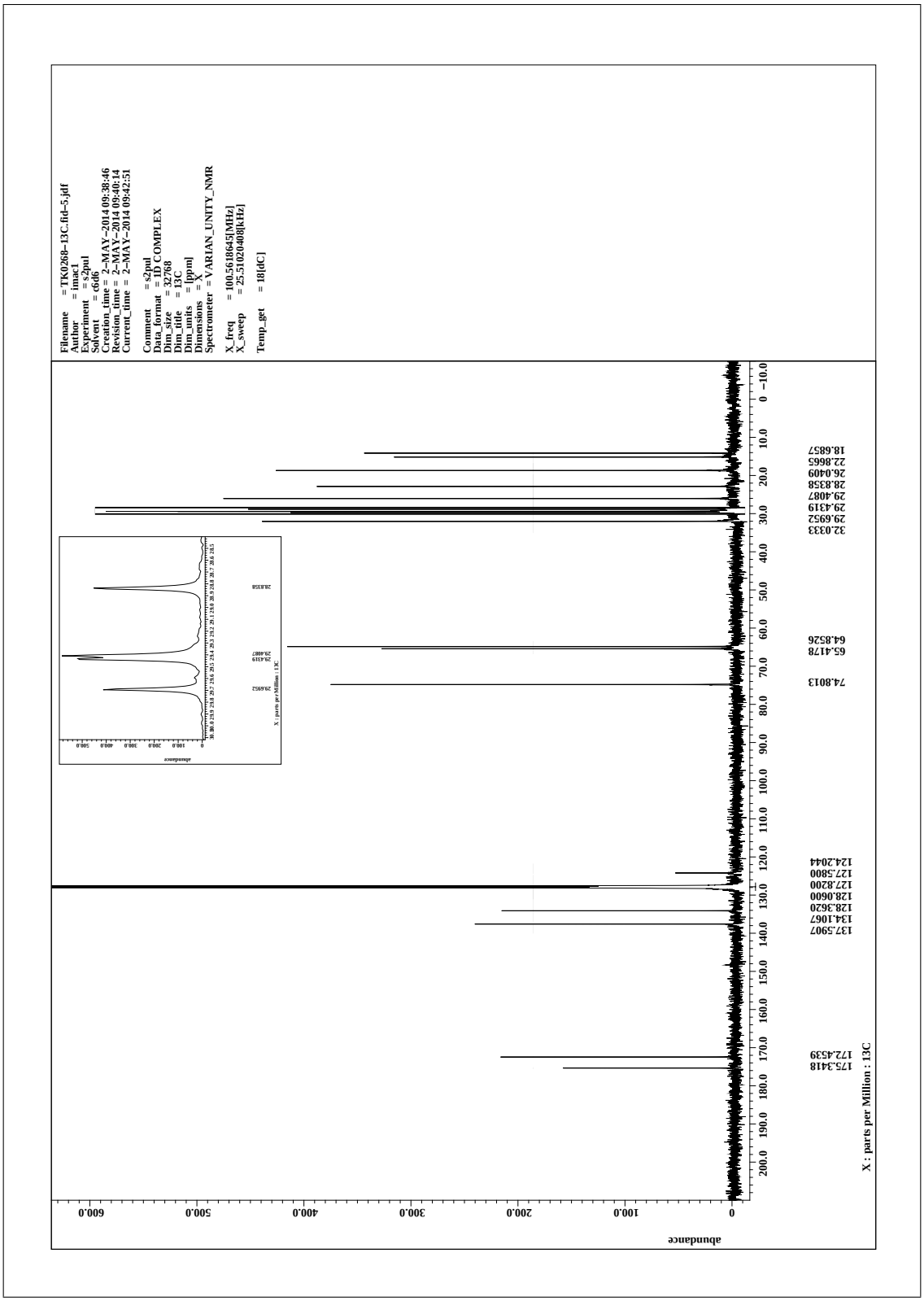

Figure S38. ^{13}C NMR spectrum of **M9-NC** in C_6D_6.

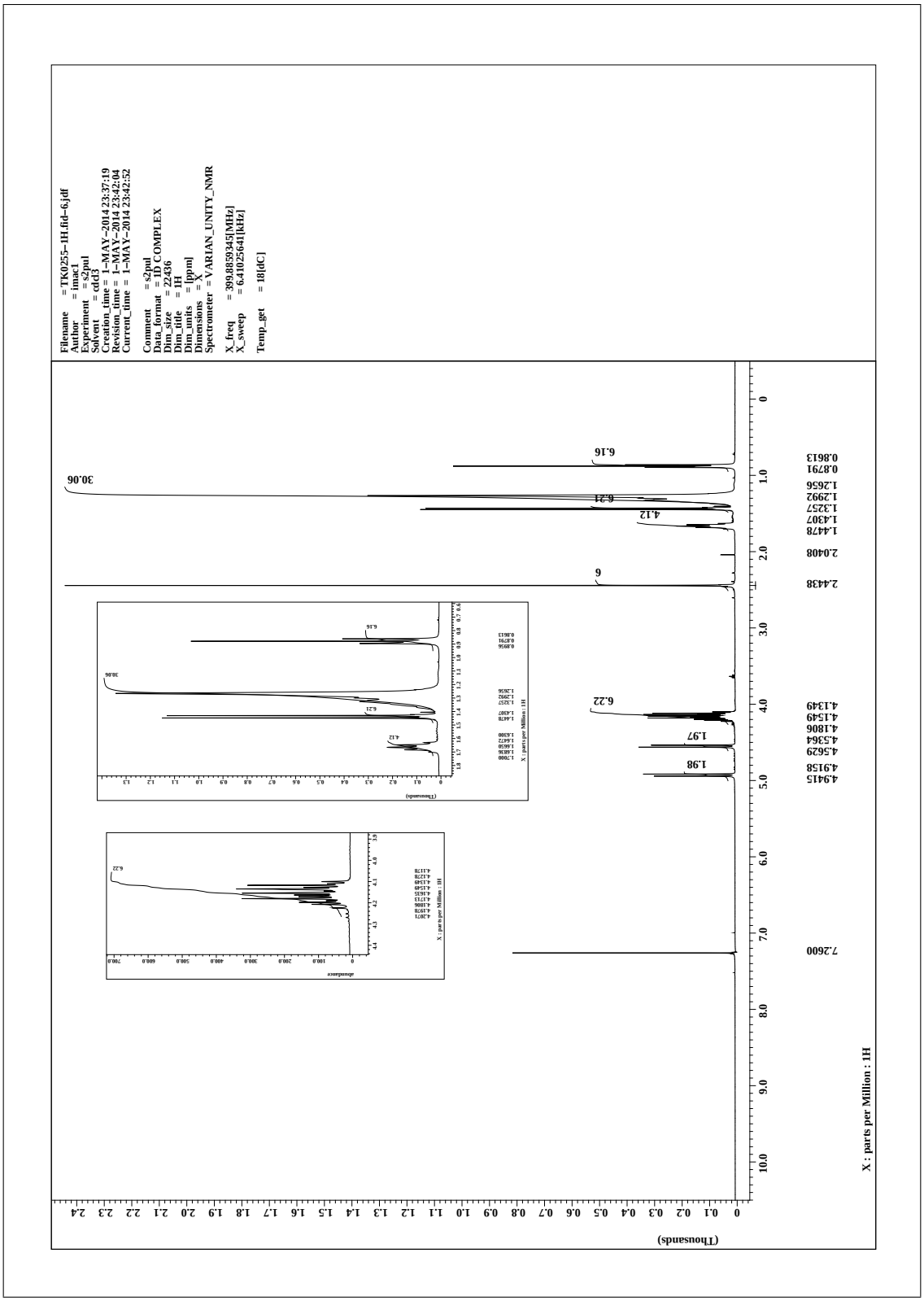

Figure S39. ^{1}H NMR spectrum of **M10-NO_2** in $CDCl_3$.

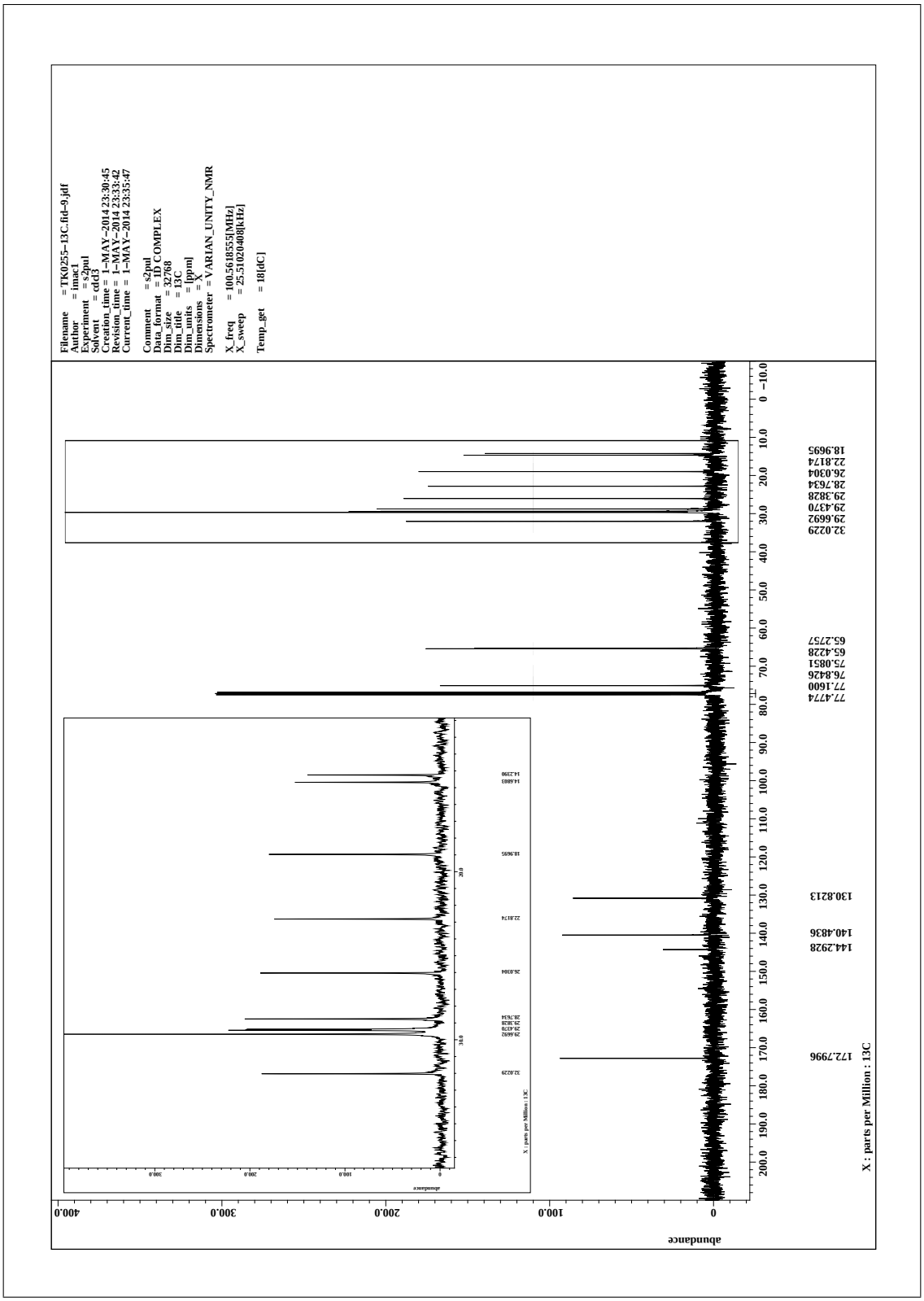

Figure S40. ^{13}C NMR spectrum of **M10-NO_2** in $CDCl_3$.

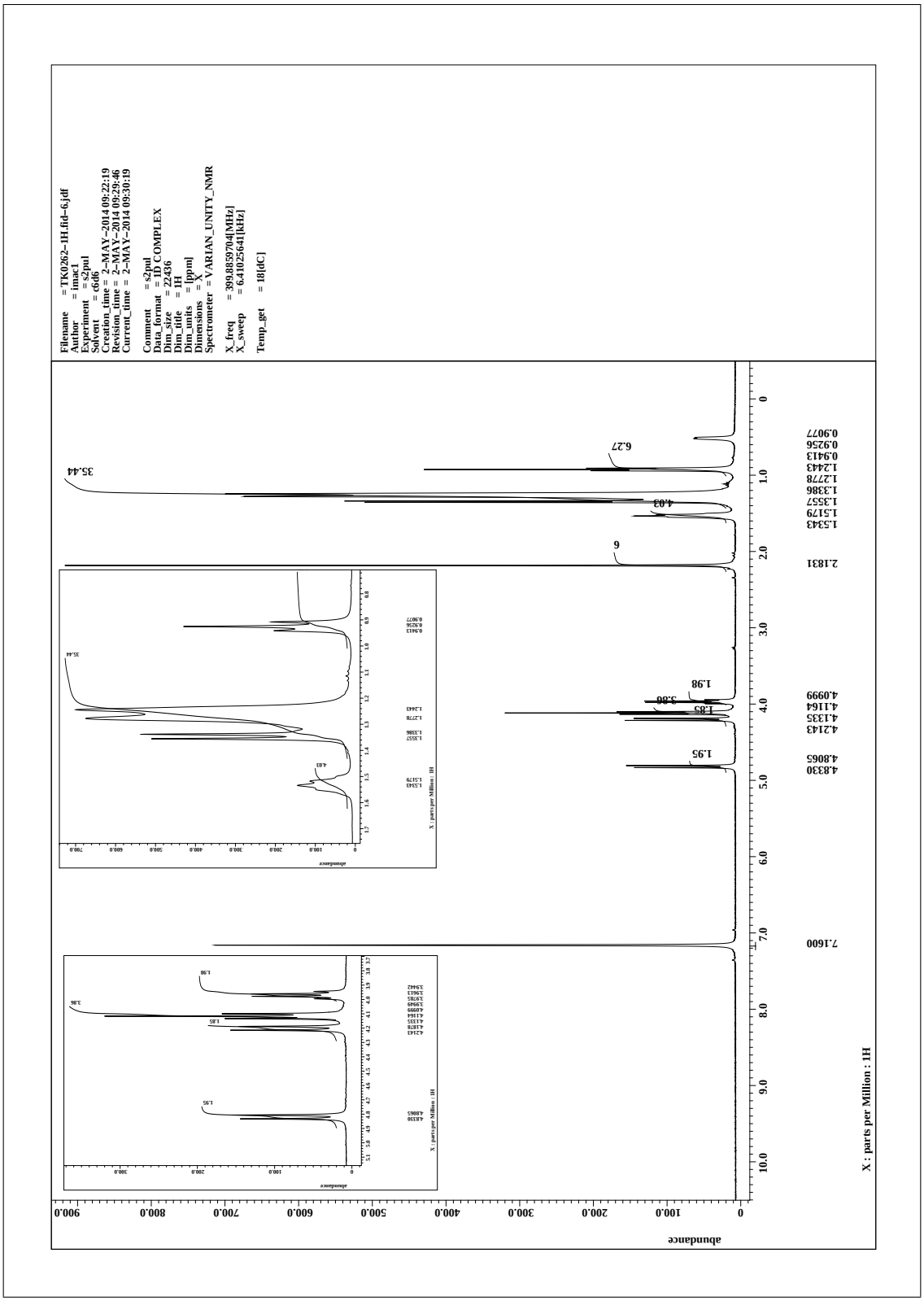

Figure S41. ^{1}H NMR spectrum of **M10-NC** in C_6D_6.

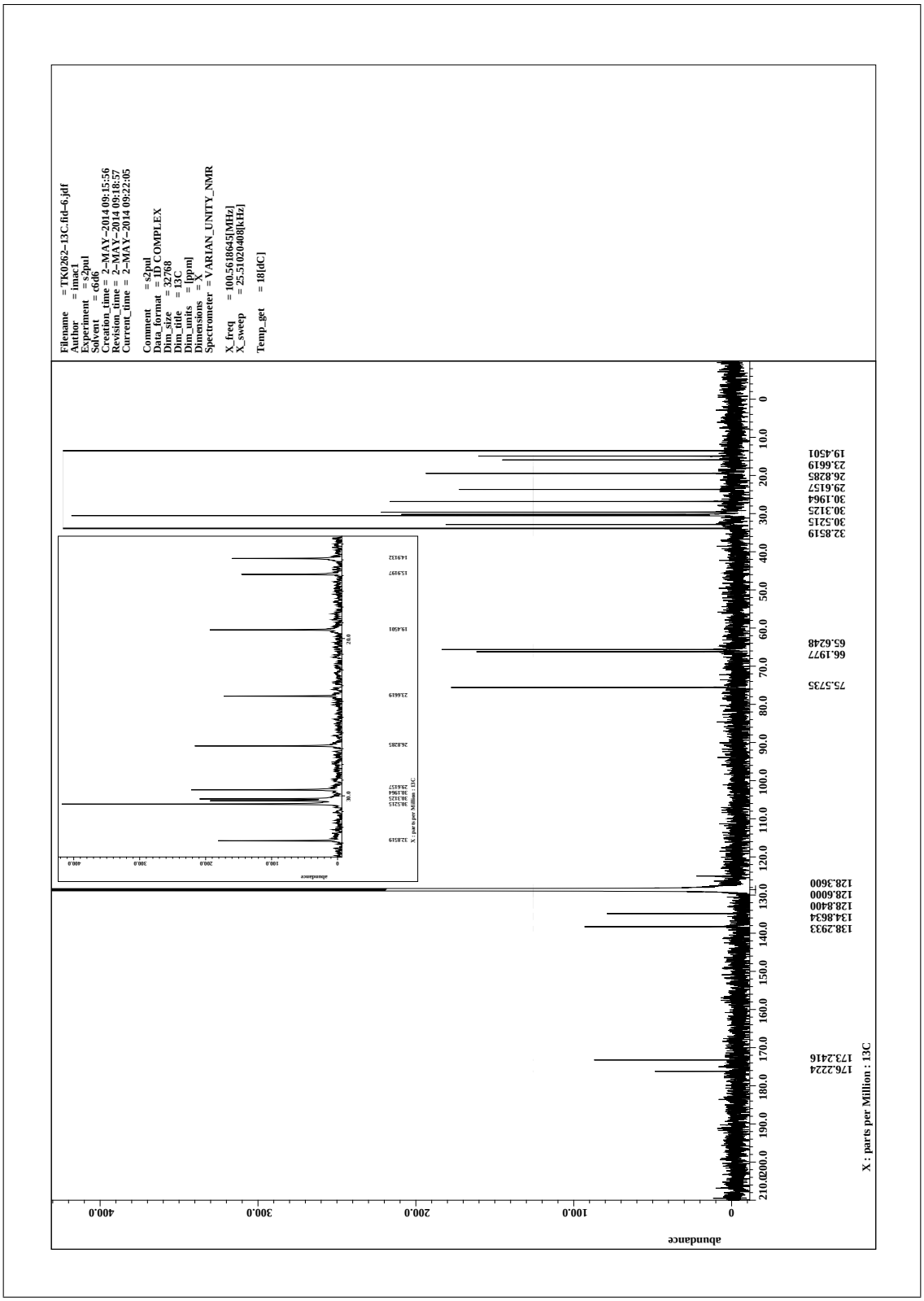

Figure S42. ^{13}C NMR spectrum of **M10-NC** in C_6D_6.

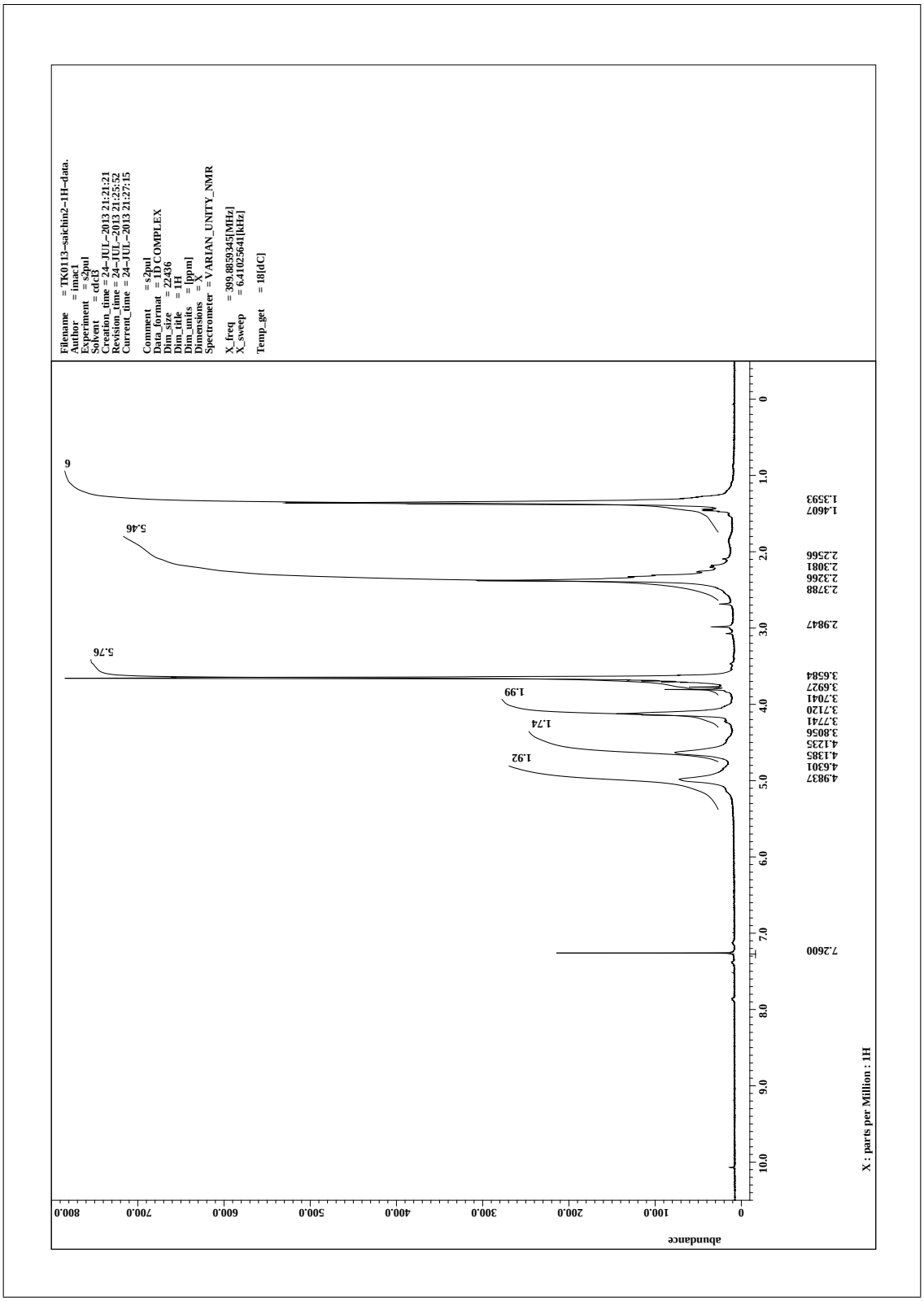

Figure S43. ^{1}H NMR spectrum of **1(40)** in $CDCl_3$.

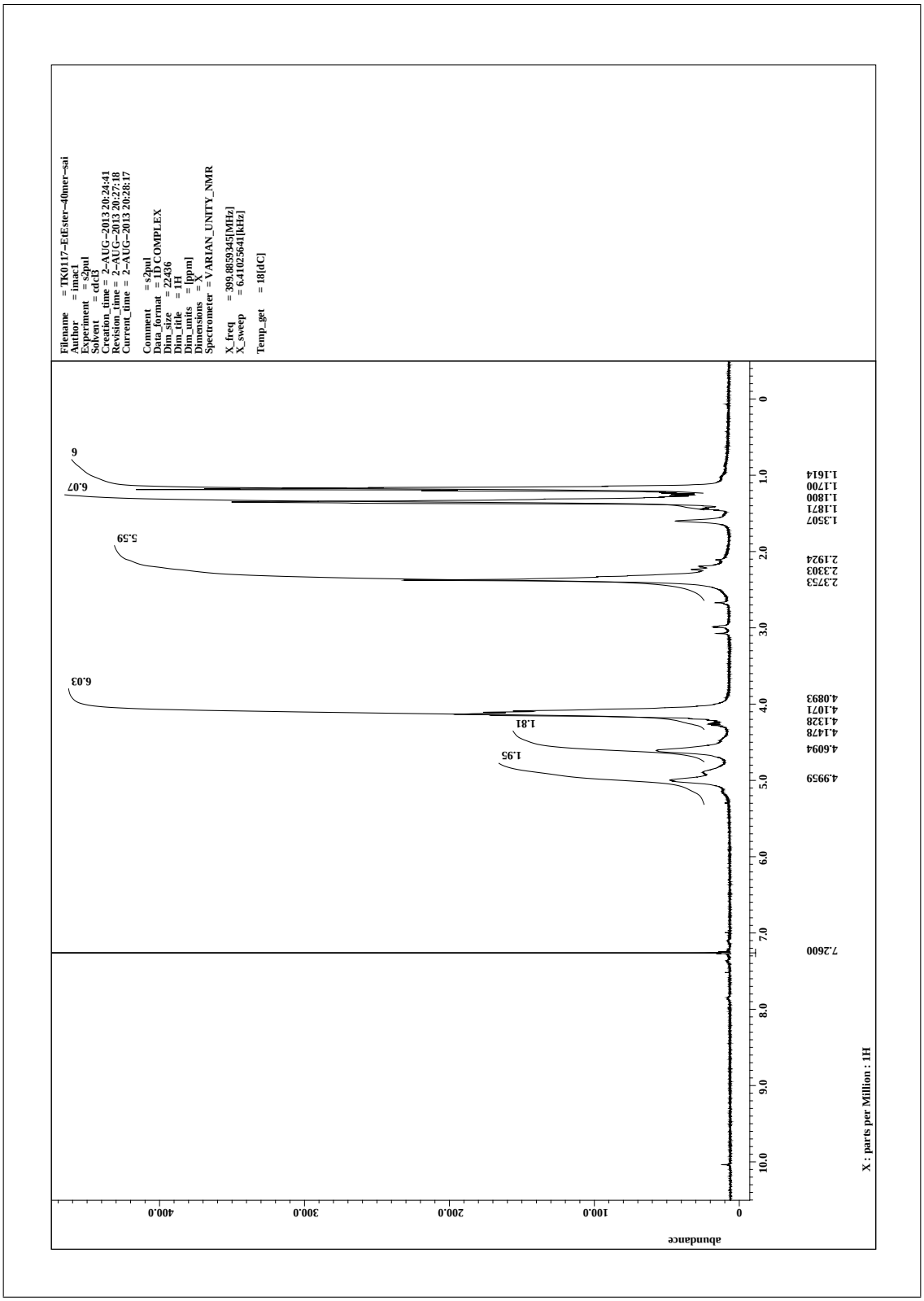

Figure S44. ^{1}H NMR spectrum of **2(40)** in $CDCl_3$.

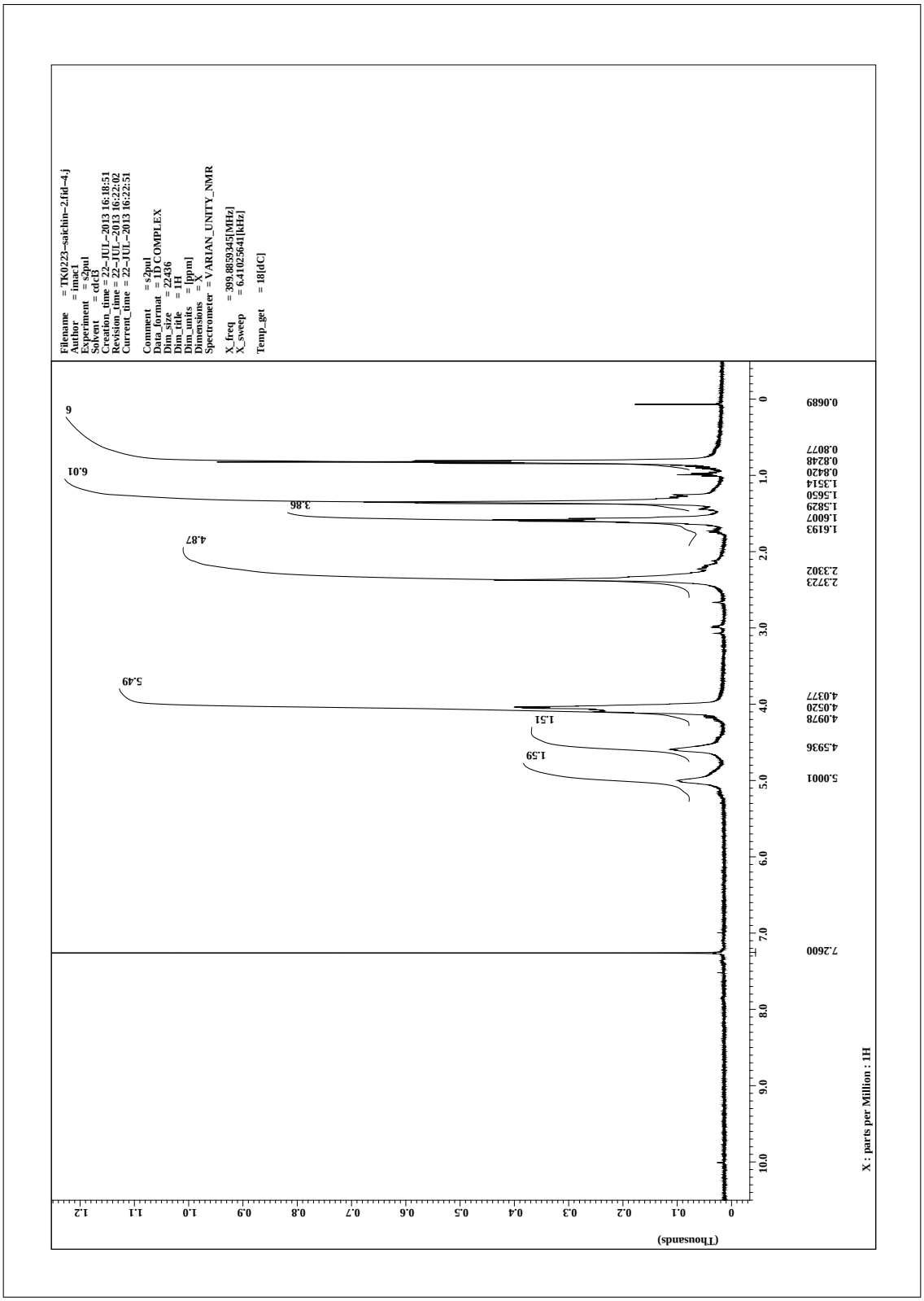

Figure S45. ^{1}H NMR spectrum of **3(40)** in $CDCl_3$.

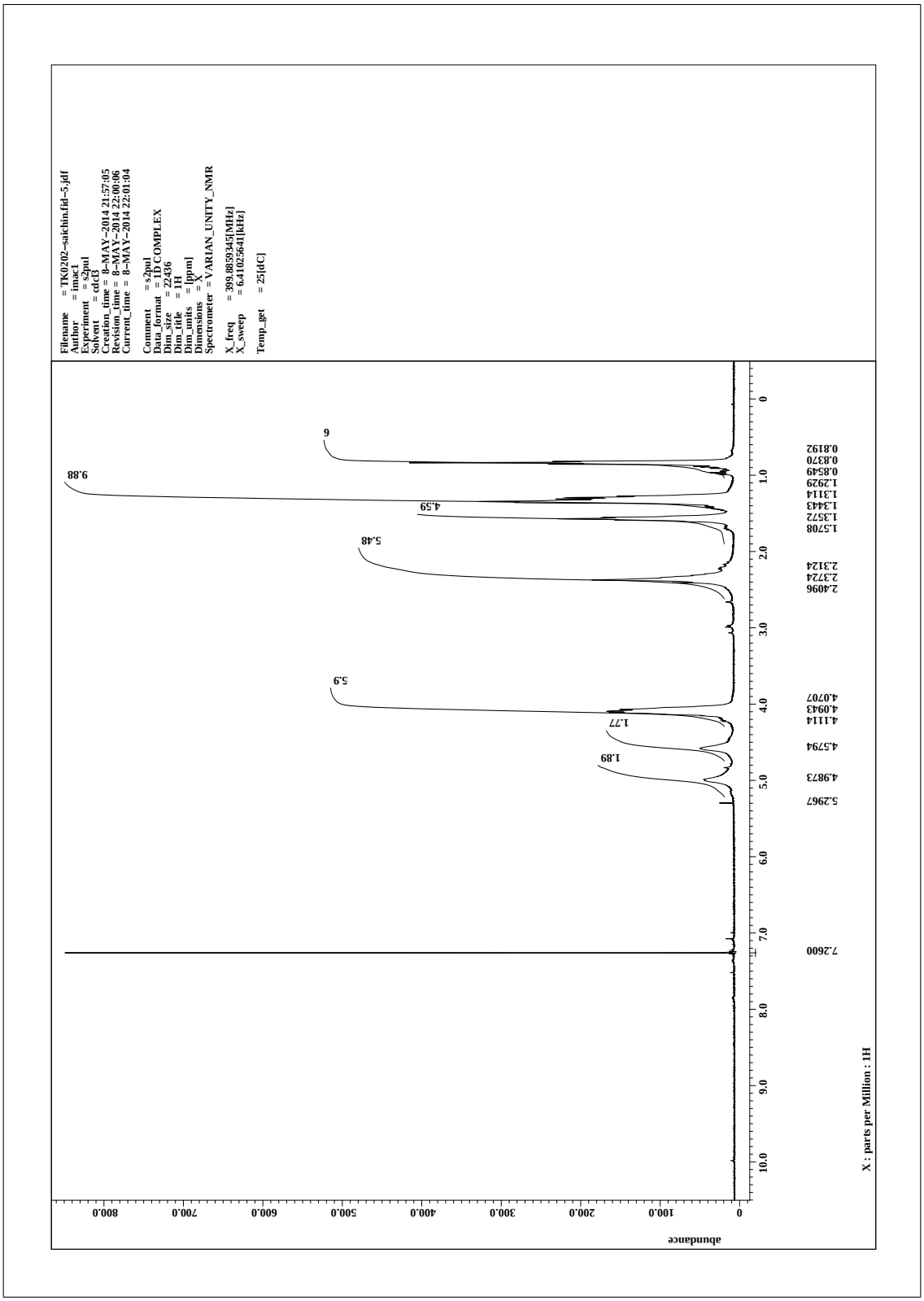

Figure S46. ^{1}H NMR spectrum of **4(40)** in $CDCl_3$.

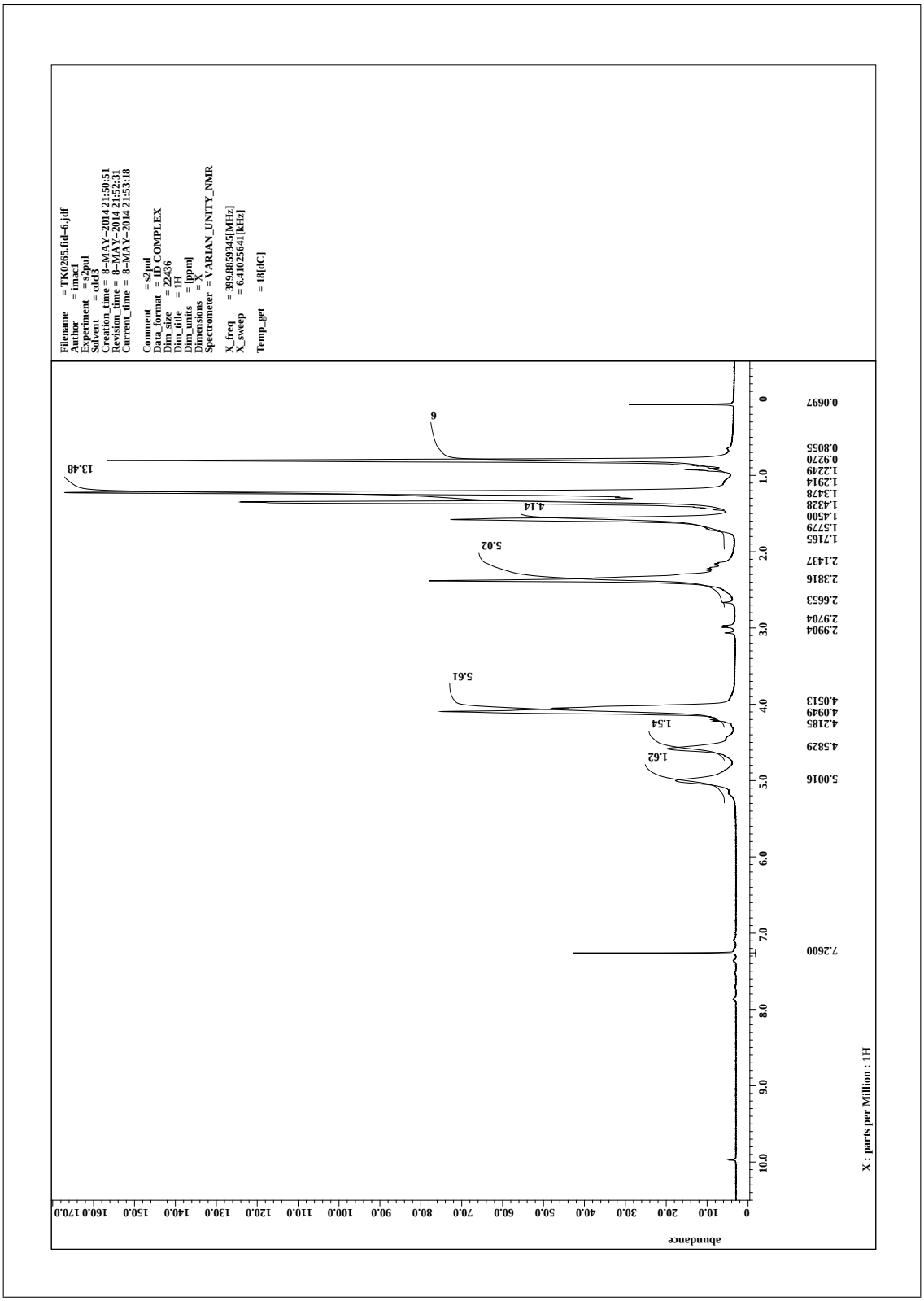

Figure S47. ^{1}H NMR spectrum of **5(40)** in $CDCl_3$.

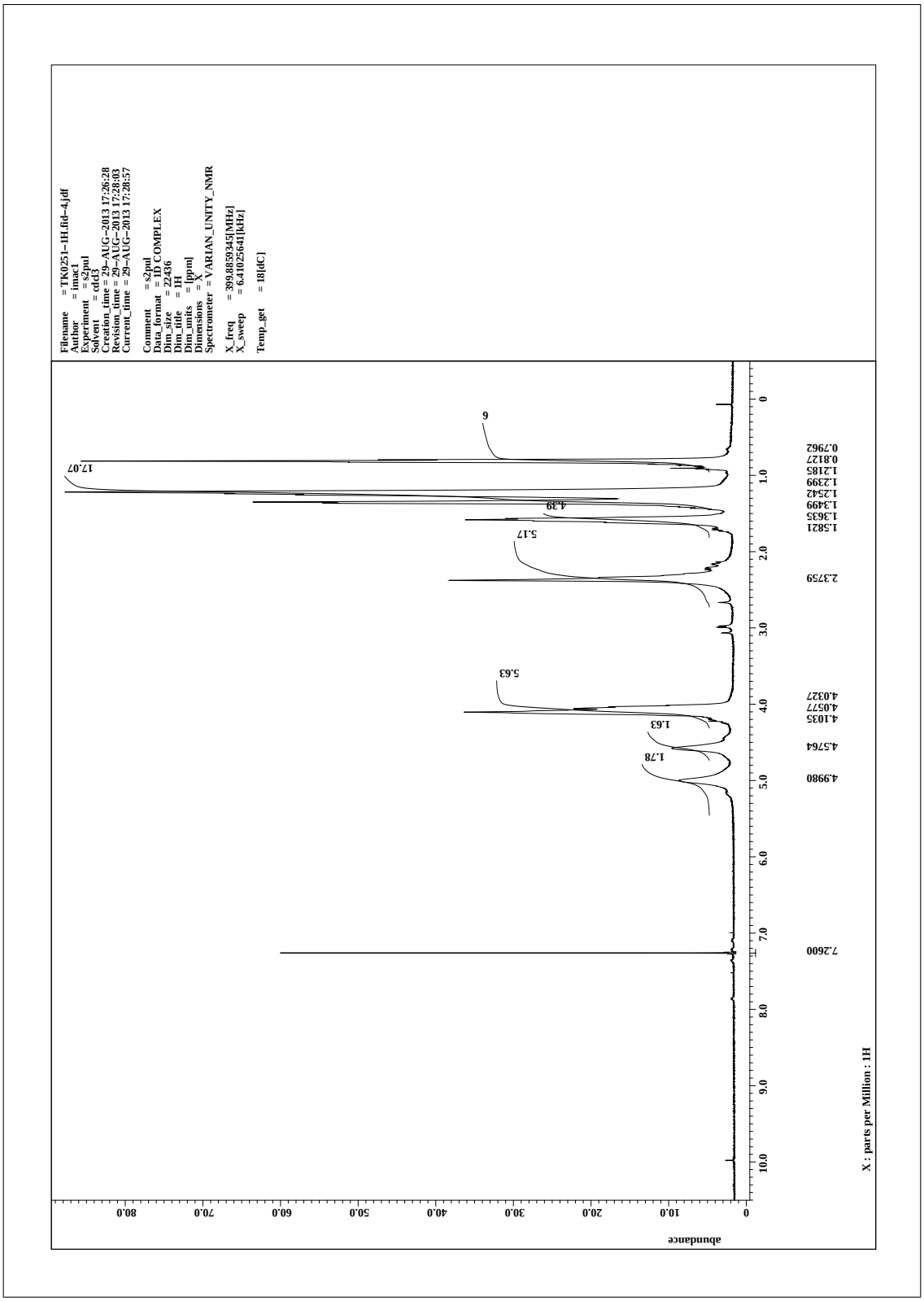

Figure S48. ^{1}H NMR spectrum of **6(40)** in $CDCl_3$.

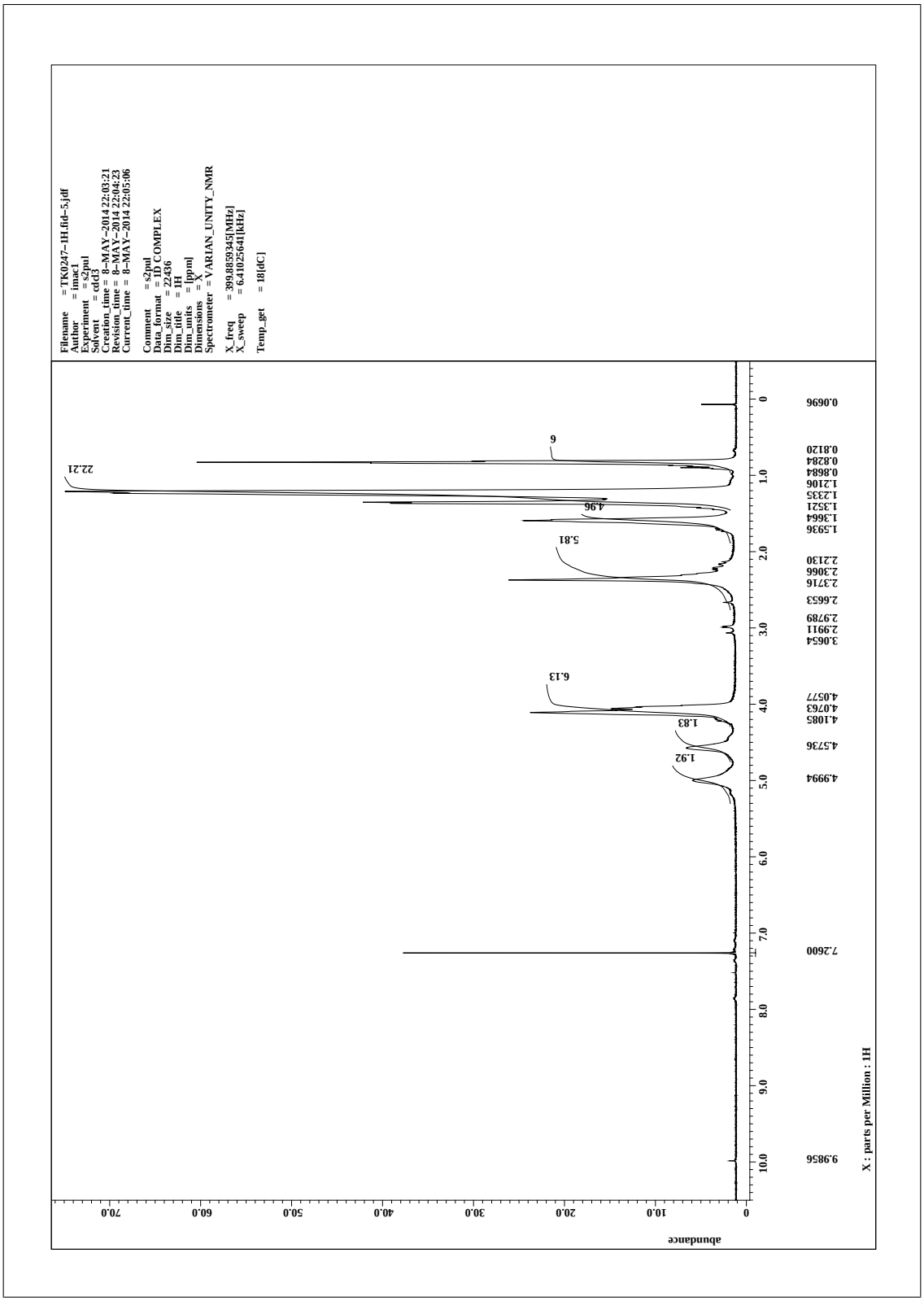

Figure S49. ^{1}H NMR spectrum of **7(40)** in $CDCl_3$.

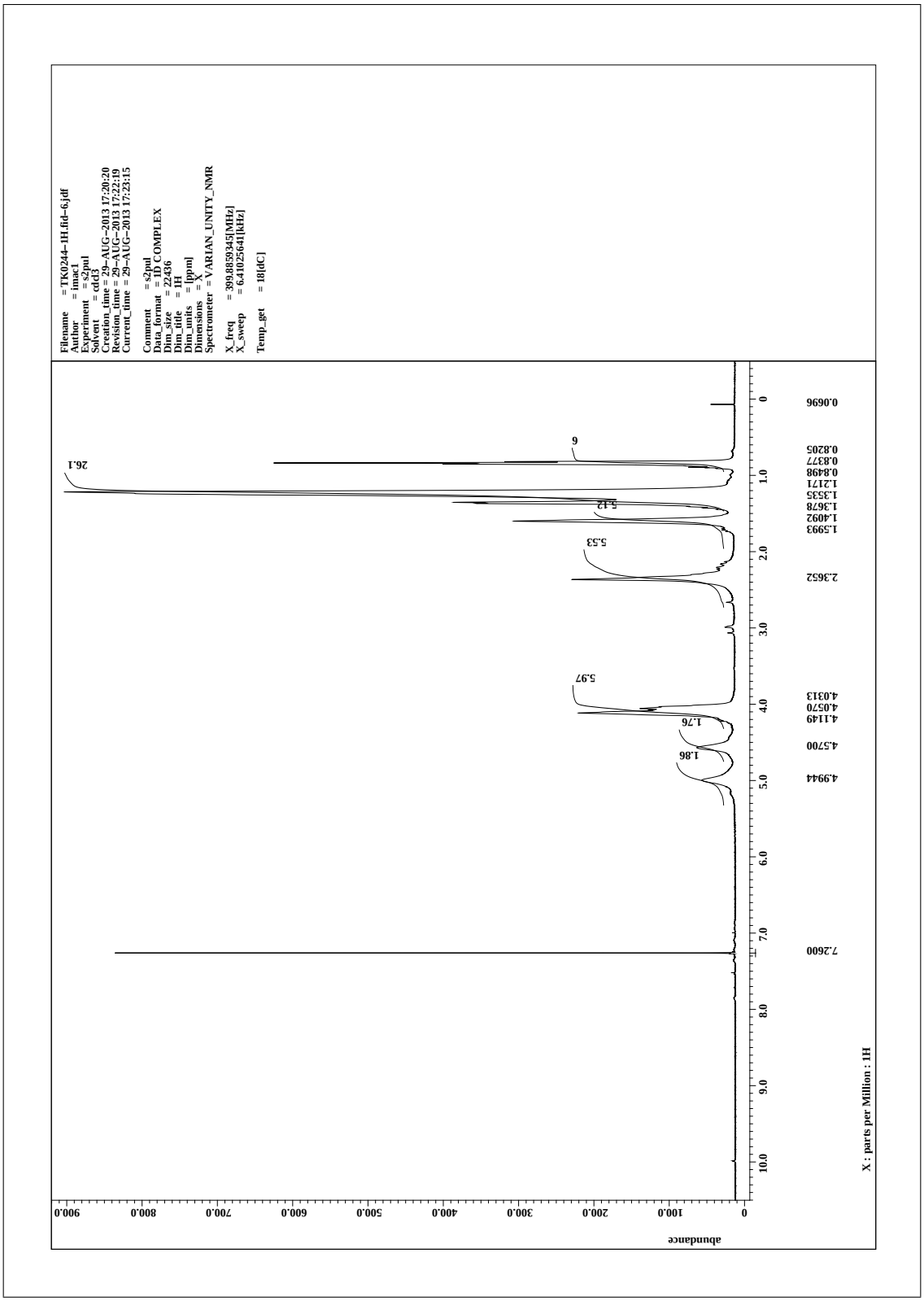

Figure S50. ^{1}H NMR spectrum of **8(40)** in $CDCl_3$.

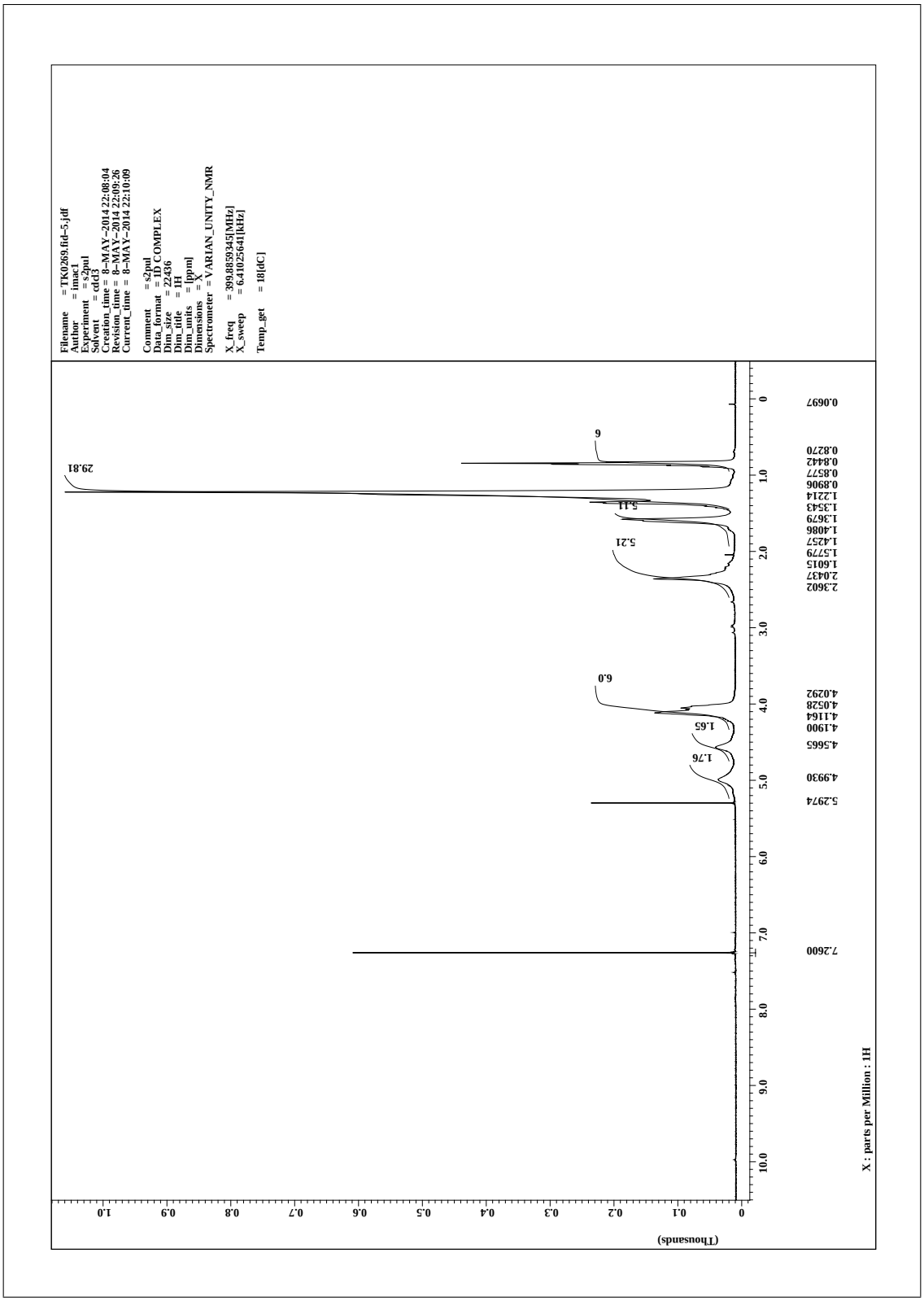

Figure S51. ^{1}H NMR spectrum of **9(40)** in $CDCl_3$.

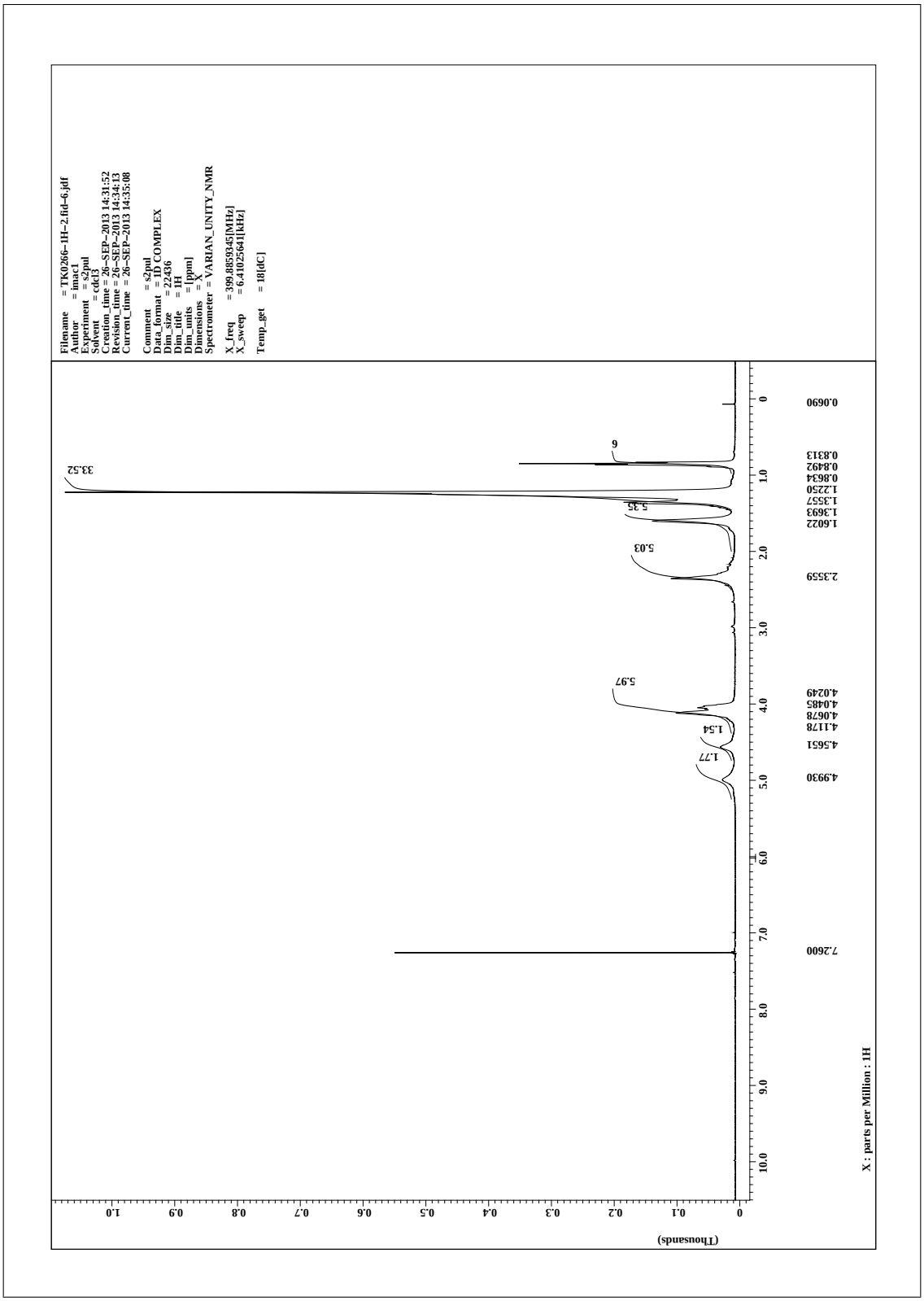

Figure S52. ^{1}H NMR spectrum of **10(40)** in $CDCl_3$.

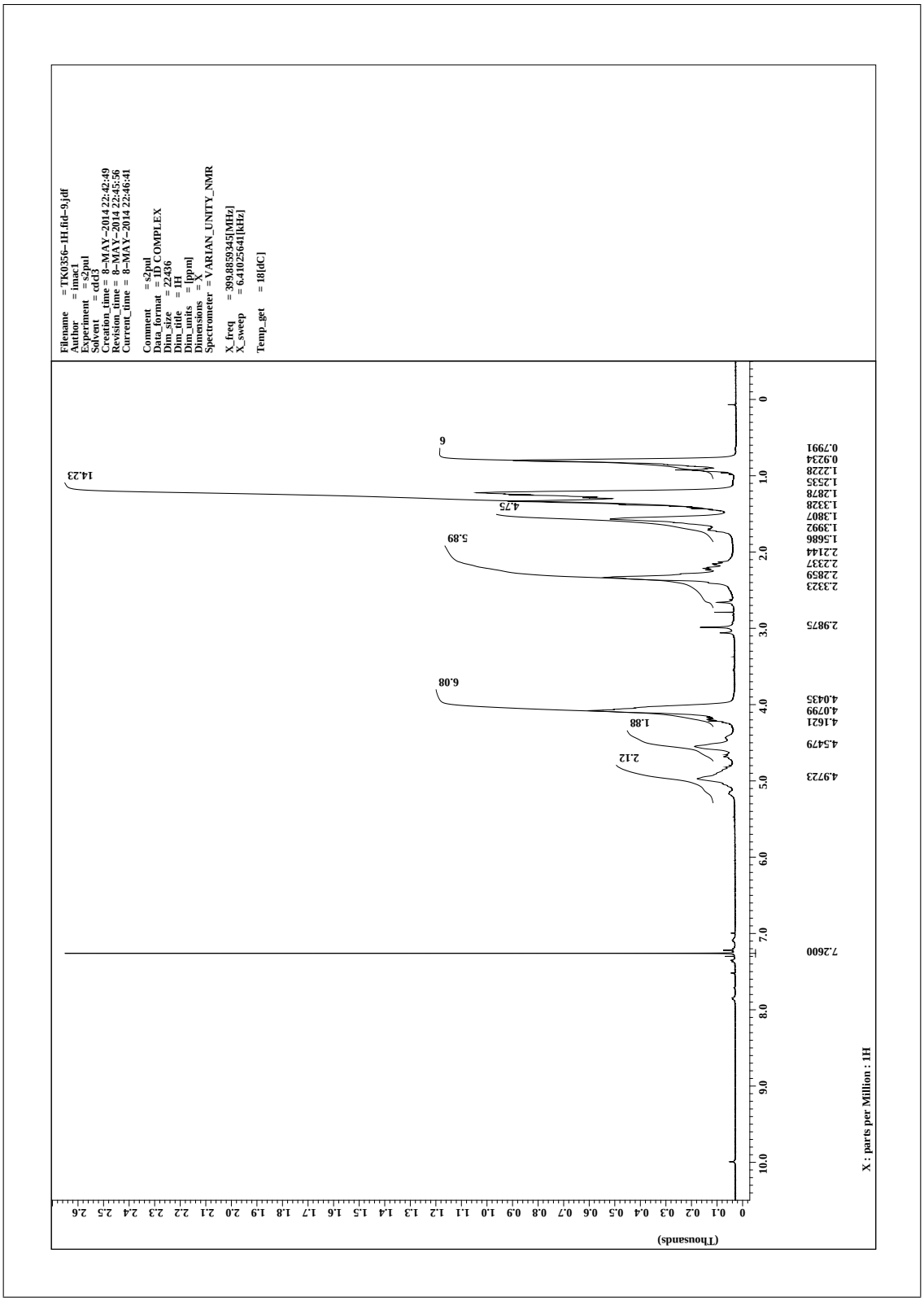

Figure S53. ^{1}H NMR spectrum of **5(20)** in $CDCl_3$.

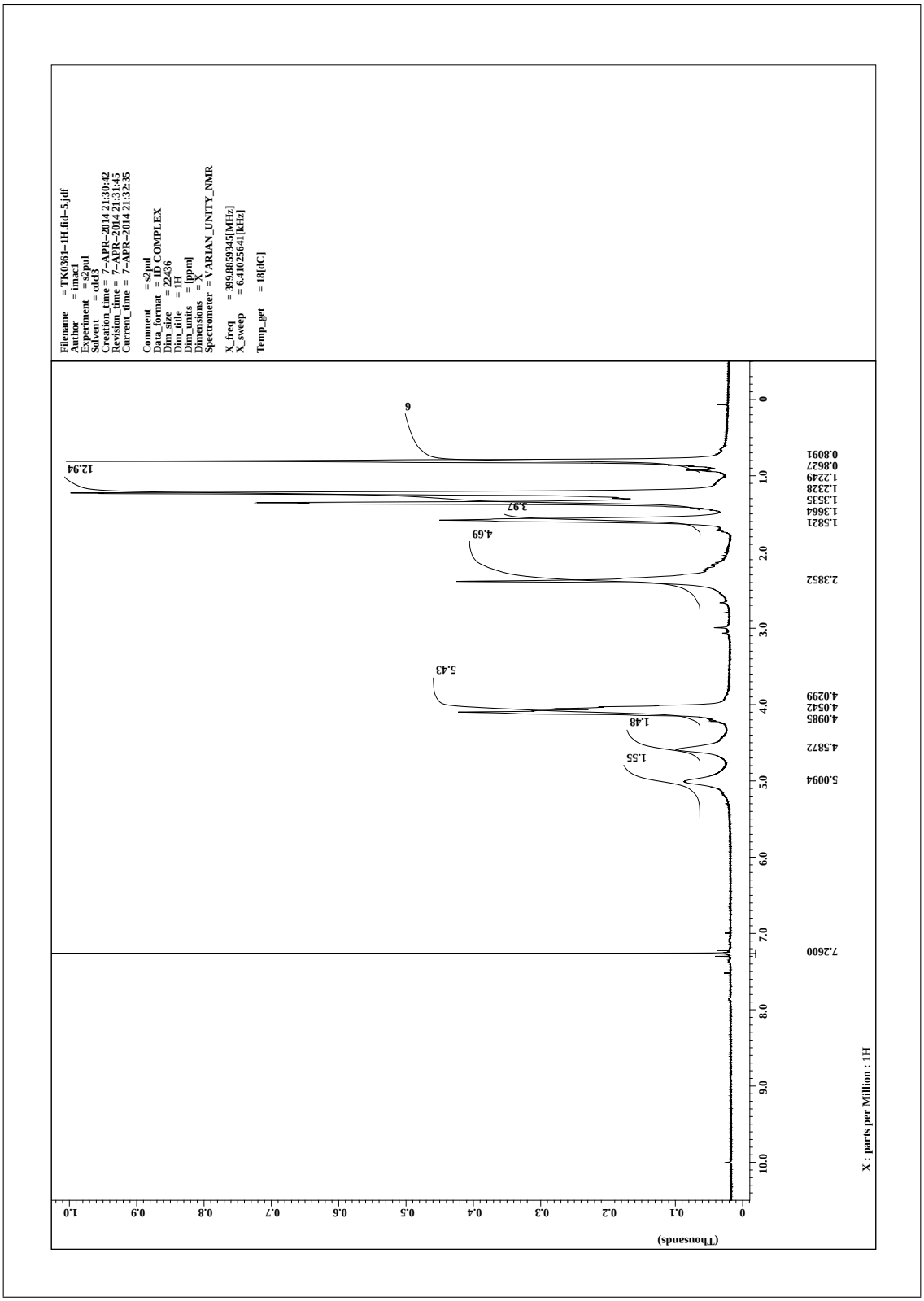

Figure S54. ^{1}H NMR spectrum of **5(60)** in $CDCl_3$.

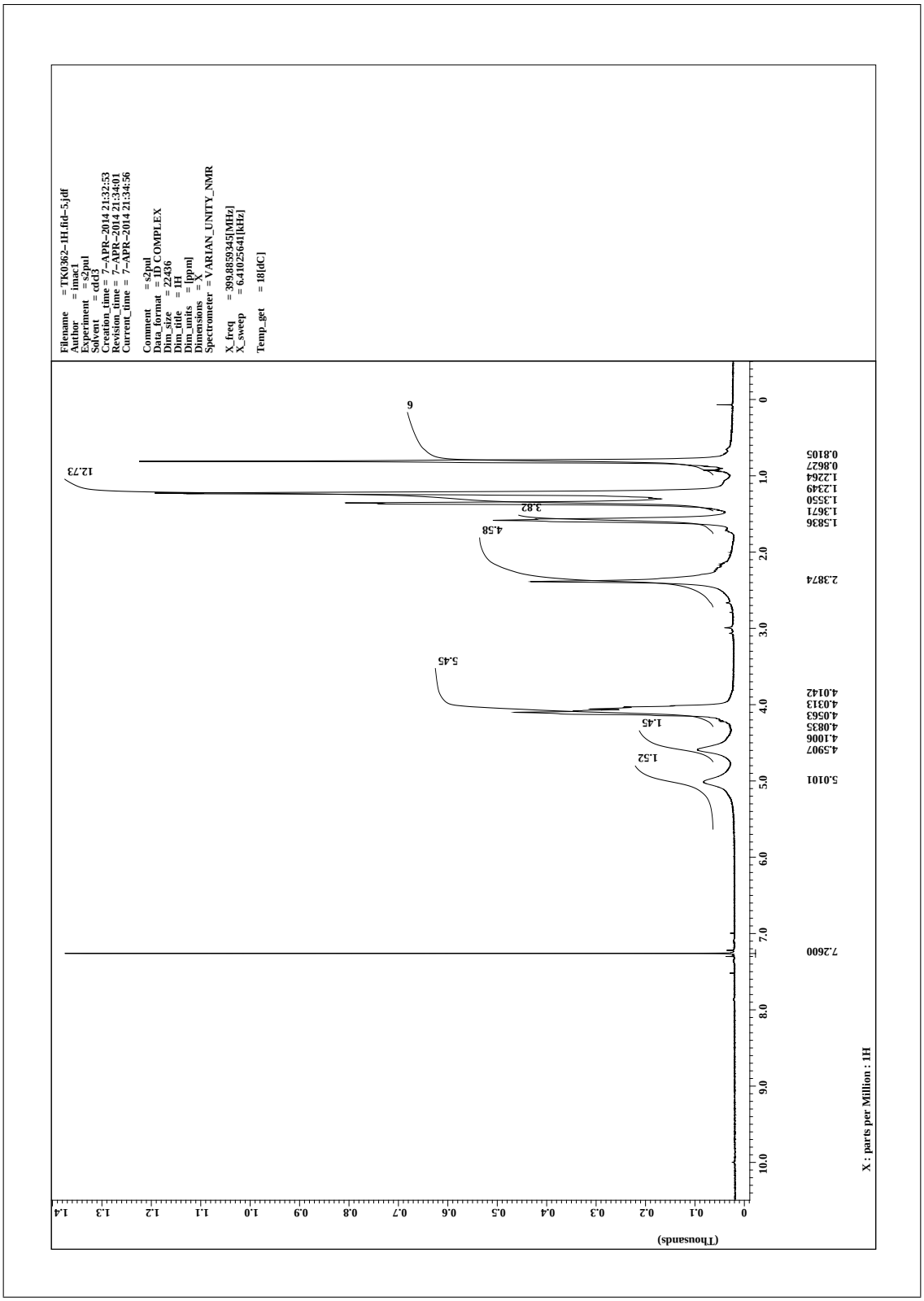

Figure S55. ^{1}H NMR spectrum of **5(80)** in $CDCl_3$.

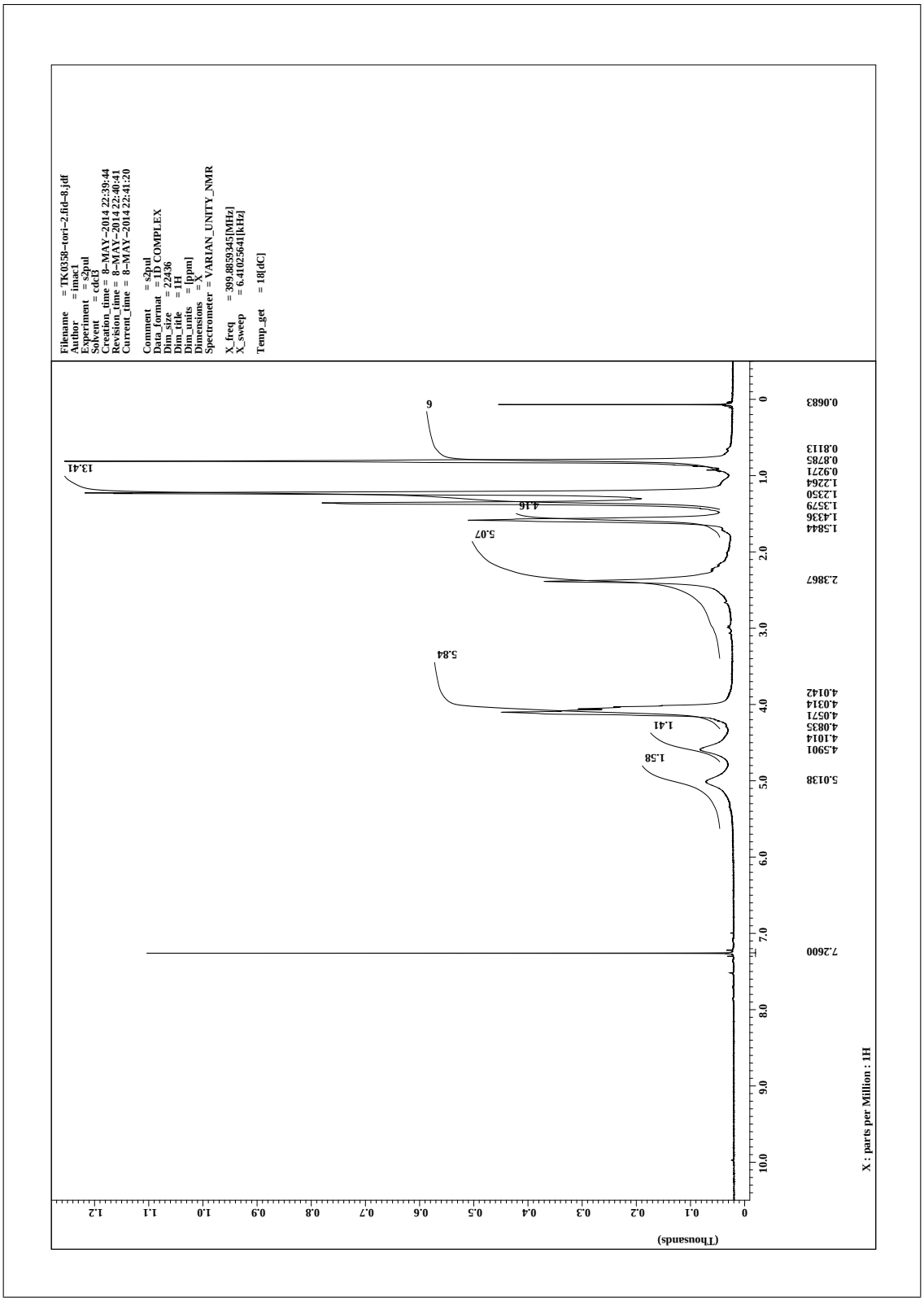

Figure S56. ^{1}H NMR spectrum of **5(100)** in $CDCl_3$.

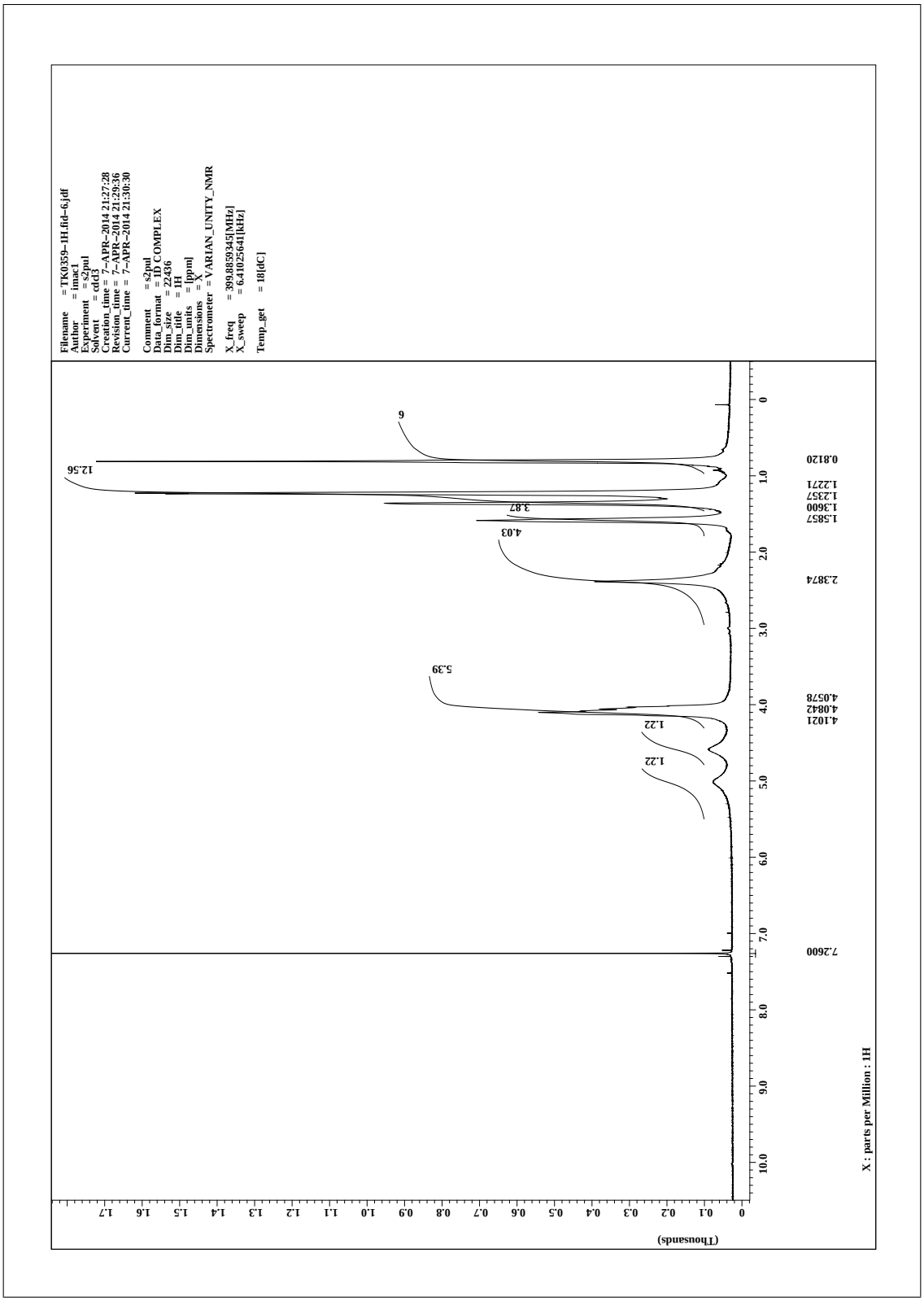

Figure S57. ^{1}H NMR spectrum of **5(150)** in $CDCl_3$.

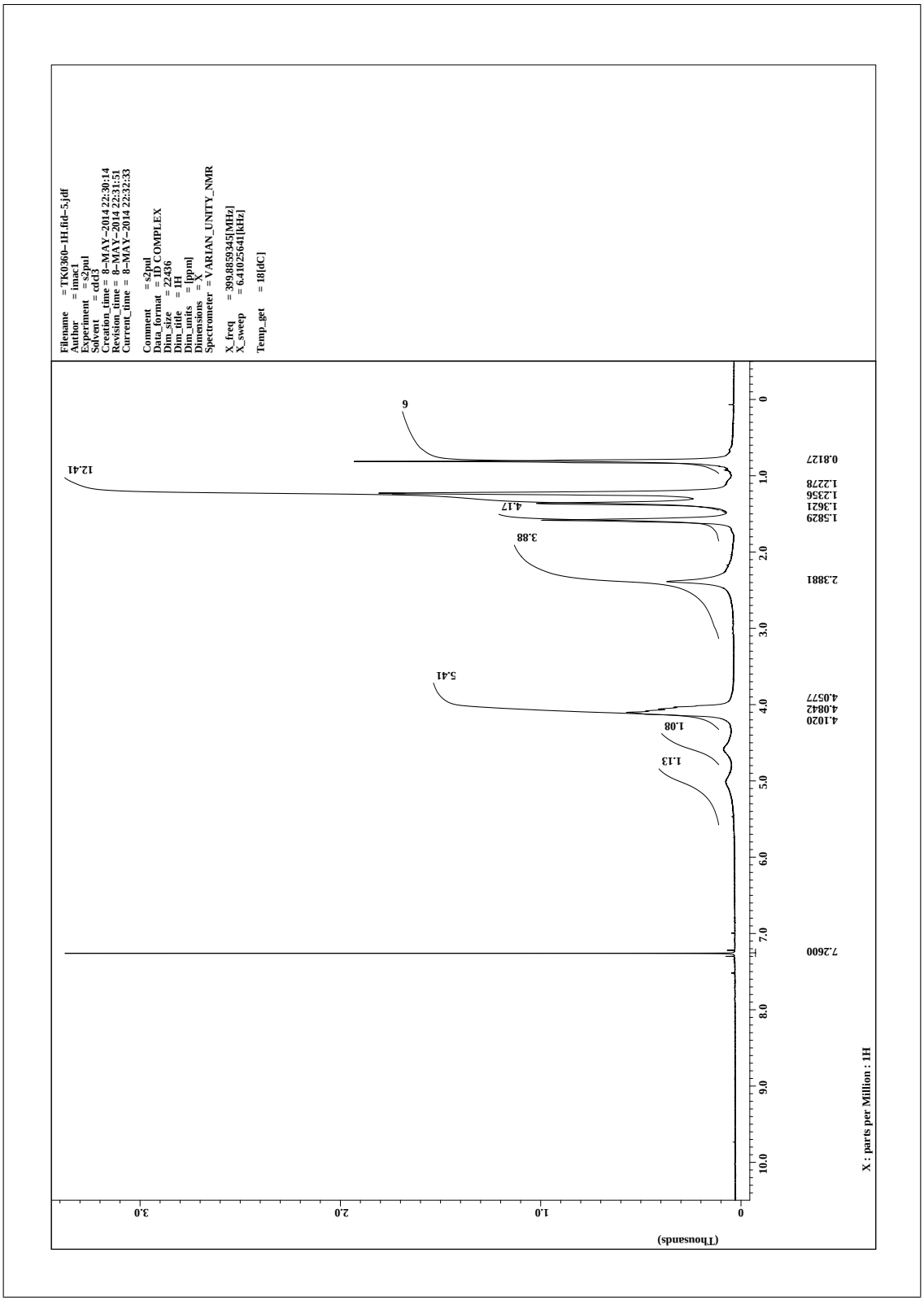

Figure S58. ^{1}H NMR spectrum of **5(200)** in $CDCl_3$.

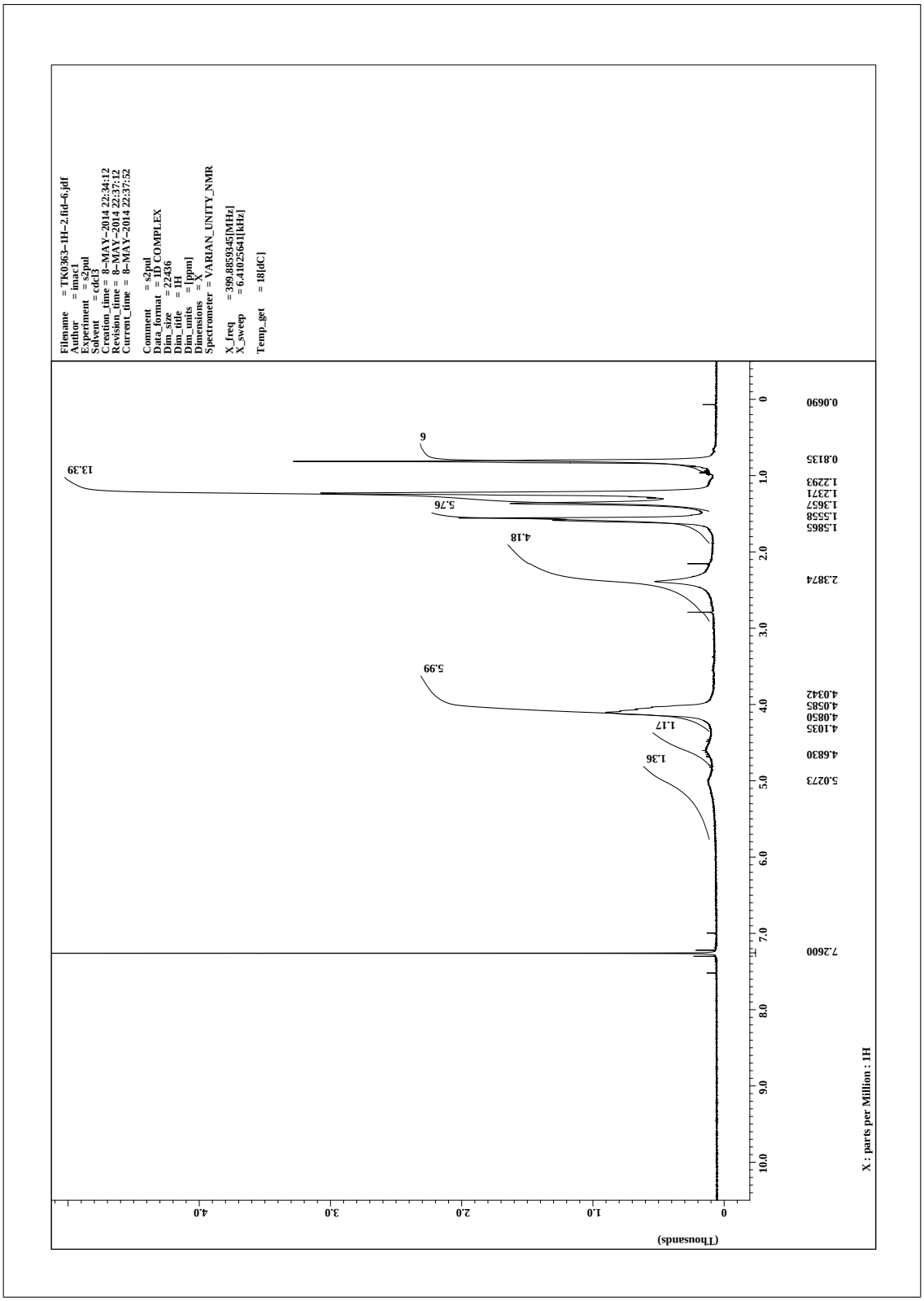

Figure S59. ^{1}H NMR spectrum of **5(300)** in $CDCl_3$.

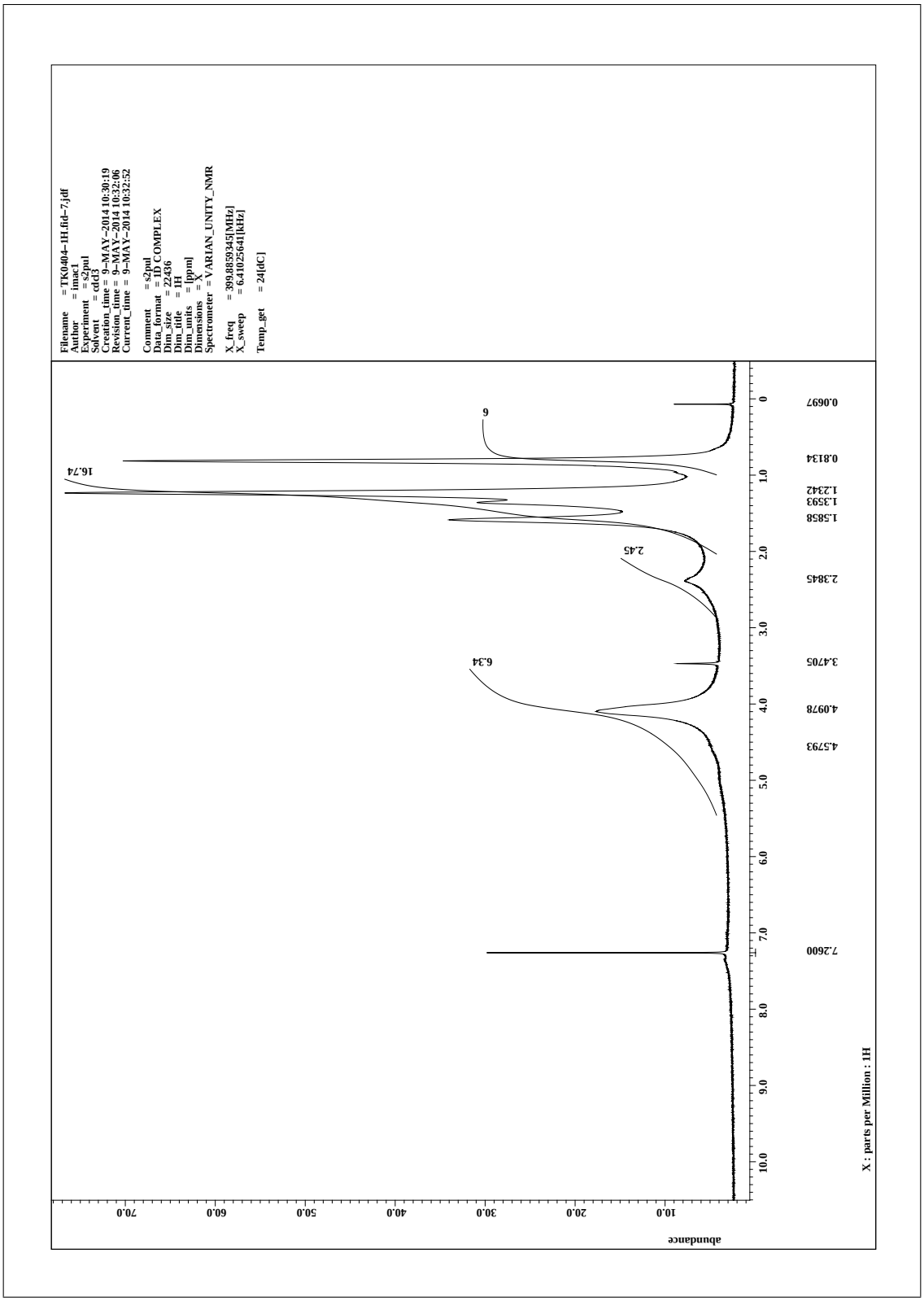

Figure S60. ^{1}H NMR spectrum of **5(1000-50)** in $CDCl_3$.

2 UV-vis and CD Spectra of New Compounds

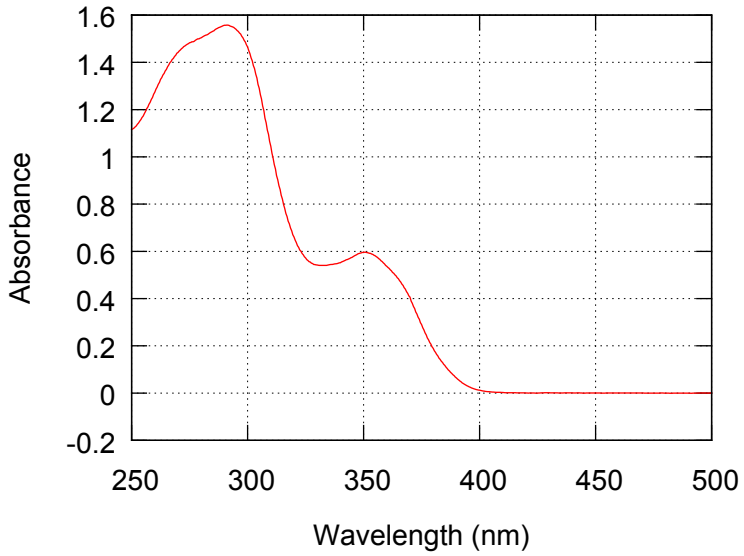

Figure S61. UV-vis absorption spectrum of **(*S*)-BQ** in $CHCl_3$ (2.54×10^{-2} g/L, path length = 10 mm).

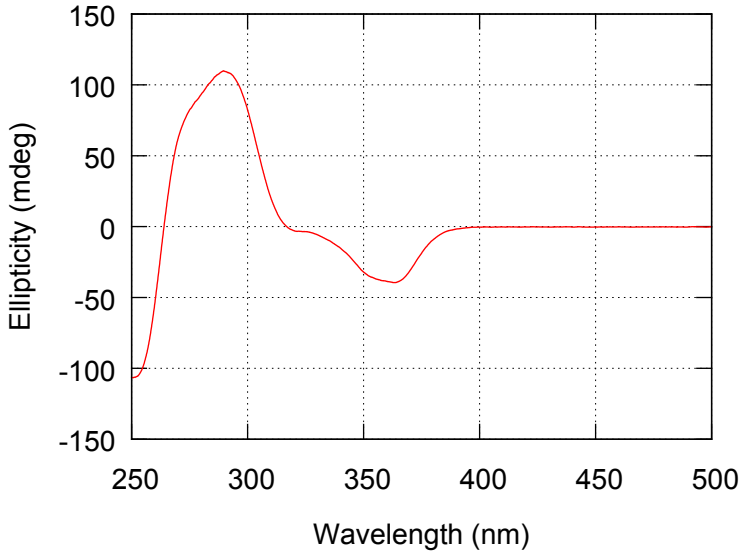

Figure S62. CD spectrum of **(*S*)-BQ** in $CHCl_3$ (2.54×10^{-2} g/L, path length = 10 mm).

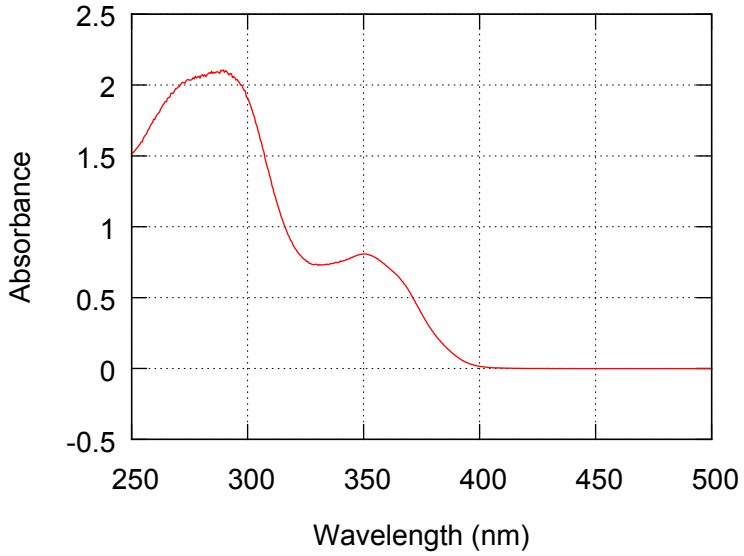

Figure S63. UV-vis absorption spectrum of **(*S*)-BQ** in CH_2Cl_2 (3.01×10^{-2} g/L, path length = 10 mm).

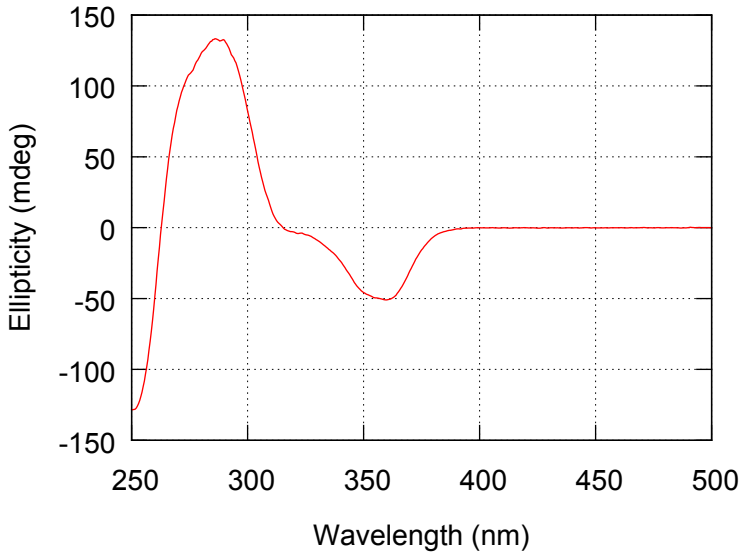

Figure S64. CD spectrum of **(*S*)-BQ** in CH_2Cl_2 (3.01×10^{-2} g/L, path length = 10 mm).

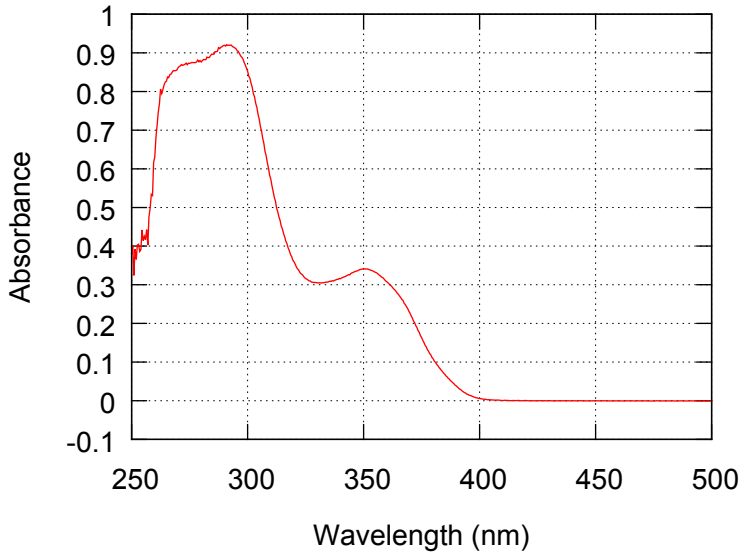

Figure S65. UV-vis absorption spectrum of **(*S*)-BQ** in 1,1,2-TCE (1.86×10^{-2} g/L, path length = 10 mm).

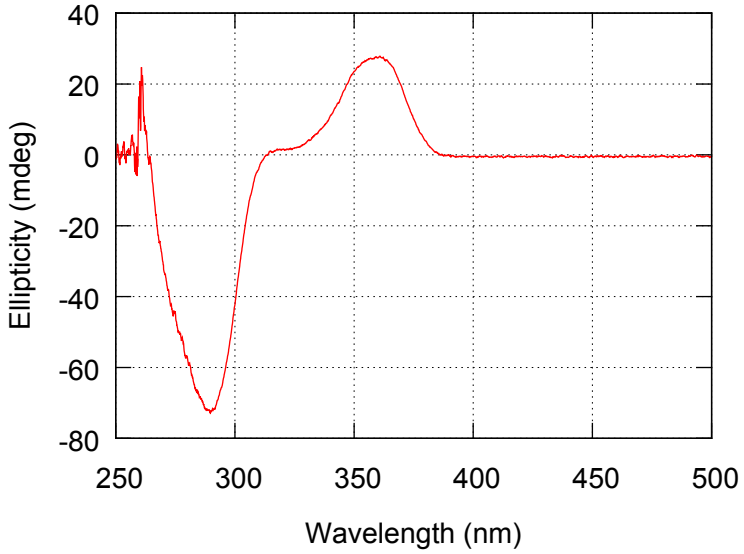

Figure S66. CD spectrum of **(*S*)-BQ** in 1,1,2-TCE (1.86×10^{-2} g/L, path length = 10 mm).

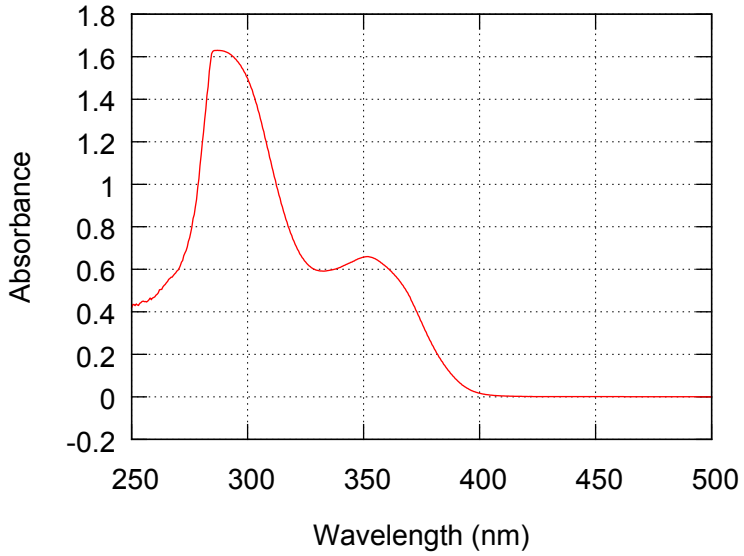

Figure S67. UV-vis absorption spectrum of **(*S*)-BQ** in Toluene (3.01×10^{-2} g/L, path length = 10 mm).

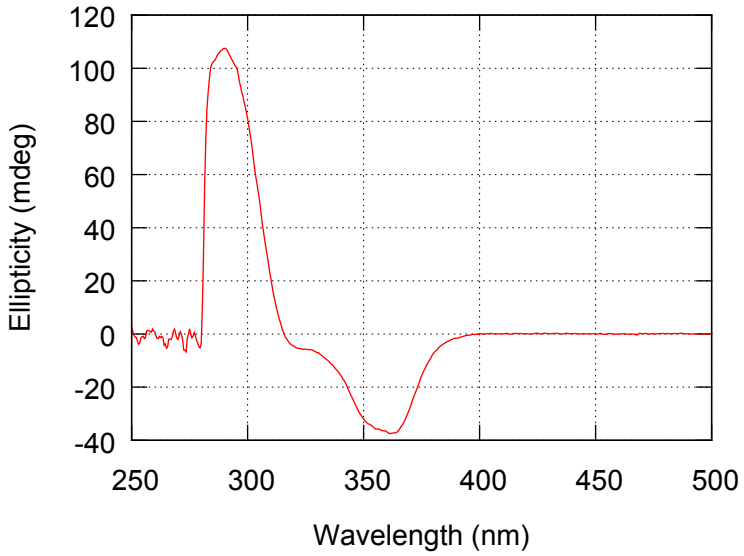

Figure S68. CD spectrum of **(*S*)-BQ** in Toluene (3.01×10^{-2} g/L, path length = 10 mm).

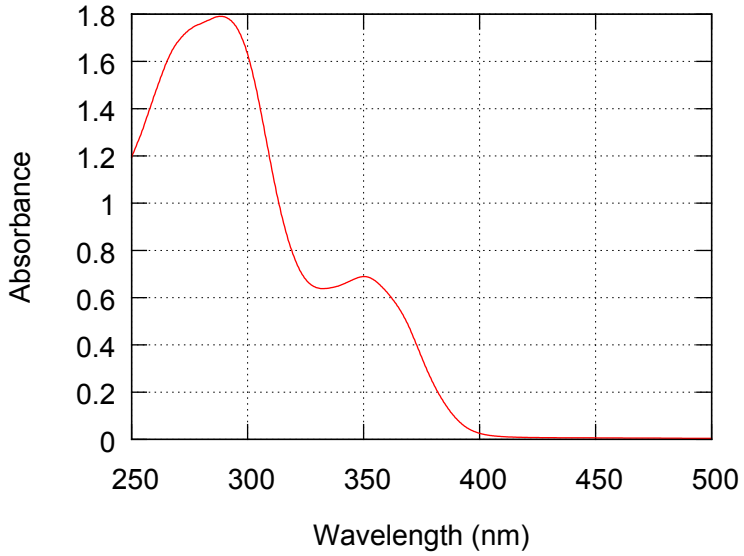

Figure S69. UV-vis absorption spectrum of **(*S*)-BQ** in THF (3.01×10^{-2} g/L, path length = 10 mm).

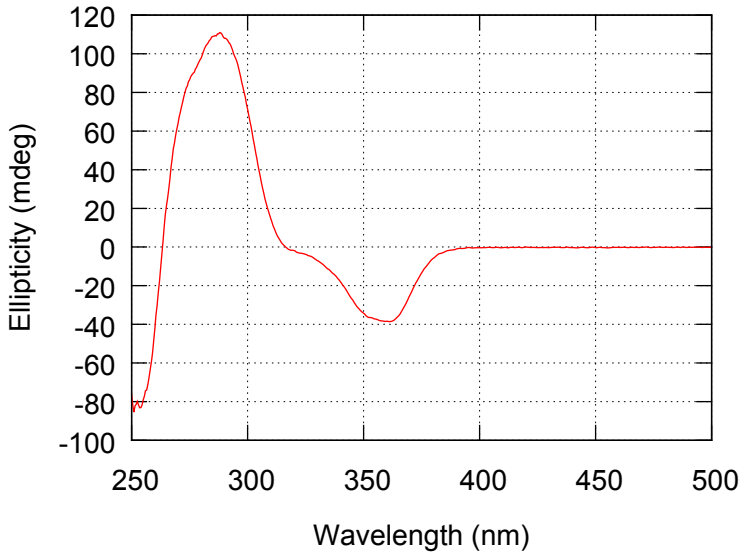

Figure S70. CD spectrum of **(*S*)-BQ** in THF (3.01×10^{-2} g/L, path length = 10 mm).

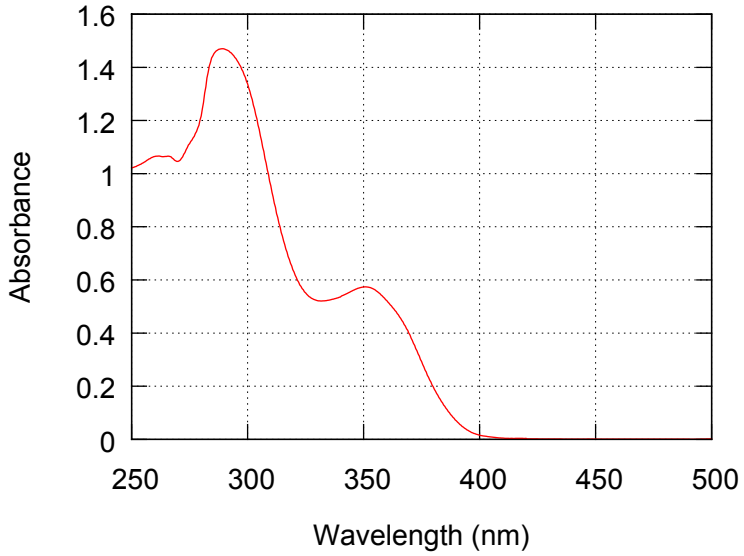

Figure S71. UV-vis absorption spectrum of **(*S*)-BQ** in 1,4-Dioxane (3.01×10^{-2} g/L, path length = 10 mm).

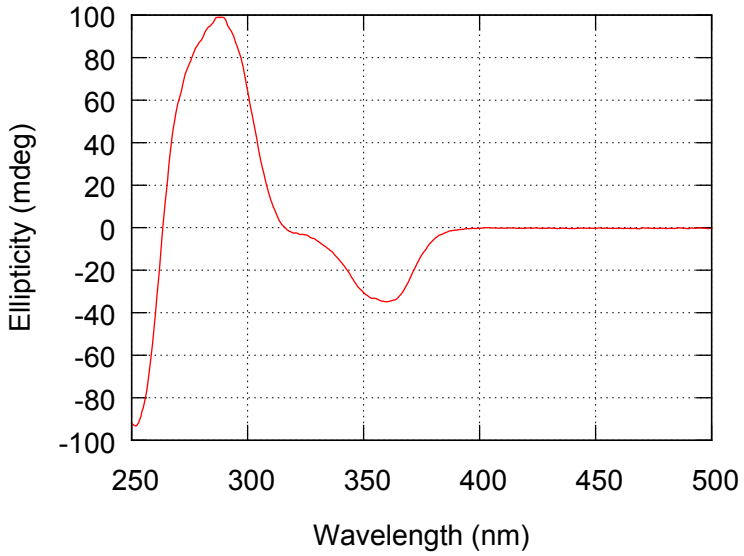

Figure S72. CD spectrum of **(*S*)-BQ** in 1,4-Dioxane (3.01×10^{-2} g/L, path length = 10 mm).

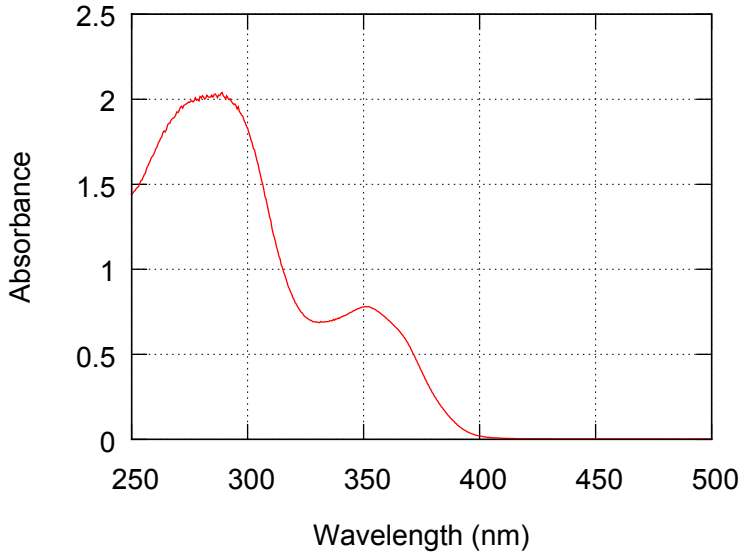

Figure S73. UV-vis absorption spectrum of **(*S*)-BQ** in 1,2-DME (3.01×10^{-2} g/L, path length = 10 mm).

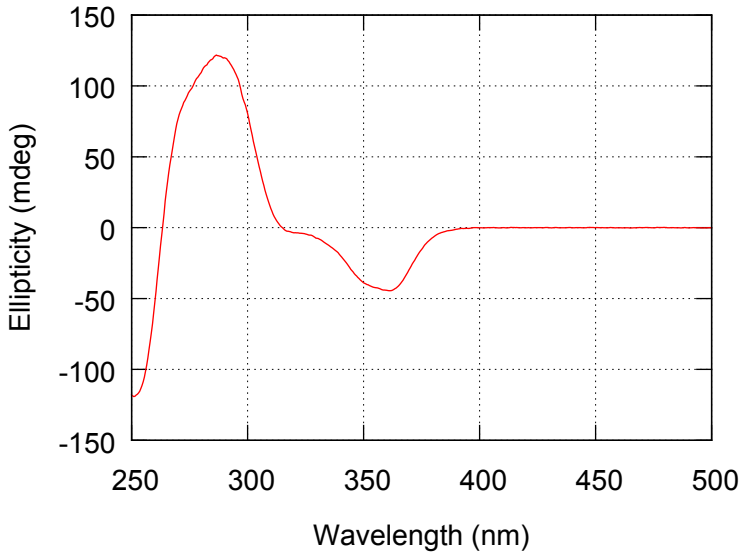

Figure S74. CD spectrum of **(*S*)-BQ** in 1,2-DME (3.01×10^{-2} g/L, path length = 10 mm).

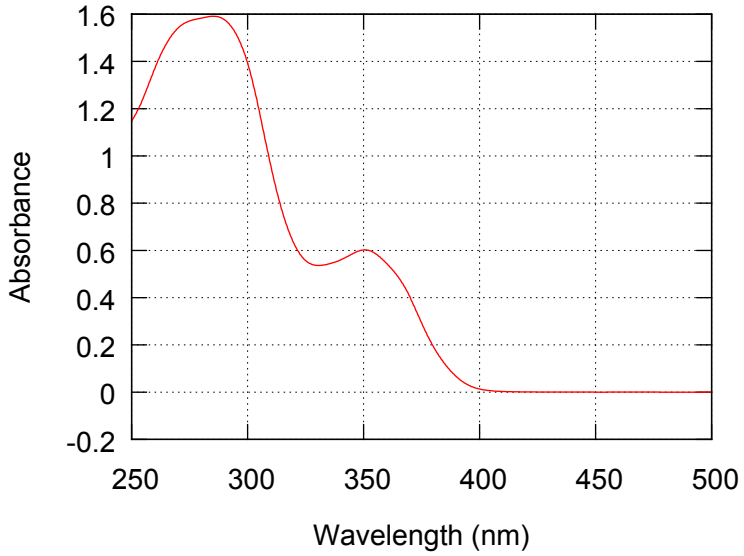

Figure S75. UV-vis absorption spectrum of **(*S*)-BQ** in Et_2O (3.01×10^{-2} g/L, path length = 10 mm).

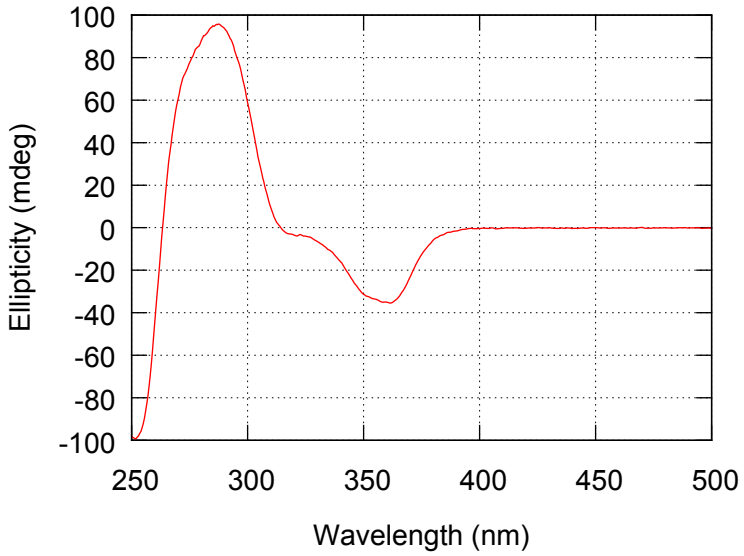

Figure S76. CD spectrum of **(*S*)-BQ** in Et_2O (3.01×10^{-2} g/L, path length = 10 mm).

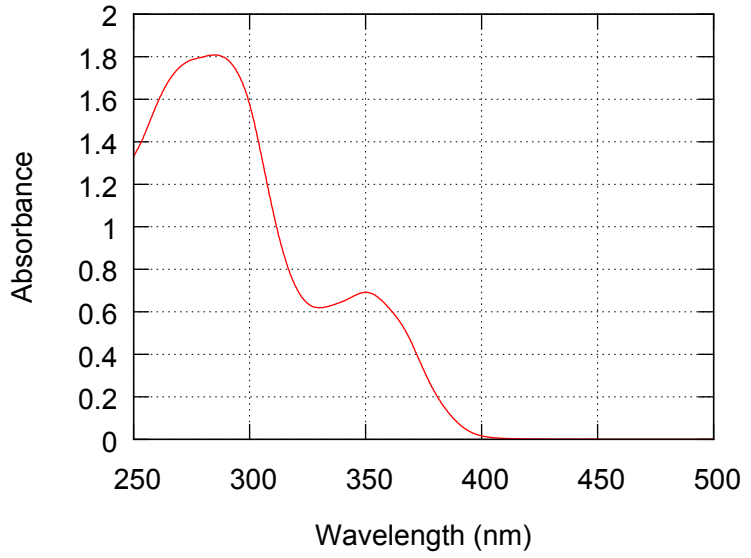

Figure S77. UV-vis absorption spectrum of **(*S*)-BQ** in MTBE (3.01×10^{-2} g/L, path length = 10 mm).

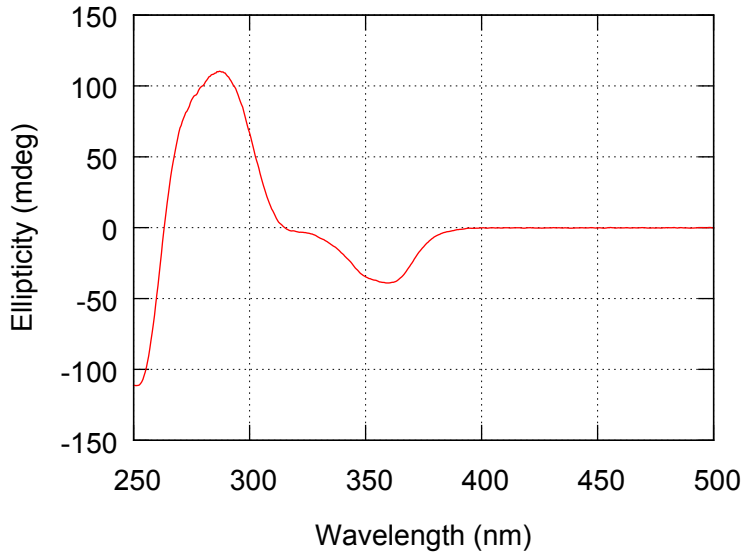

Figure S78. CD spectrum of **(*S*)-BQ** in MTBE (3.01×10^{-2} g/L, path length = 10 mm).

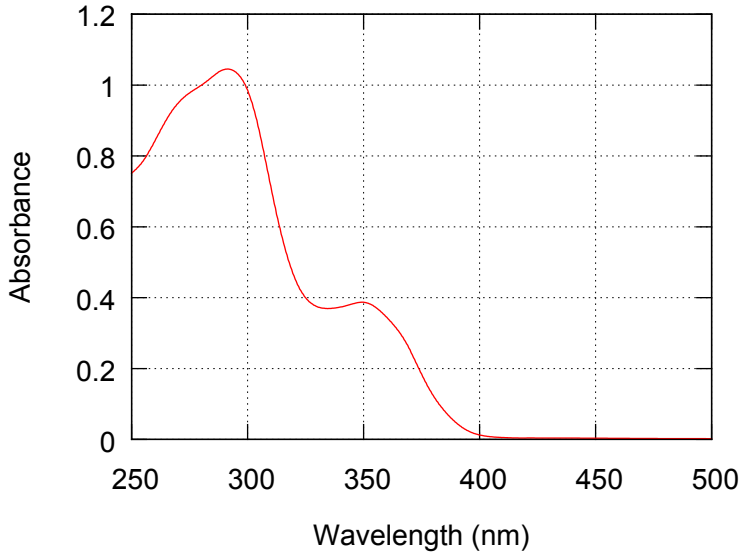

Figure S79. UV-vis absorption spectrum of **1(40)** in $CHCl_3$ (2.37×10^{-2} g/L, path length = 10 mm).

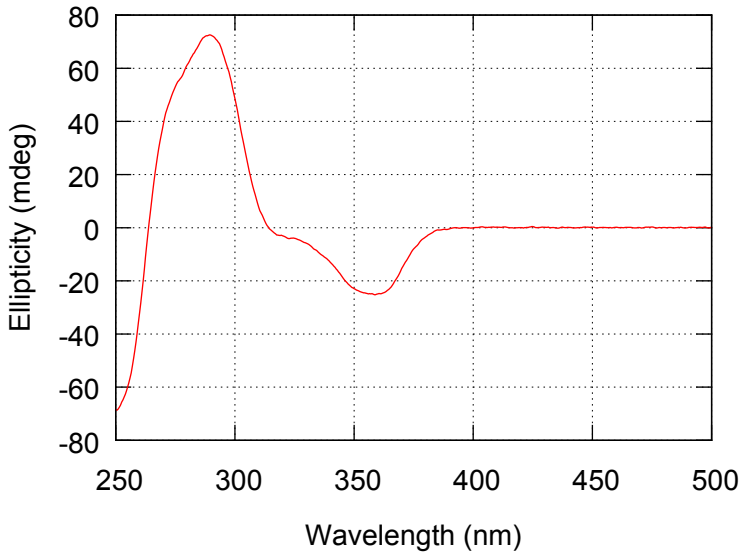

Figure S80. CD spectrum of **1(40)** in $CHCl_3$ (2.37×10^{-2} g/L, path length = 10 mm).

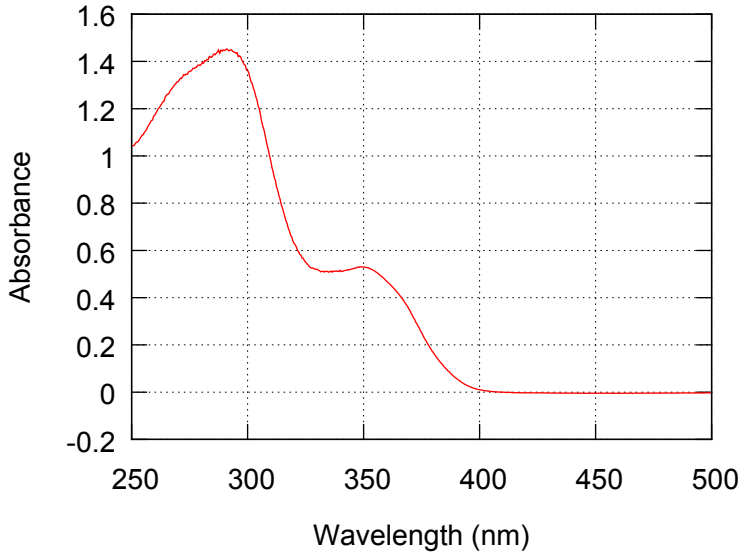

Figure S81. UV-vis absorption spectrum of **1(40)** in CH_2Cl_2 (2.75×10^{-2} g/L, path length = 10 mm).

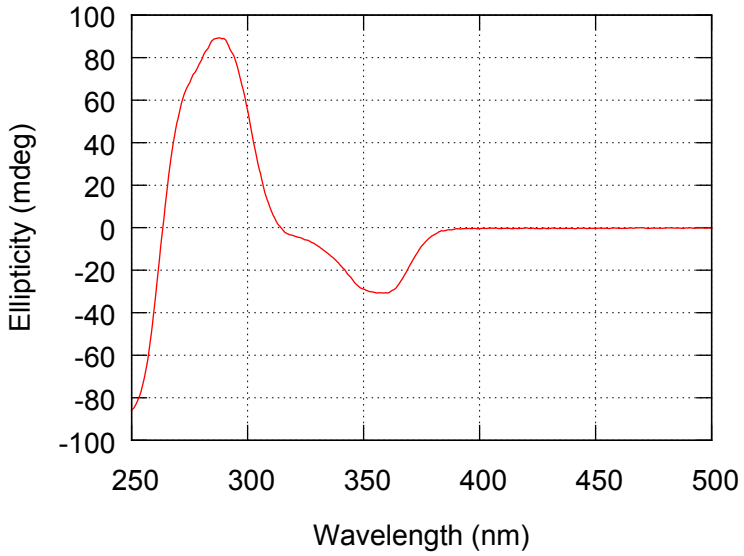

Figure S82. CD spectrum of **1(40)** in CH_2Cl_2 (2.75×10^{-2} g/L, path length = 10 mm).

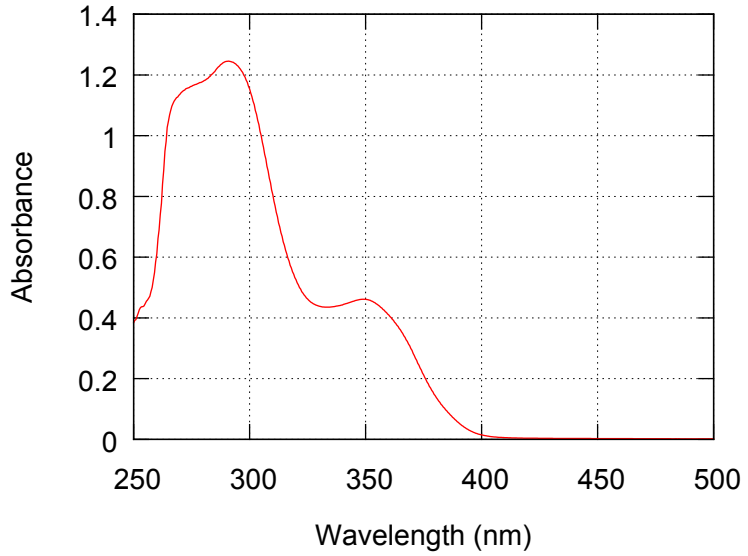

Figure S83. UV-vis absorption spectrum of **1(40)** in 1,1,2-TCE (3.2×10^{-2} g/L, path length = 10 mm).

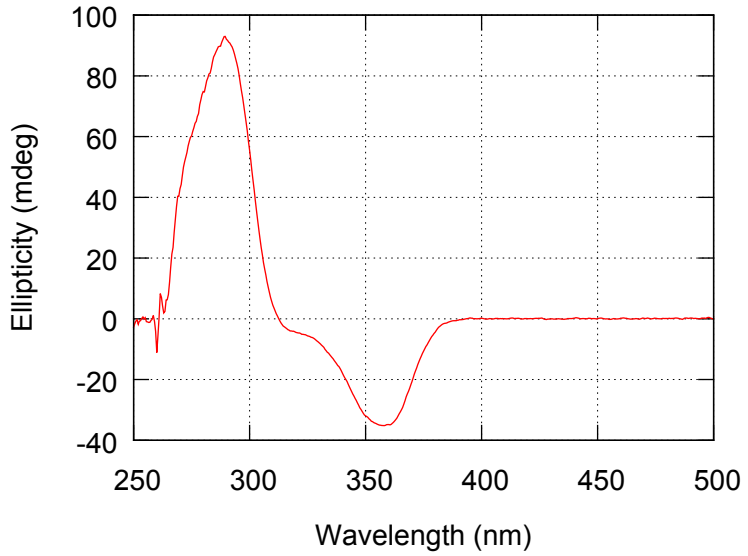

Figure S84. CD spectrum of **1(40)** in 1,1,2-TCE (3.2×10^{-2} g/L, path length = 10 mm).

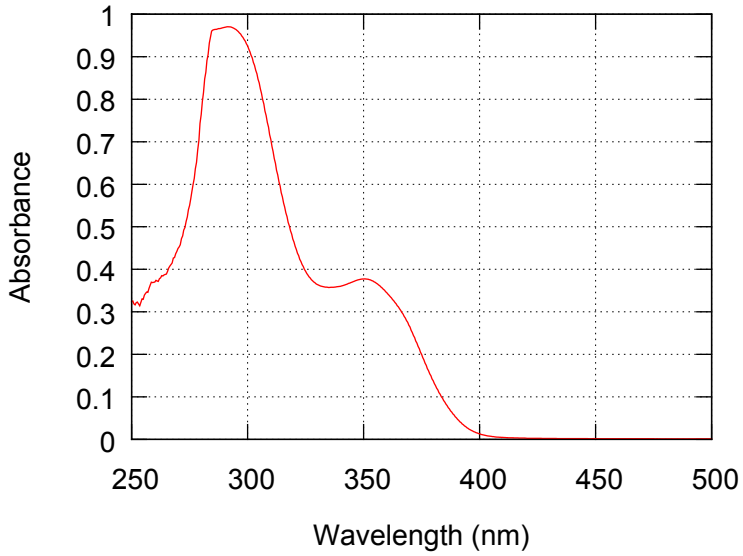

Figure S85. UV-vis absorption spectrum of **1(40)** in Toluene (3.2×10^{-2} g/L, path length = 10 mm).

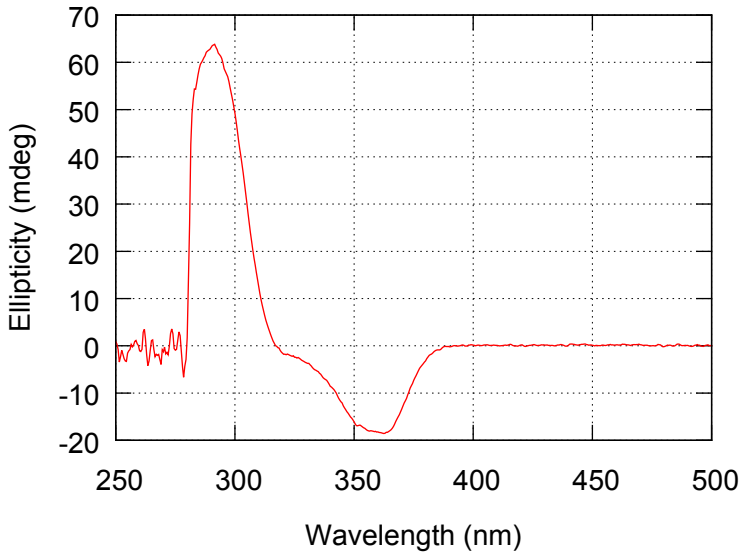

Figure S86. CD spectrum of **1(40)** in Toluene (3.2×10^{-2} g/L, path length = 10 mm).

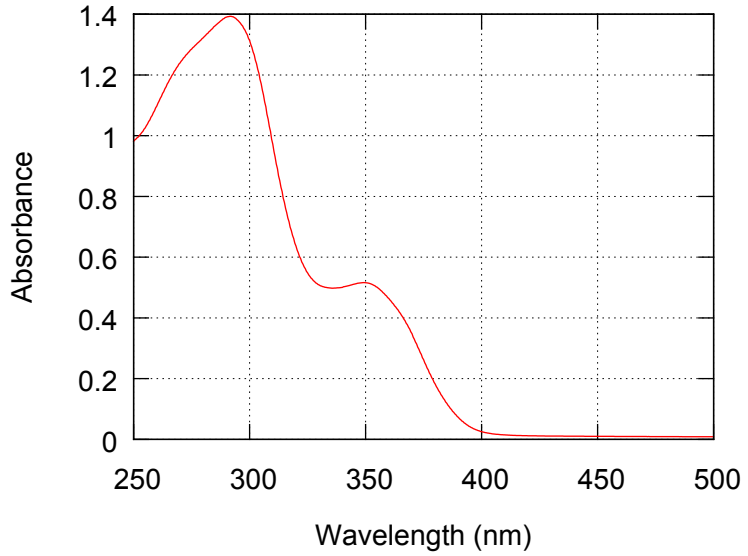

Figure S87. UV-vis absorption spectrum of **1(40)** in THF (2.37×10^{-2} g/L, path length = 10 mm).

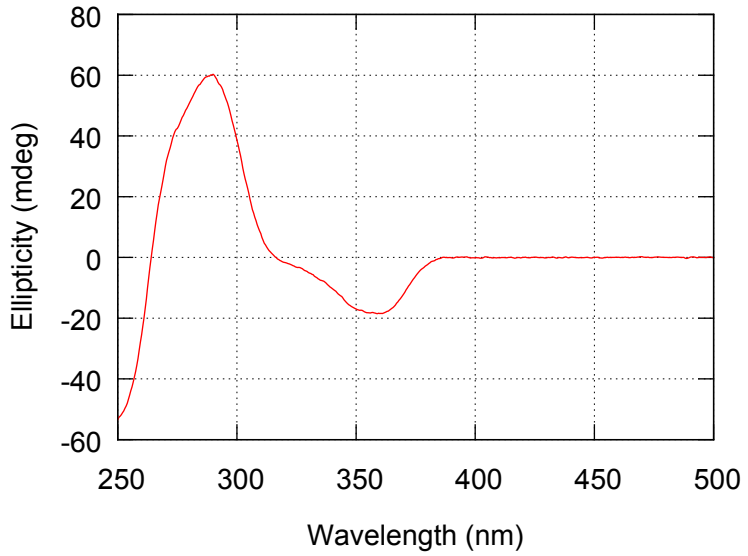

Figure S88. CD spectrum of **1(40)** in THF (2.37×10^{-2} g/L, path length = 10 mm).

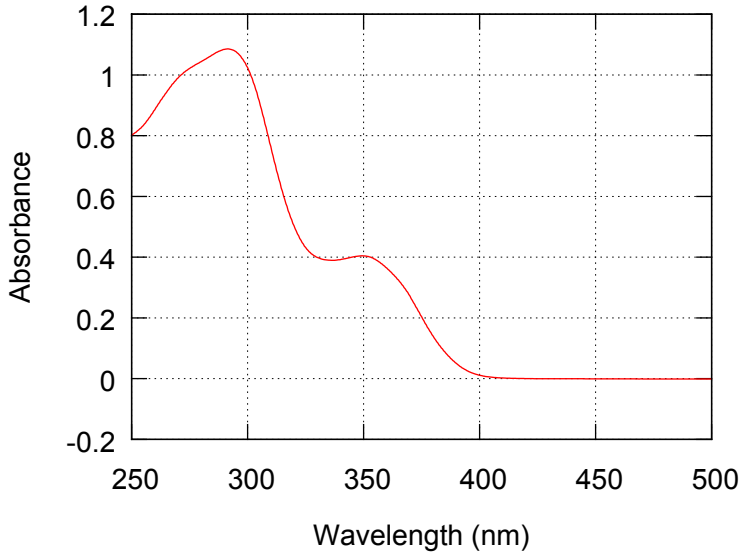

Figure S89. UV-vis absorption spectrum of **1(40)** in 1,4-Dioxane (3.2×10^{-2} g/L, path length = 10 mm).

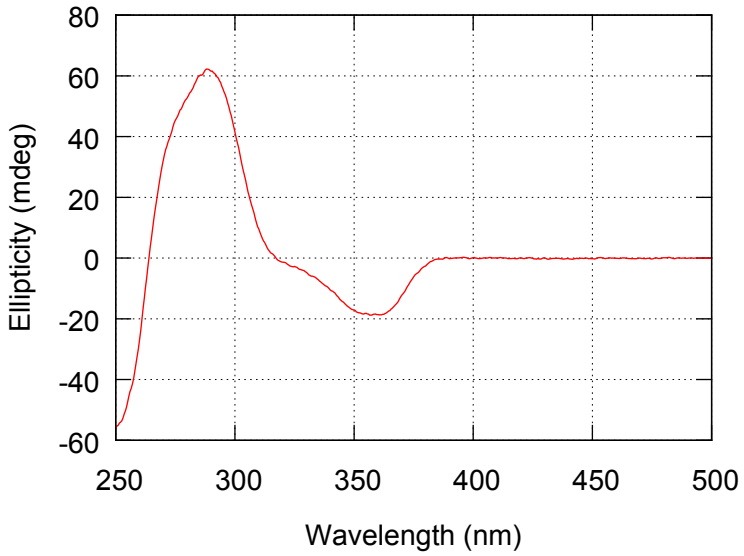

Figure S90. CD spectrum of **1(40)** in 1,4-Dioxane (3.2×10^{-2} g/L, path length = 10 mm).

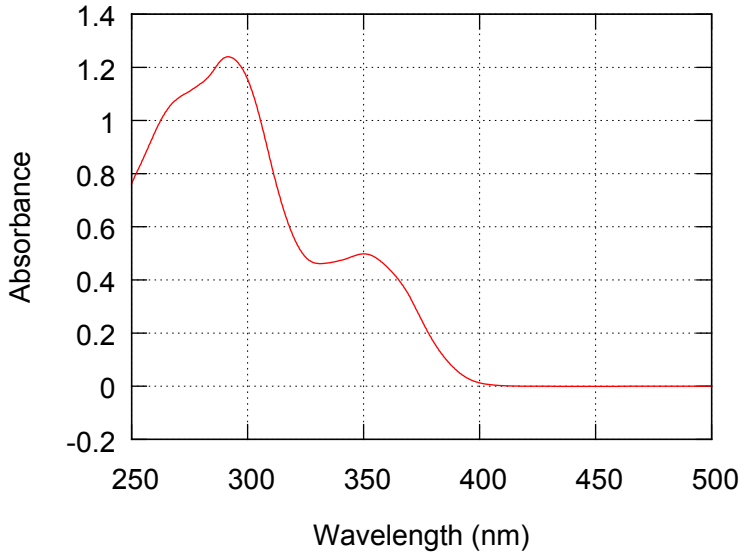

Figure S91. UV-vis absorption spectrum of **1(40)** in 1,2-DME (3.2×10^{-2} g/L, path length = 10 mm).

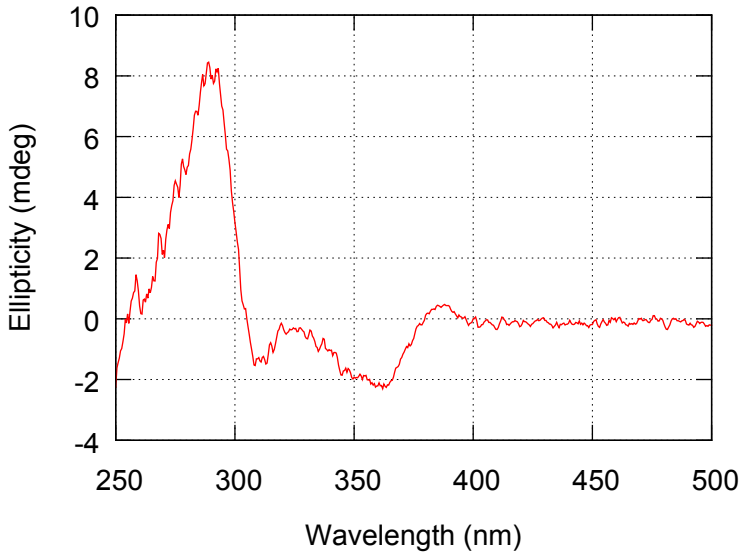

Figure S92. CD spectrum of **1(40)** in 1,2-DME (3.2×10^{-2} g/L, path length = 10 mm).

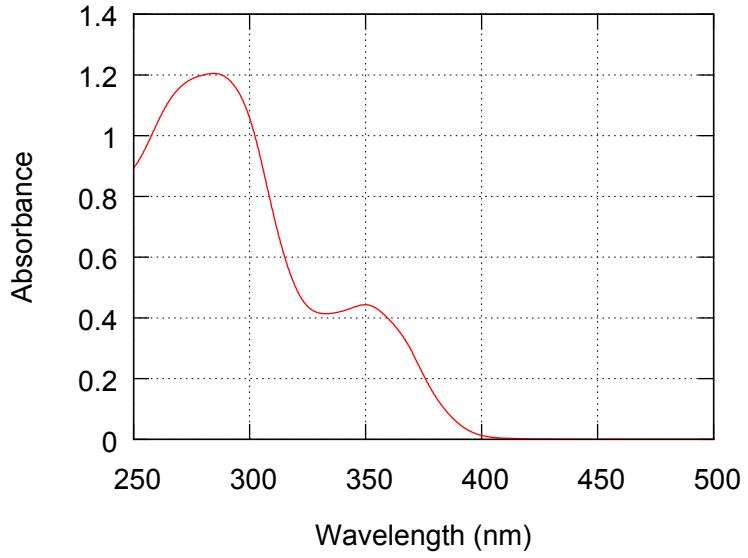

Figure S93. UV-vis absorption spectrum of **1(40)** in Et_2O (2.37×10^{-2} g/L, path length = 10 mm).

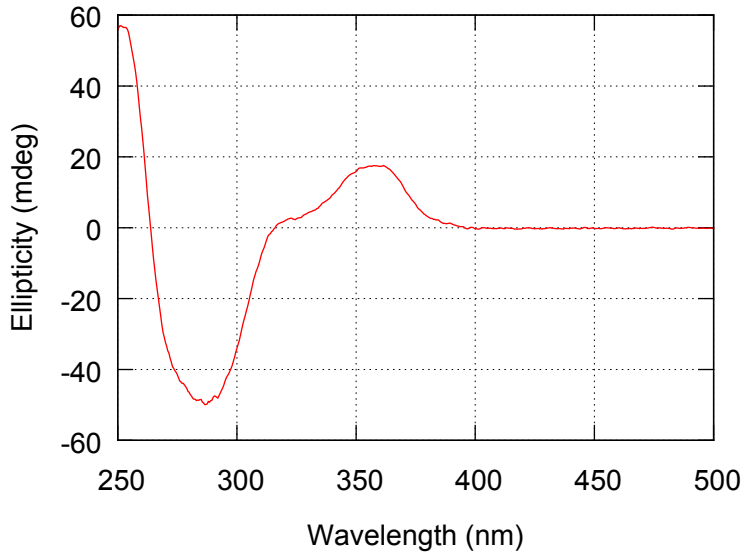

Figure S94. CD spectrum of **1(40)** in Et_2O (2.37×10^{-2} g/L, path length = 10 mm).

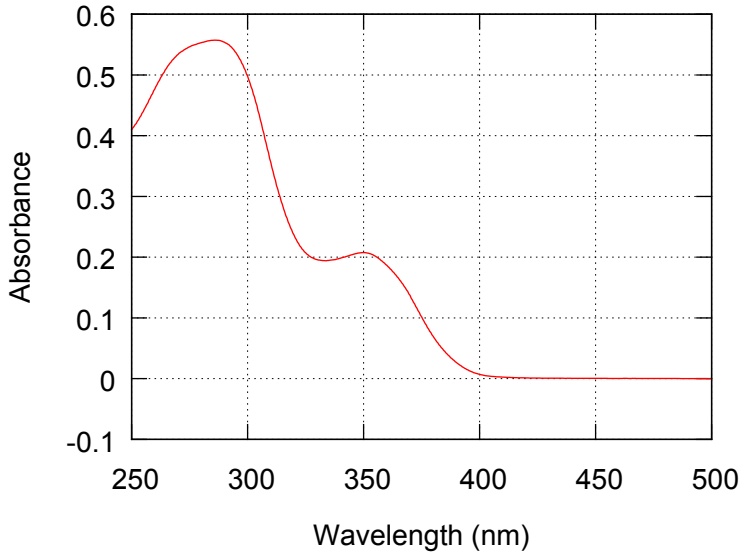

Figure S95. UV-vis absorption spectrum of **1(40)** in MTBE (3.2×10^{-2} g/L, path length = 10 mm).

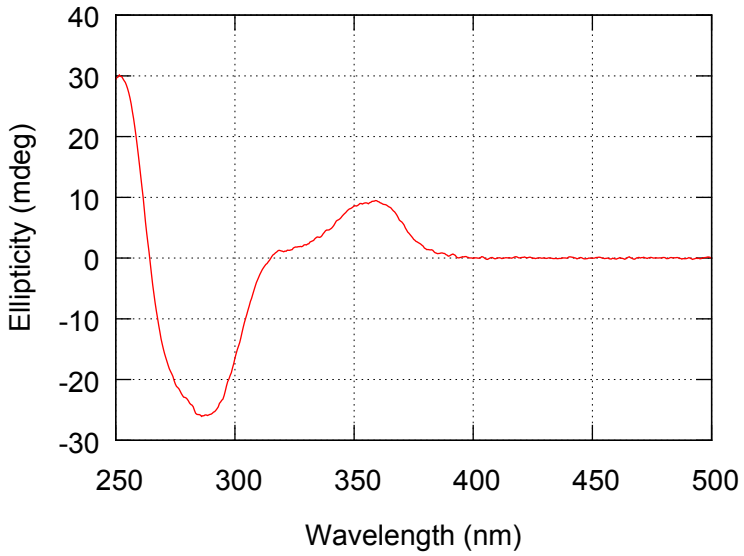

Figure S96. CD spectrum of **1(40)** in MTBE (3.2×10^{-2} g/L, path length = 10 mm).

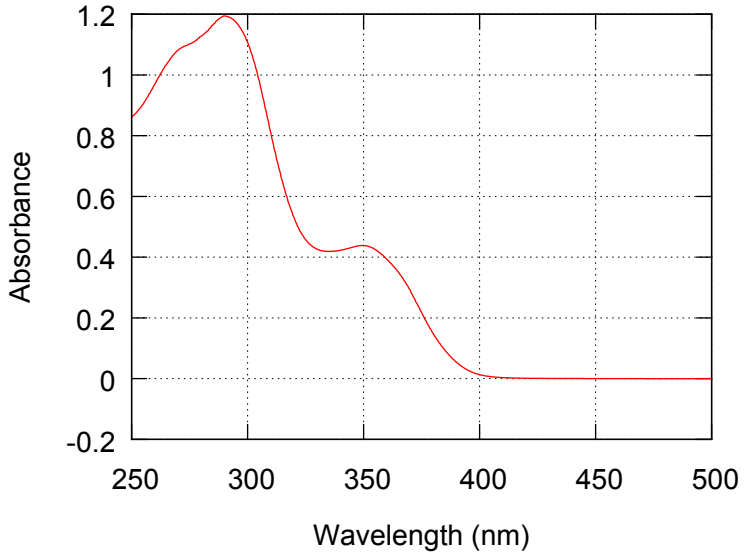

Figure S97. UV-vis absorption spectrum of **1(40)** in 2-MeTHF (3.2×10^{-2} g/L, path length = 10 mm).

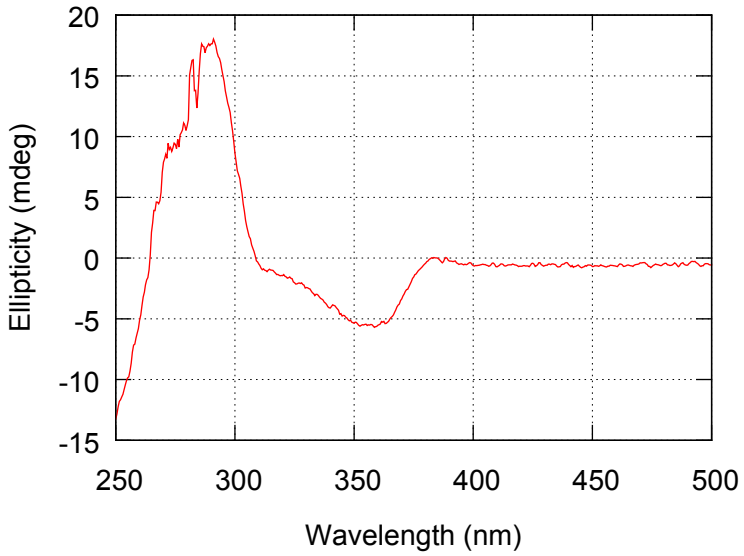

Figure S98. CD spectrum of **1(40)** in 2-MeTHF (3.2×10^{-2} g/L, path length = 10 mm).

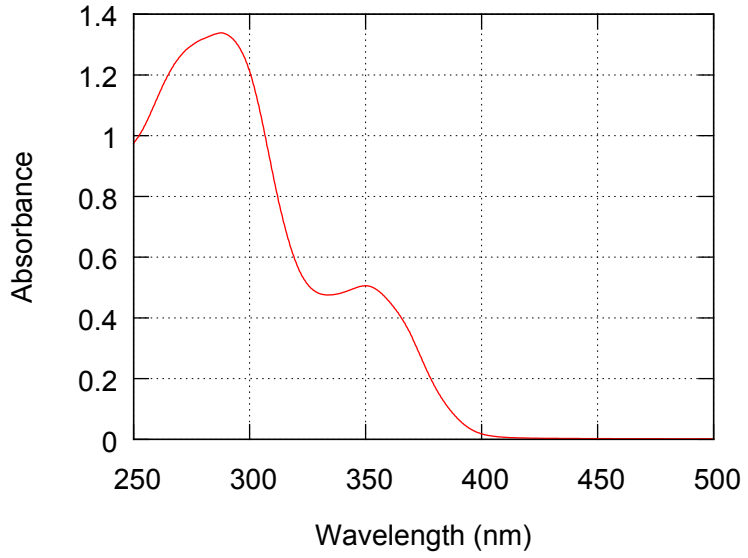

Figure S99. UV-vis absorption spectrum of **1(40)** in CPME (3.2×10^{-2} g/L, path length = 10 mm).

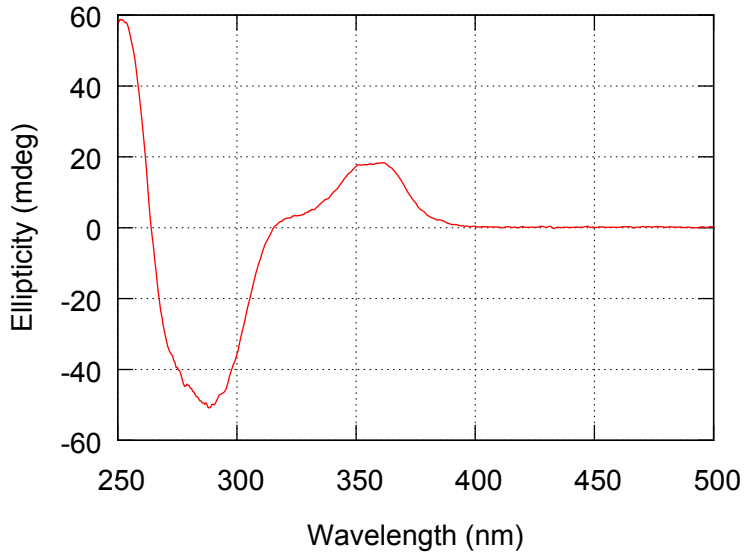

Figure S100. CD spectrum of **1(40)** in CPME (3.2×10^{-2} g/L, path length = 10 mm).

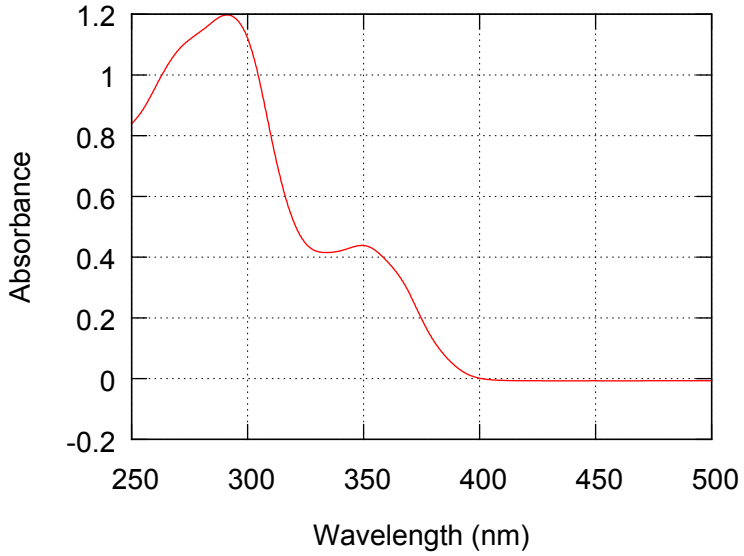

Figure S101. UV-vis absorption spectrum of **2(40)** in $CHCl_3$ (2.85×10^{-2} g/L, path length = 10 mm).

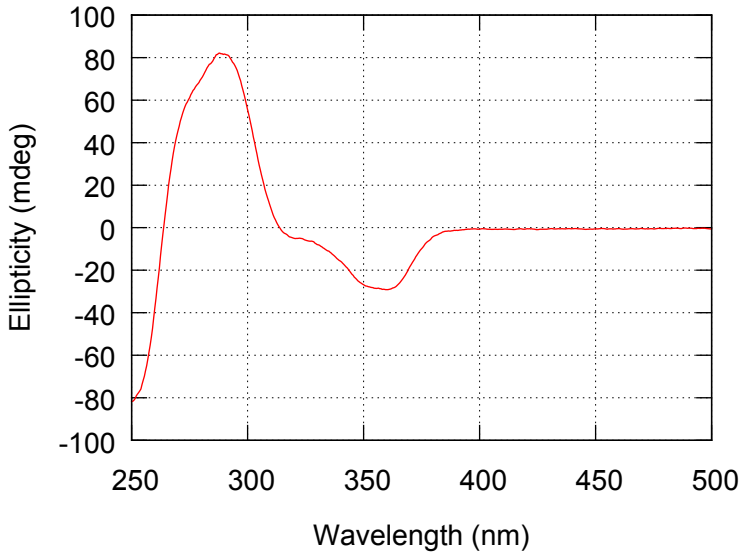

Figure S102. CD spectrum of **2(40)** in $CHCl_3$ (2.85×10^{-2} g/L, path length = 10 mm).

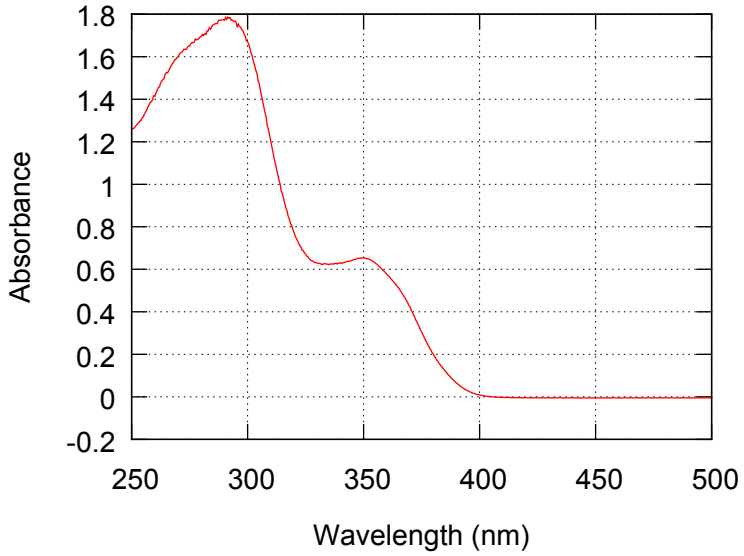

Figure S103. UV-vis absorption spectrum of **2(40)** in CH_2Cl_2 (2.98×10^{-2} g/L, path length = 10 mm).

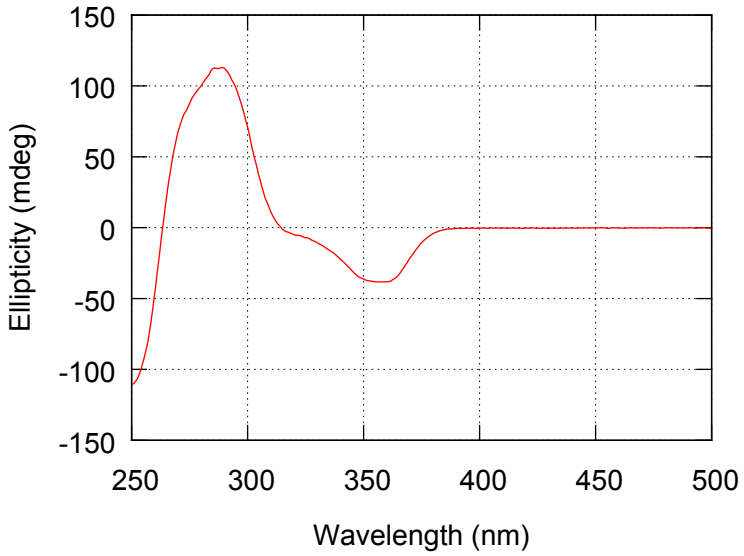

Figure S104. CD spectrum of **2(40)** in CH_2Cl_2 (2.98×10^{-2} g/L, path length = 10 mm).

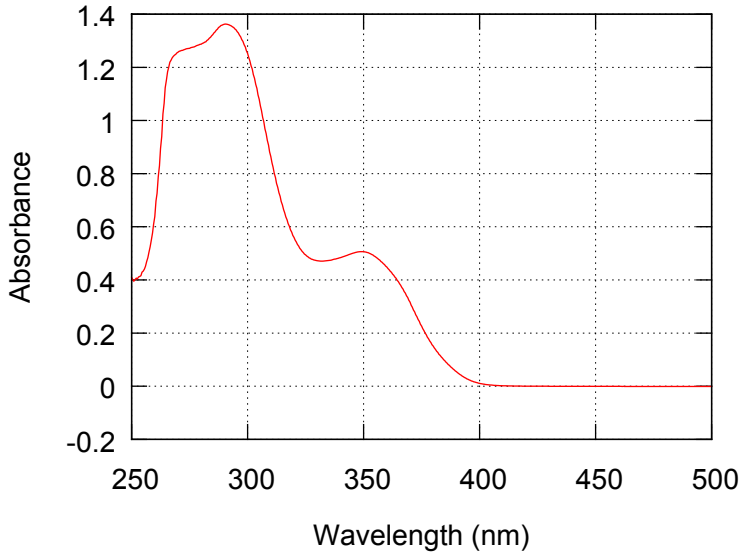

Figure S105. UV-vis absorption spectrum of **2(40)** in 1,1,2-TCE (2.85×10^{-2} g/L, path length = 10 mm).

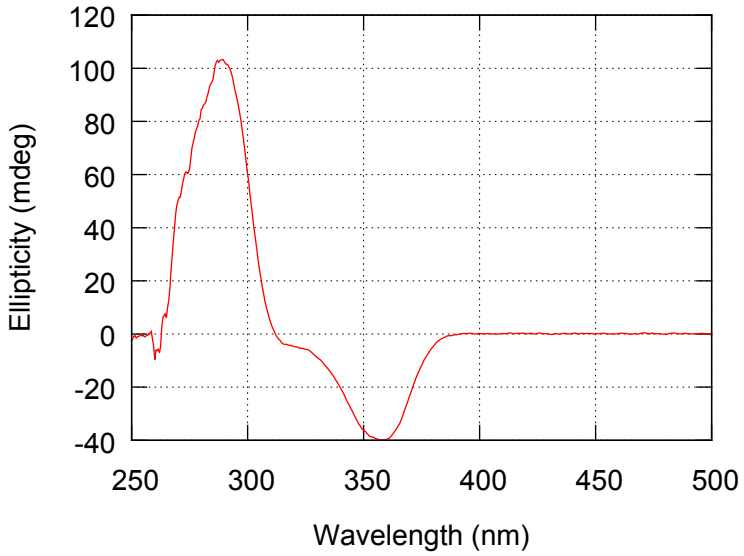

Figure S106. CD spectrum of **2(40)** in 1,1,2-TCE (2.85×10^{-2} g/L, path length = 10 mm).

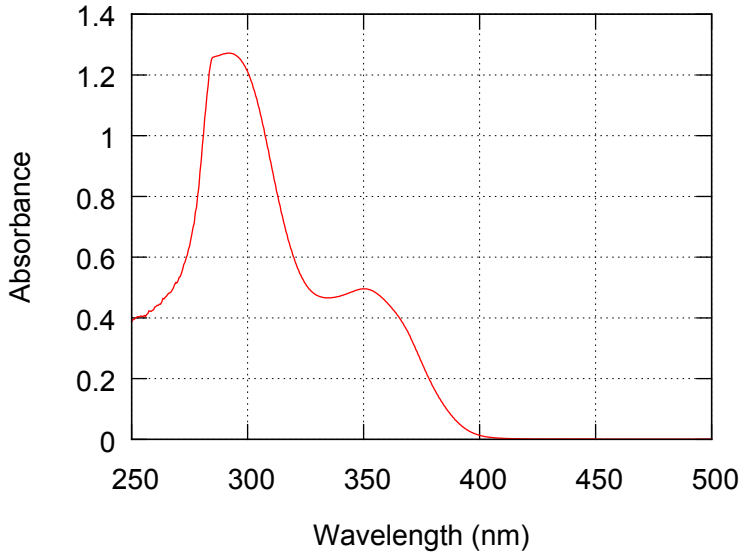

Figure S107. UV-vis absorption spectrum of **2(40)** in Toluene (2.85×10^{-2} g/L, path length = 10 mm).

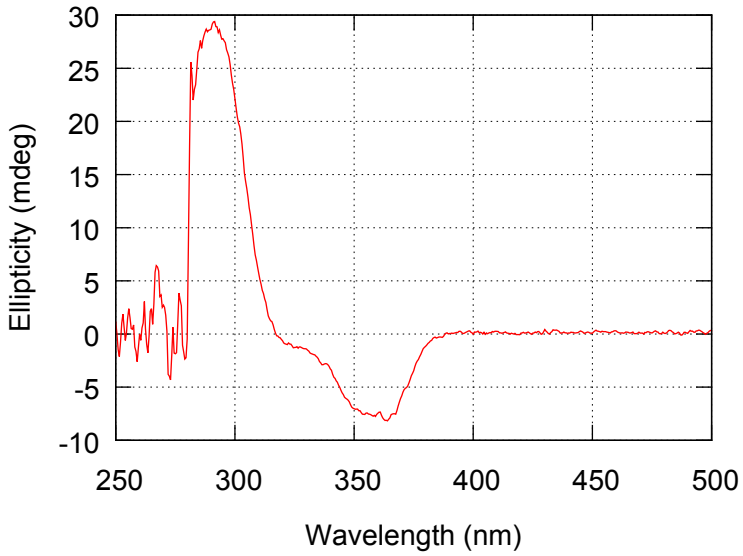

Figure S108. CD spectrum of **2(40)** in Toluene (2.85×10^{-2} g/L, path length = 10 mm).

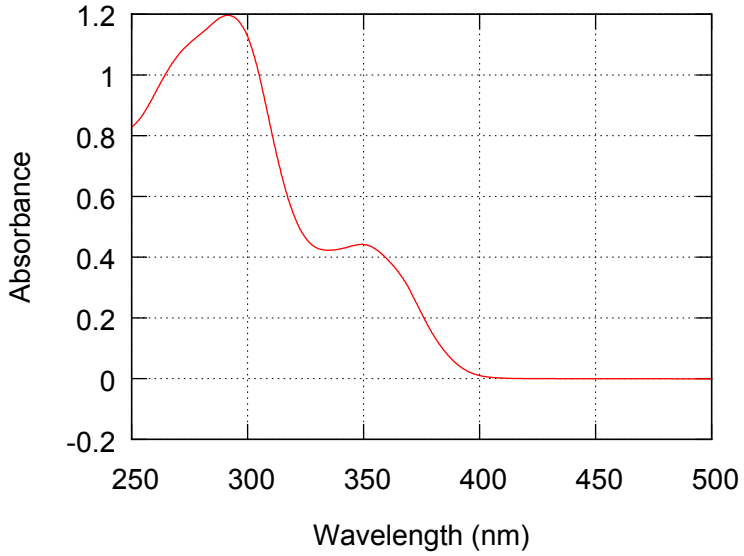

Figure S109. UV-vis absorption spectrum of **2(40)** in THF (2.85×10^{-2} g/L, path length = 10 mm).

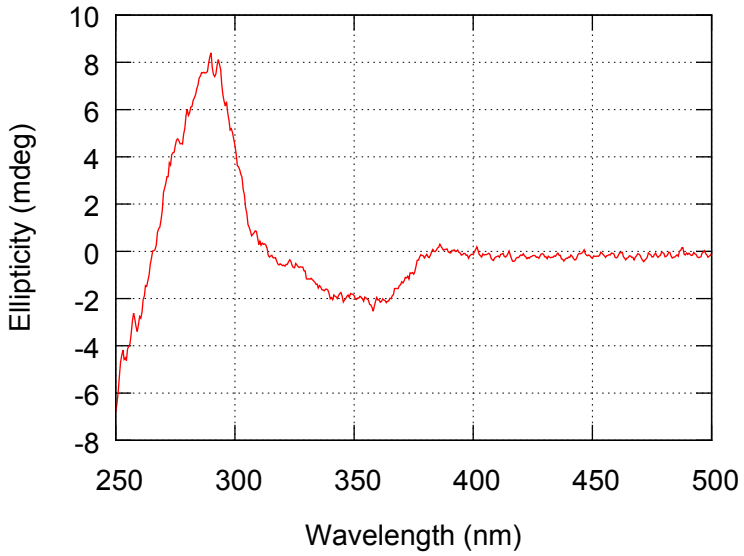

Figure S110. CD spectrum of **2(40)** in THF (2.85×10^{-2} g/L, path length = 10 mm).

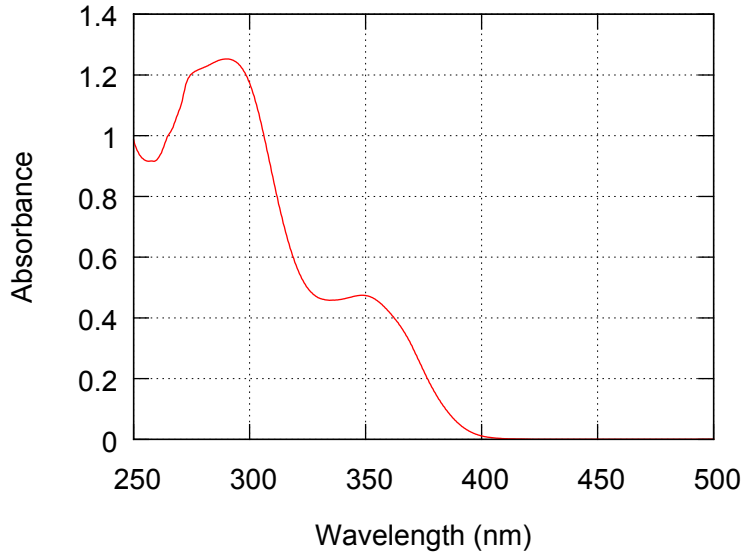

Figure S111. UV-vis absorption spectrum of **2(40)** in 1,4-Dioxane (2.85×10^{-2} g/L, path length = 10 mm).

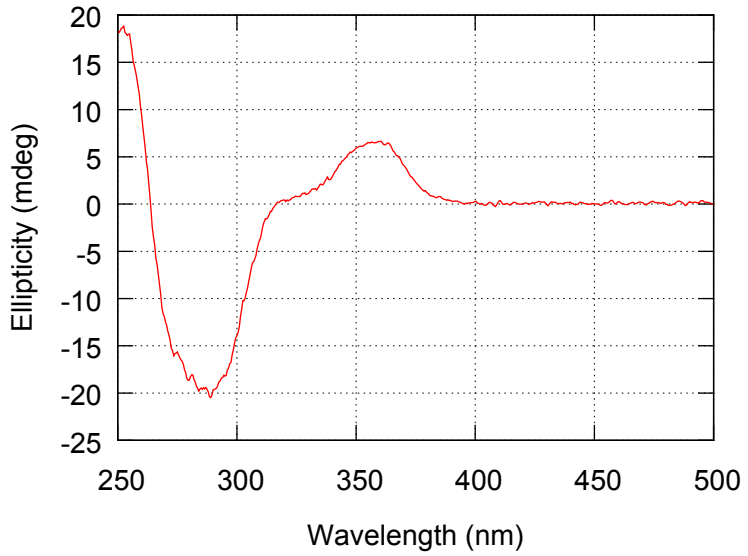

Figure S112. CD spectrum of **2(40)** in 1,4-Dioxane (2.85×10^{-2} g/L, path length = 10 mm).

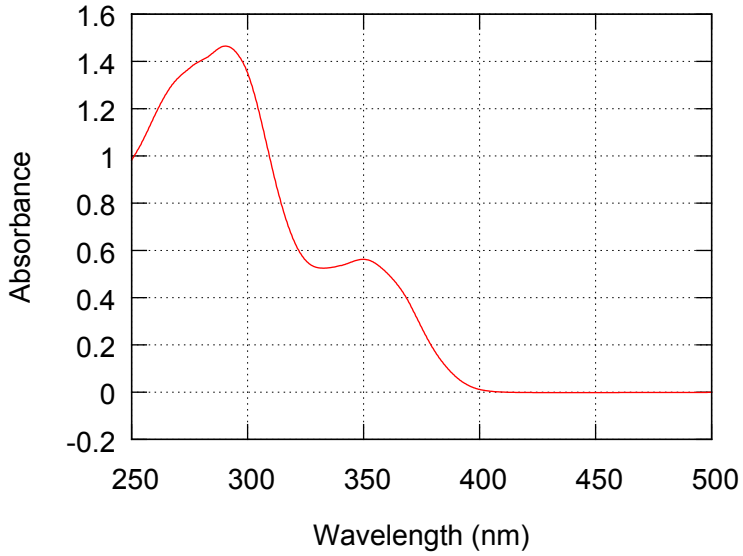

Figure S113. UV-vis absorption spectrum of **2(40)** in 1,2-DME (2.98×10^{-2} g/L, path length = 10 mm).

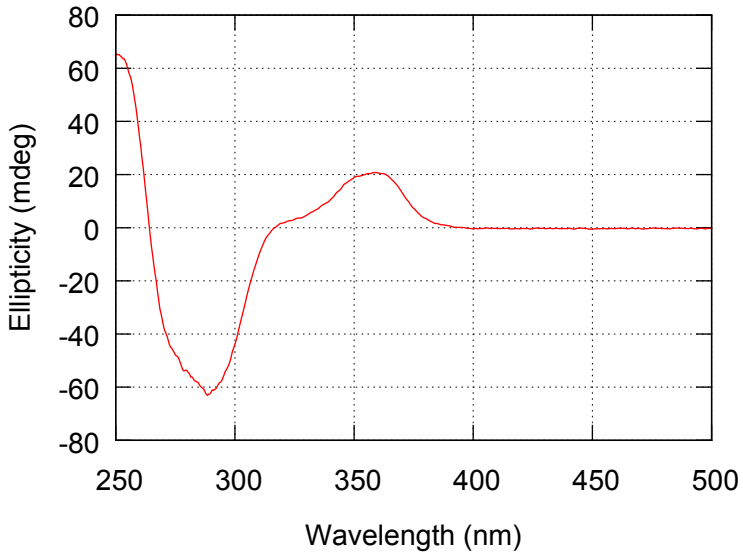

Figure S114. CD spectrum of **2(40)** in 1,2-DME (2.98×10^{-2} g/L, path length = 10 mm).

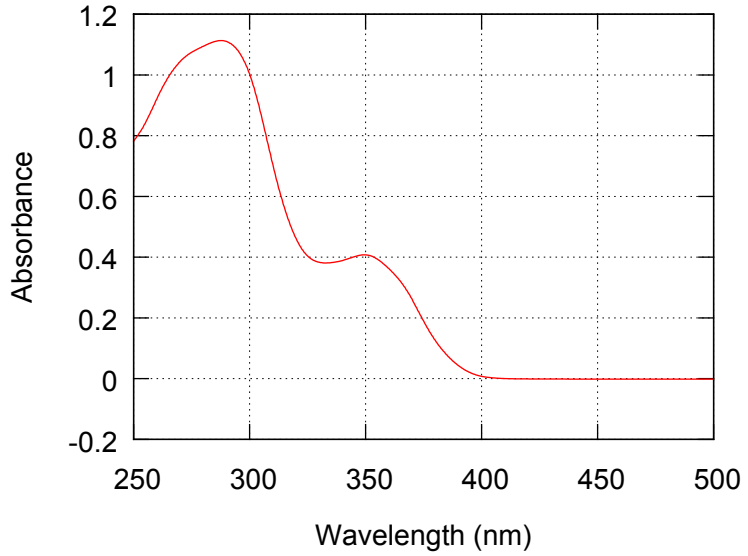

Figure S115. UV-vis absorption spectrum of **2(40)** in Et_2O (2.85×10^{-2} g/L, path length = 10 mm).

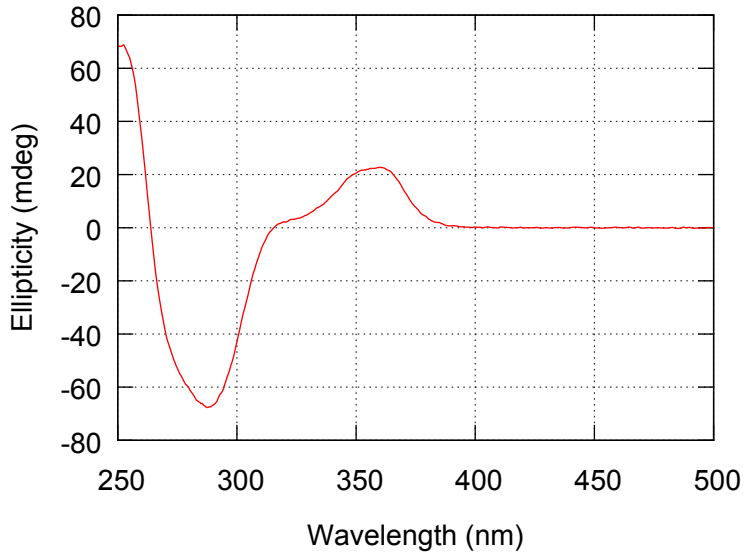

Figure S116. CD spectrum of **2(40)** in Et_2O (2.85×10^{-2} g/L, path length = 10 mm).

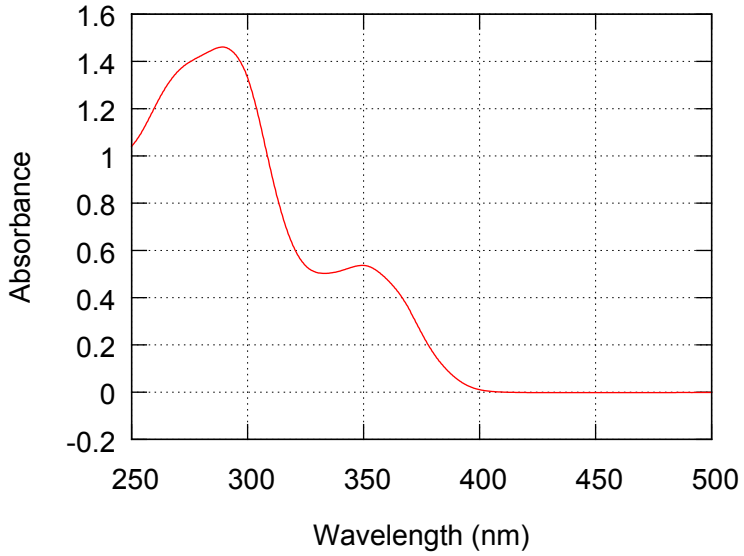

Figure S117. UV-vis absorption spectrum of **2(40)** in MTBE (2.98×10^{-2} g/L, path length = 10 mm).

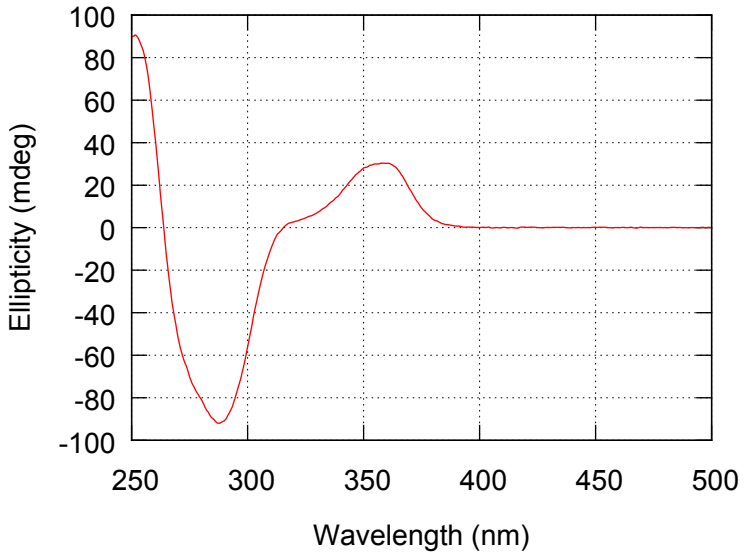

Figure S118. CD spectrum of **2(40)** in MTBE (2.98×10^{-2} g/L, path length = 10 mm).

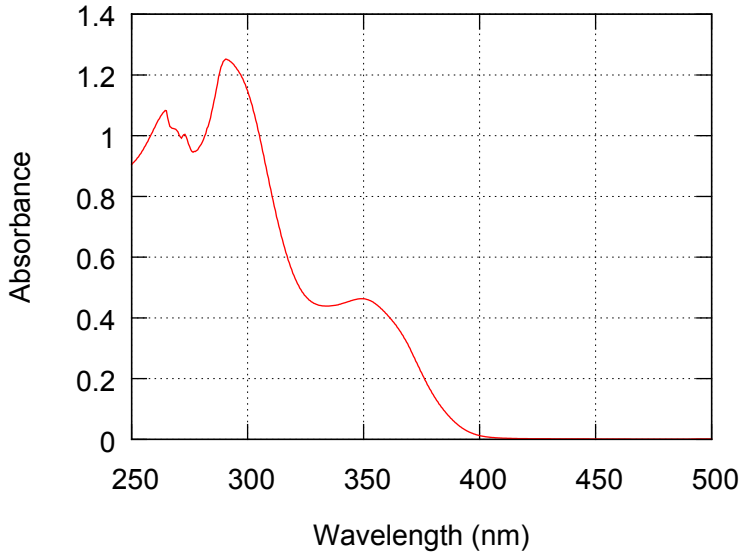

Figure S119. UV-vis absorption spectrum of **2(40)** in 2-MeTHF (2.85×10^{-2} g/L, path length = 10 mm).

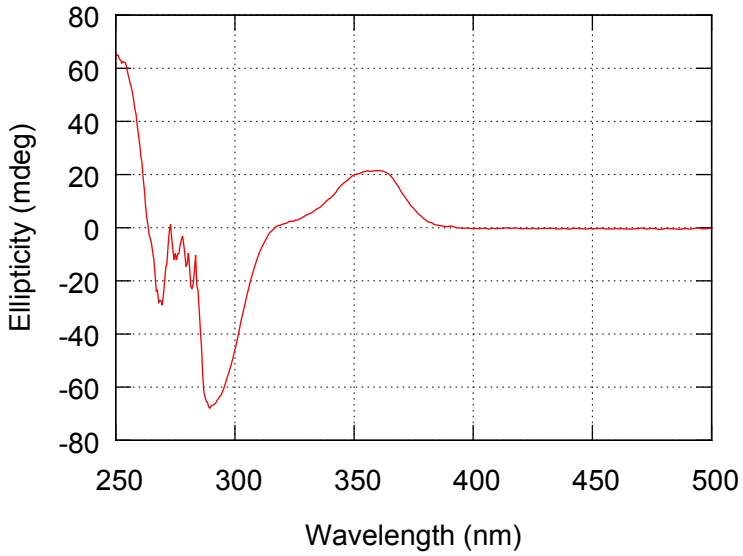

Figure S120. CD spectrum of **2(40)** in 2-MeTHF (2.85×10^{-2} g/L, path length = 10 mm).

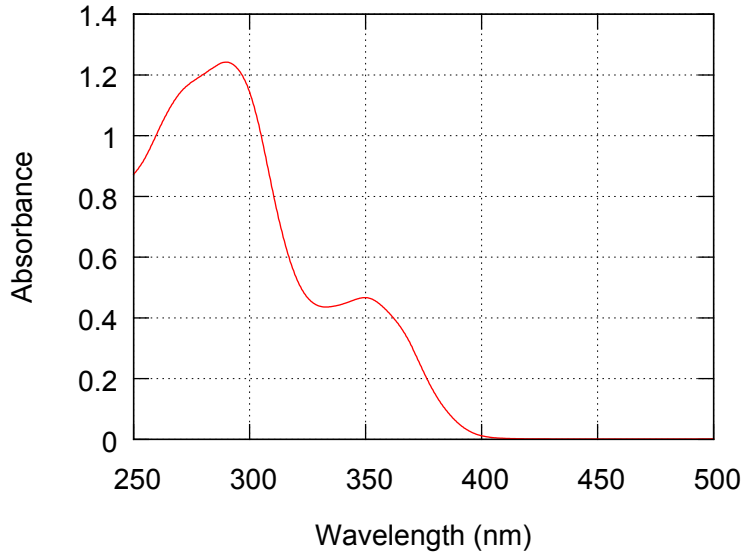

Figure S121. UV-vis absorption spectrum of **2(40)** in CPME (2.85×10^{-2} g/L, path length = 10 mm).

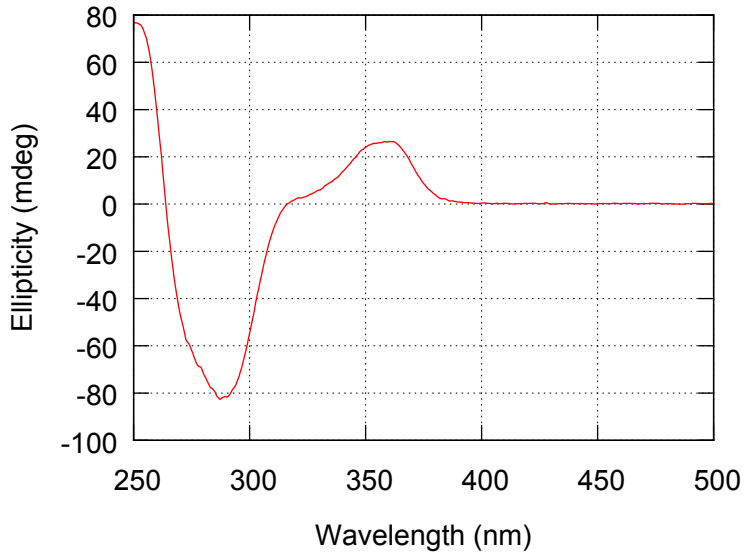

Figure S122. CD spectrum of **2(40)** in CPME (2.85×10^{-2} g/L, path length = 10 mm).

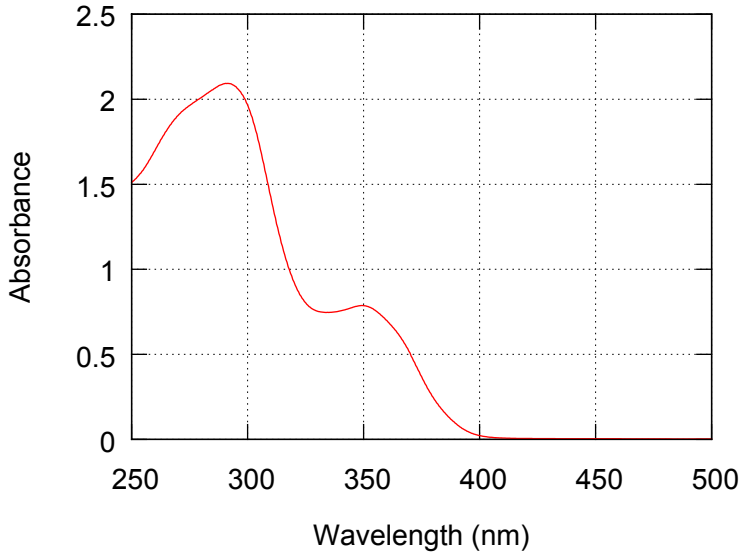

Figure S123. UV-vis absorption spectrum of **3(40)** in $CHCl_3$ (4.62×10^{-2} g/L, path length = 10 mm).

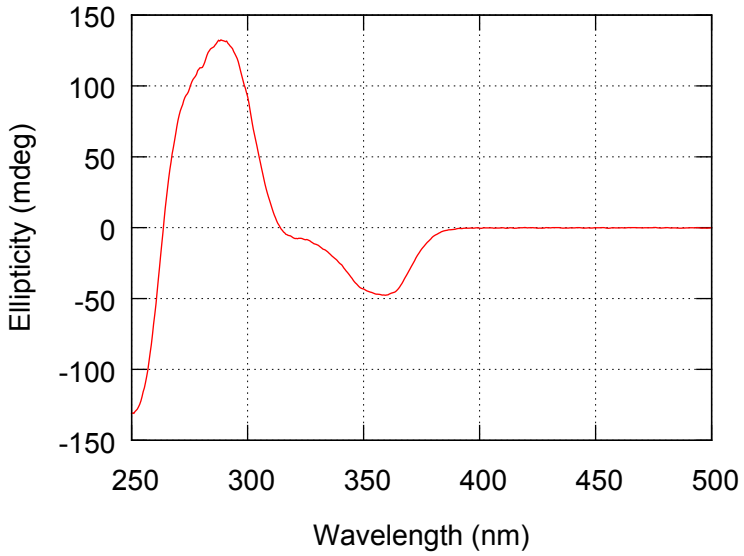

Figure S124. CD spectrum of **3(40)** in $CHCl_3$ (4.62×10^{-2} g/L, path length = 10 mm).

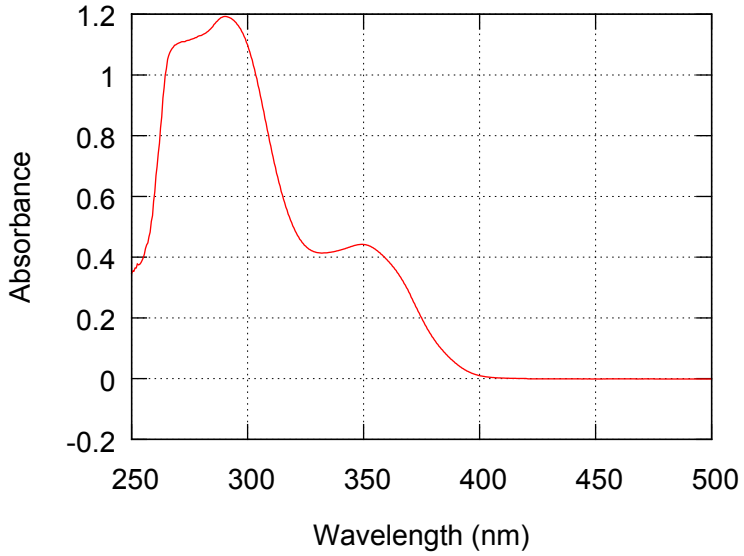

Figure S125. UV-vis absorption spectrum of **3(40)** in 1,1,2-TCE (3.05×10^{-2} g/L, path length = 10 mm).

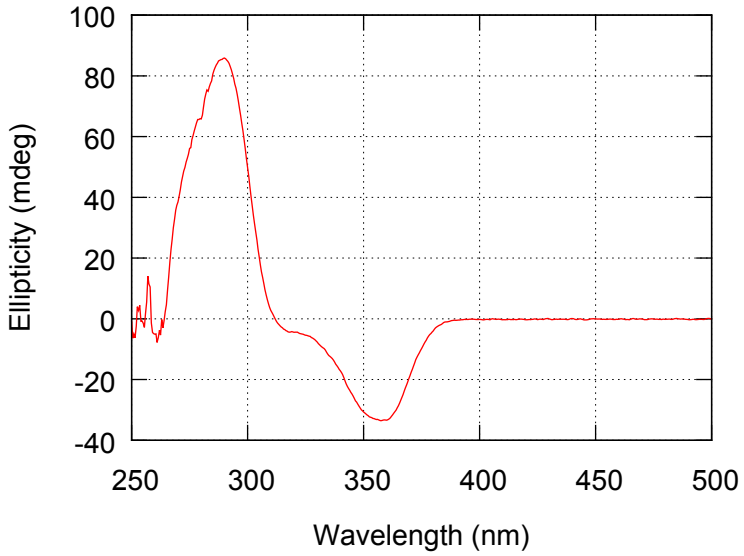

Figure S126. CD spectrum of **3(40)** in 1,1,2-TCE (3.05×10^{-2} g/L, path length = 10 mm).

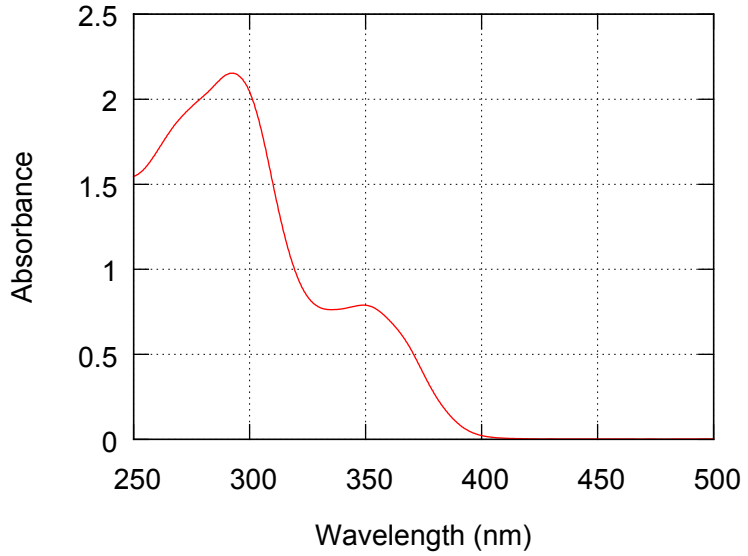

Figure S127. UV-vis absorption spectrum of **3(40)** in THF (4.62×10^{-2} g/L, path length = 10 mm).

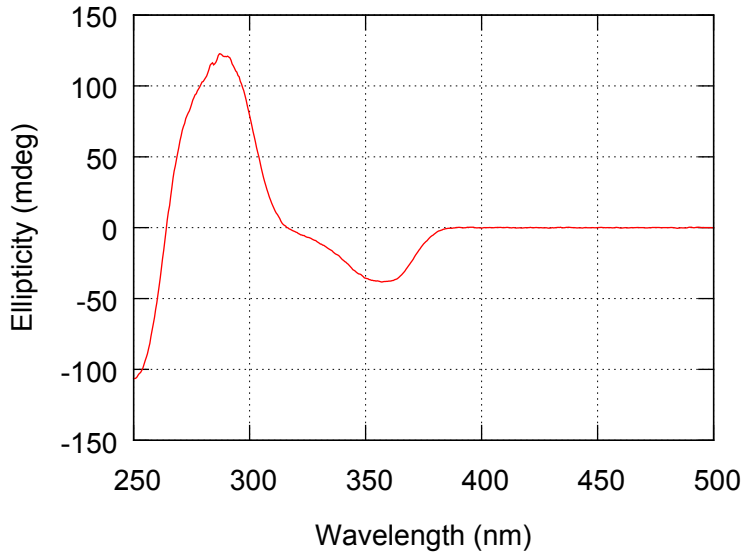

Figure S128. CD spectrum of **3(40)** in THF (4.62×10^{-2} g/L, path length = 10 mm).

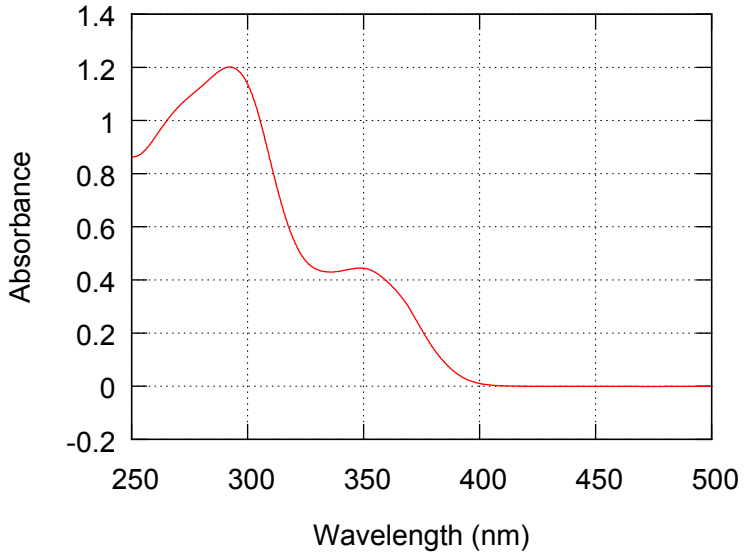

Figure S129. UV-vis absorption spectrum of **3(40)** in 1,4-Dioxane (3.05×10^{-2} g/L, path length = 10 mm).

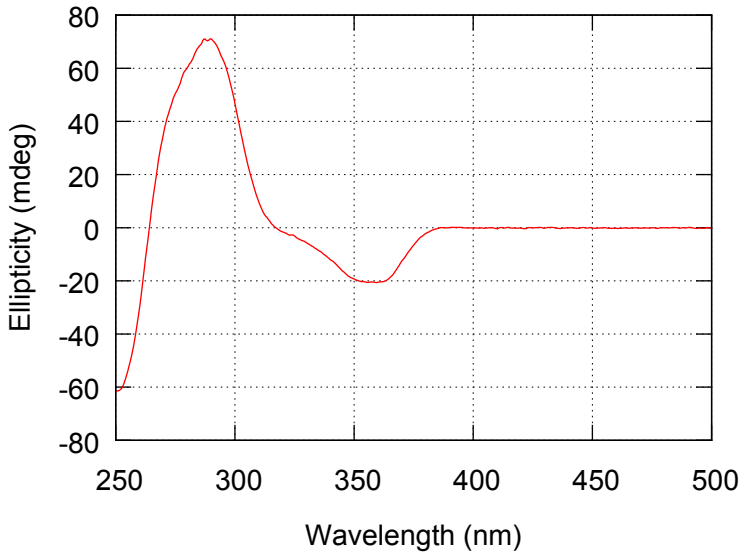

Figure S130. CD spectrum of **3(40)** in 1,4-Dioxane (3.05×10^{-2} g/L, path length = 10 mm).

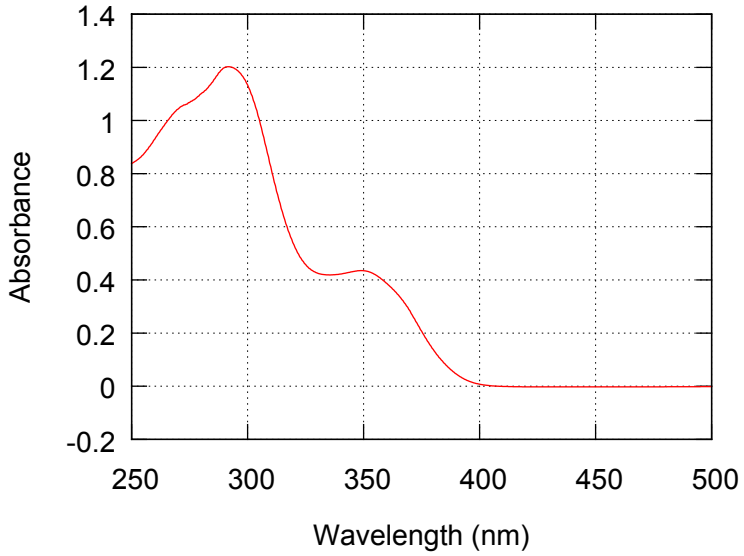

Figure S131. UV-vis absorption spectrum of **3(40)** in 2-MeTHF (3.05×10^{-2} g/L, path length = 10 mm).

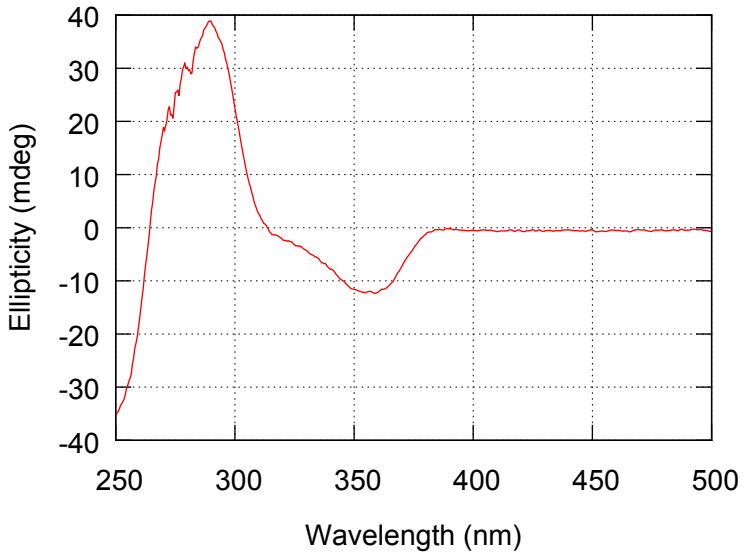

Figure S132. CD spectrum of **3(40)** in 2-MeTHF (3.05×10^{-2} g/L, path length = 10 mm).

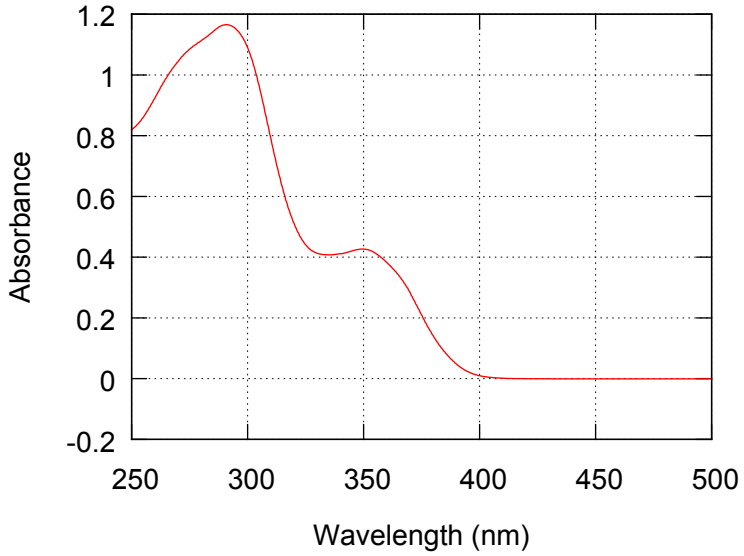

Figure S133. UV-vis absorption spectrum of **3(40)** in 1,2-DME (3.05×10^{-2} g/L, path length = 10 mm).

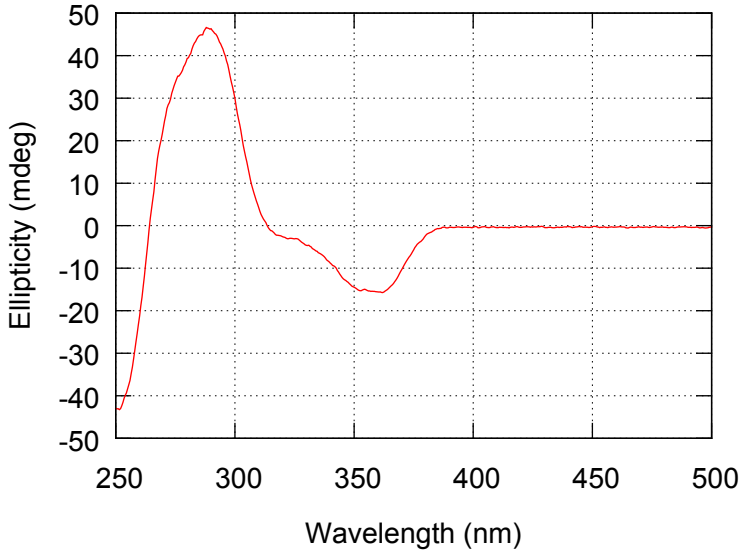

Figure S134. CD spectrum of **3(40)** in 1,2-DME (3.05×10^{-2} g/L, path length = 10 mm).

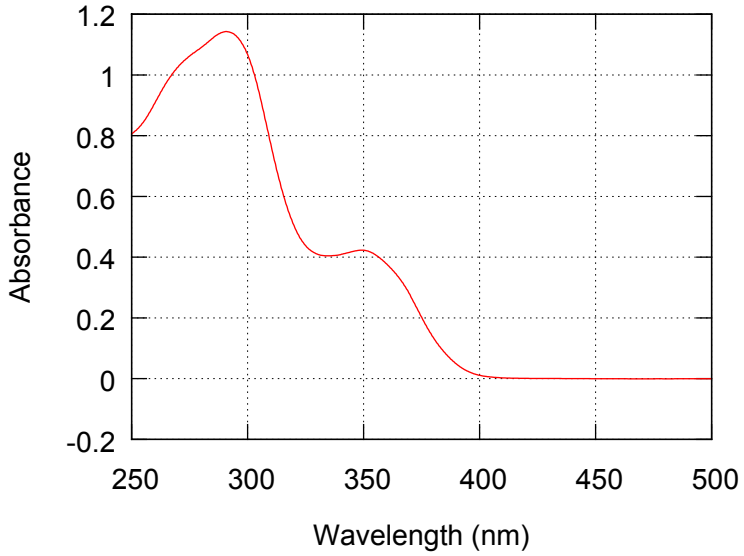

Figure S135. UV-vis absorption spectrum of **3(40)** in CPME (3.05×10^{-2} g/L, path length = 10 mm).

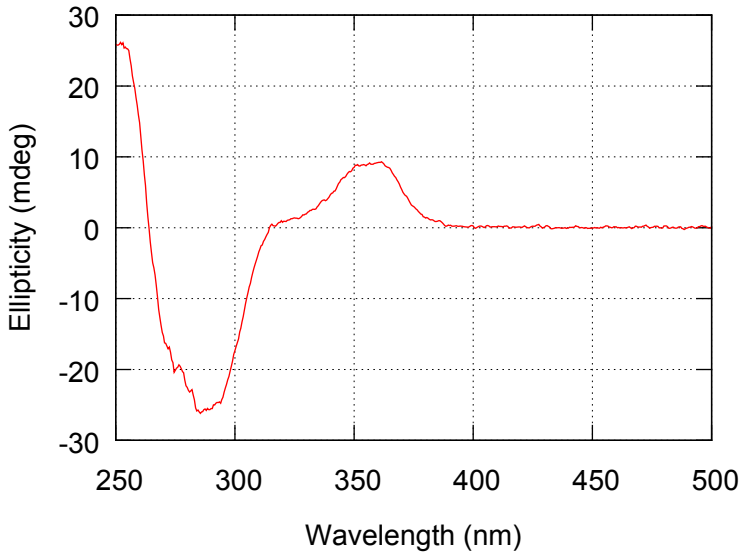

Figure S136. CD spectrum of **3(40)** in CPME (3.05×10^{-2} g/L, path length = 10 mm).

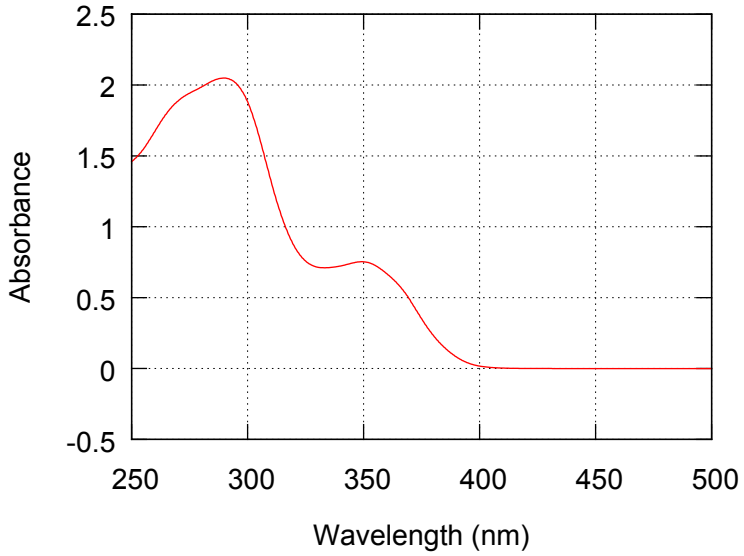

Figure S137. UV-vis absorption spectrum of **3(40)** in Et_2O (4.62×10^{-2} g/L, path length = 10 mm).

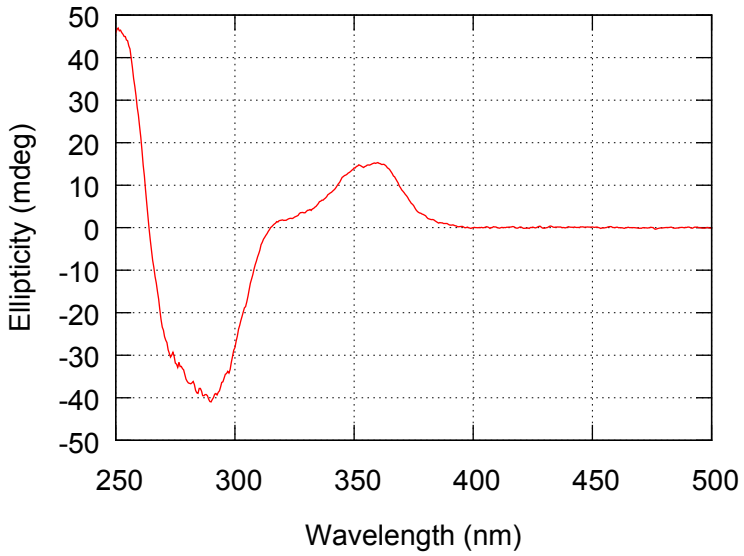

Figure S138. CD spectrum of **3(40)** in Et_2O (4.62×10^{-2} g/L, path length = 10 mm).

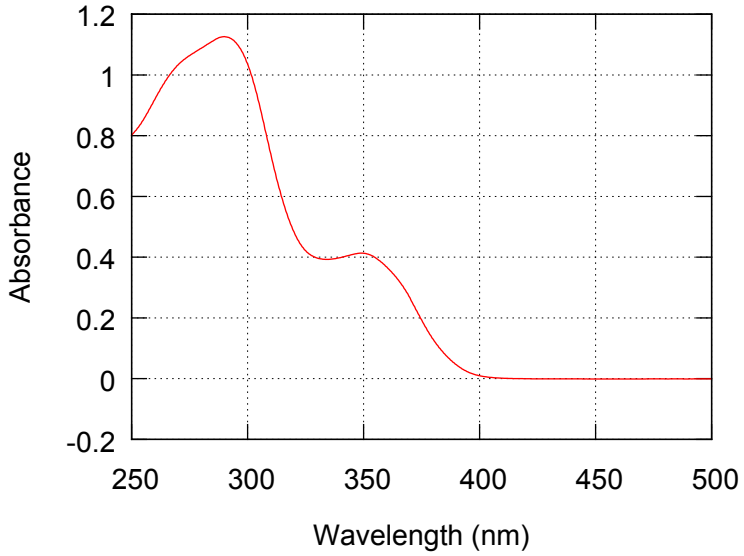

Figure S139. UV-vis absorption spectrum of **3(40)** in MTBE (3.05×10^{-2} g/L, path length = 10 mm).

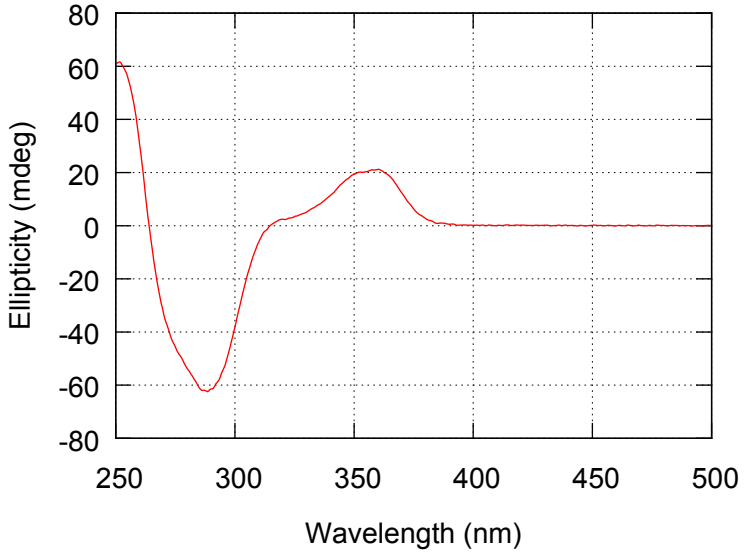

Figure S140. CD spectrum of **3(40)** in MTBE (3.05×10^{-2} g/L, path length = 10 mm).

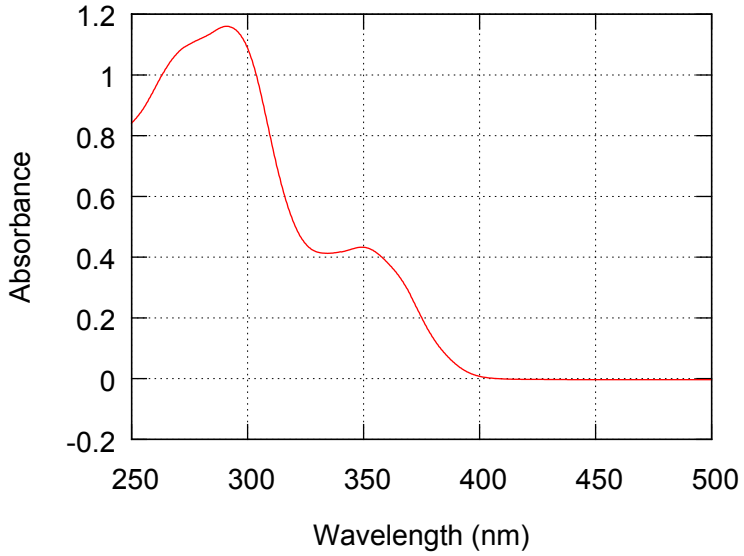

Figure S141. UV-vis absorption spectrum of **4(40)** in $CHCl_3$ (3.01×10^{-2} g/L, path length = 10 mm).

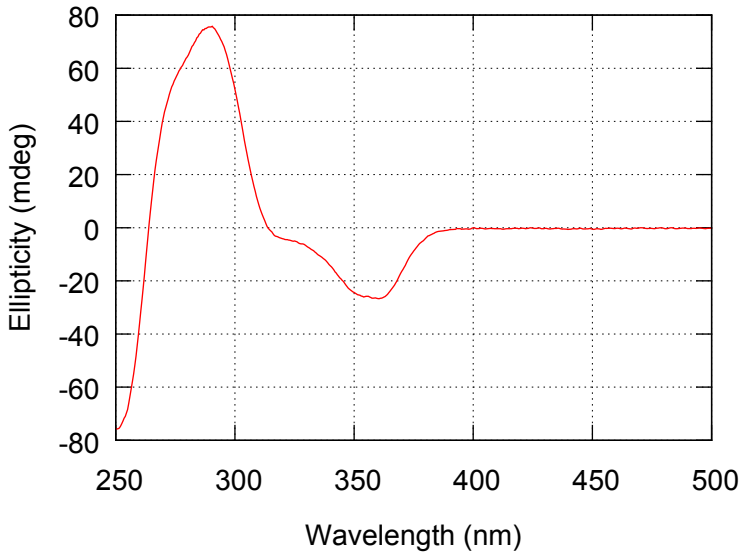

Figure S142. CD spectrum of **4(40)** in $CHCl_3$ (3.01×10^{-2} g/L, path length = 10 mm).

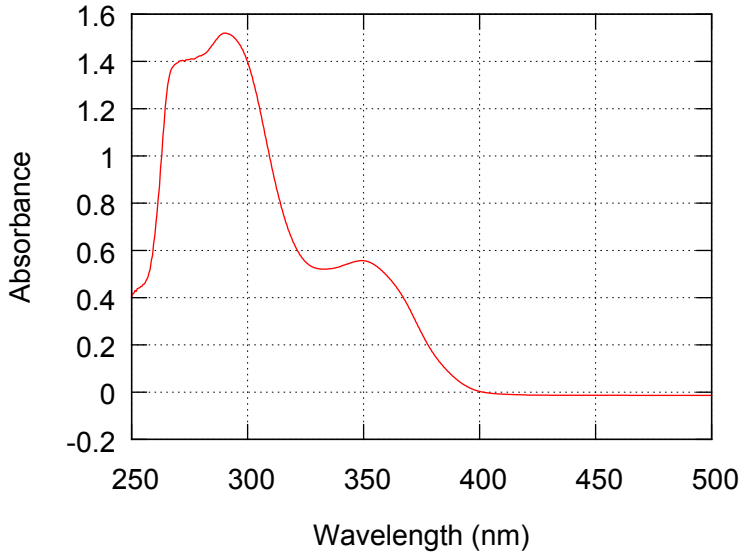

Figure S143. UV-vis absorption spectrum of **4(40)** in 1,1,2-TCE (2.99×10^{-2} g/L, path length = 10 mm).

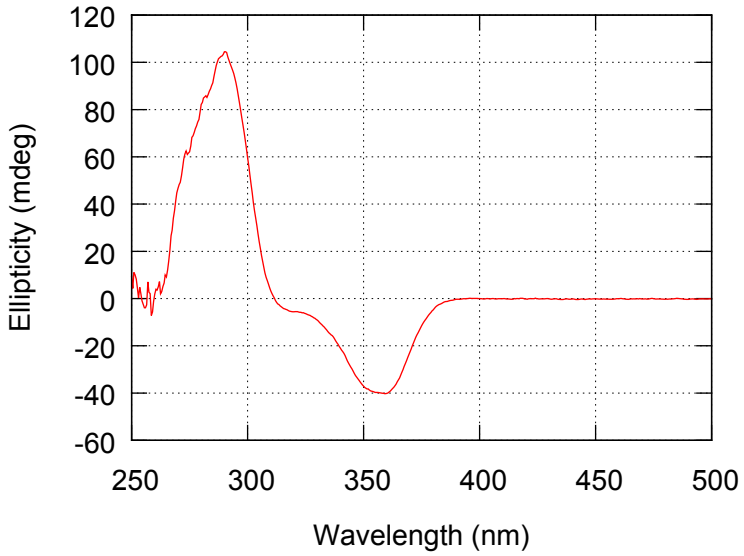

Figure S144. CD spectrum of **4(40)** in 1,1,2-TCE (2.99×10^{-2} g/L, path length = 10 mm).

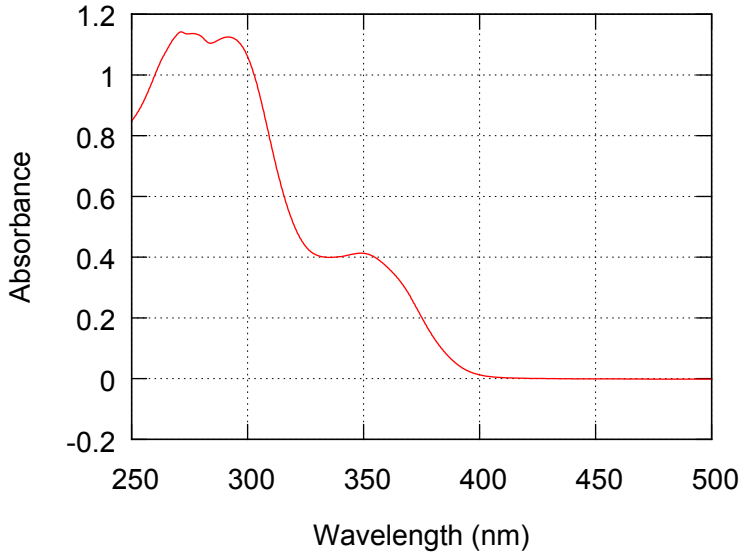

Figure S145. UV-vis absorption spectrum of **4(40)** in THF (3.01×10^{-2} g/L, path length = 10 mm).

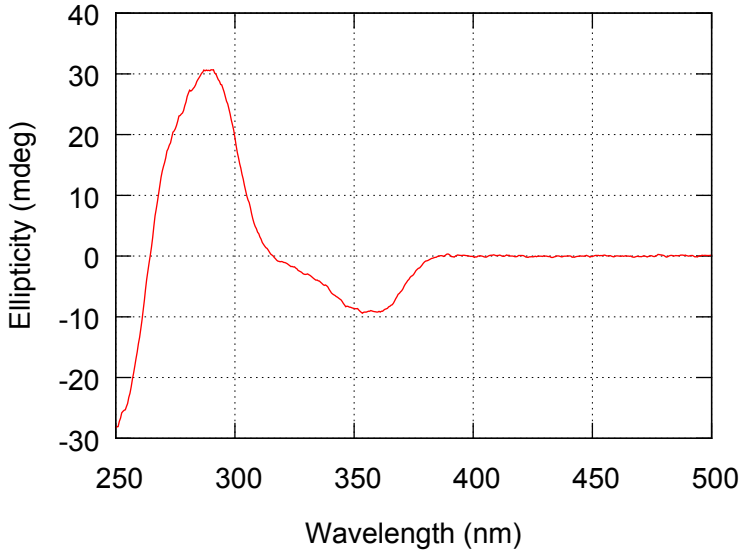

Figure S146. CD spectrum of **4(40)** in THF (3.01×10^{-2} g/L, path length = 10 mm).

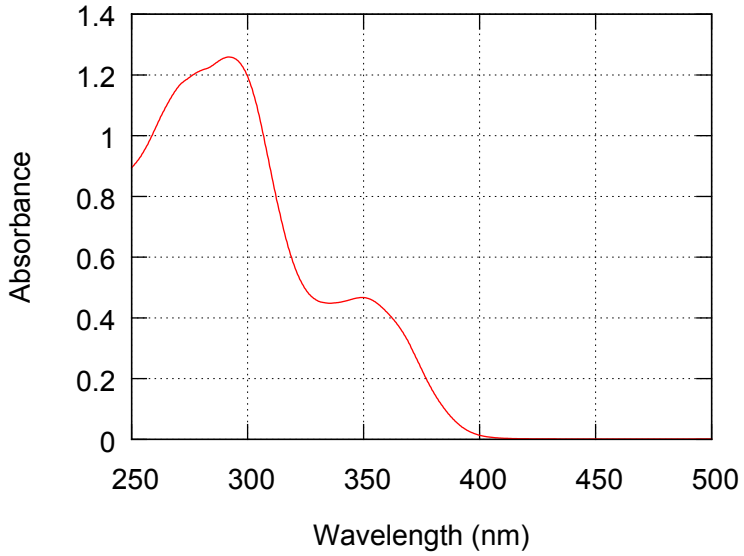

Figure S147. UV-vis absorption spectrum of **4(40)** in 1,4-Dioxane (3.01×10^{-2} g/L, path length = 10 mm).

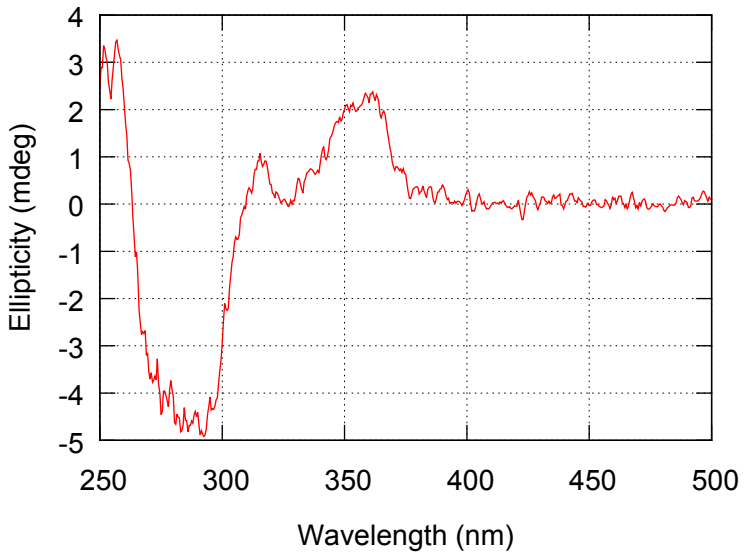

Figure S148. CD spectrum of **4(40)** in 1,4-Dioxane (3.01×10^{-2} g/L, path length = 10 mm).

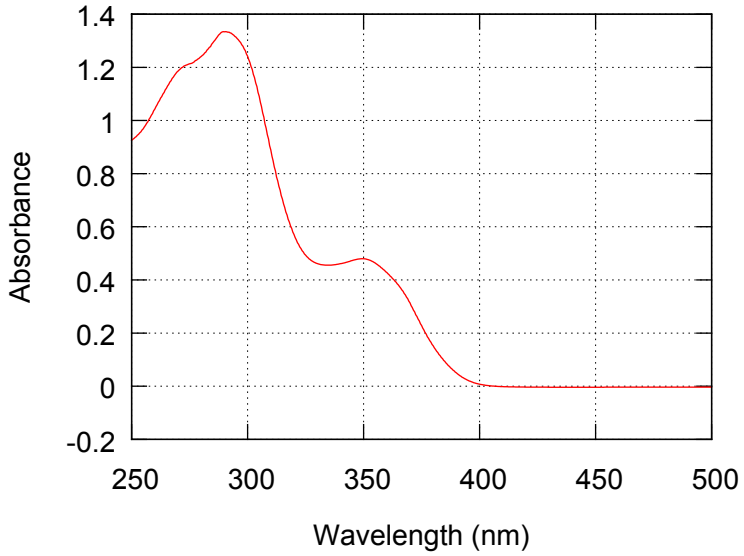

Figure S149. UV-vis absorption spectrum of **4(40)** in 2-MeTHF (3.01×10^{-2} g/L, path length = 10 mm).

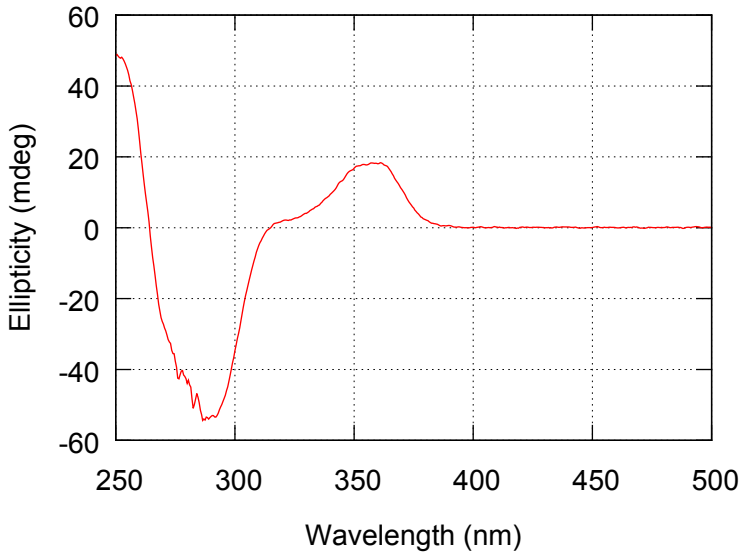

Figure S150. CD spectrum of **4(40)** in 2-MeTHF (3.01×10^{-2} g/L, path length = 10 mm).

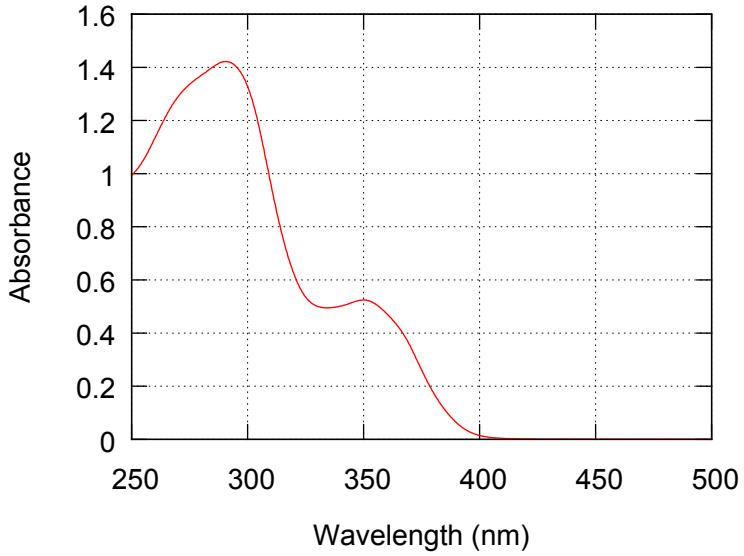

Figure S151. UV-vis absorption spectrum of **4(40)** in 1,2-DME (2.99×10^{-2} g/L, path length = 10 mm).

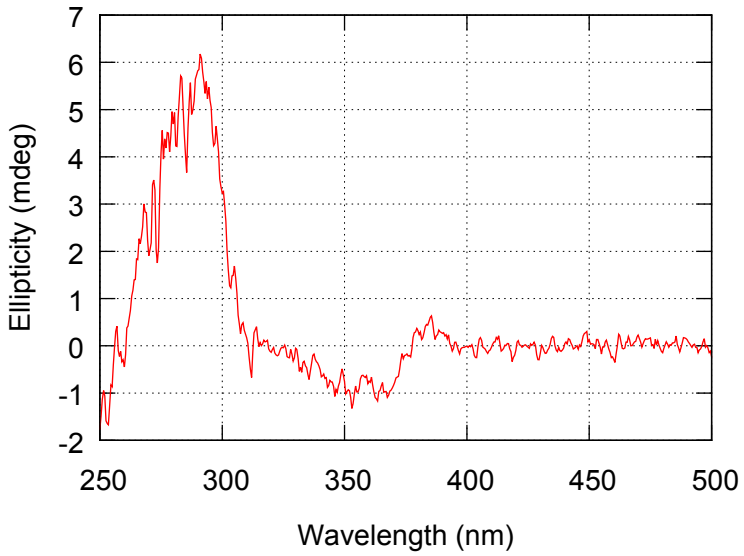

Figure S152. CD spectrum of **4(40)** in 1,2-DME (2.99×10^{-2} g/L, path length = 10 mm).

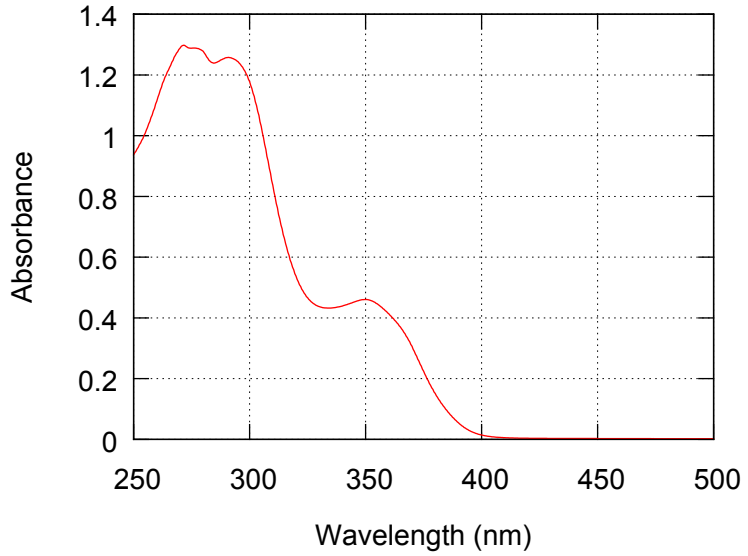

Figure S153. UV-vis absorption spectrum of **4(40)** in CPME (3.01×10^{-2} g/L, path length = 10 mm).

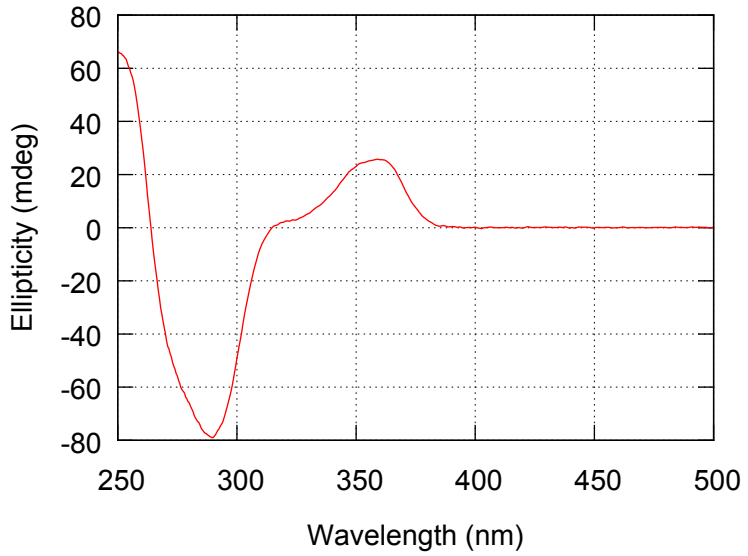

Figure S154. CD spectrum of **4(40)** in CPME (3.01×10^{-2} g/L, path length = 10 mm).

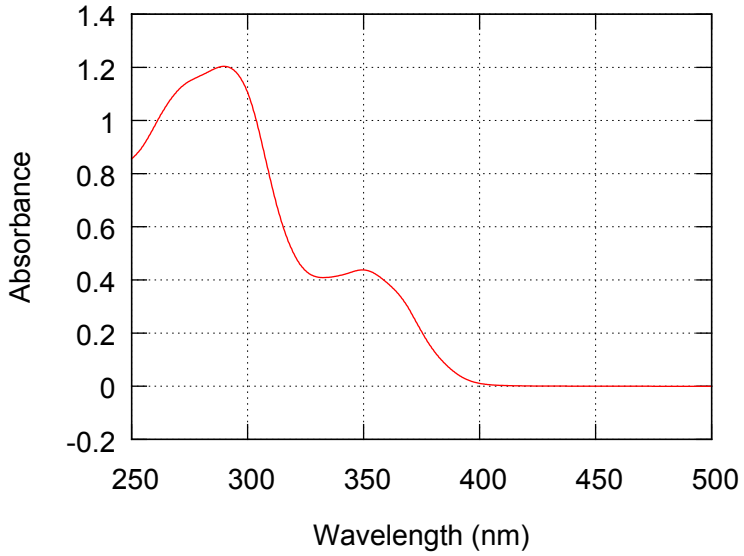

Figure S155. UV-vis absorption spectrum of **4(40)** in Et_2O (3.01×10^{-2} g/L, path length = 10 mm).

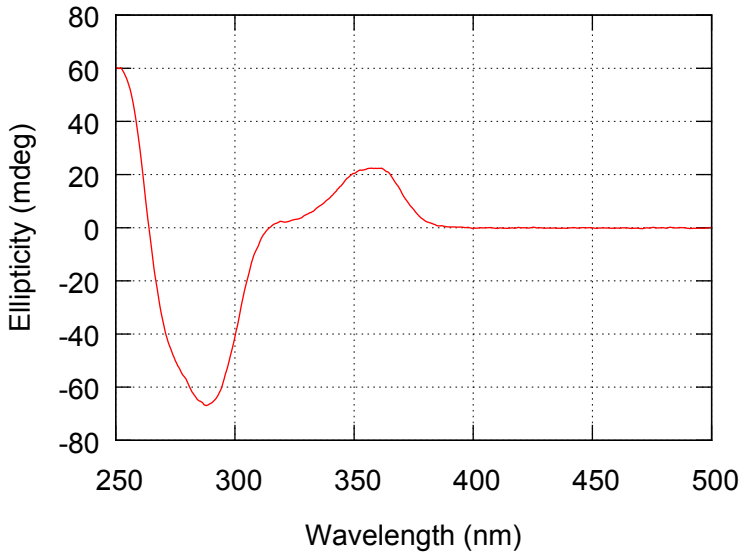

Figure S156. CD spectrum of **4(40)** in Et_2O (3.01×10^{-2} g/L, path length = 10 mm).

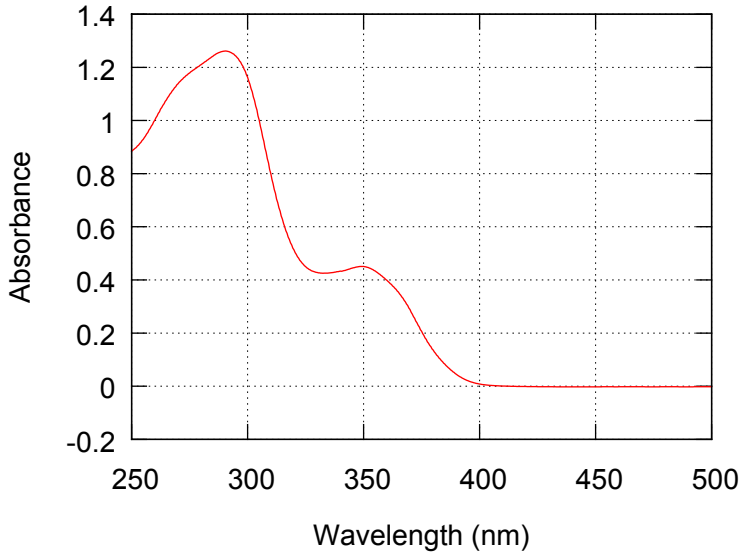

Figure S157. UV-vis absorption spectrum of **4(40)** in MTBE (3.01×10^{-2} g/L, path length = 10 mm).

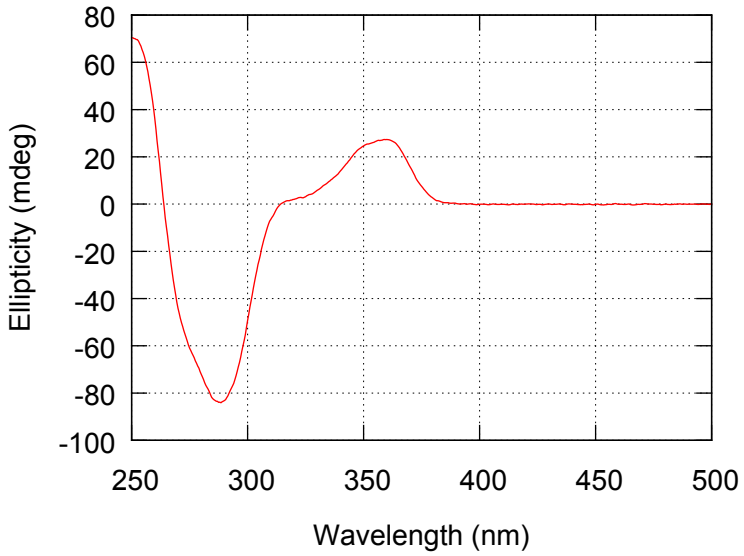

Figure S158. CD spectrum of **4(40)** in MTBE (3.01×10^{-2} g/L, path length = 10 mm).

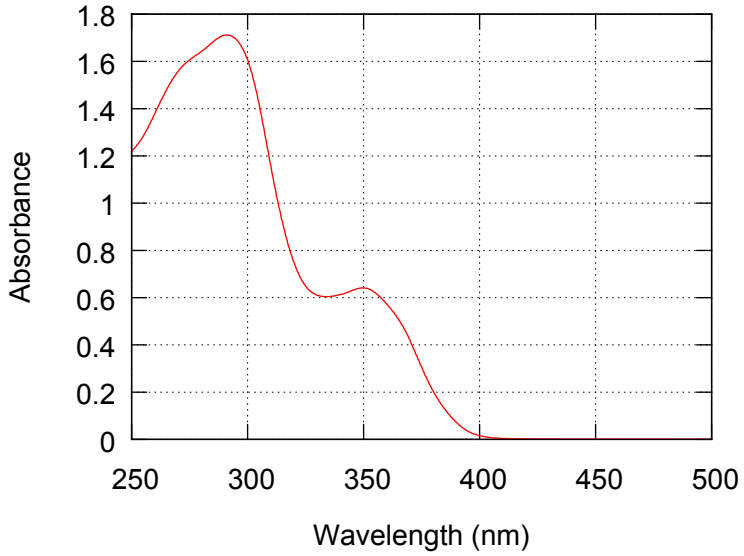

Figure S159. UV-vis absorption spectrum of **5(40)** in $CHCl_3$ (3×10^{-2} g/L, path length = 10 mm).

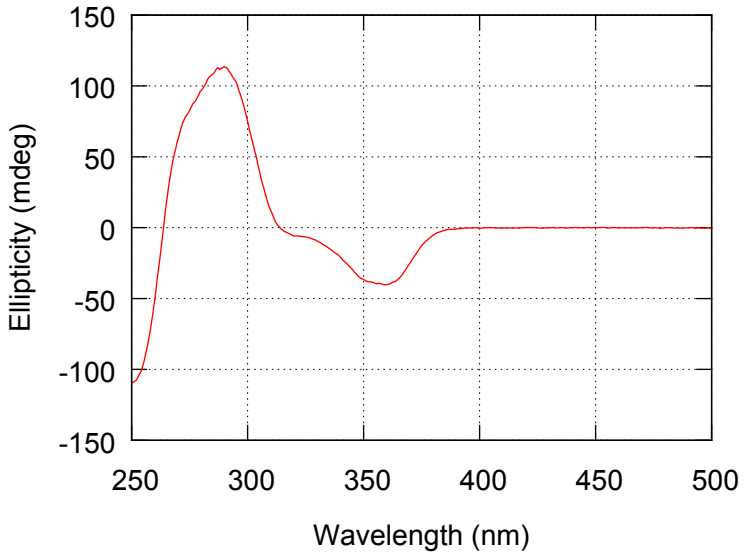

Figure S160. CD spectrum of **5(40)** in $CHCl_3$ (3×10^{-2} g/L, path length = 10 mm).

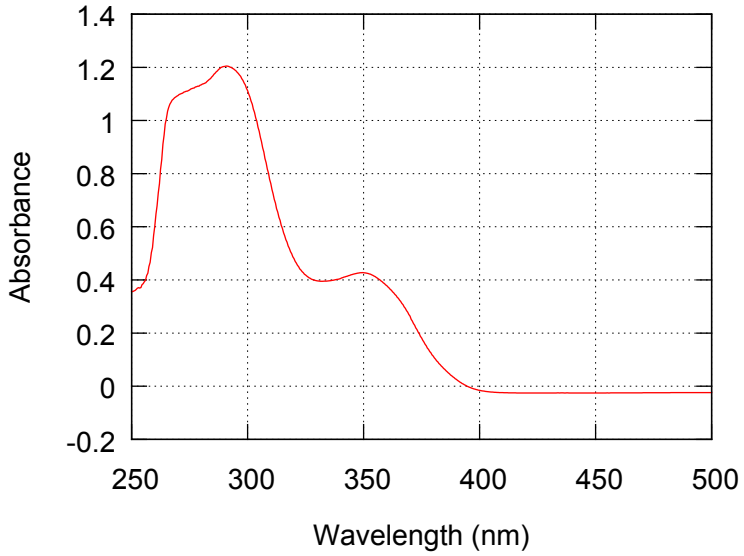

Figure S161. UV-vis absorption spectrum of **5(40)** in 1,1,2-TCE (2.46×10^{-2} g/L, path length = 10 mm).

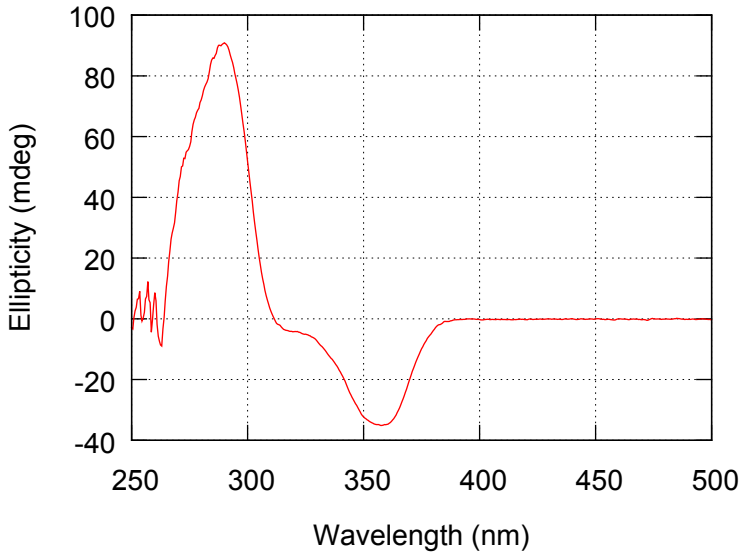

Figure S162. CD spectrum of **5(40)** in 1,1,2-TCE (2.46×10^{-2} g/L, path length = 10 mm).

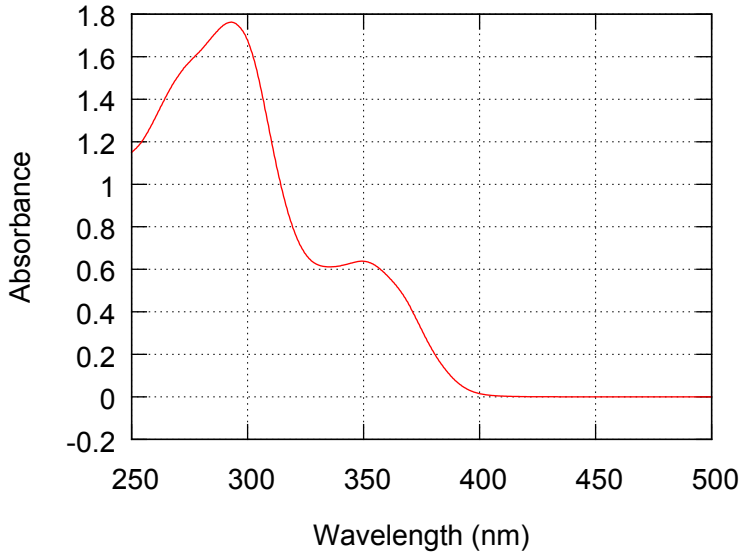

Figure S163. UV-vis absorption spectrum of **5(40)** in THF (3×10^{-2} g/L, path length = 10 mm).

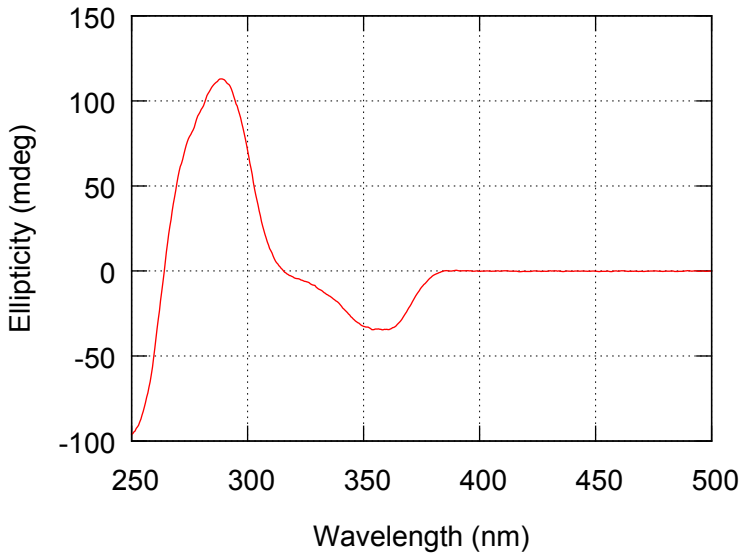

Figure S164. CD spectrum of **5(40)** in THF (3×10^{-2} g/L, path length = 10 mm).

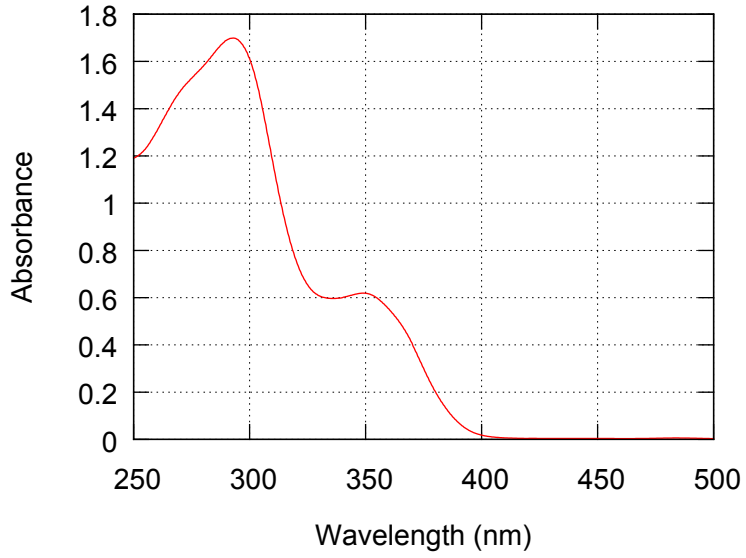

Figure S165. UV-vis absorption spectrum of **5(40)** in 1,4-Dioxane (3×10^{-2} g/L, path length = 10 mm).

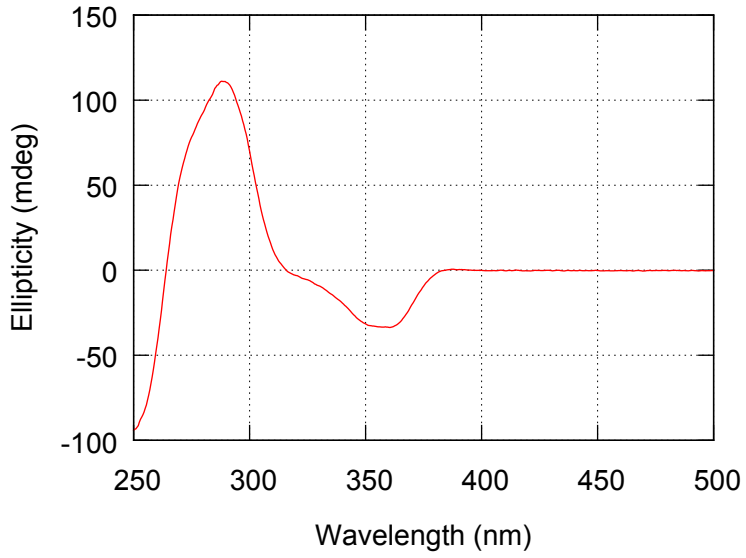

Figure S166. CD spectrum of **5(40)** in 1,4-Dioxane (3×10^{-2} g/L, path length = 10 mm).

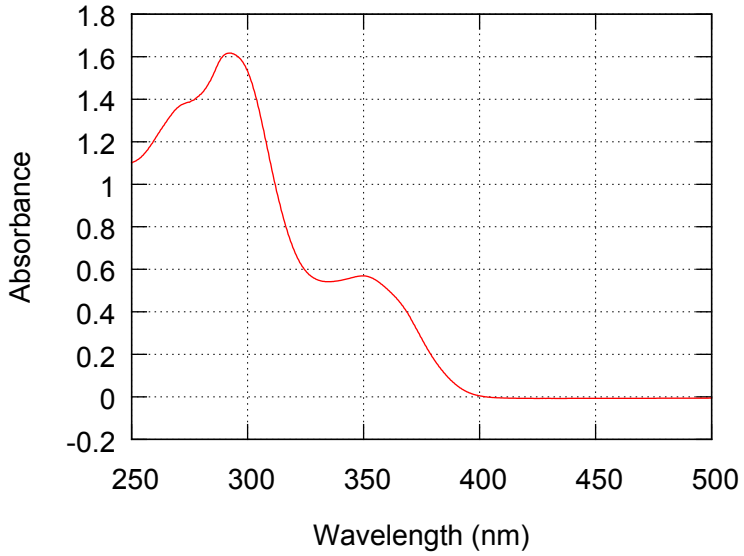

Figure S167. UV-vis absorption spectrum of **5(40)** in 2-MeTHF (3×10^{-2} g/L, path length = 10 mm).

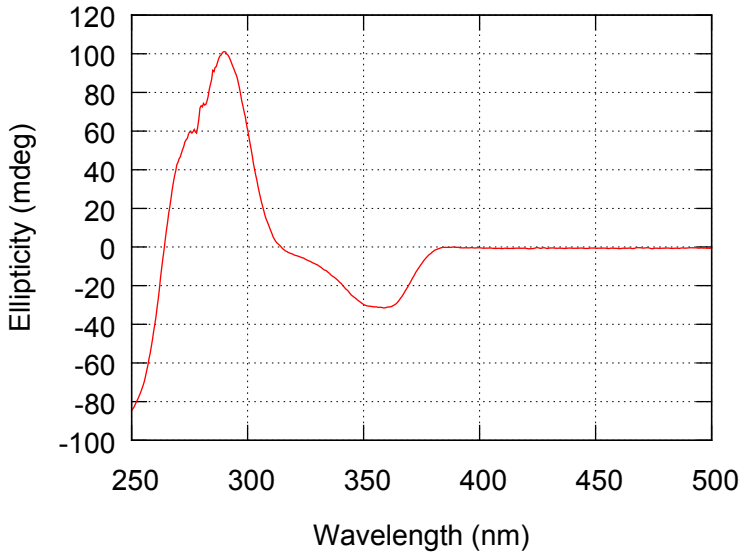

Figure S168. CD spectrum of **5(40)** in 2-MeTHF (3×10^{-2} g/L, path length = 10 mm).

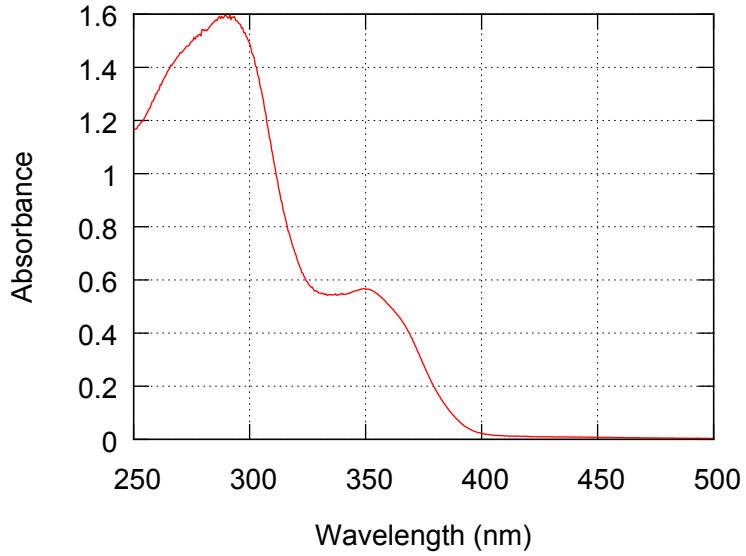

Figure S169. UV-vis absorption spectrum of **5(40)** in 1,2-DME (3.49×10^{-2} g/L, path length = 10 mm).

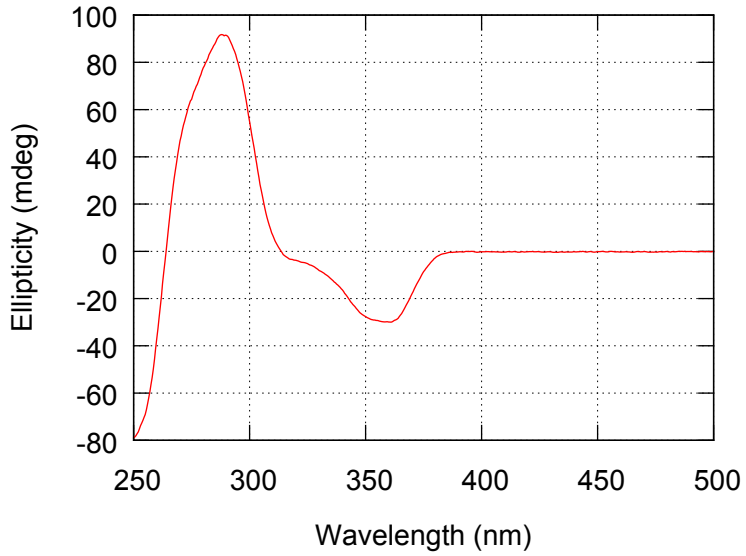

Figure S170. CD spectrum of **5(40)** in 1,2-DME (3.49×10^{-2} g/L, path length = 10 mm).

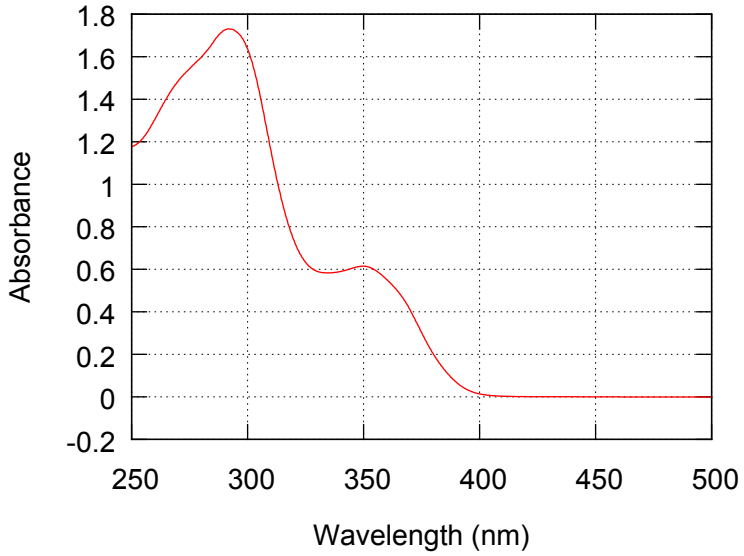

Figure S171. UV-vis absorption spectrum of **5(40)** in CPME (3×10^{-2} g/L, path length = 10 mm).

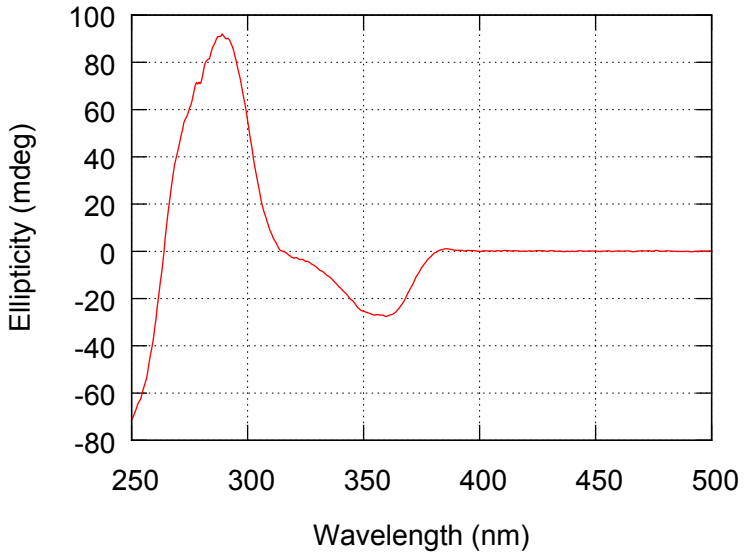

Figure S172. CD spectrum of **5(40)** in CPME (3×10^{-2} g/L, path length = 10 mm).

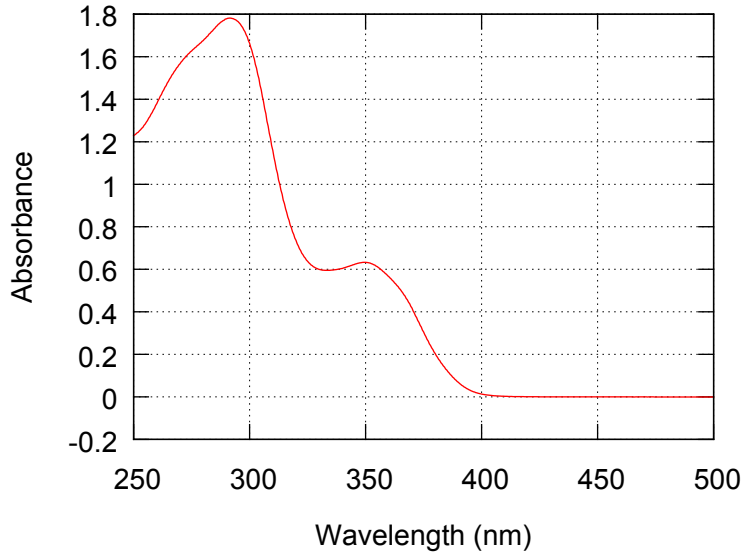

Figure S173. UV-vis absorption spectrum of **5(40)** in Et_2O (3×10^{-2} g/L, path length = 10 mm).

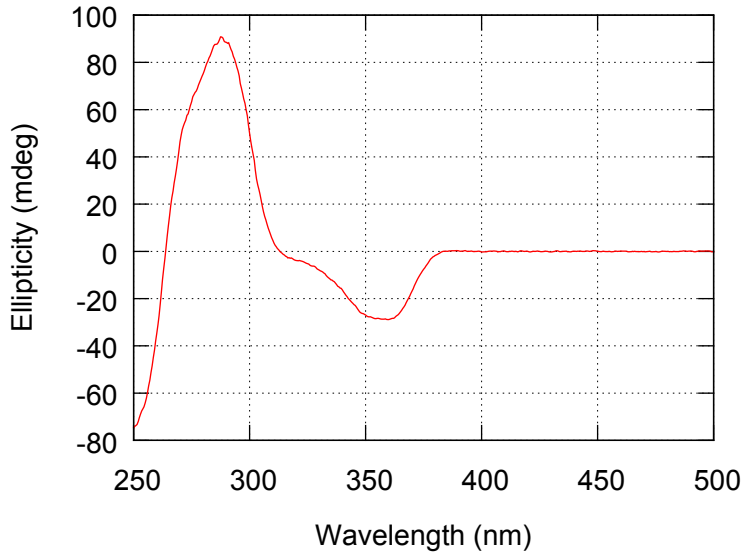

Figure S174. CD spectrum of **5(40)** in Et_2O (3×10^{-2} g/L, path length = 10 mm).

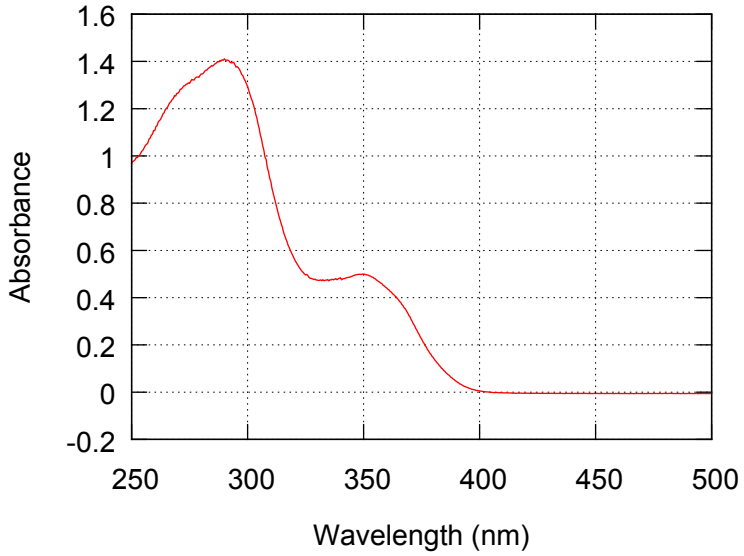

Figure S175. UV-vis absorption spectrum of **5(40)** in MTBE (3.49×10^{-2} g/L, path length = 10 mm).

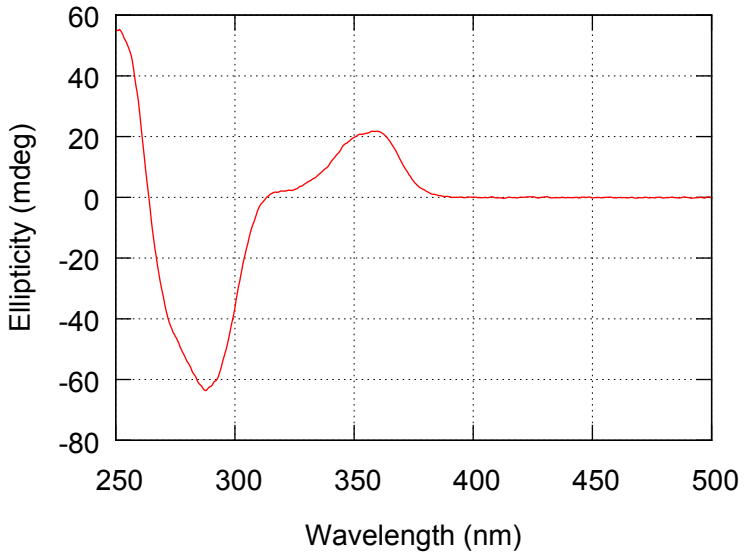

Figure S176. CD spectrum of **5(40)** in MTBE (3.49×10^{-2} g/L, path length = 10 mm).

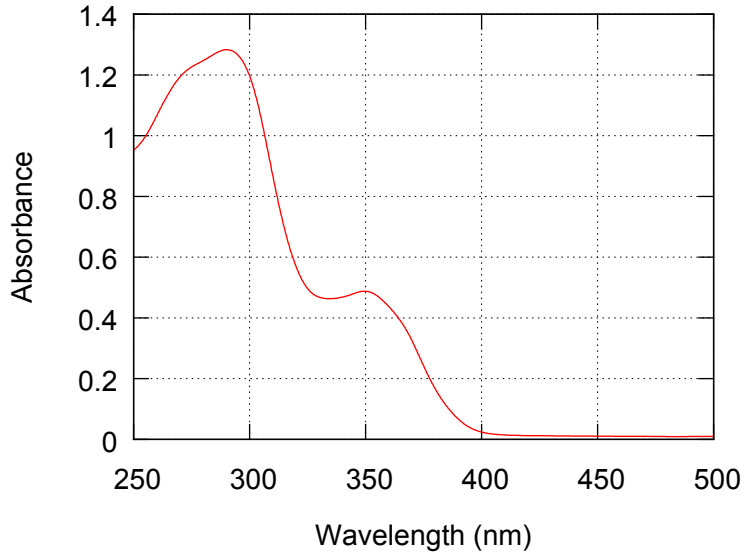

Figure S177. UV-vis absorption spectrum of **6(40)** in $CHCl_3$ (3.01×10^{-2} g/L, path length = 10 mm).

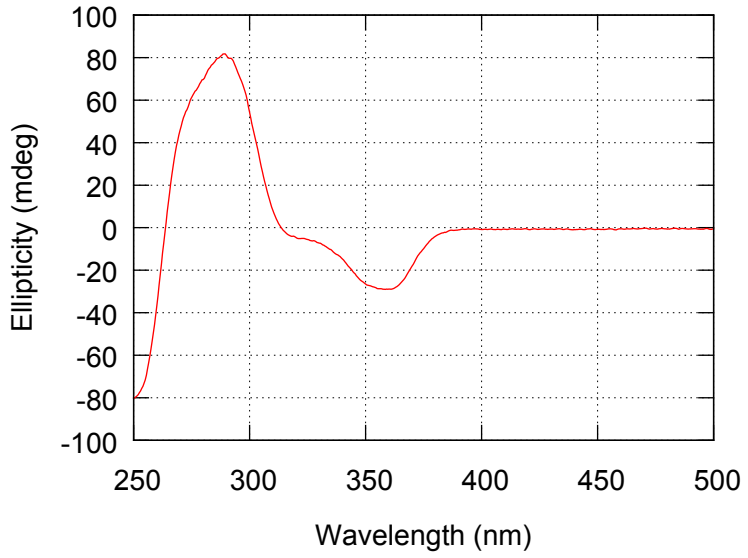

Figure S178. CD spectrum of **6(40)** in $CHCl_3$ (3.01×10^{-2} g/L, path length = 10 mm).

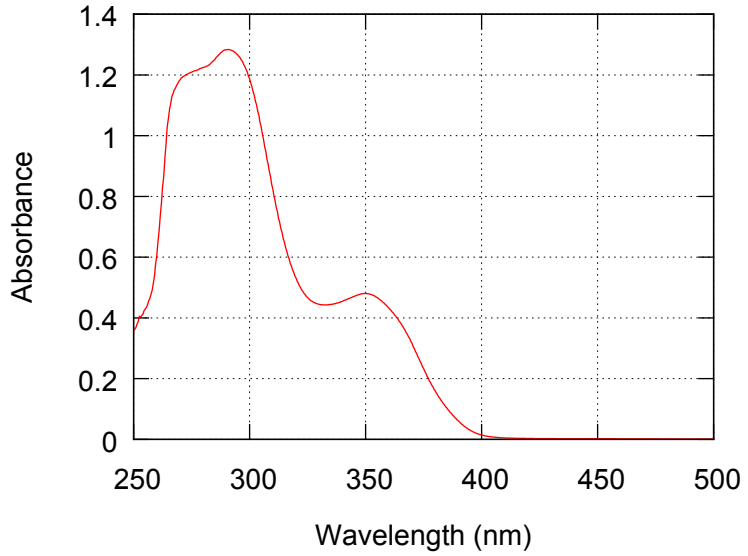

Figure S179. UV-vis absorption spectrum of **6(40)** in 1,1,2-TCE (3.01×10^{-2} g/L, path length = 10 mm).

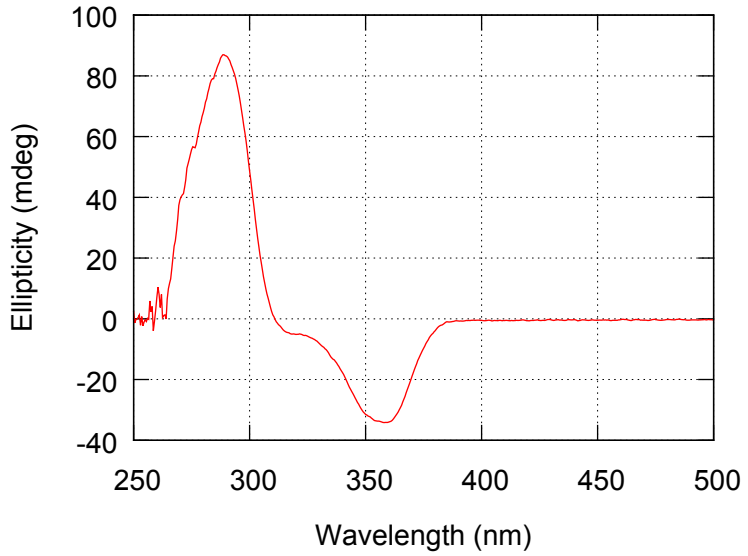

Figure S180. CD spectrum of **6(40)** in 1,1,2-TCE (3.01×10^{-2} g/L, path length = 10 mm).

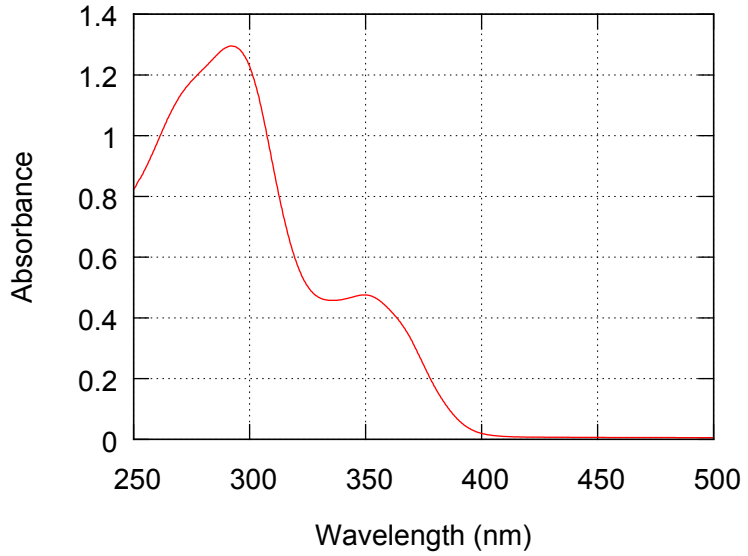

Figure S181. UV-vis absorption spectrum of **6(40)** in THF (3.01×10^{-2} g/L, path length = 10 mm).

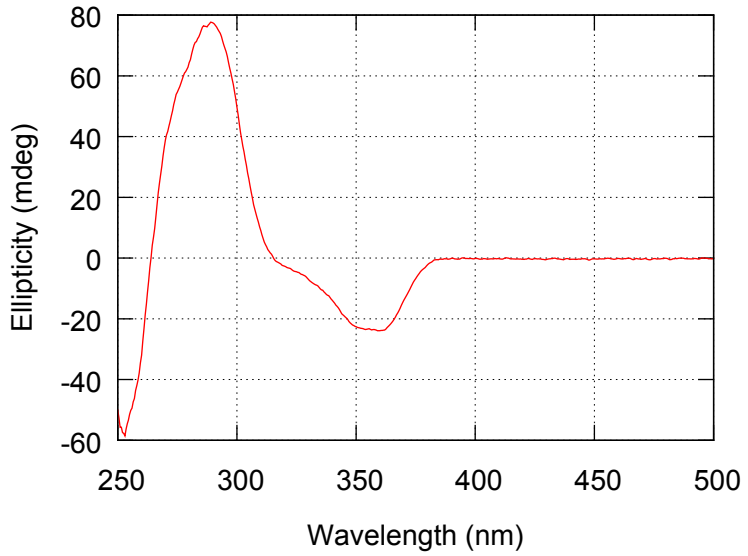

Figure S182. CD spectrum of **6(40)** in THF (3.01×10^{-2} g/L, path length = 10 mm).

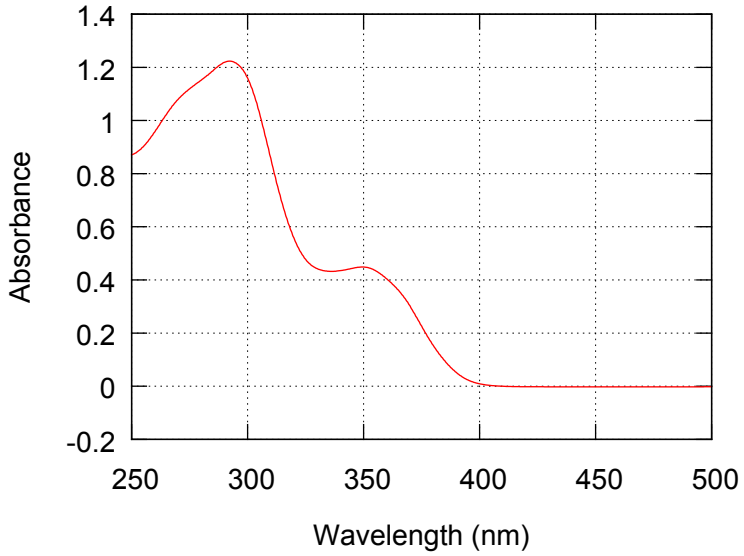

Figure S183. UV-vis absorption spectrum of **6(40)** in 1,4-Dioxane (3.01×10^{-2} g/L, path length = 10 mm).

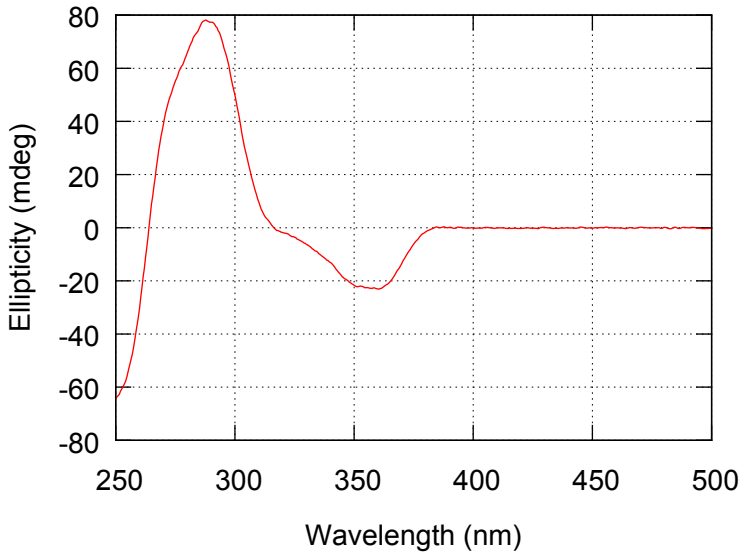

Figure S184. CD spectrum of **6(40)** in 1,4-Dioxane (3.01×10^{-2} g/L, path length = 10 mm).

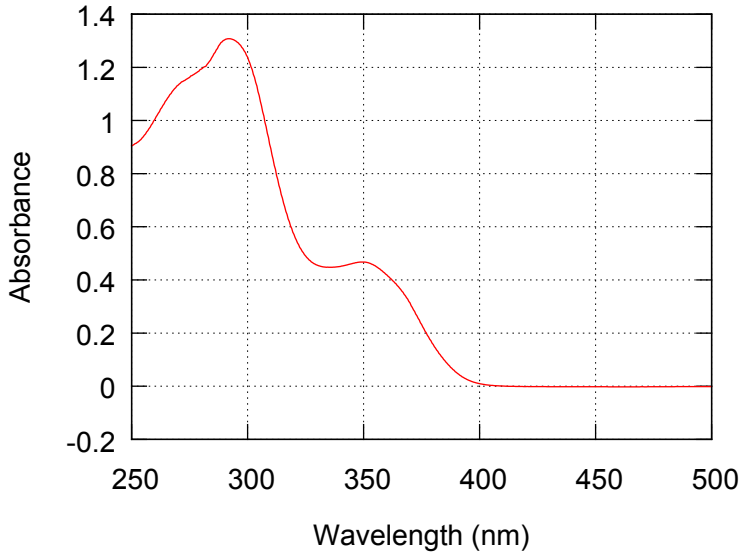

Figure S185. UV-vis absorption spectrum of **6(40)** in 2-MeTHF (3.01×10^{-2} g/L, path length = 10 mm).

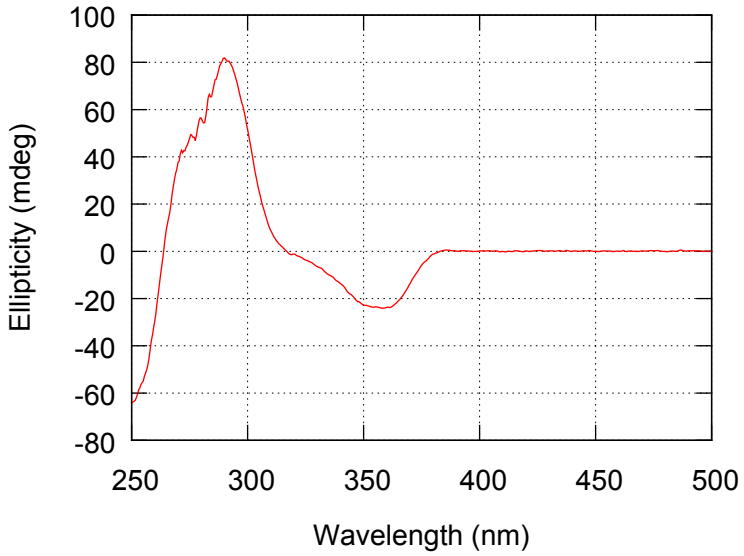

Figure S186. CD spectrum of **6(40)** in 2-MeTHF (3.01×10^{-2} g/L, path length = 10 mm).

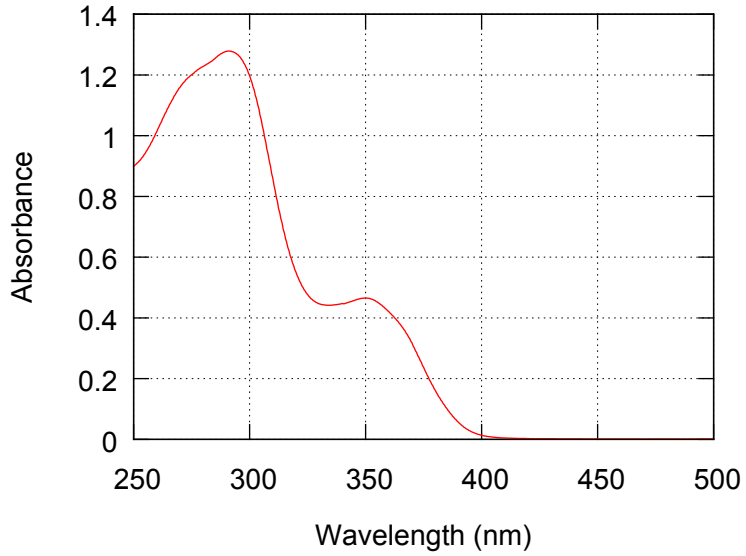

Figure S187. UV-vis absorption spectrum of **6(40)** in 1,2-DME (3.01×10^{-2} g/L, path length = 10 mm).

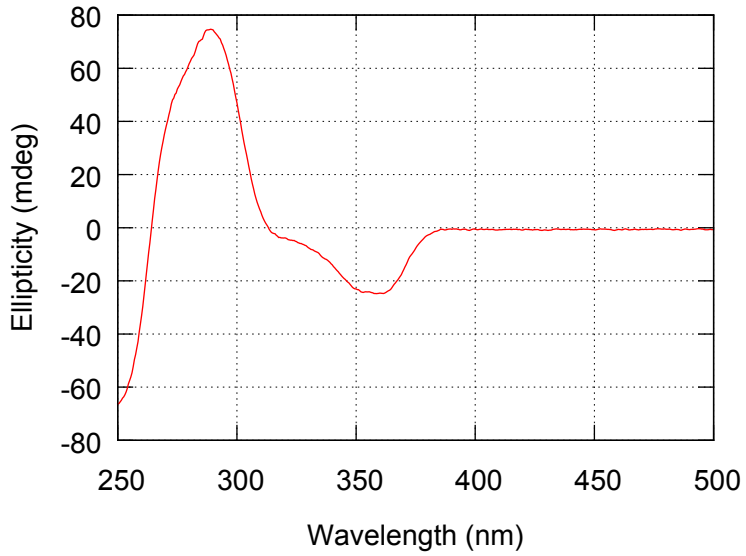

Figure S188. CD spectrum of **6(40)** in 1,2-DME (3.01×10^{-2} g/L, path length = 10 mm).

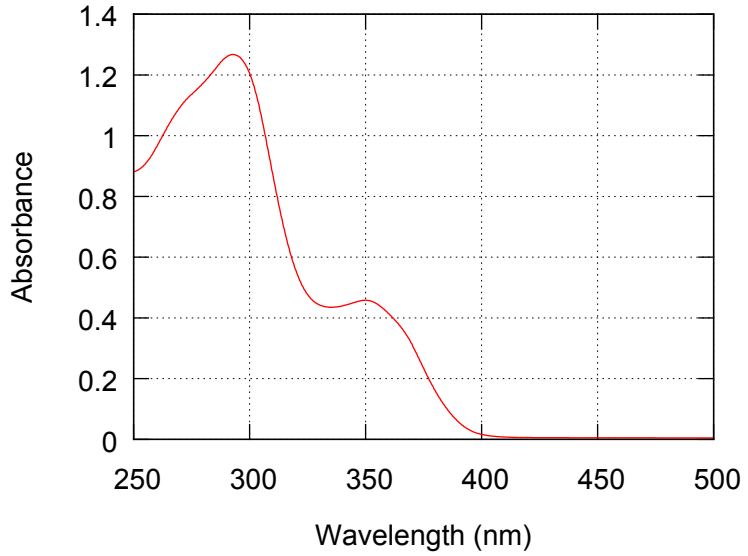

Figure S189. UV-vis absorption spectrum of **6(40)** in CPME (3.01×10^{-2} g/L, path length = 10 mm).

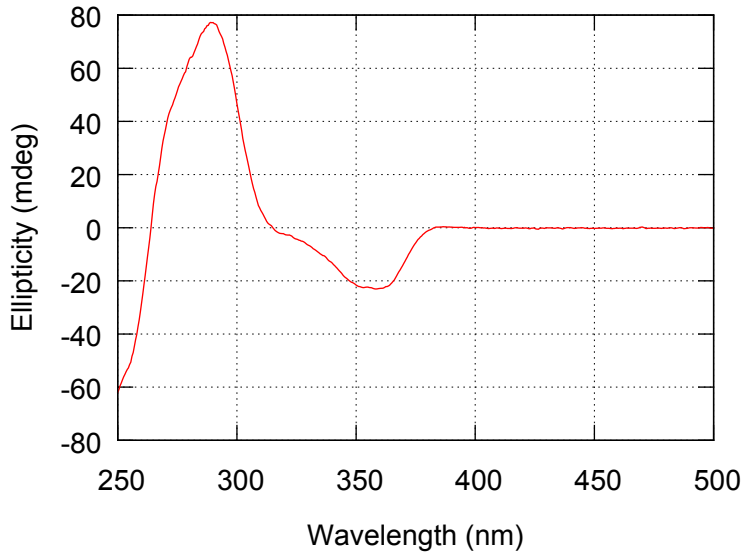

Figure S190. CD spectrum of **6(40)** in CPME (3.01×10^{-2} g/L, path length = 10 mm).

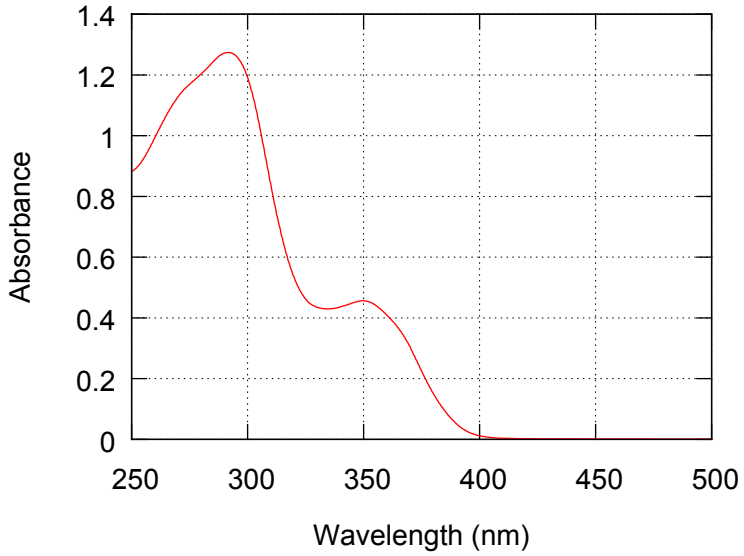

Figure S191. UV-vis absorption spectrum of **6(40)** in Et_2O (3.01×10^{-2} g/L, path length = 10 mm).

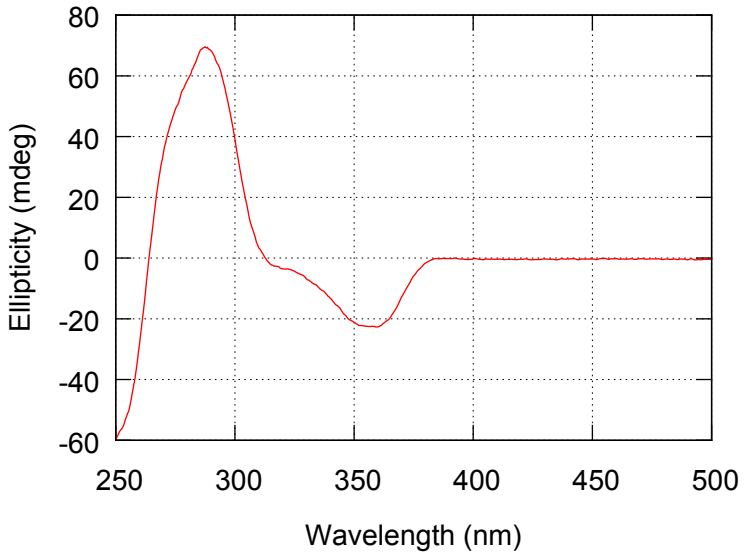

Figure S192. CD spectrum of **6(40)** in Et_2O (3.01×10^{-2} g/L, path length = 10 mm).

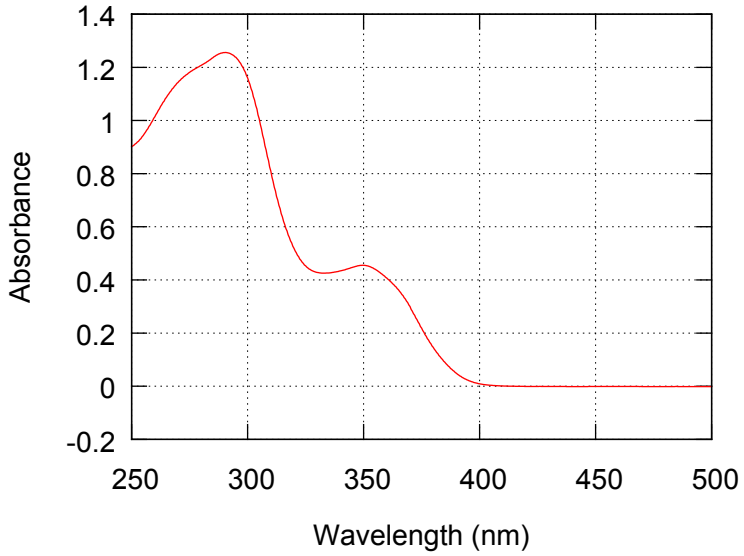

Figure S193. UV-vis absorption spectrum of **6(40)** in MTBE (3.01×10^{-2} g/L, path length = 10 mm).

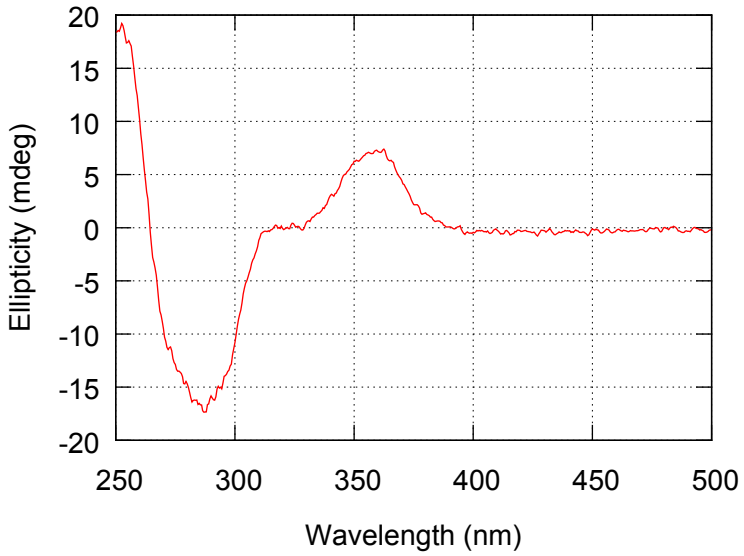

Figure S194. CD spectrum of **6(40)** in MTBE (3.01×10^{-2} g/L, path length = 10 mm).

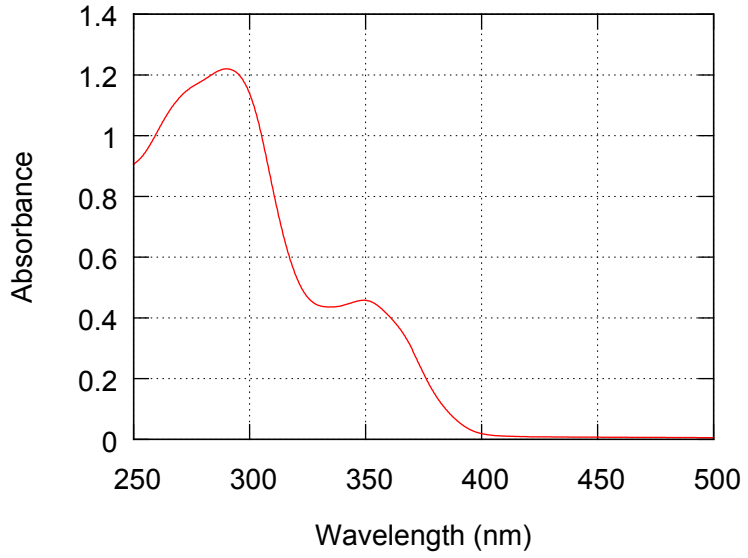

Figure S195. UV-vis absorption spectrum of **7(40)** in $CHCl_3$ (2.99×10^{-2} g/L, path length = 10 mm).

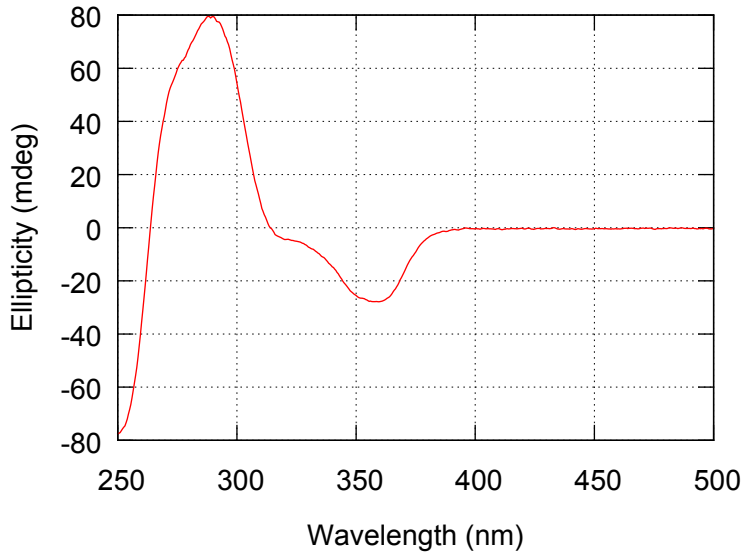

Figure S196. CD spectrum of **7(40)** in $CHCl_3$ (2.99×10^{-2} g/L, path length = 10 mm).

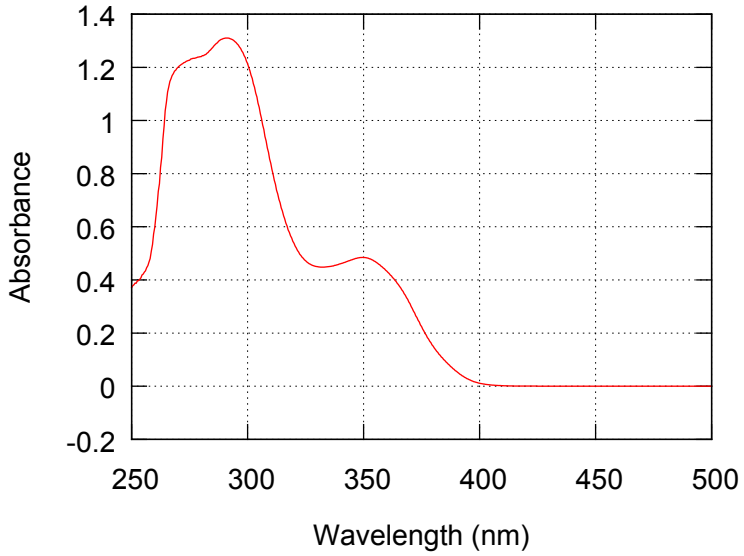

Figure S197. UV-vis absorption spectrum of **7(40)** in 1,1,2-TCE (2.99×10^{-2} g/L, path length = 10 mm).

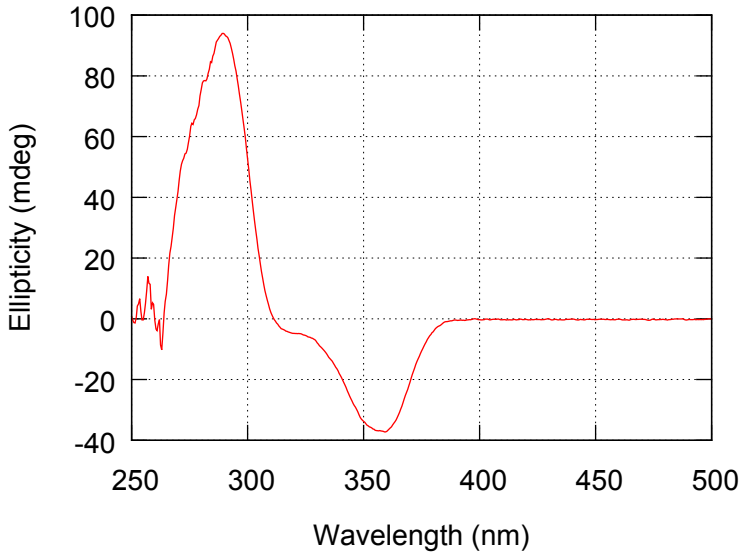

Figure S198. CD spectrum of **7(40)** in 1,1,2-TCE (2.99×10^{-2} g/L, path length = 10 mm).

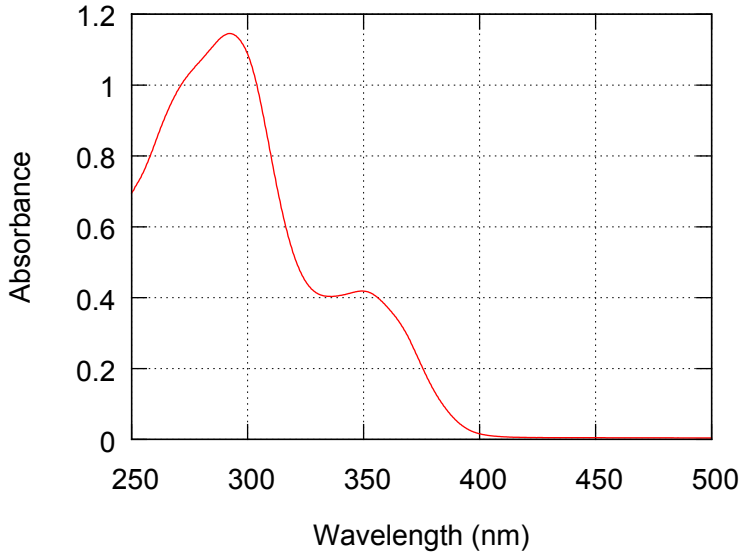

Figure S199. UV-vis absorption spectrum of **7(40)** in THF (2.99×10^{-2} g/L, path length = 10 mm).

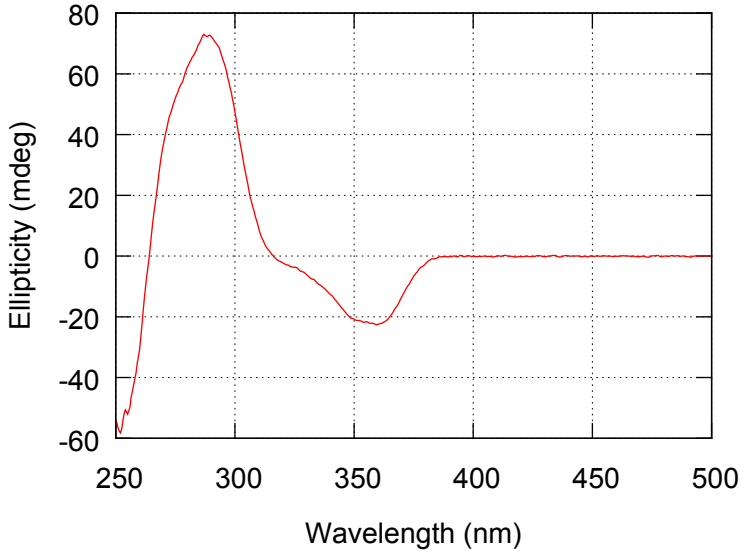

Figure S200. CD spectrum of **7(40)** in THF (2.99×10^{-2} g/L, path length = 10 mm).

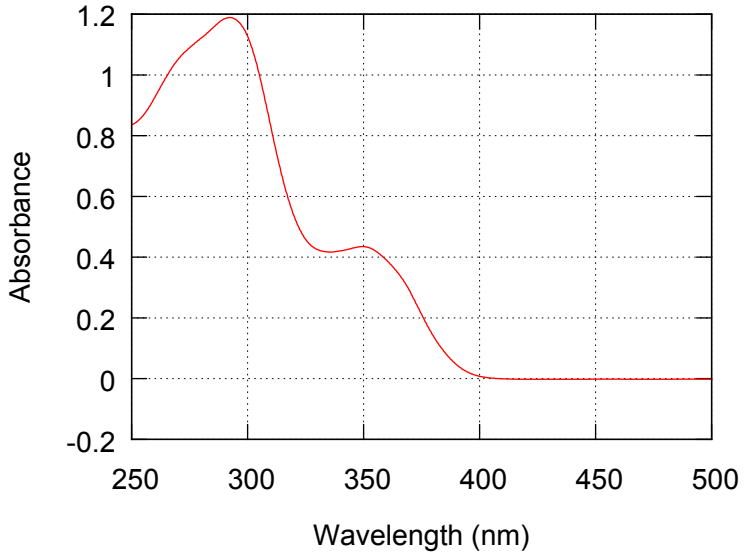

Figure S201. UV-vis absorption spectrum of **7(40)** in 1,4-Dioxane (2.99×10^{-2} g/L, path length = 10 mm).

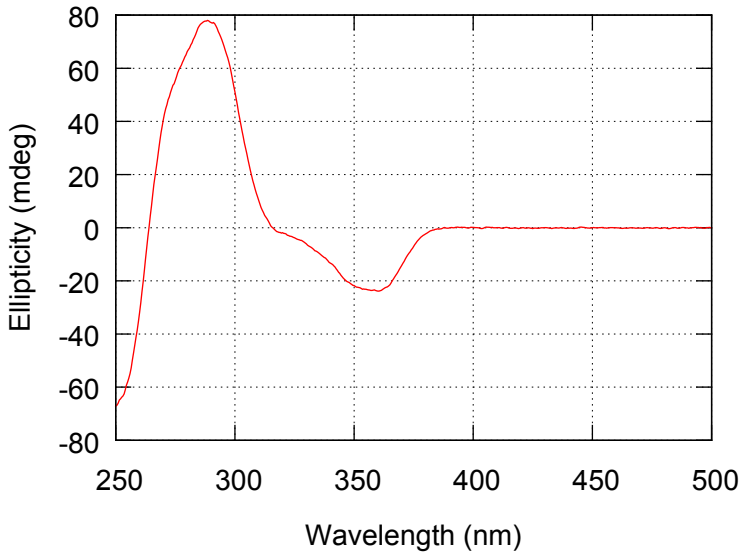

Figure S202. CD spectrum of **7(40)** in 1,4-Dioxane (2.99×10^{-2} g/L, path length = 10 mm).

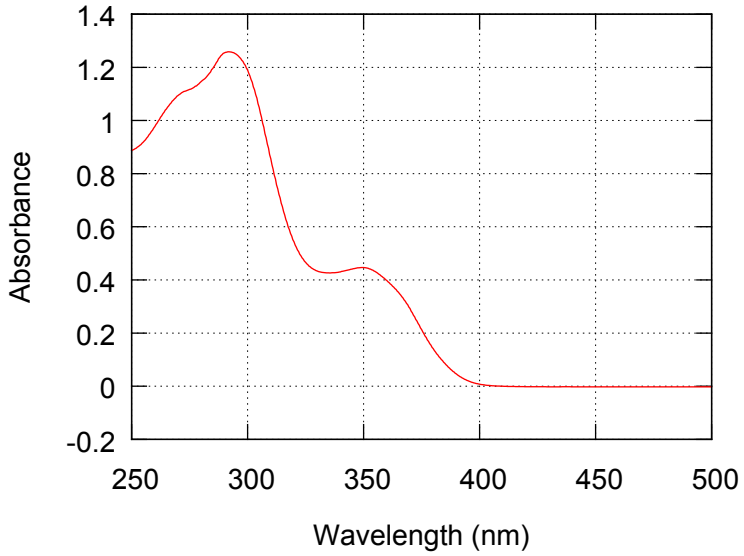

Figure S203. UV-vis absorption spectrum of **7(40)** in 2-MeTHF (2.99×10^{-2} g/L, path length = 10 mm).

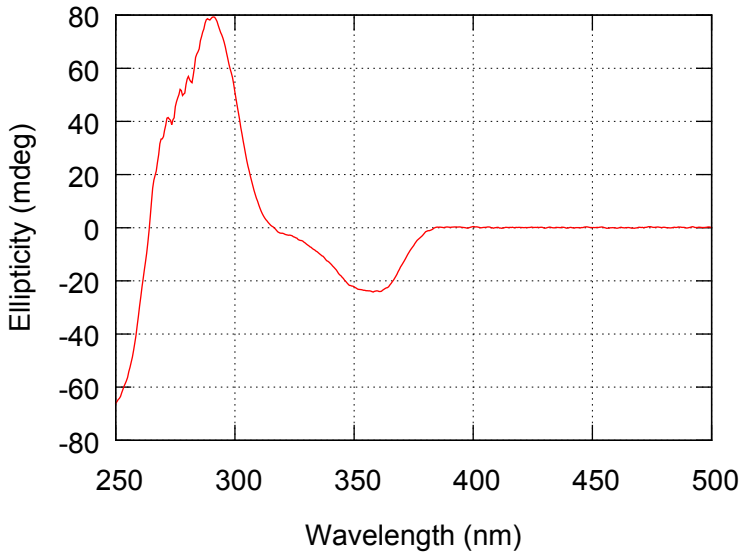

Figure S204. CD spectrum of **7(40)** in 2-MeTHF (2.99×10^{-2} g/L, path length = 10 mm).

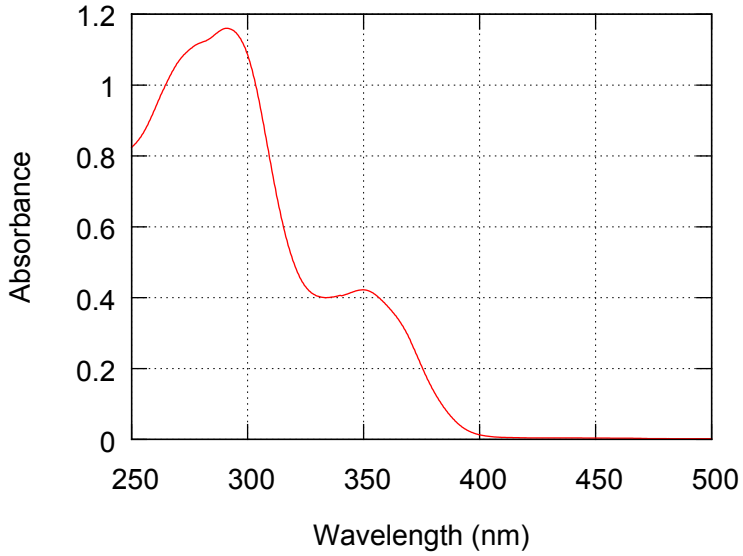

Figure S205. UV-vis absorption spectrum of **7(40)** in 1,2-DME (2.99×10^{-2} g/L, path length = 10 mm).

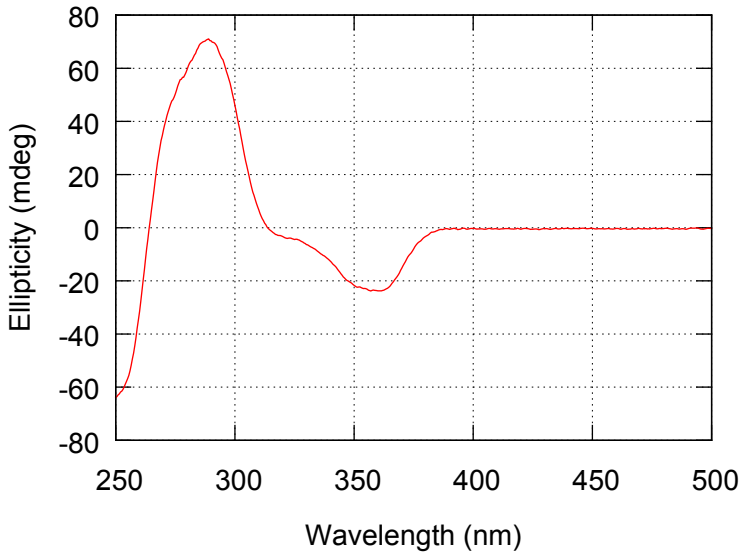

Figure S206. CD spectrum of **7(40)** in 1,2-DME (2.99×10^{-2} g/L, path length = 10 mm).

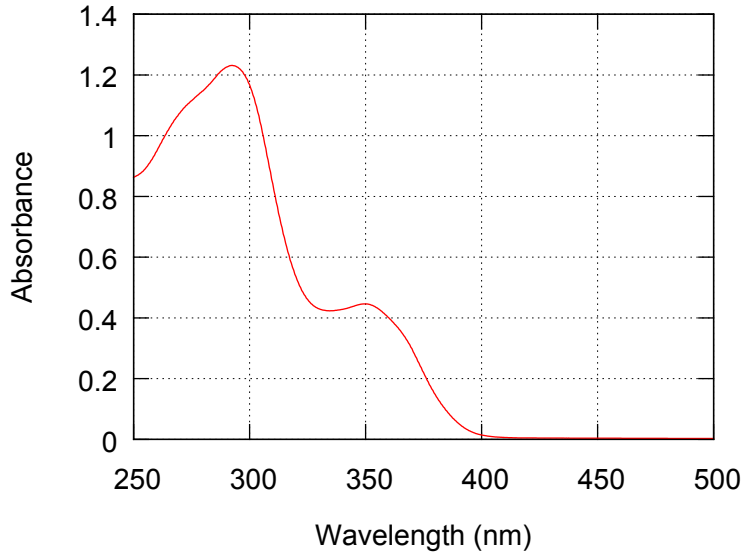

Figure S207. UV-vis absorption spectrum of **7(40)** in CPME (2.99×10^{-2} g/L, path length = 10 mm).

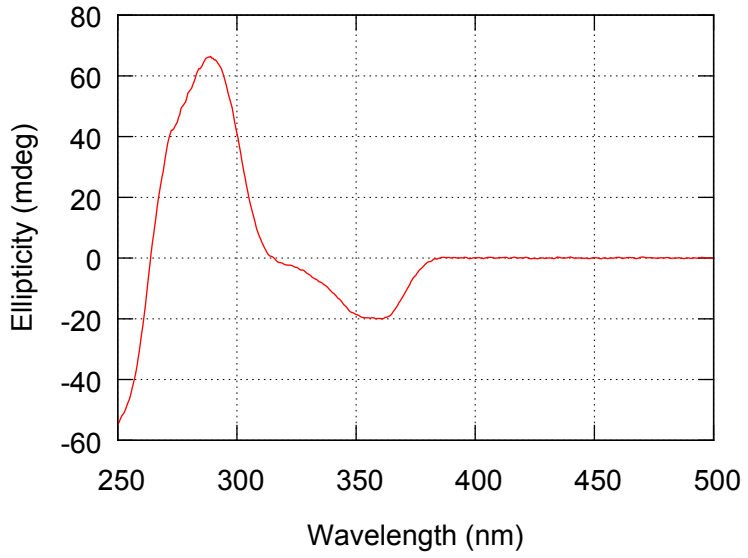

Figure S208. CD spectrum of **7(40)** in CPME (2.99×10^{-2} g/L, path length = 10 mm).

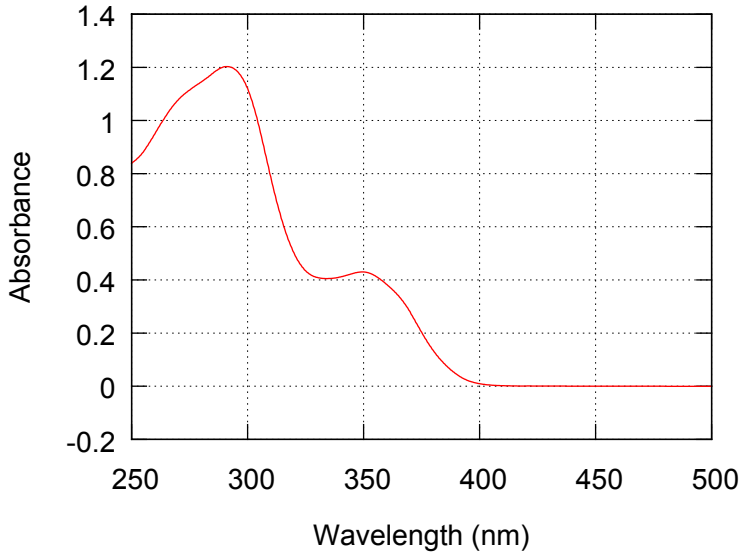

Figure S209. UV-vis absorption spectrum of **7(40)** in Et_2O (2.99×10^{-2} g/L, path length = 10 mm).

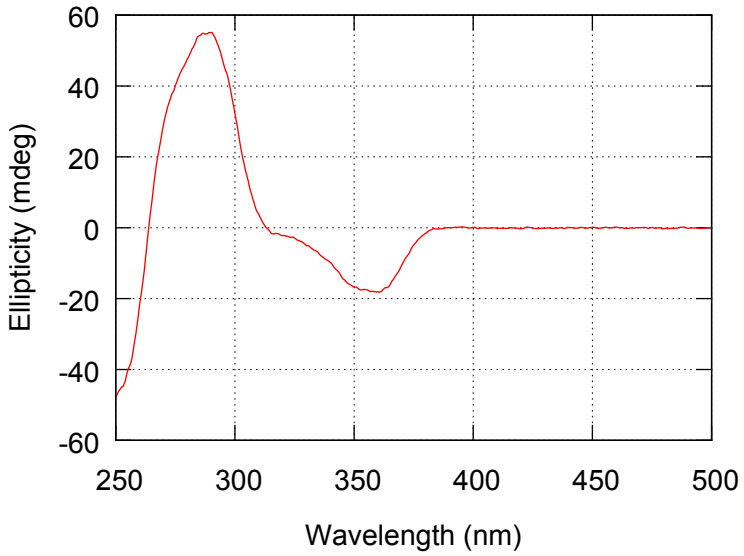

Figure S210. CD spectrum of **7(40)** in Et_2O (2.99×10^{-2} g/L, path length = 10 mm).

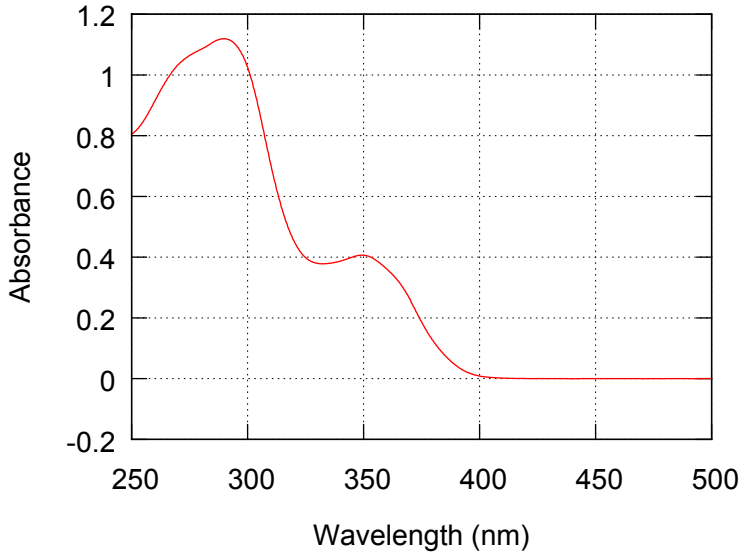

Figure S211. UV-vis absorption spectrum of **7(40)** in MTBE (2.99×10^{-2} g/L, path length = 10 mm).

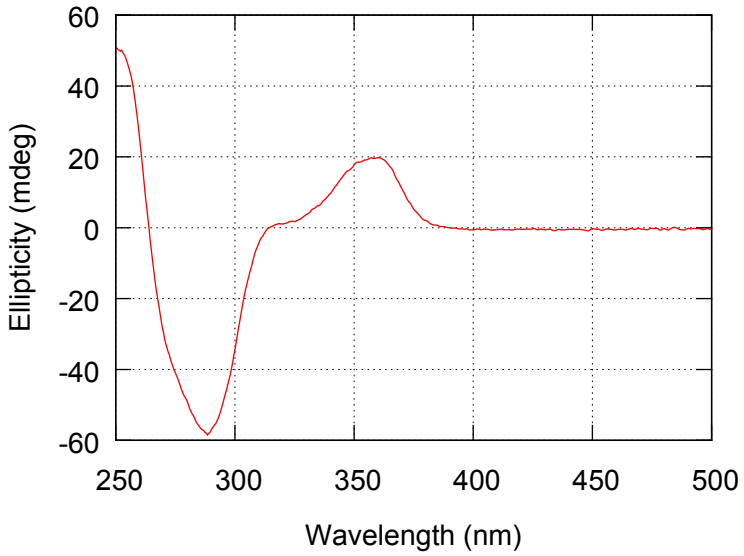

Figure S212. CD spectrum of **7(40)** in MTBE (2.99×10^{-2} g/L, path length = 10 mm).

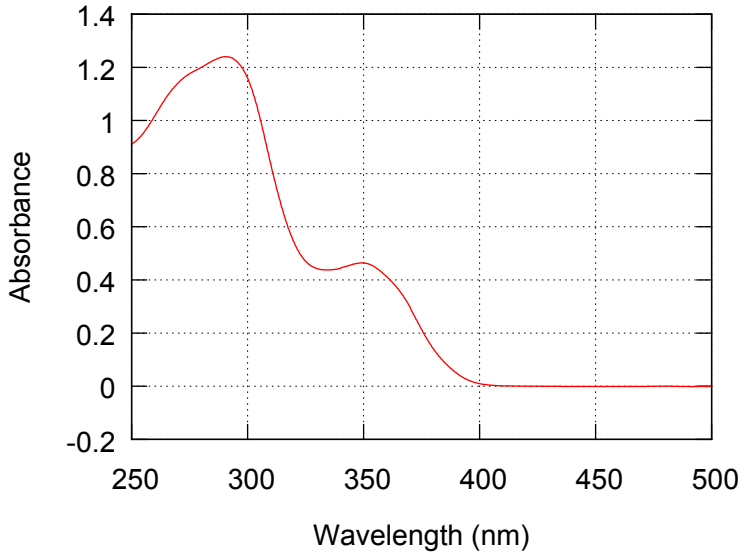

Figure S213. UV-vis absorption spectrum of **8(40)** in $CHCl_3$ (3.02×10^{-2} g/L, path length = 10 mm).

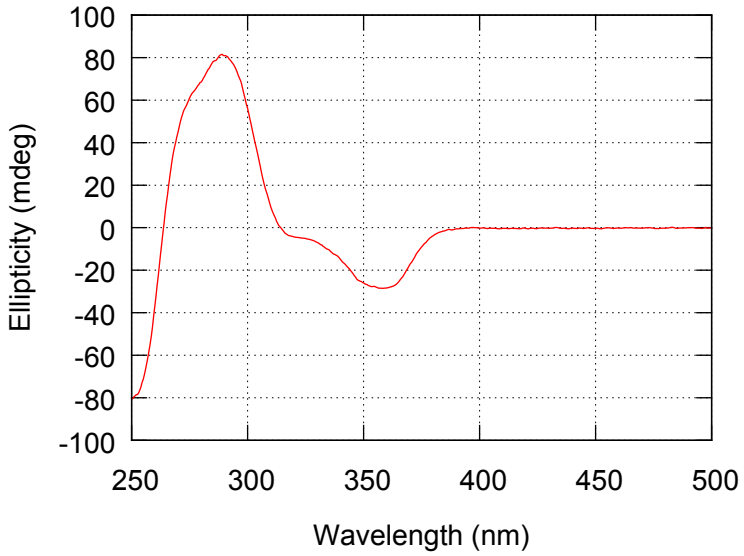

Figure S214. CD spectrum of **8(40)** in $CHCl_3$ (3.02×10^{-2} g/L, path length = 10 mm).

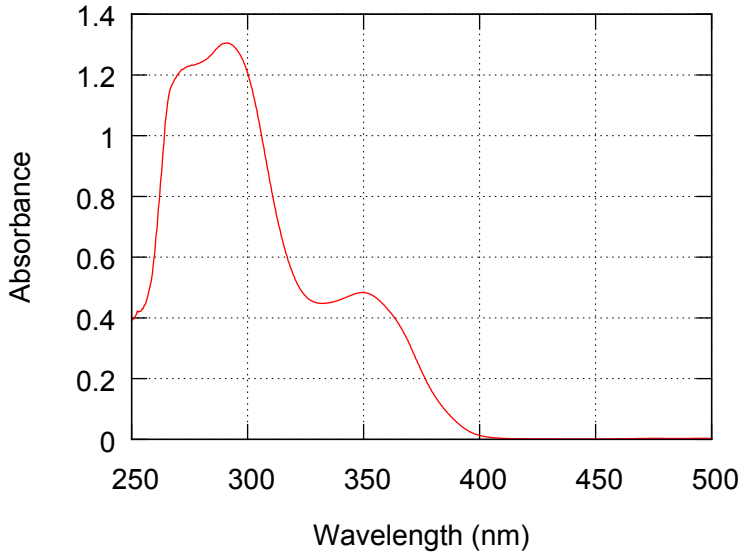

Figure S215. UV-vis absorption spectrum of **8(40)** in 1,1,2-TCE (3.02×10^{-2} g/L, path length = 10 mm).

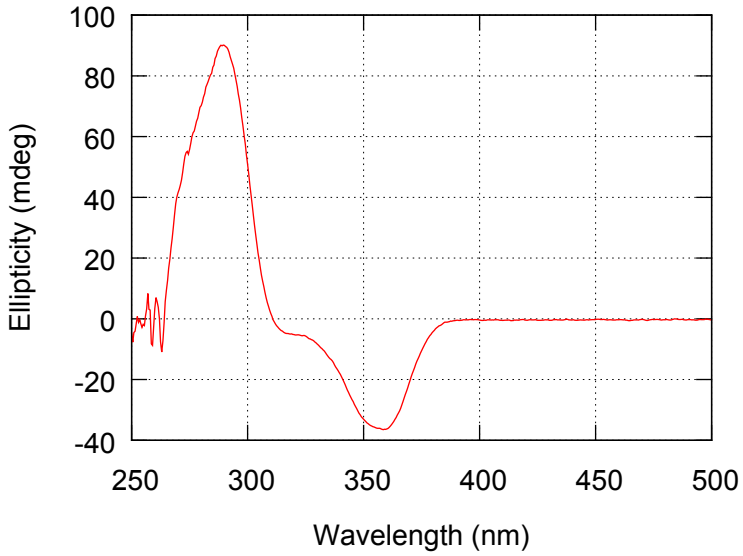

Figure S216. CD spectrum of **8(40)** in 1,1,2-TCE (3.02×10^{-2} g/L, path length = 10 mm).

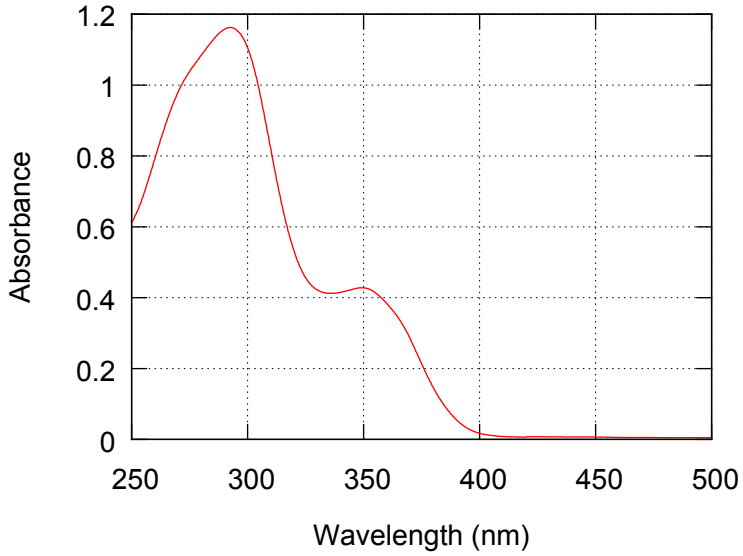

Figure S217. UV-vis absorption spectrum of **8(40)** in THF (3.02×10^{-2} g/L, path length = 10 mm).

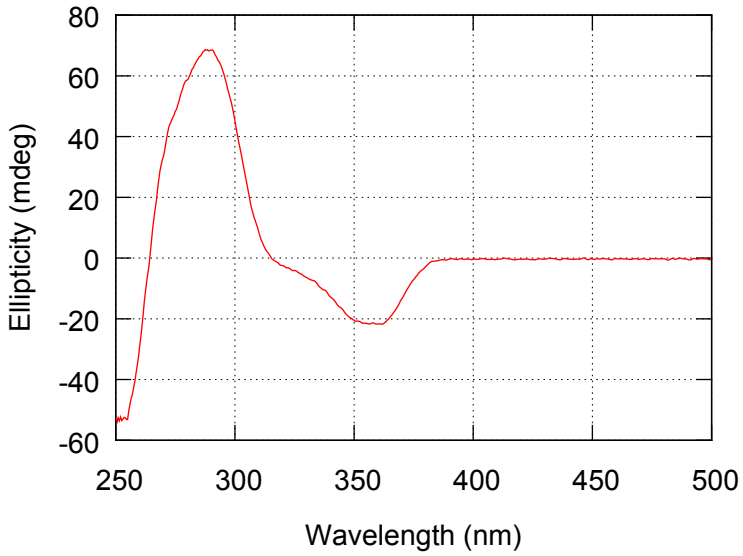

Figure S218. CD spectrum of **8(40)** in THF (3.02×10^{-2} g/L, path length = 10 mm).

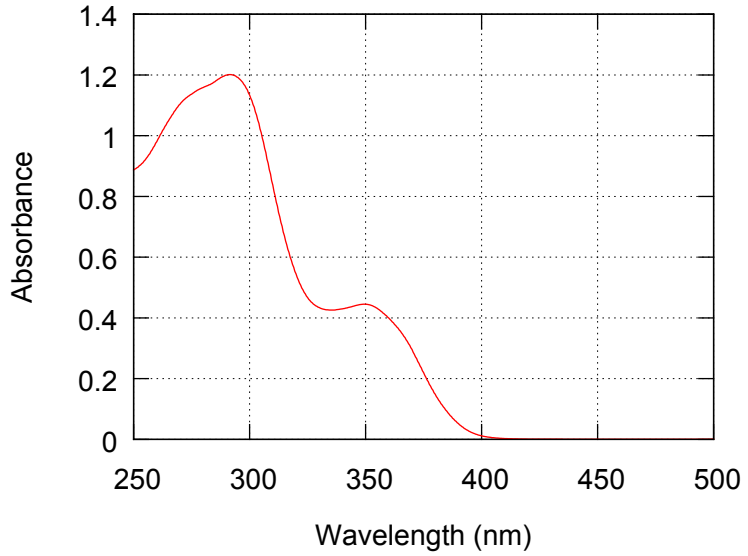

Figure S219. UV-vis absorption spectrum of **8(40)** in 1,4-Dioxane (3.02×10^{-2} g/L, path length = 10 mm).

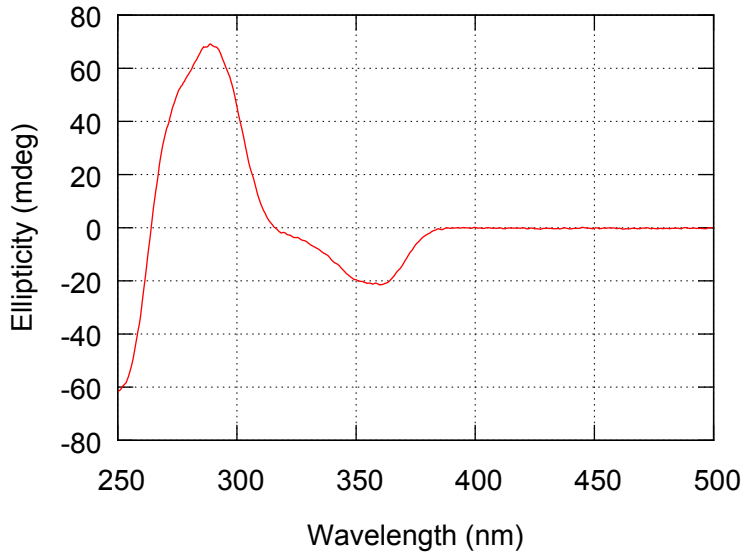

Figure S220. CD spectrum of **8(40)** in 1,4-Dioxane (3.02×10^{-2} g/L, path length = 10 mm).

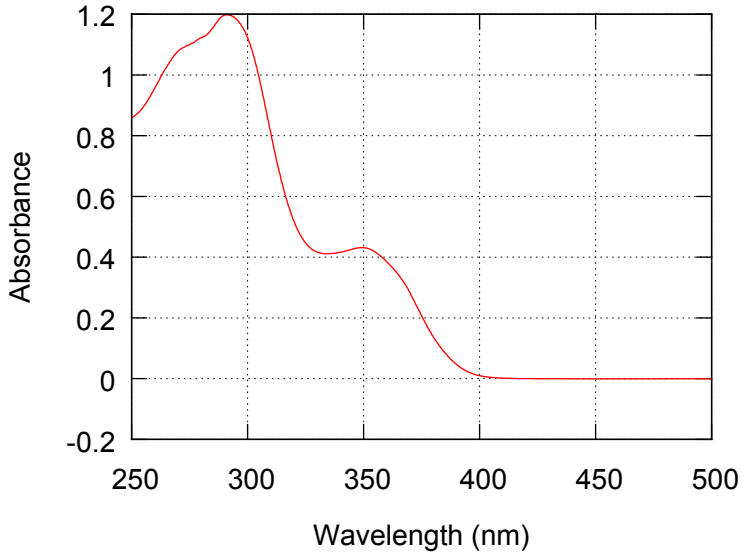

Figure S221. UV-vis absorption spectrum of **8(40)** in 2-MeTHF (3.02×10^{-2} g/L, path length = 10 mm).

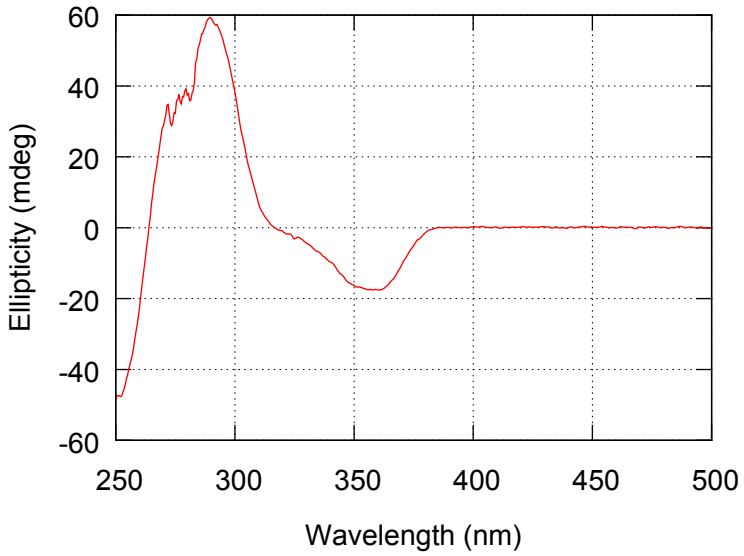

Figure S222. CD spectrum of **8(40)** in 2-MeTHF (3.02×10^{-2} g/L, path length = 10 mm).

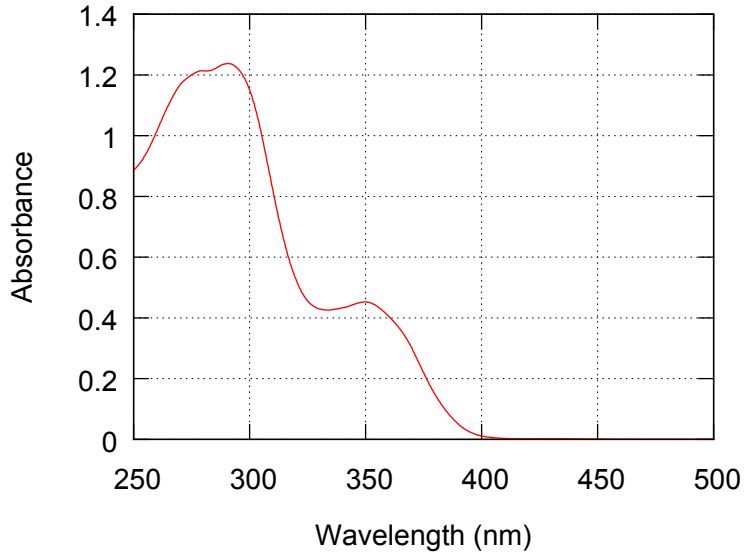

Figure S223. UV-vis absorption spectrum of **8(40)** in 1,2-DME (3.02×10^{-2} g/L, path length = 10 mm).

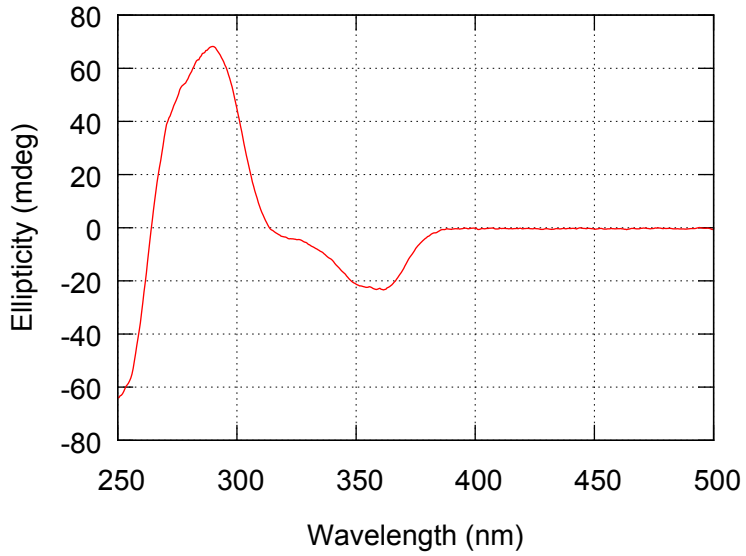

Figure S224. CD spectrum of **8(40)** in 1,2-DME (3.02×10^{-2} g/L, path length = 10 mm).

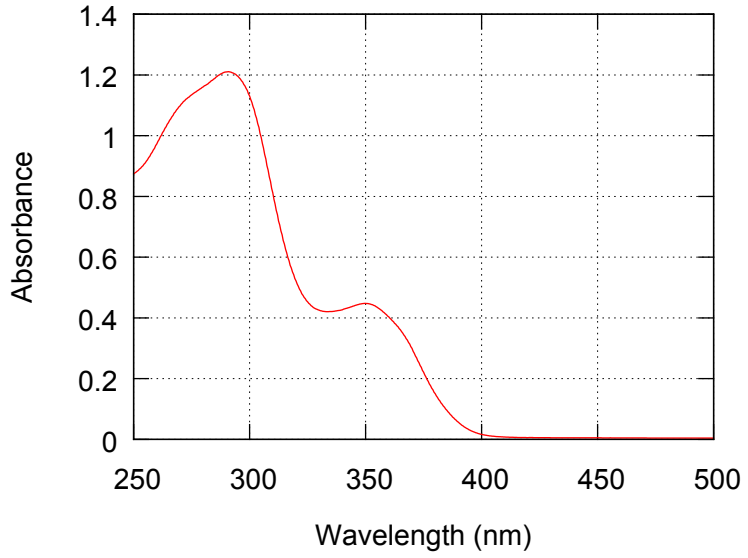

Figure S225. UV-vis absorption spectrum of **8(40)** in CPME (3.02×10^{-2} g/L, path length = 10 mm).

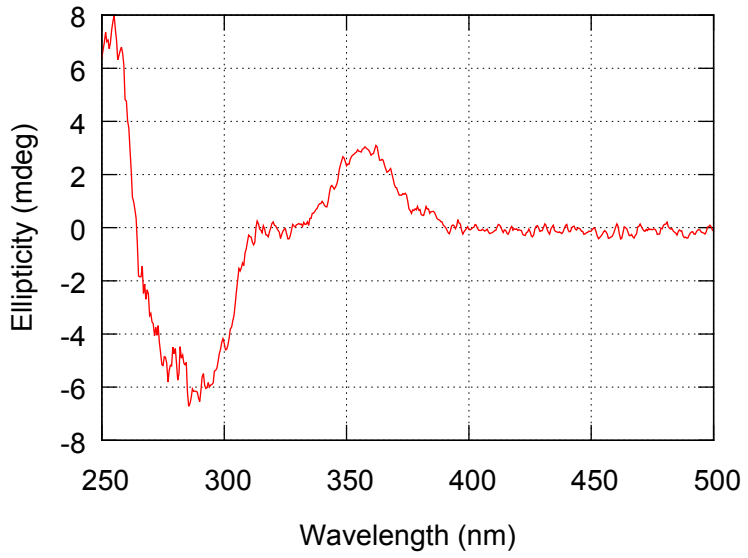

Figure S226. CD spectrum of **8(40)** in CPME (3.02×10^{-2} g/L, path length = 10 mm).

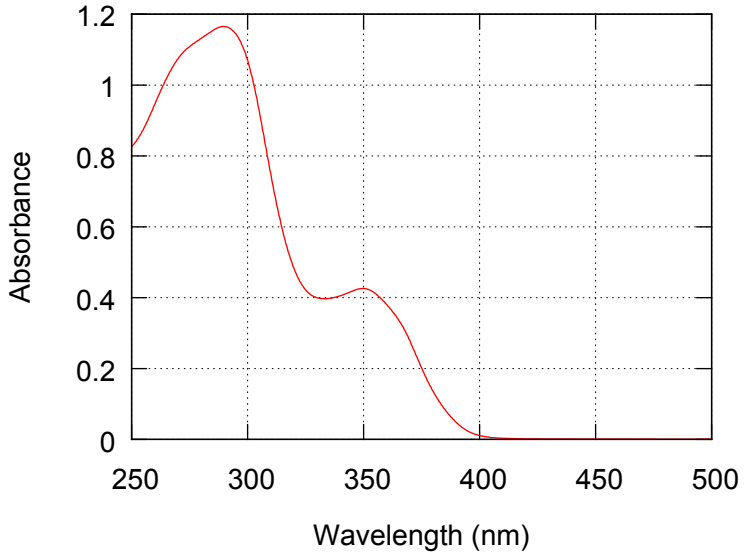

Figure S227. UV-vis absorption spectrum of **8(40)** in Et_2O (3.02×10^{-2} g/L, path length = 10 mm).

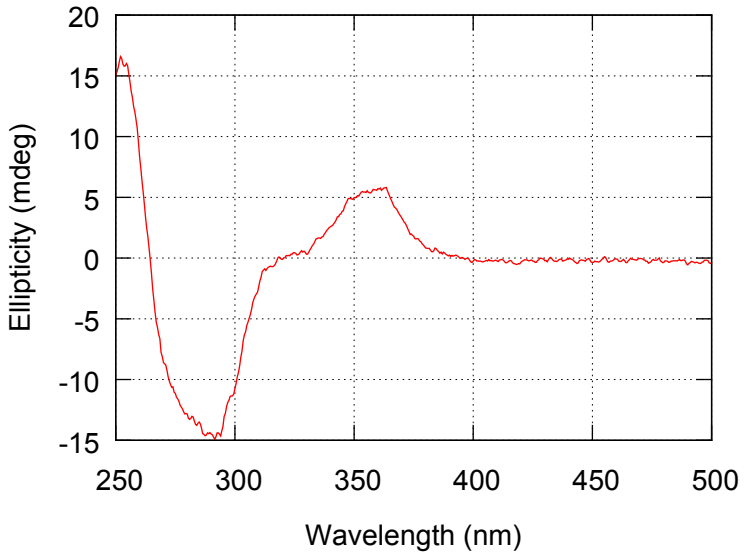

Figure S228. CD spectrum of **8(40)** in Et_2O (3.02×10^{-2} g/L, path length = 10 mm).

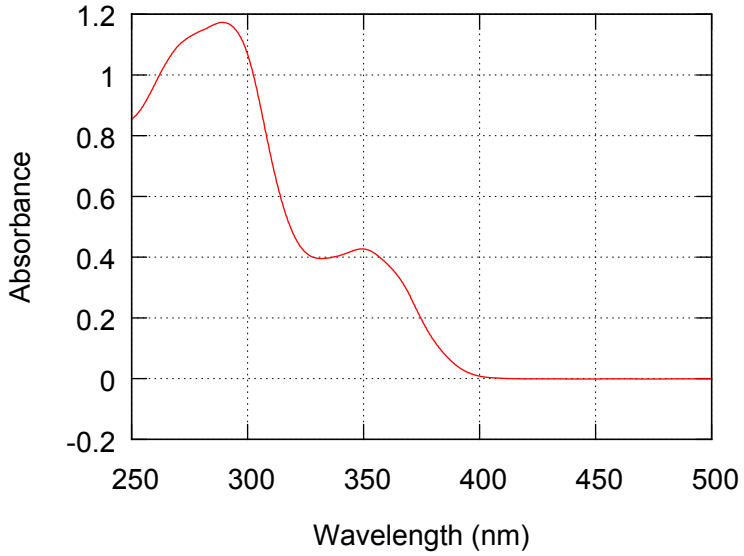

Figure S229. UV-vis absorption spectrum of **8(40)** in MTBE (3.02×10^{-2} g/L, path length = 10 mm).

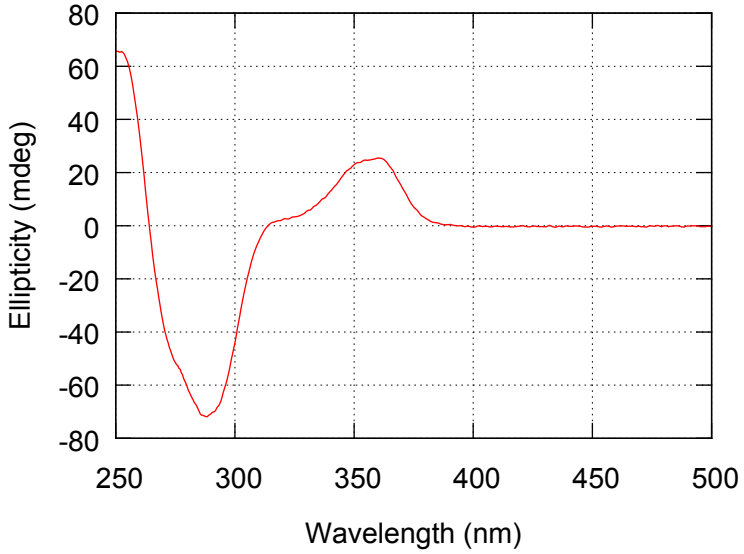

Figure S230. CD spectrum of **8(40)** in MTBE (3.02×10^{-2} g/L, path length = 10 mm).

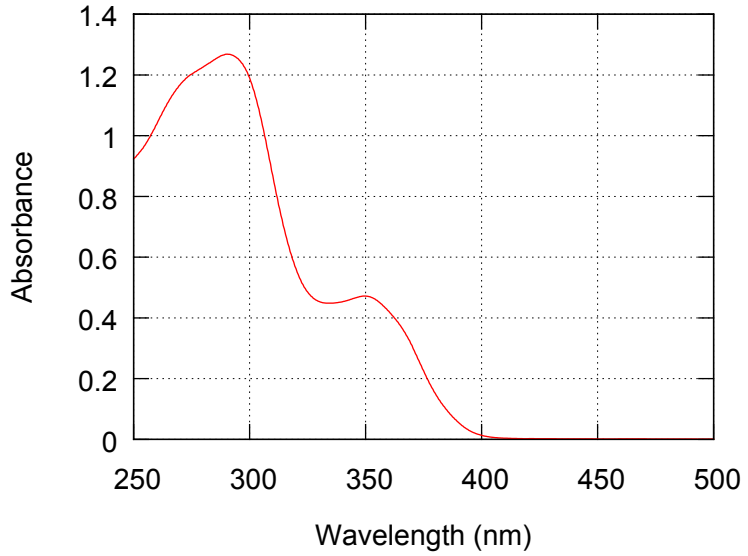

Figure S231. UV-vis absorption spectrum of **9(40)** in $CHCl_3$ (3.14×10^{-2} g/L, path length = 10 mm).

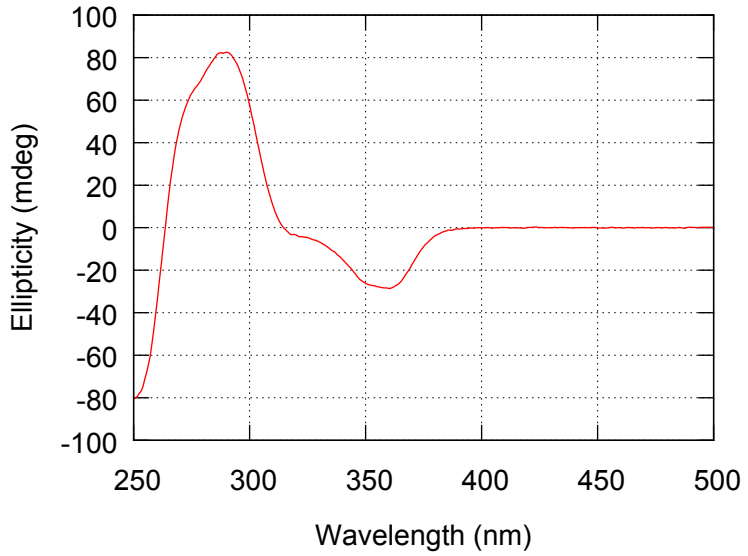

Figure S232. CD spectrum of **9(40)** in $CHCl_3$ (3.14×10^{-2} g/L, path length = 10 mm).

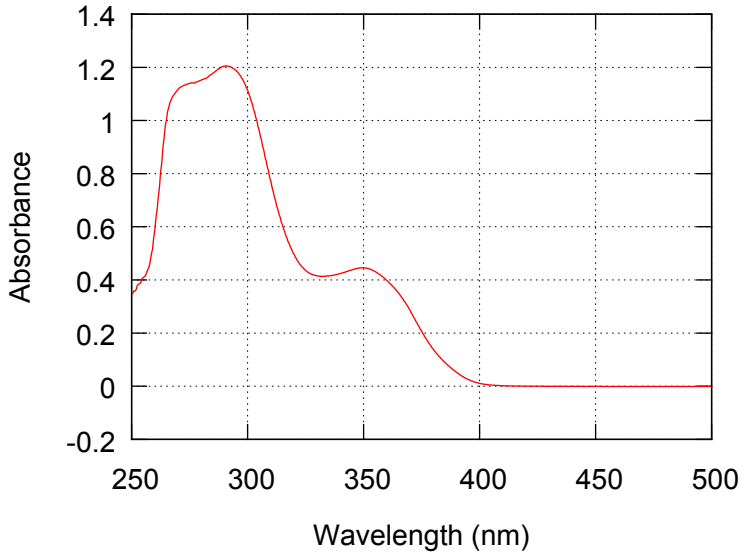

Figure S233. UV-vis absorption spectrum of **9(40)** in 1,1,2-TCE (3.14×10^{-2} g/L, path length = 10 mm).

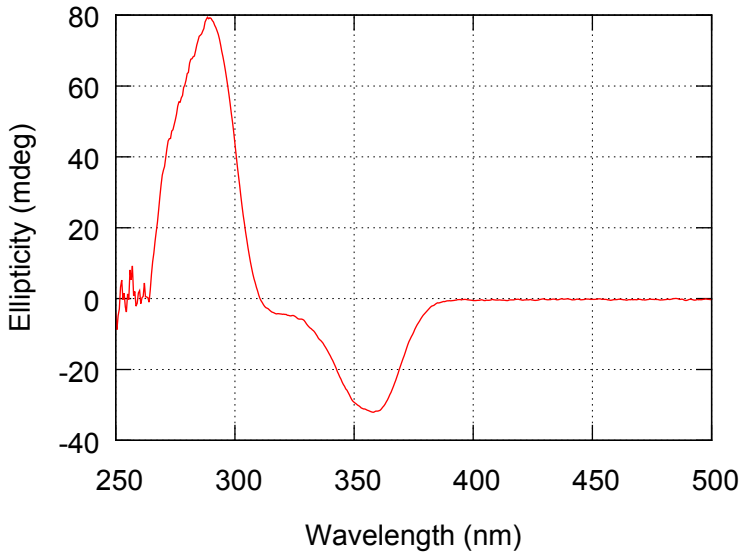

Figure S234. CD spectrum of **9(40)** in 1,1,2-TCE (3.14×10^{-2} g/L, path length = 10 mm).

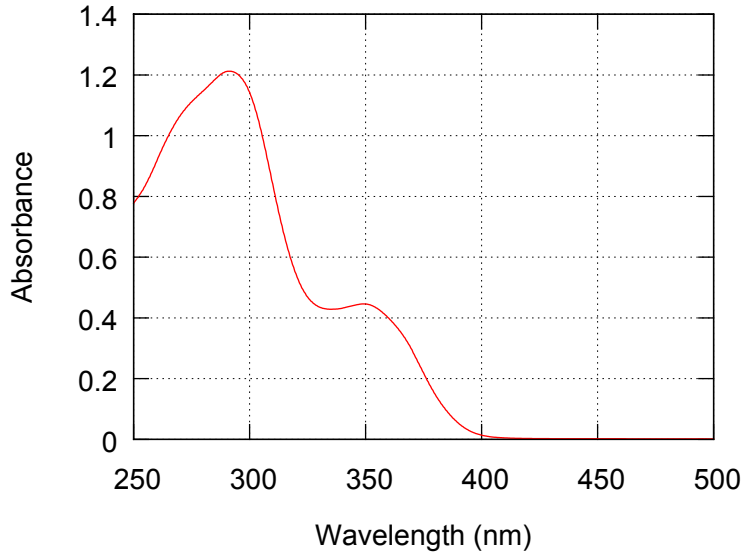

Figure S235. UV-vis absorption spectrum of **9(40)** in THF (3.14×10^{-2} g/L, path length = 10 mm).

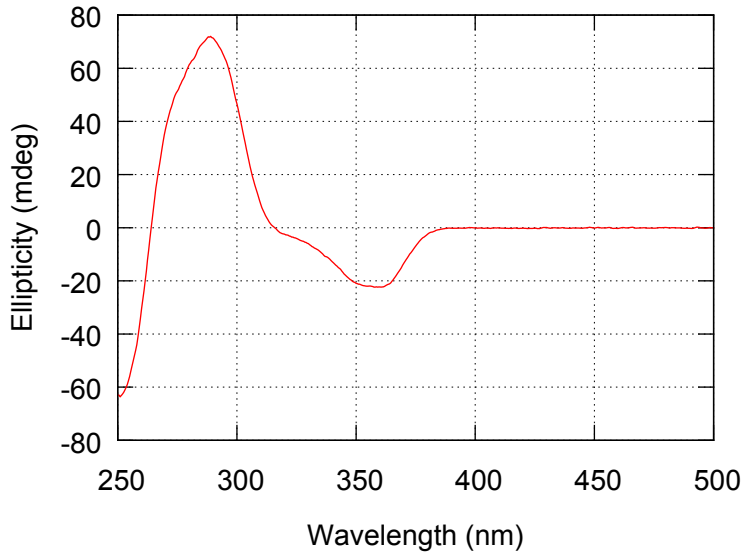

Figure S236. CD spectrum of **9(40)** in THF (3.14×10^{-2} g/L, path length = 10 mm).

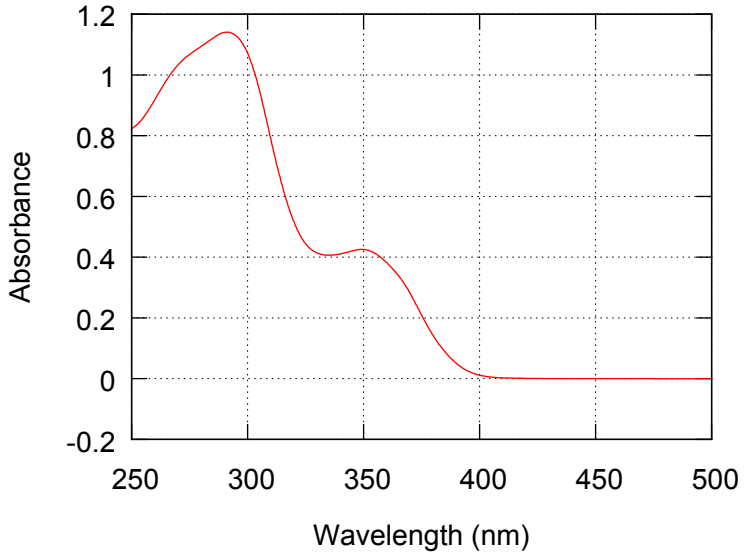

Figure S237. UV-vis absorption spectrum of **9(40)** in 1,4-Dioxane (3.14×10^{-2} g/L, path length = 10 mm).

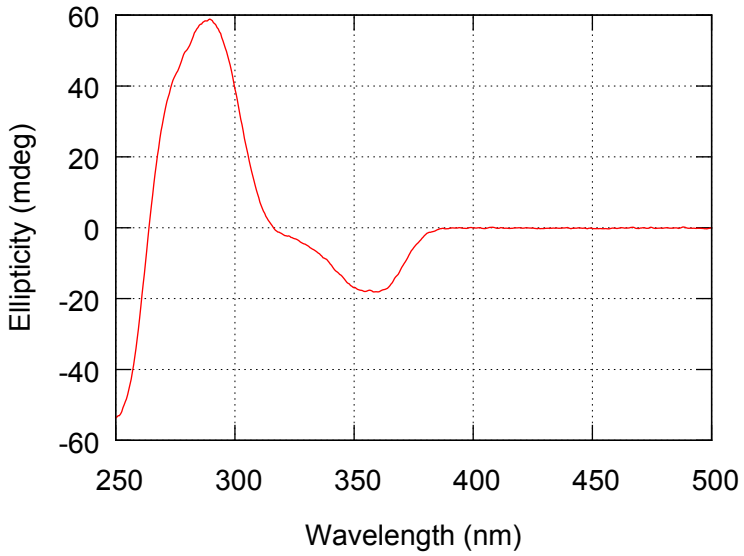

Figure S238. CD spectrum of **9(40)** in 1,4-Dioxane (3.14×10^{-2} g/L, path length = 10 mm).

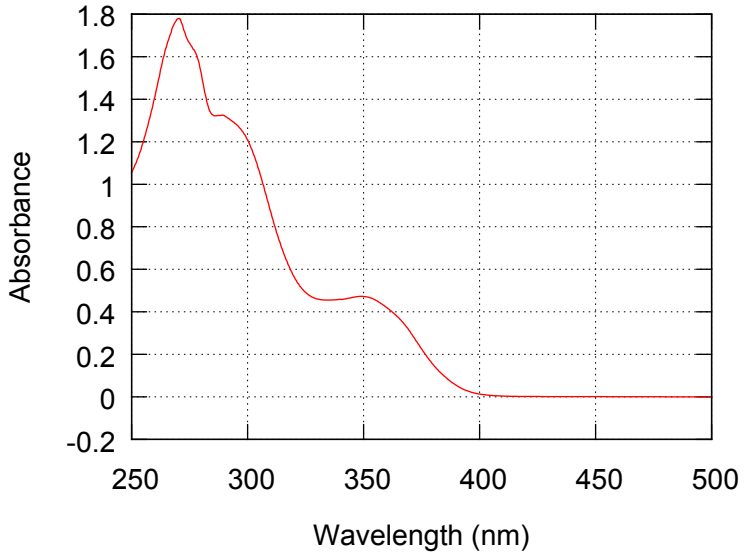

Figure S239. UV-vis absorption spectrum of **9(40)** in 2-MeTHF (3.14×10^{-2} g/L, path length = 10 mm).

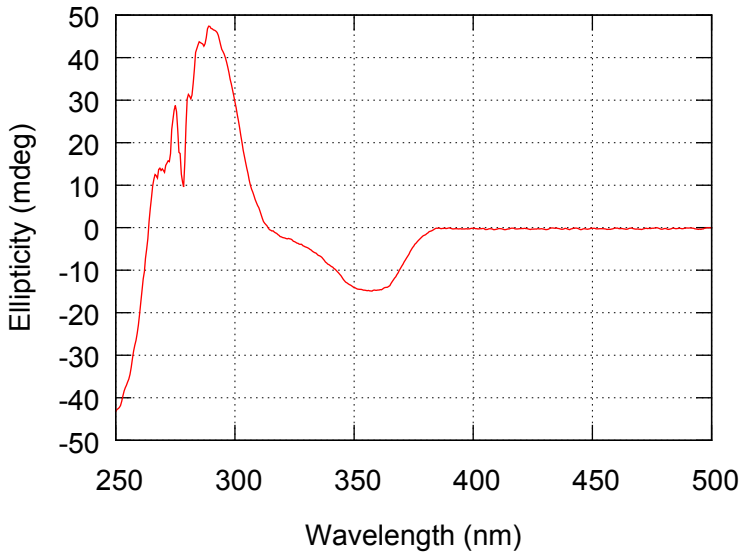

Figure S240. CD spectrum of **9(40)** in 2-MeTHF (3.14×10^{-2} g/L, path length = 10 mm).

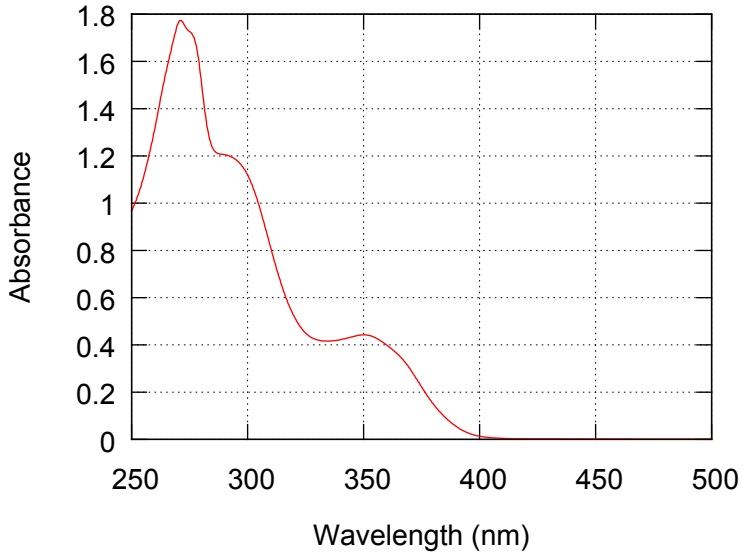

Figure S241. UV-vis absorption spectrum of **9(40)** in 1,2-DME (3.14×10^{-2} g/L, path length = 10 mm).

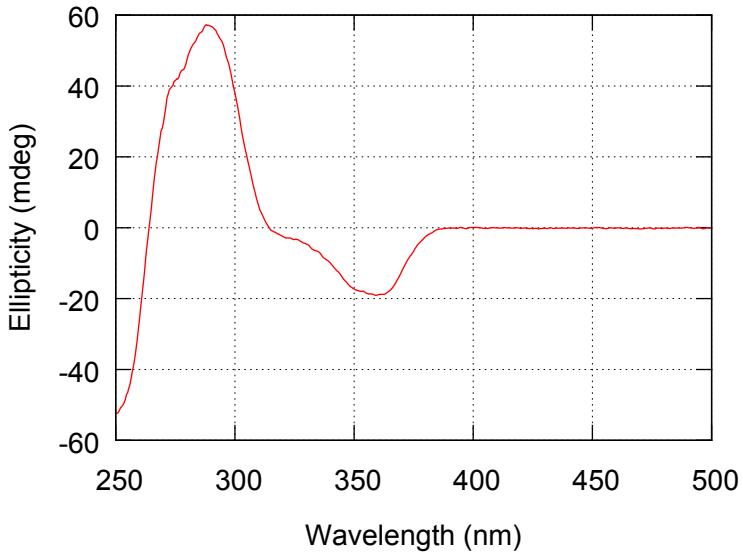

Figure S242. CD spectrum of **9(40)** in 1,2-DME (3.14×10^{-2} g/L, path length = 10 mm).

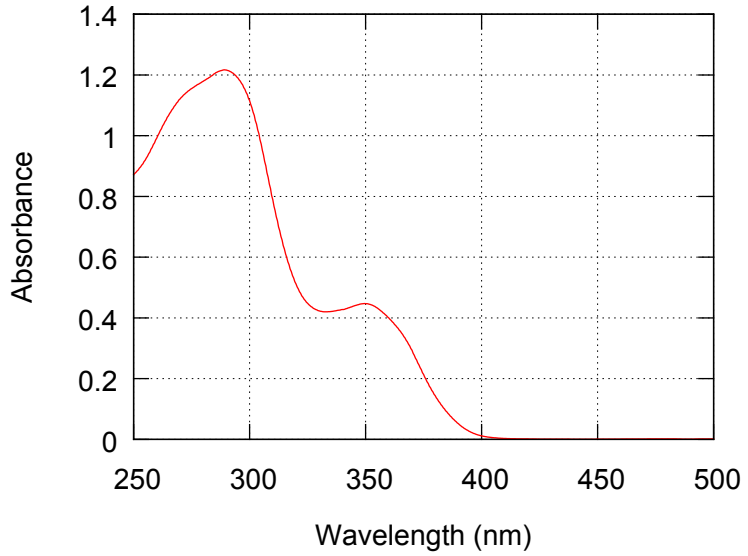

Figure S243. UV-vis absorption spectrum of **9(40)** in CPME (3.14×10^{-2} g/L, path length = 10 mm).

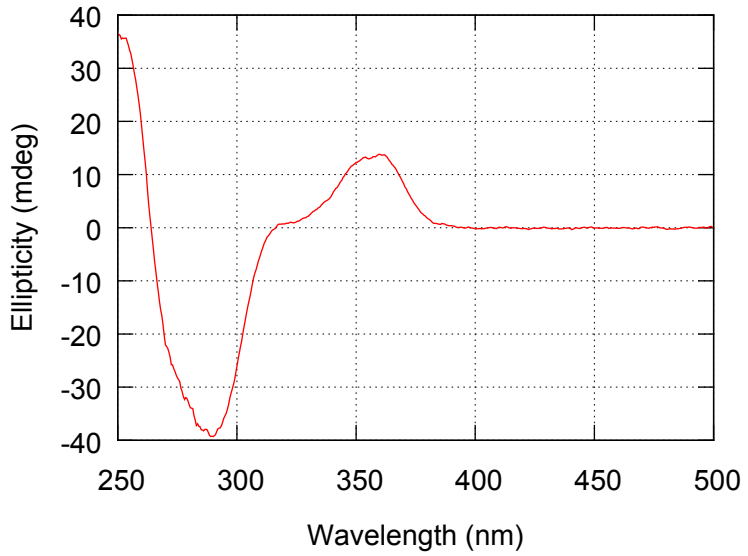

Figure S244. CD spectrum of **9(40)** in CPME (3.14×10^{-2} g/L, path length = 10 mm).

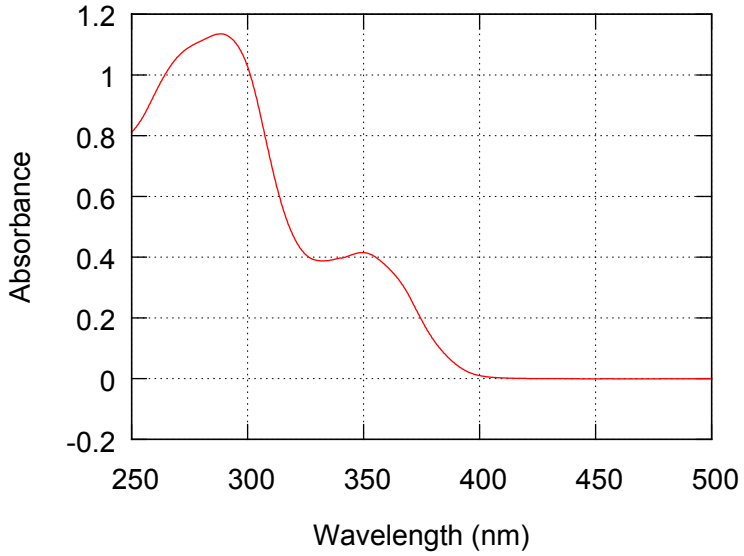

Figure S245. UV-vis absorption spectrum of **9(40)** in Et_2O (3.14×10^{-2} g/L, path length = 10 mm).

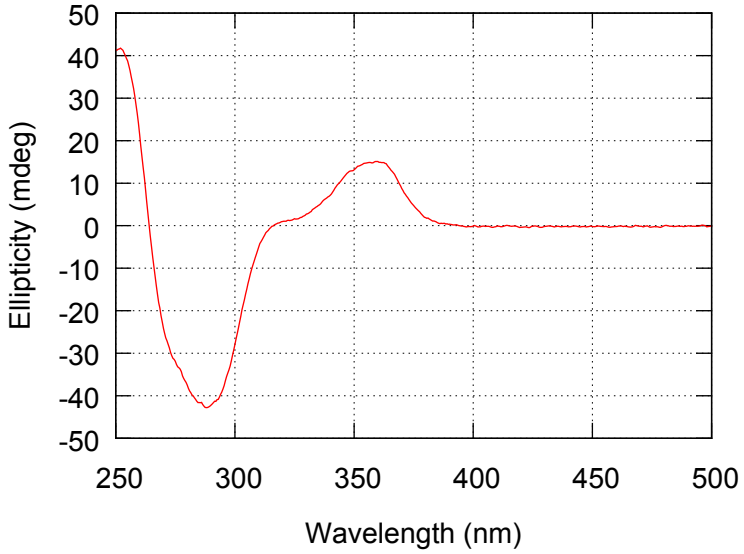

Figure S246. CD spectrum of **9(40)** in Et_2O (3.14×10^{-2} g/L, path length = 10 mm).

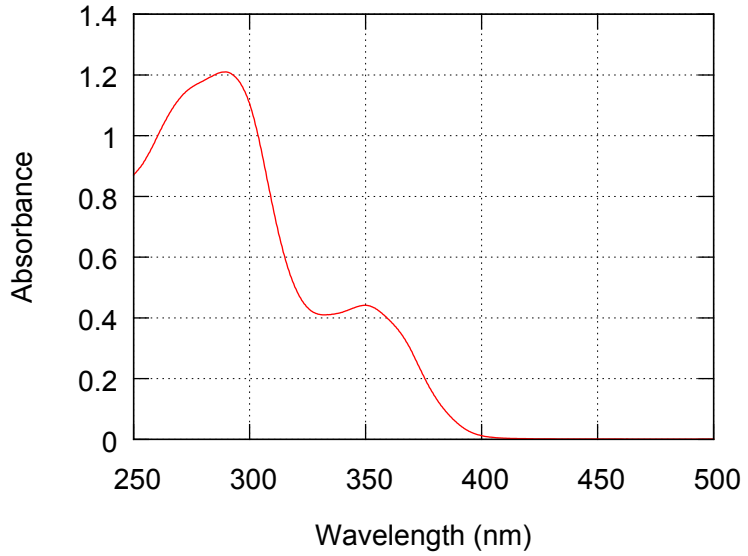

Figure S247. UV-vis absorption spectrum of **9(40)** in MTBE (3.14×10^{-2} g/L, path length = 10 mm).

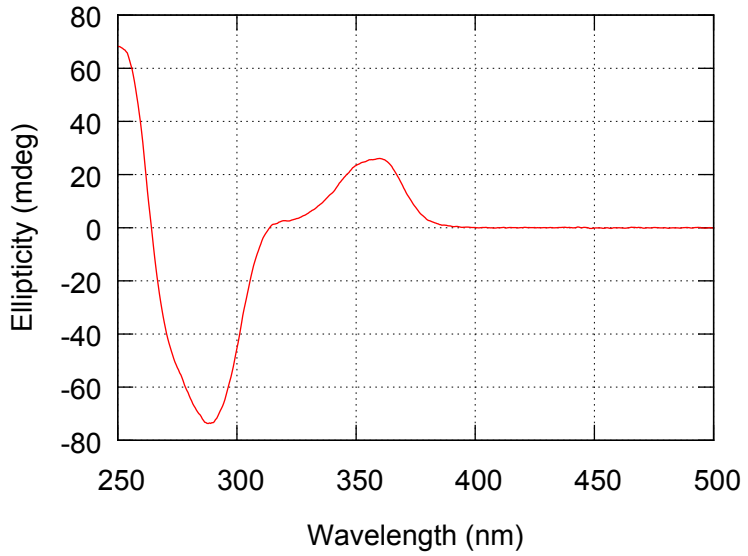

Figure S248. CD spectrum of **9(40)** in MTBE (3.14×10^{-2} g/L, path length = 10 mm).

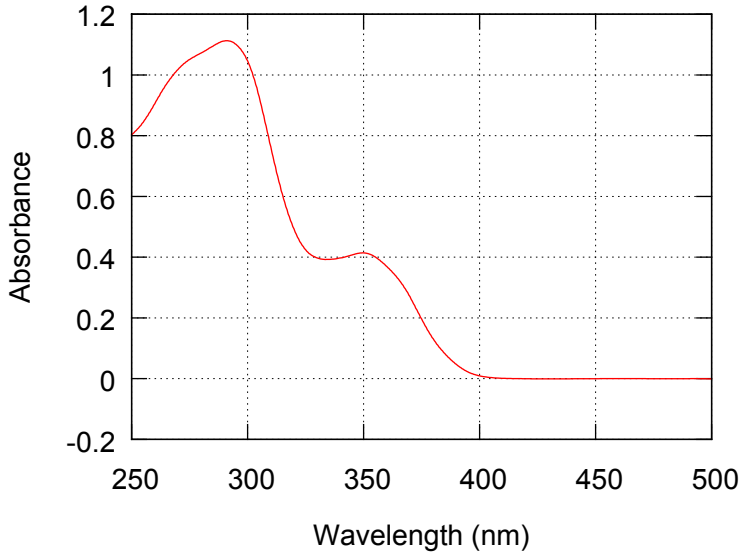

Figure S249. UV-vis absorption spectrum of **10(40)** in $CHCl_3$ (2.68×10^{-2} g/L, path length = 10 mm).

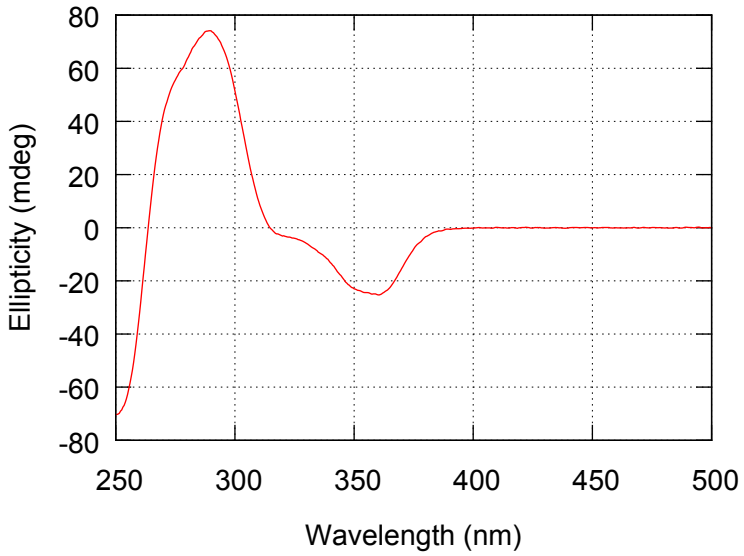

Figure S250. CD spectrum of **10(40)** in $CHCl_3$ (2.68×10^{-2} g/L, path length = 10 mm).

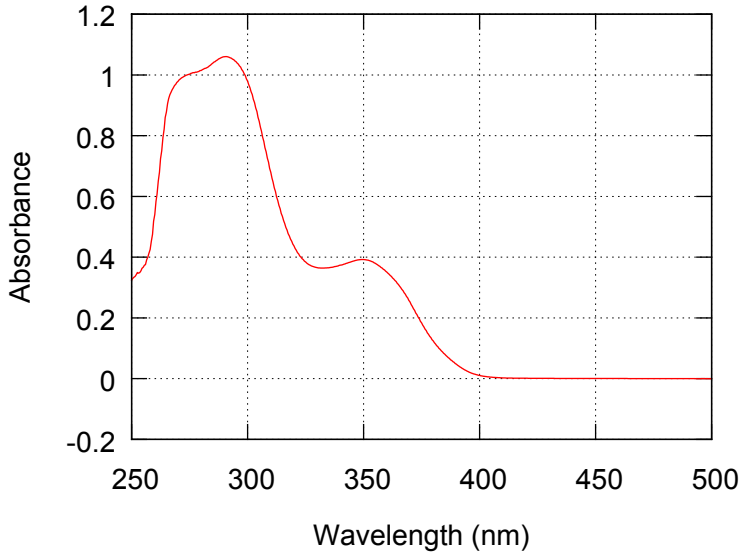

Figure S251. UV-vis absorption spectrum of **10(40)** in 1,1,2-TCE (2.68×10^{-2} g/L, path length = 10 mm).

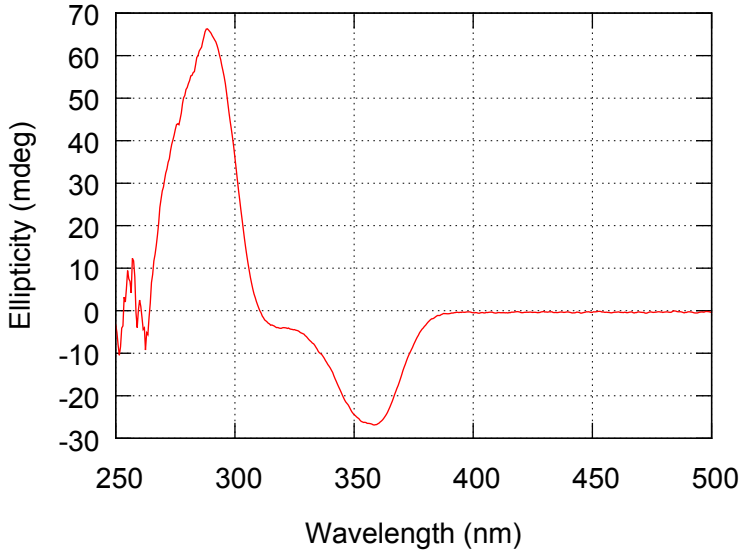

Figure S252. CD spectrum of **10(40)** in 1,1,2-TCE (2.68×10^{-2} g/L, path length = 10 mm).

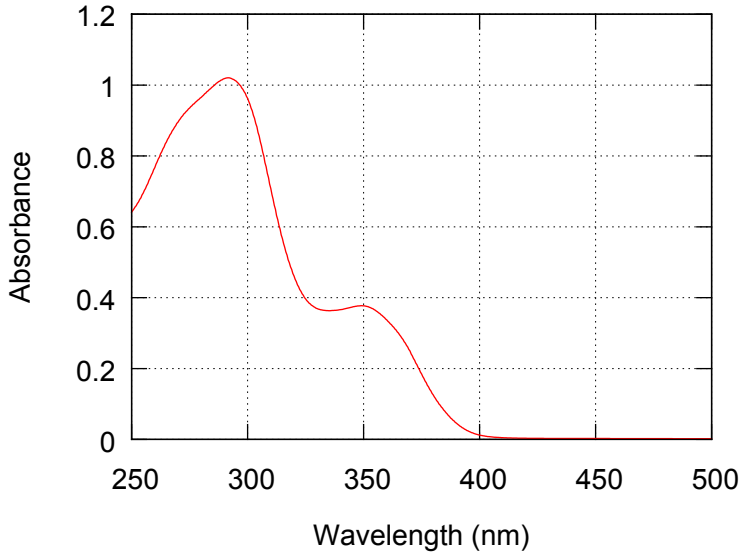

Figure S253. UV-vis absorption spectrum of **10(40)** in THF (2.68×10^{-2} g/L, path length = 10 mm).

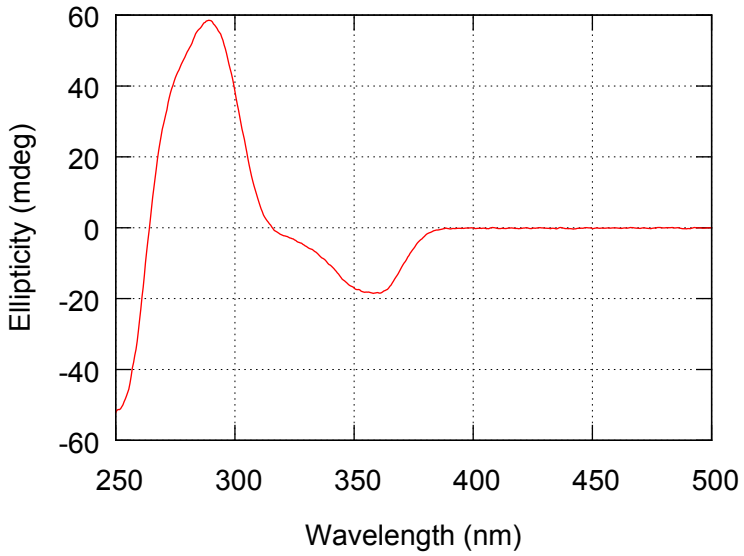

Figure S254. CD spectrum of **10(40)** in THF (2.68×10^{-2} g/L, path length = 10 mm).

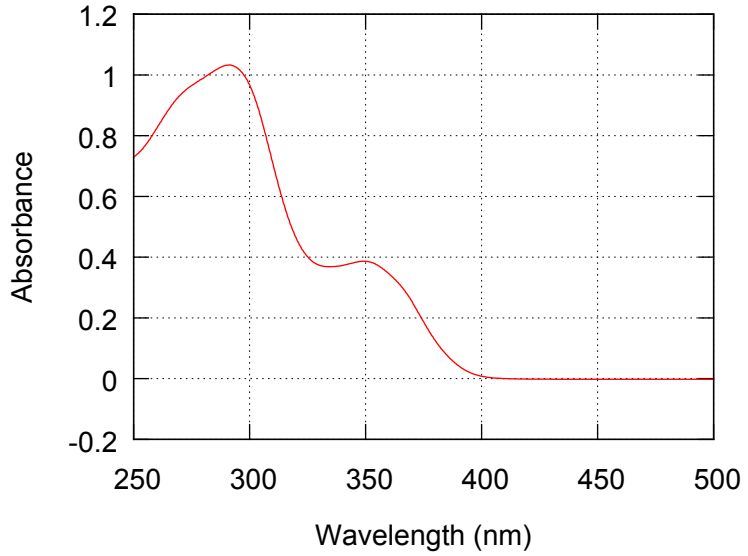

Figure S255. UV-vis absorption spectrum of **10(40)** in 1,4-Dioxane (2.68×10^{-2} g/L, path length = 10 mm).

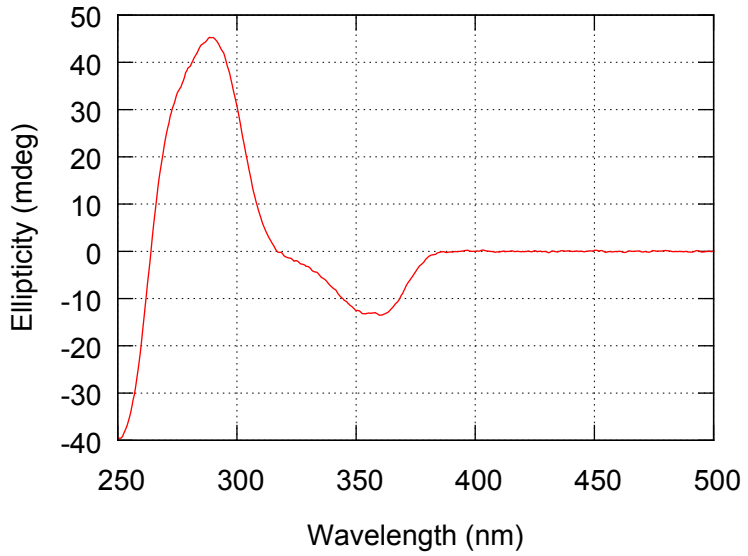

Figure S256. CD spectrum of **10(40)** in 1,4-Dioxane (2.68×10^{-2} g/L, path length = 10 mm).

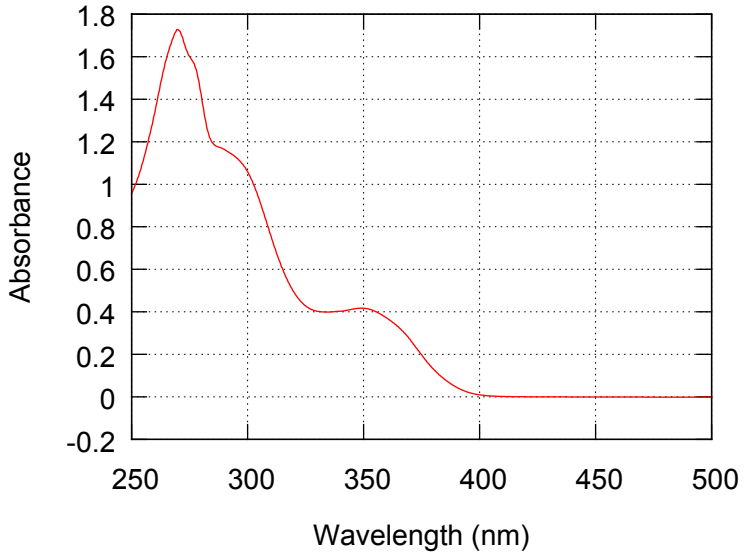

Figure S257. UV-vis absorption spectrum of **10(40)** in 2-MeTHF (2.68×10^{-2} g/L, path length = 10 mm).

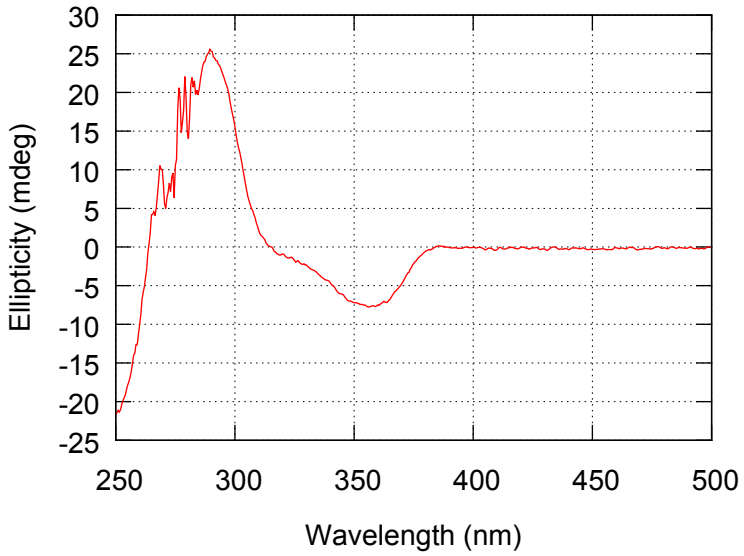

Figure S258. CD spectrum of **10(40)** in 2-MeTHF (2.68×10^{-2} g/L, path length = 10 mm).

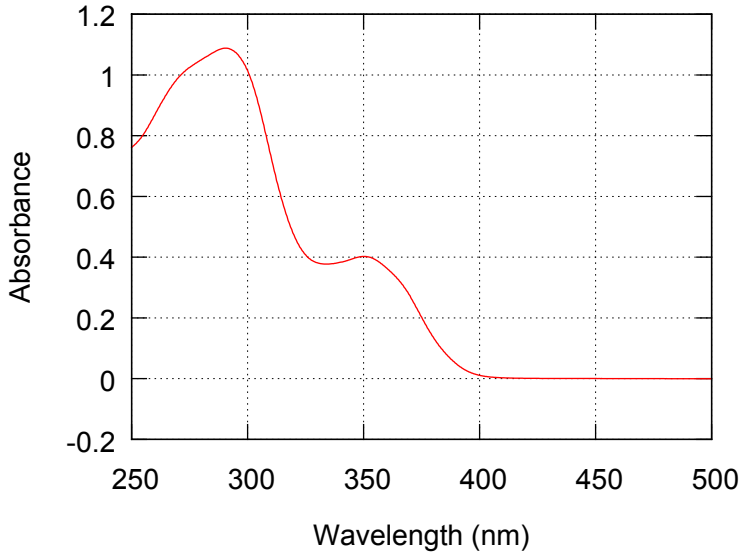

Figure S259. UV-vis absorption spectrum of **10(40)** in 1,2-DME (2.68×10^{-2} g/L, path length = 10 mm).

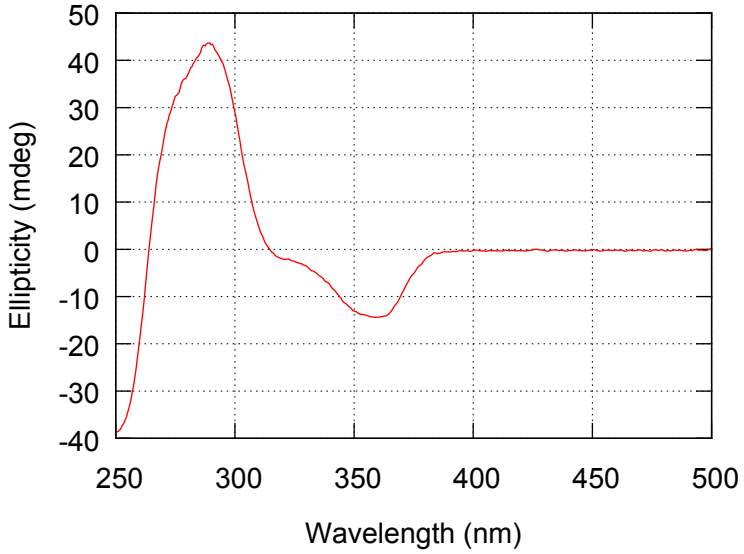

Figure S260. CD spectrum of **10(40)** in 1,2-DME (2.68×10^{-2} g/L, path length = 10 mm).

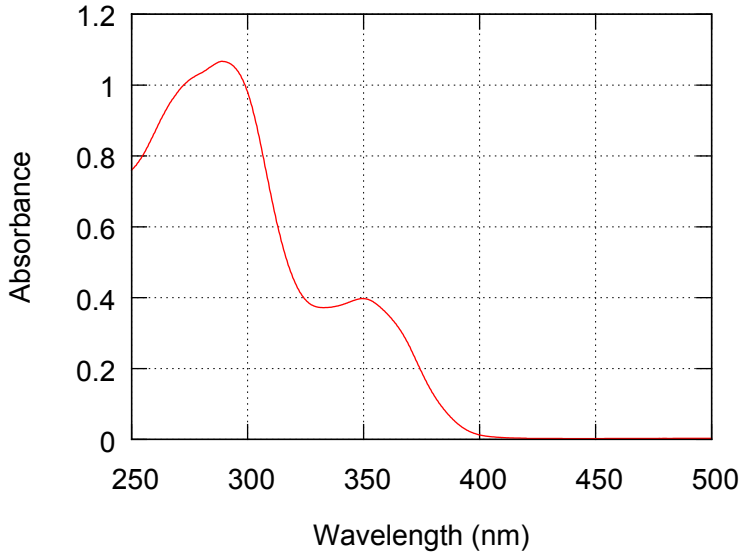

Figure S261. UV-vis absorption spectrum of **10(40)** in CPME (2.68×10^{-2} g/L, path length = 10 mm).

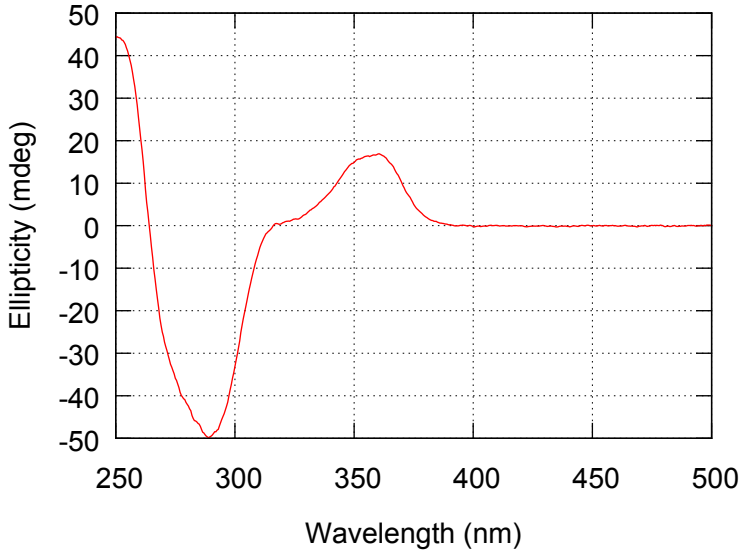

Figure S262. CD spectrum of **10(40)** in CPME (2.68×10^{-2} g/L, path length = 10 mm).

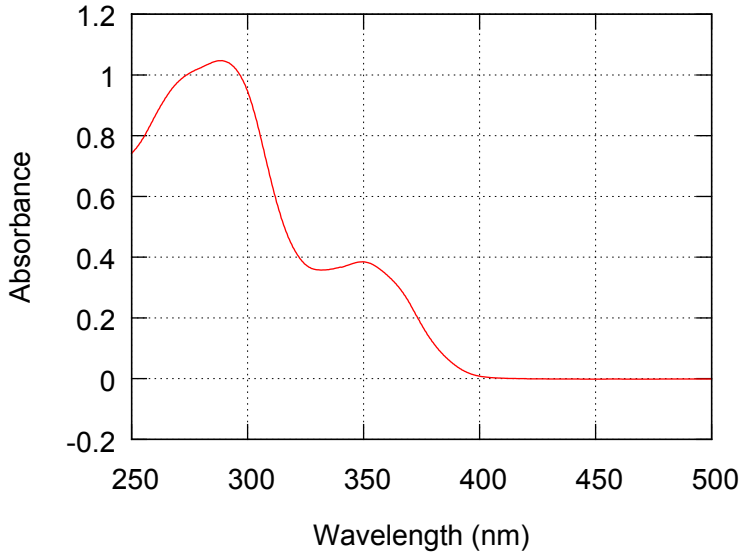

Figure S263. UV-vis absorption spectrum of **10(40)** in Et_2O (2.68×10^{-2} g/L, path length = 10 mm).

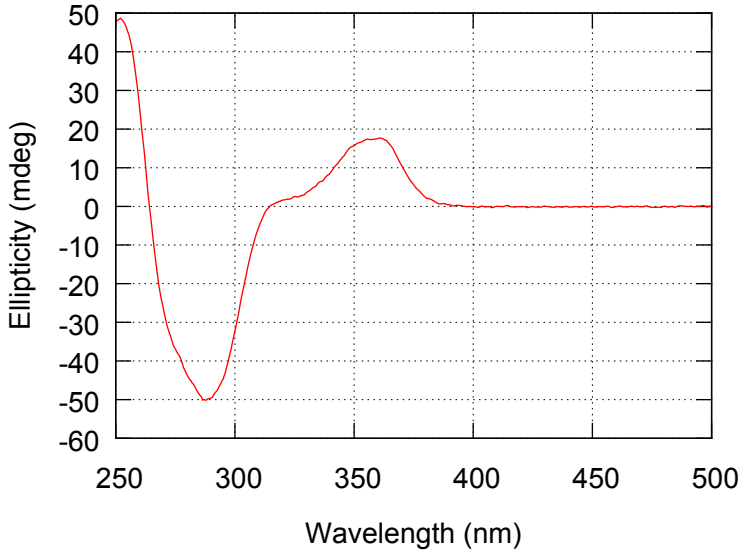

Figure S264. CD spectrum of **10(40)** in Et_2O (2.68×10^{-2} g/L, path length = 10 mm).

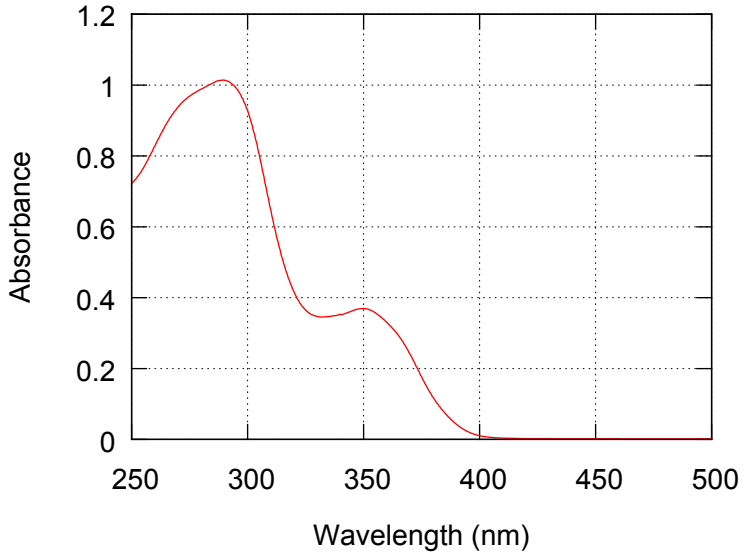

Figure S265. UV-vis absorption spectrum of **10(40)** in MTBE (2.68×10^{-2} g/L, path length = 10 mm).

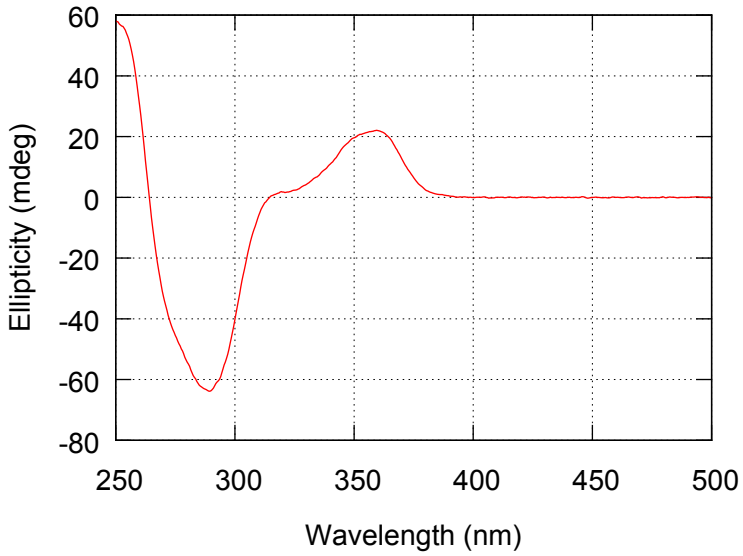

Figure S266. CD spectrum of **10(40)** in MTBE (2.68×10^{-2} g/L, path length = 10 mm).

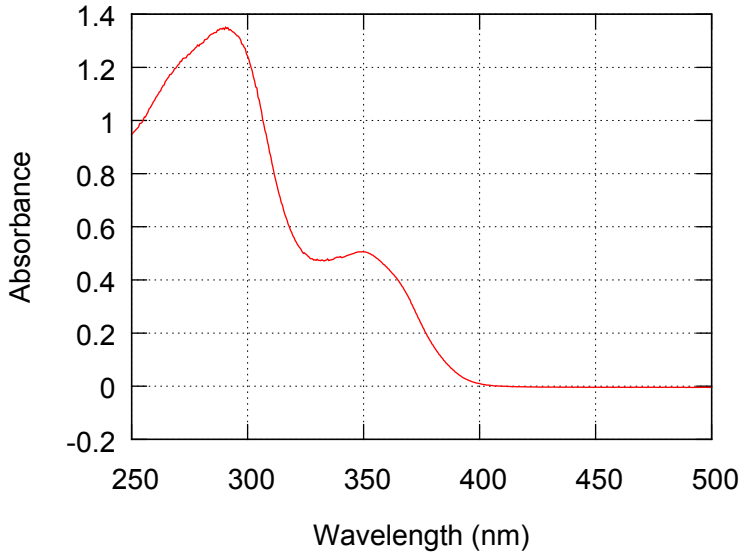

Figure S267. UV-vis absorption spectrum of **5(20)** in MTBE (3.34×10^{-2} g/L, path length = 10 mm).

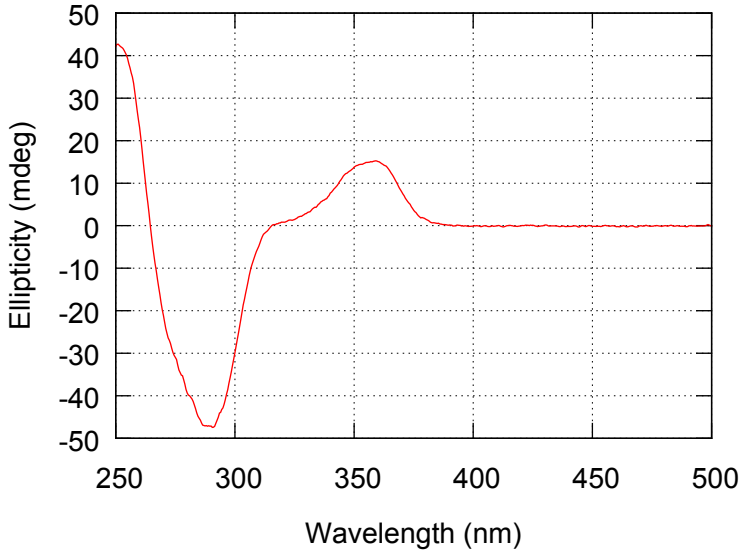

Figure S268. CD spectrum of **5(20)** in MTBE (3.34×10^{-2} g/L, path length = 10 mm).

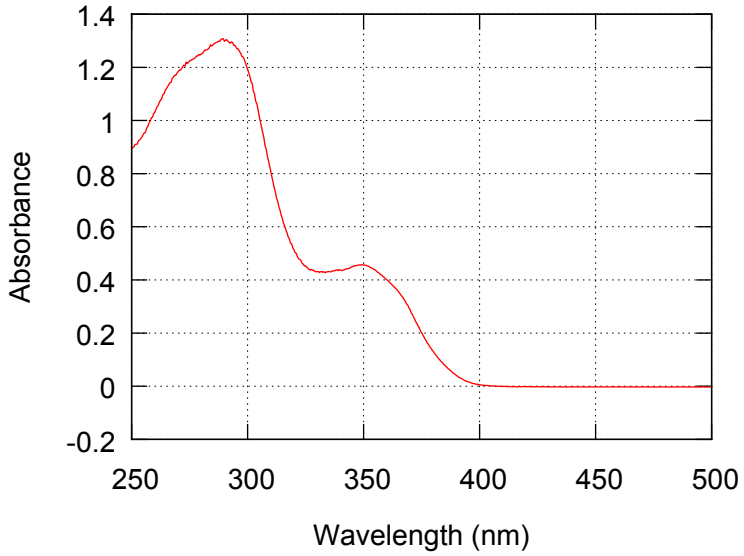

Figure S269. UV-vis absorption spectrum of **5(60)** in MTBE (2.99×10^{-2} g/L, path length = 10 mm).

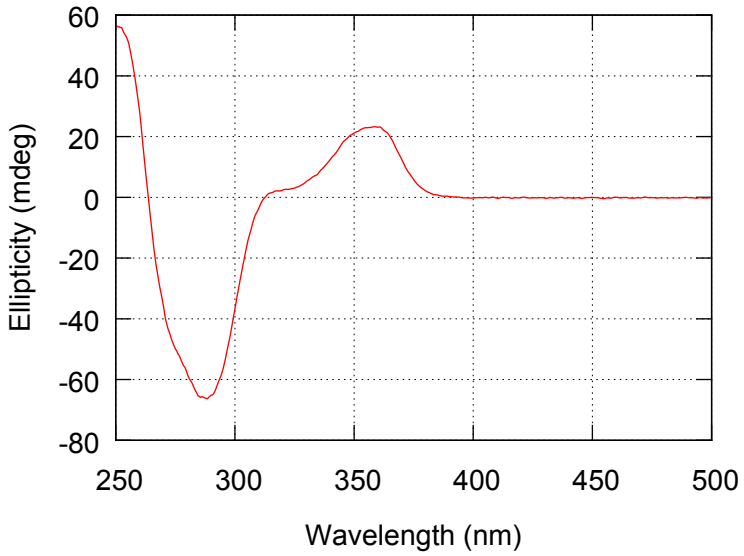

Figure S270. CD spectrum of **5(60)** in MTBE (2.99×10^{-2} g/L, path length = 10 mm).

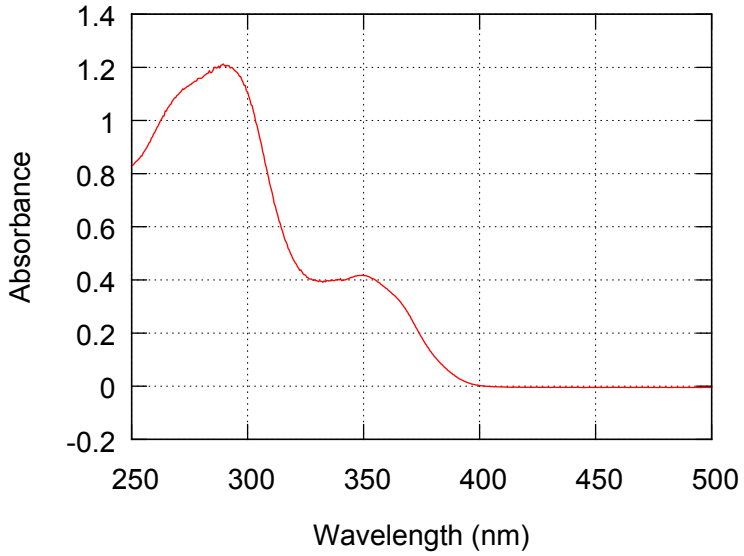

Figure S271. UV-vis absorption spectrum of **5(80)** in MTBE (2.86×10^{-2} g/L, path length = 10 mm).

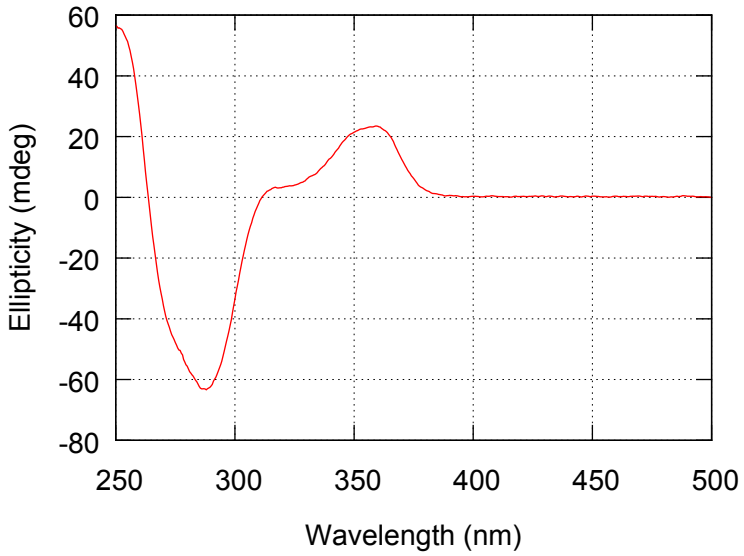

Figure S272. CD spectrum of **5(80)** in MTBE (2.86×10^{-2} g/L, path length = 10 mm).

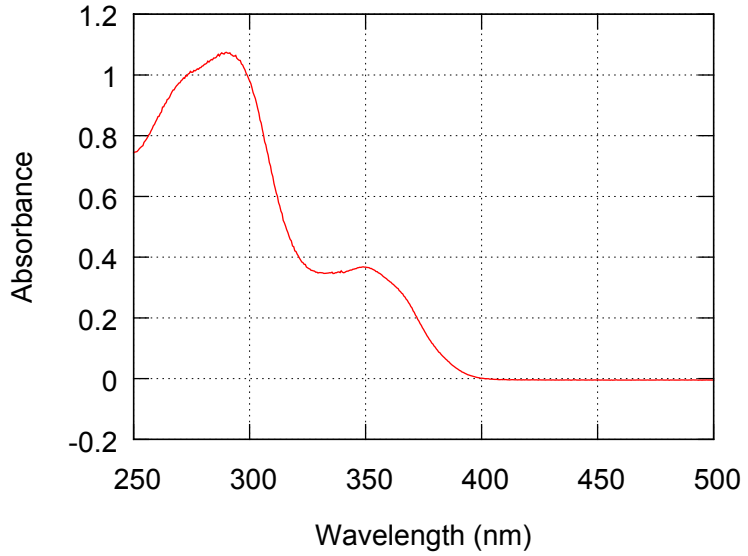

Figure S273. UV-vis absorption spectrum of **5(100)** in MTBE (2.38×10^{-2} g/L, path length = 10 mm).

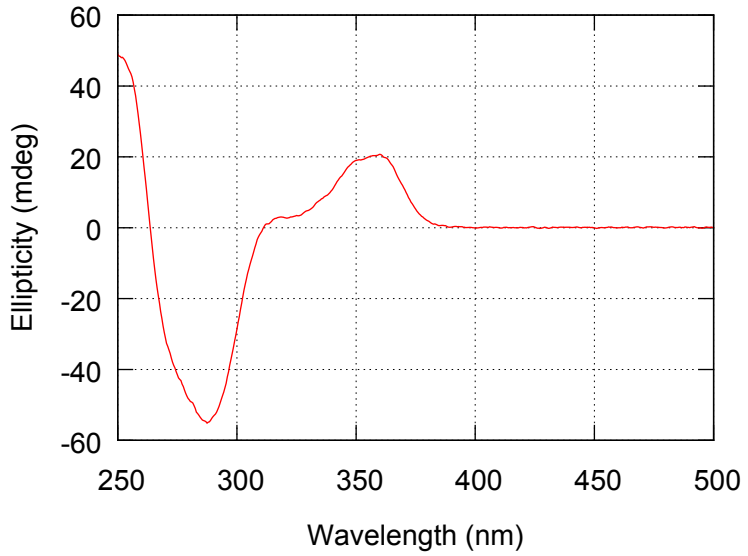

Figure S274. CD spectrum of **5(100)** in MTBE (2.38×10^{-2} g/L, path length = 10 mm).

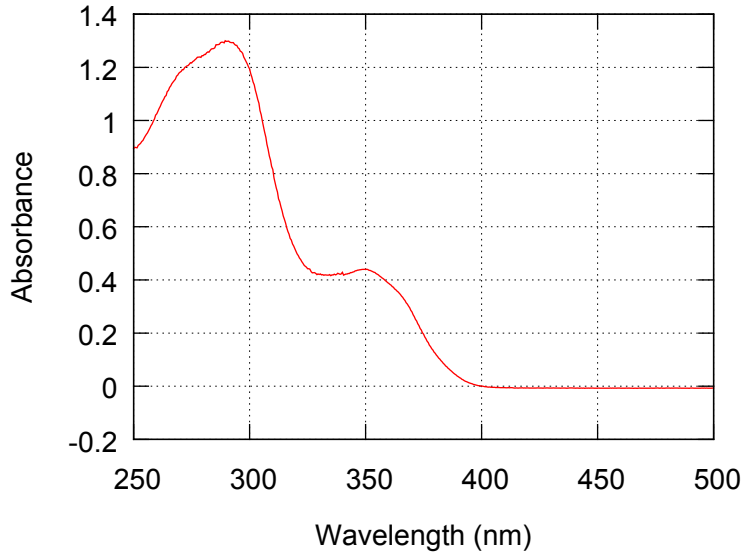

Figure S275. UV-vis absorption spectrum of **5(150)** in MTBE (3.33×10^{-2} g/L, path length = 10 mm).

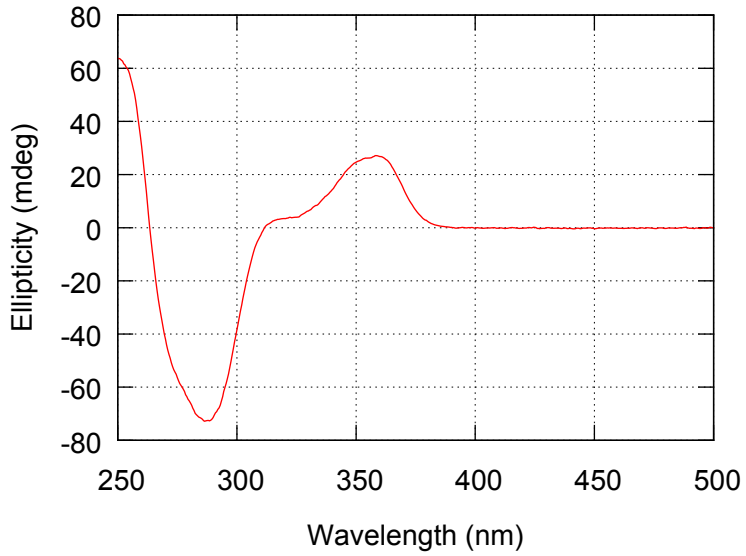

Figure S276. CD spectrum of **5(150)** in MTBE (3.33×10^{-2} g/L, path length = 10 mm).

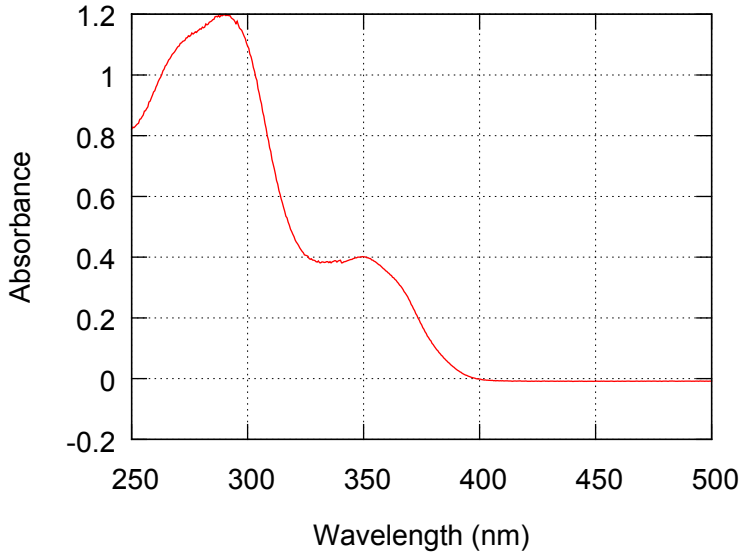

Figure S277. UV-vis absorption spectrum of **5(200)** in MTBE (3.68×10^{-2} g/L, path length = 10 mm).

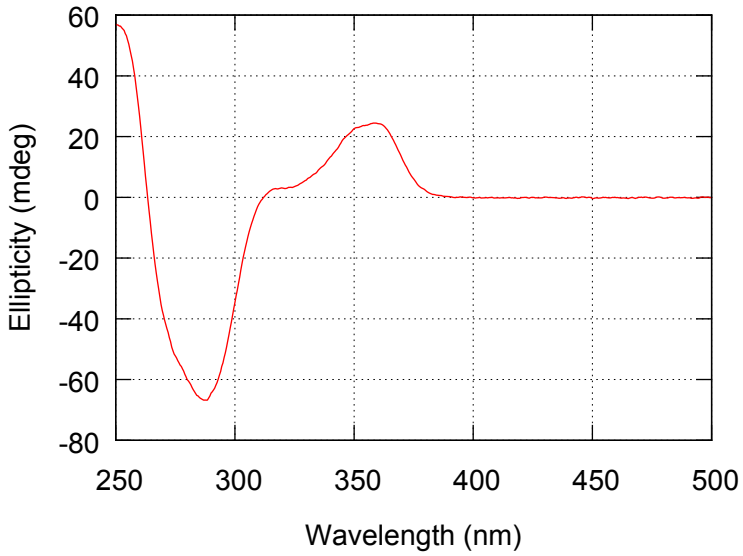

Figure S278. CD spectrum of **5(200)** in MTBE (3.68×10^{-2} g/L, path length = 10 mm).

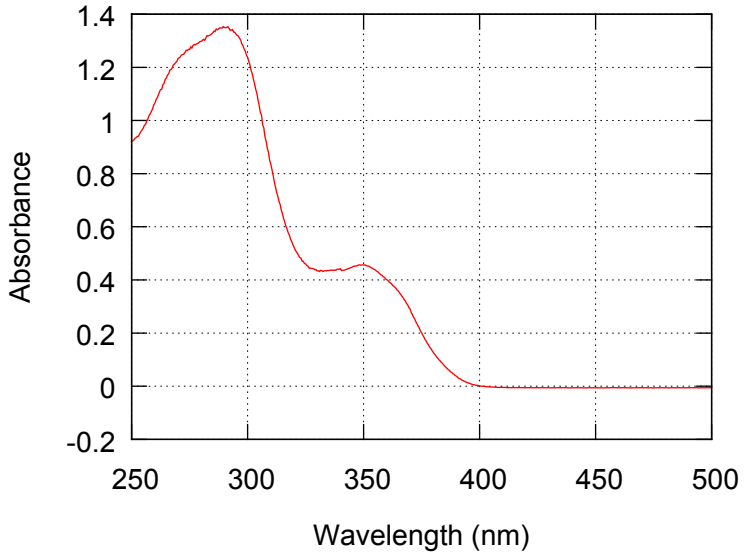

Figure S279. UV-vis absorption spectrum of **5(300)** in MTBE (3.09×10^{-2} g/L, path length = 10 mm).

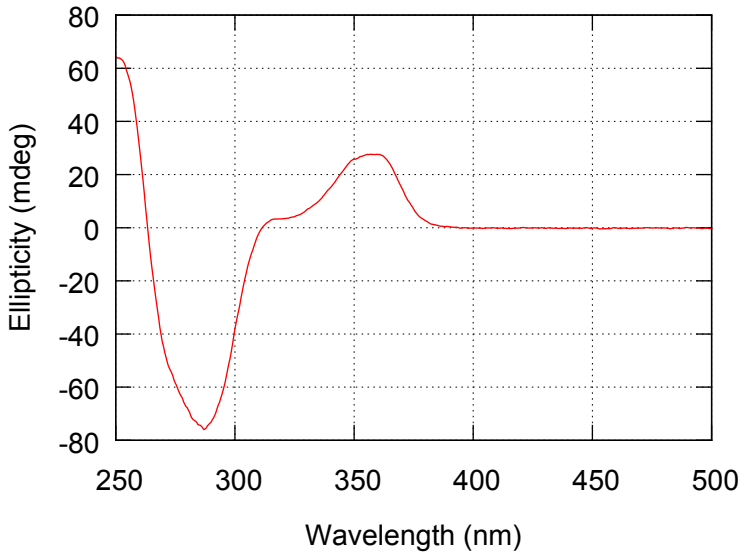

Figure S280. CD spectrum of **5(300)** in MTBE (3.09×10^{-2} g/L, path length = 10 mm).

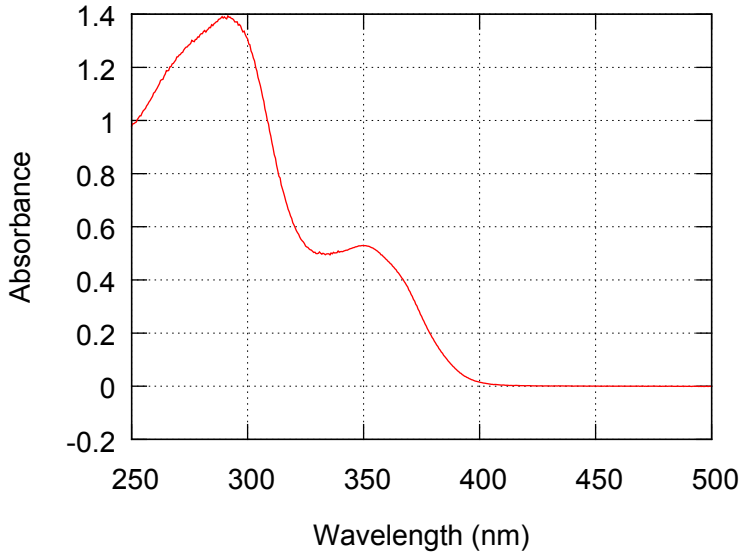

Figure S281. UV-vis absorption spectrum of **5(20)** in 1,2-DME (3.34×10^{-2} g/L, path length = 10 mm).

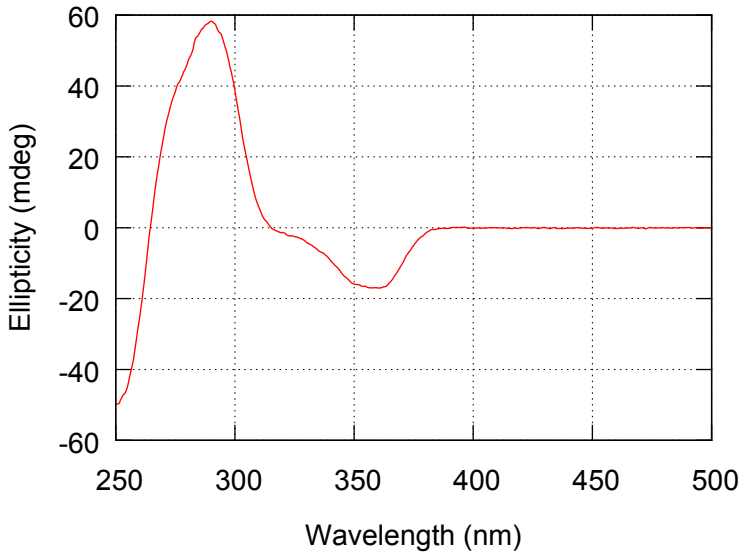

Figure S282. CD spectrum of **5(20)** in 1,2-DME (3.34×10^{-2} g/L, path length = 10 mm).

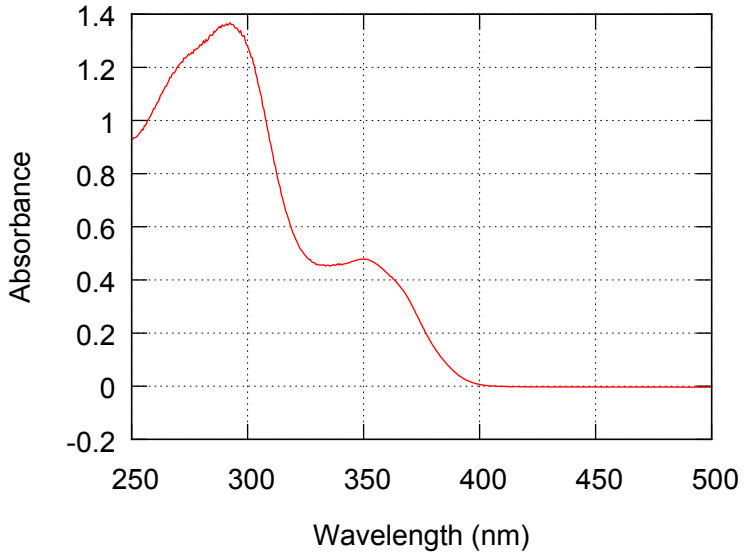

Figure S283. UV-vis absorption spectrum of **5(60)** in 1,2-DME (2.99×10^{-2} g/L, path length = 10 mm).

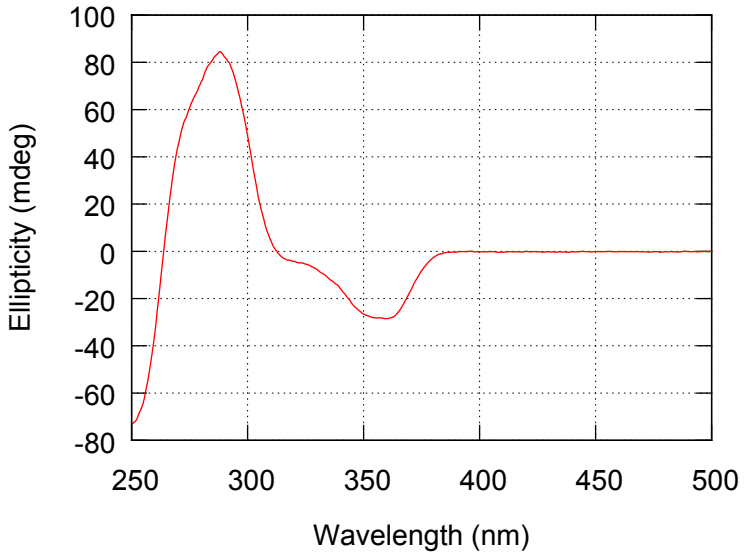

Figure S284. CD spectrum of **5(60)** in 1,2-DME (2.99×10^{-2} g/L, path length = 10 mm).

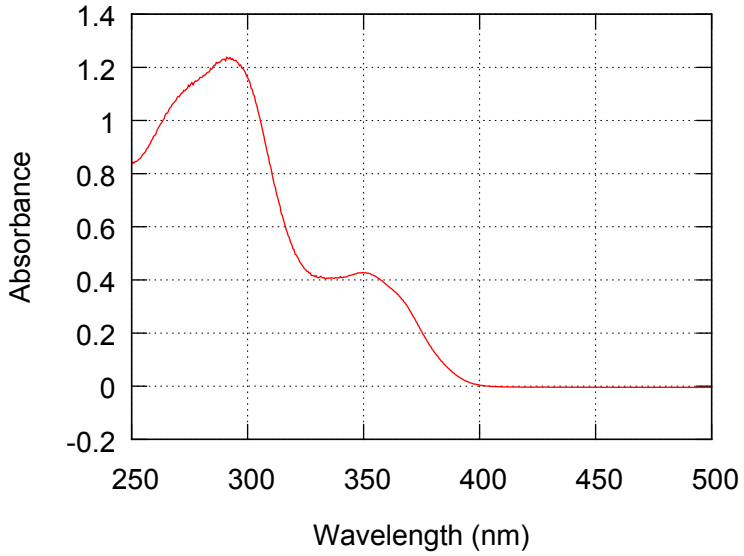

Figure S285. UV-vis absorption spectrum of **5(80)** in 1,2-DME (2.86×10^{-2} g/L, path length = 10 mm).

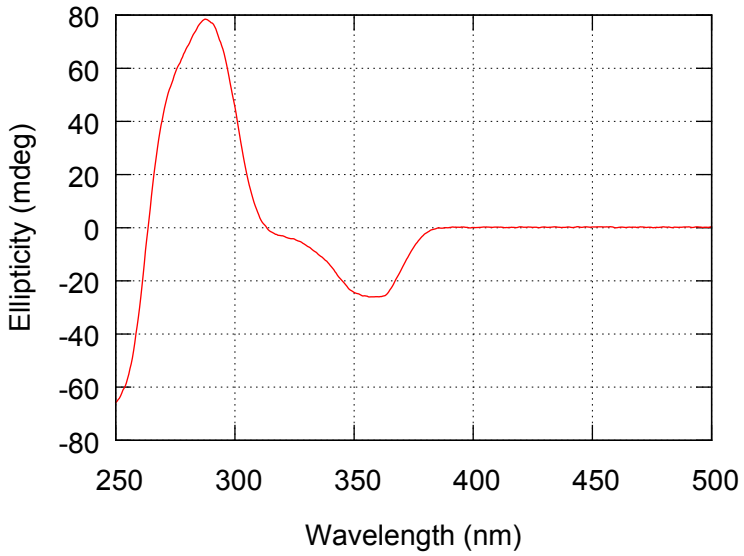

Figure S286. CD spectrum of **5(80)** in 1,2-DME (2.86×10^{-2} g/L, path length = 10 mm).

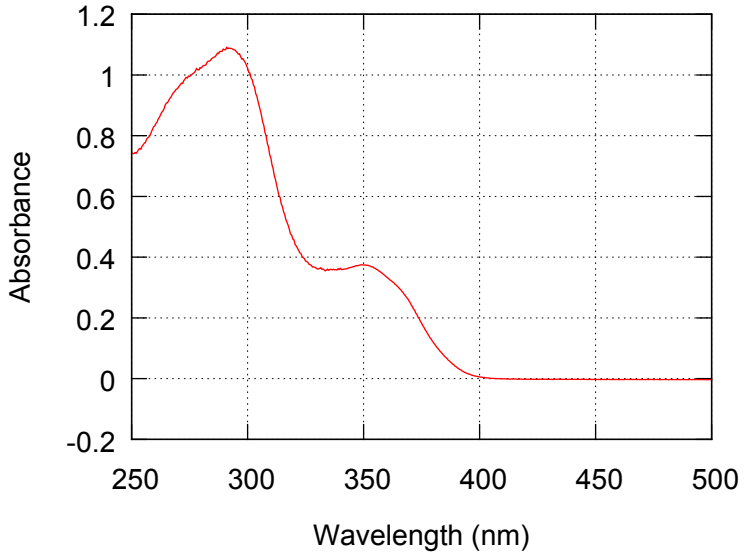

Figure S287. UV-vis absorption spectrum of **5(100)** in 1,2-DME (2.38×10^{-2} g/L, path length = 10 mm).

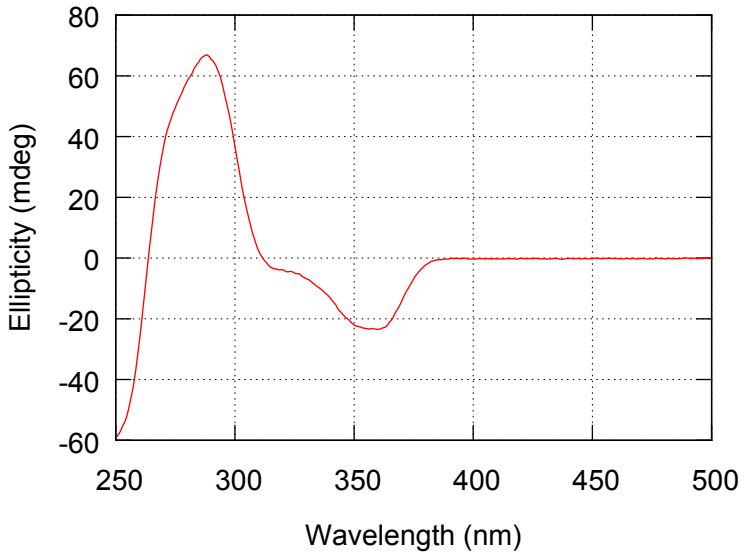

Figure S288. CD spectrum of **5(100)** in 1,2-DME (2.38×10^{-2} g/L, path length = 10 mm).

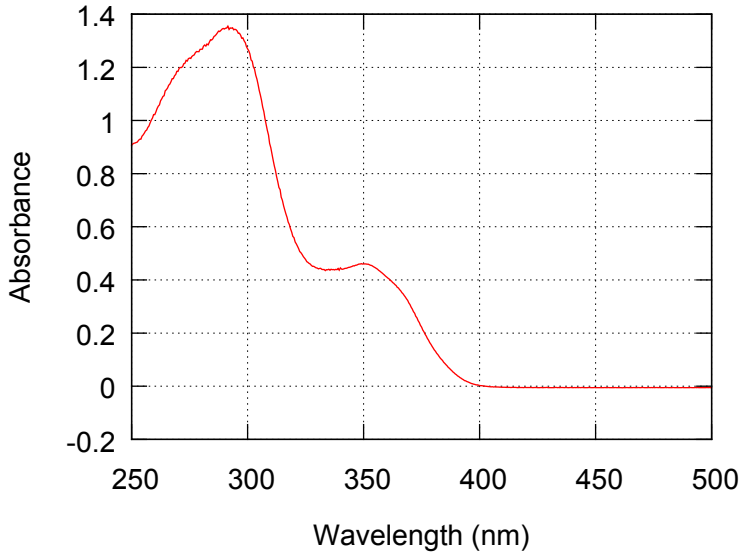

Figure S289. UV-vis absorption spectrum of **5(150)** in 1,2-DME (3.33×10^{-2} g/L, path length = 10 mm).

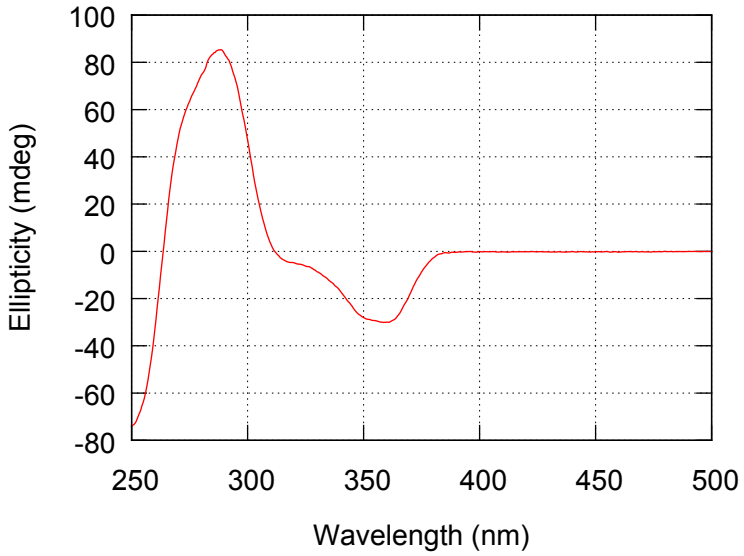

Figure S290. CD spectrum of **5(150)** in 1,2-DME (3.33×10^{-2} g/L, path length = 10 mm).

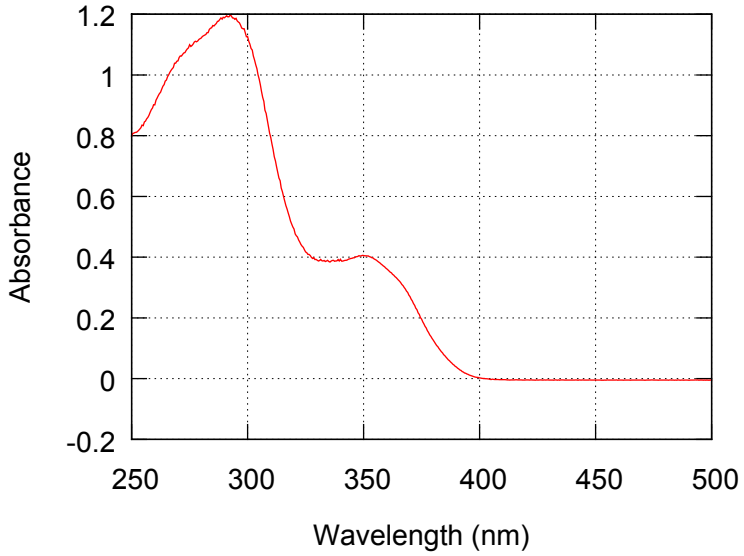

Figure S291. UV-vis absorption spectrum of **5(200)** in 1,2-DME (3.68×10^{-2} g/L, path length = 10 mm).

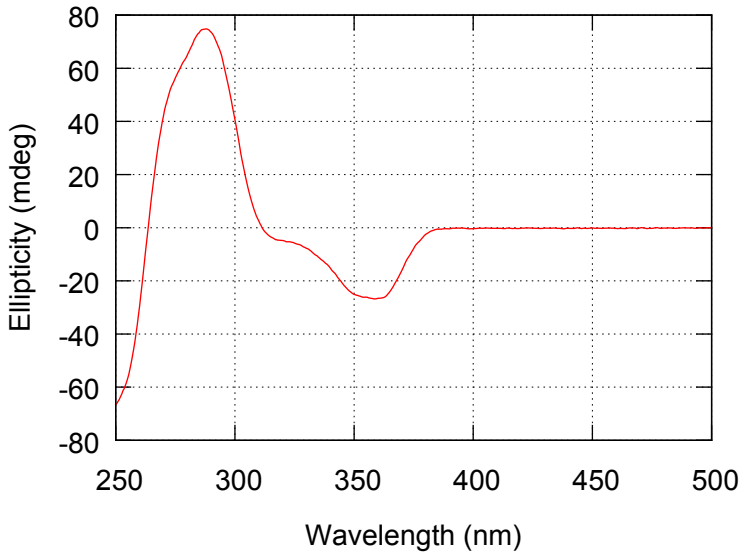

Figure S292. CD spectrum of **5(200)** in 1,2-DME (3.68×10^{-2} g/L, path length = 10 mm).

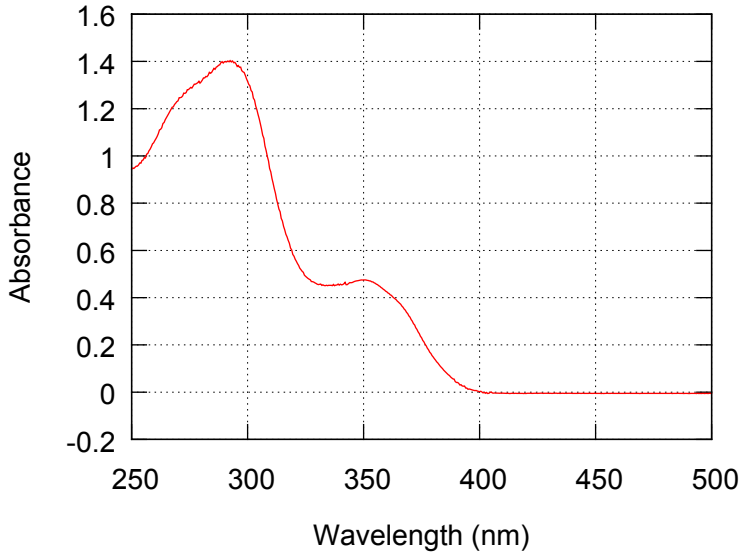

Figure S293. UV-vis absorption spectrum of **5(300)** in 1,2-DME (3.09×10^{-2} g/L, path length = 10 mm).

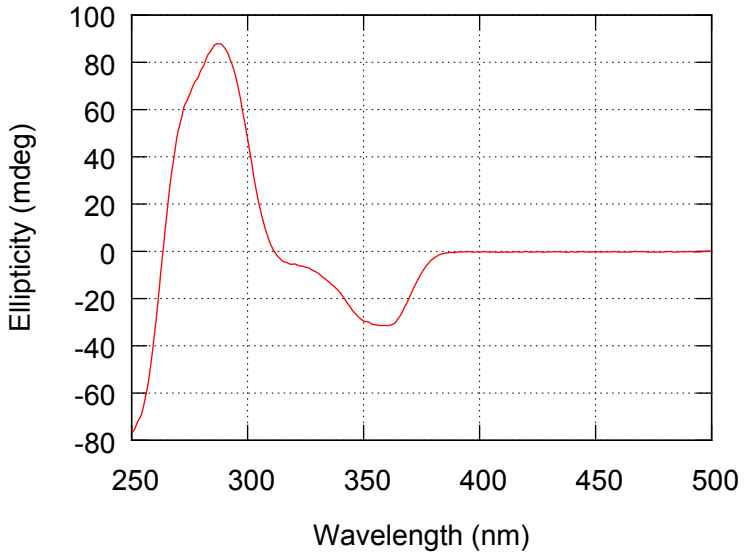

Figure S294. CD spectrum of **5(300)** in 1,2-DME (3.09×10^{-2} g/L, path length = 10 mm).

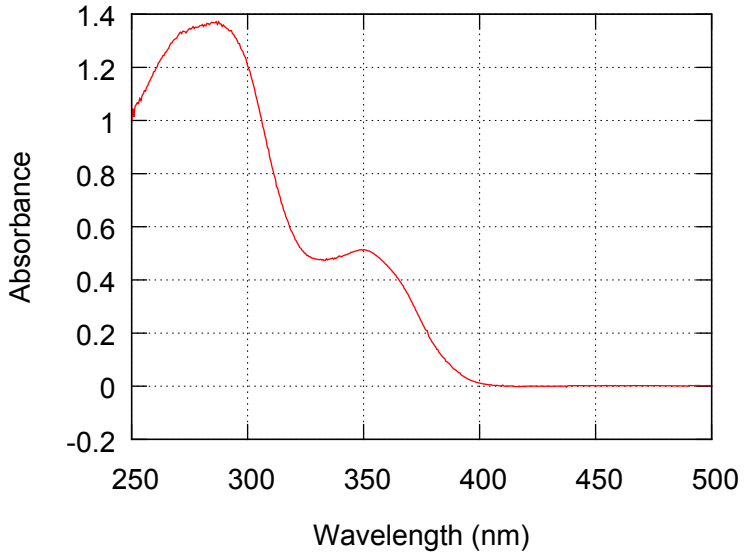

Figure S295. UV-vis absorption spectrum of **1(40)** in EtOAc (2.75×10^{-2} g/L, path length = 10 mm).

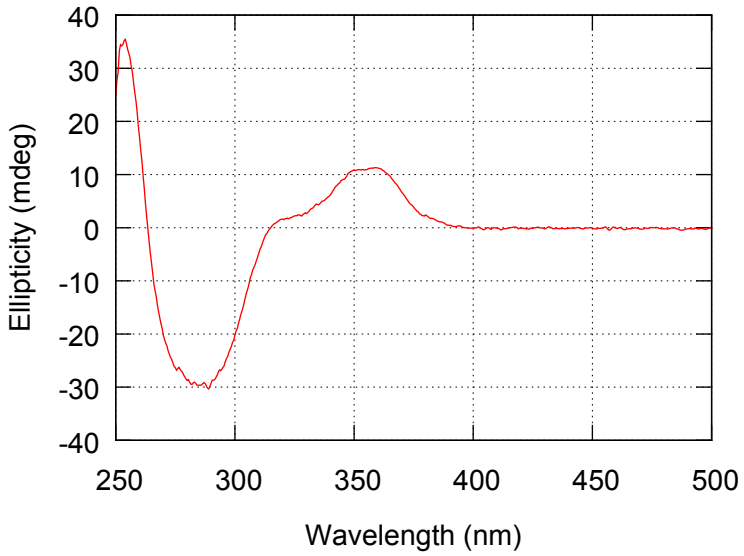

Figure S296. CD spectrum of **1(40)** in EtOAc (2.75×10^{-2} g/L, path length = 10 mm).

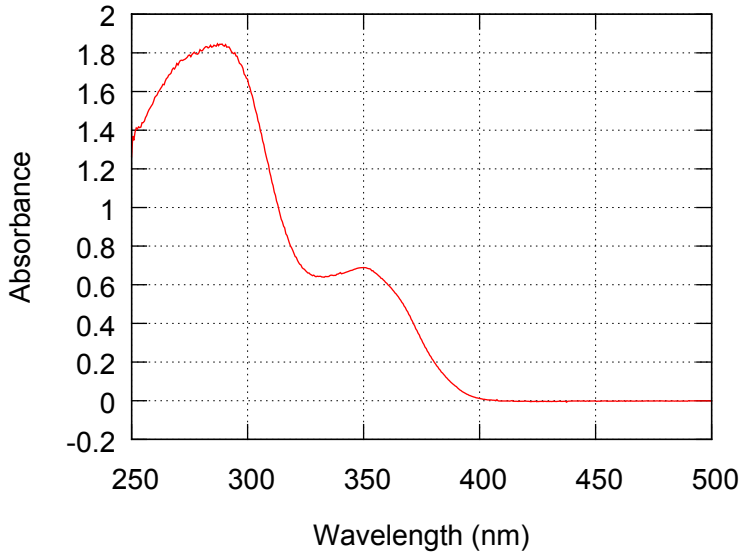

Figure S297. UV-vis absorption spectrum of **2(40)** in EtOAc (2.98×10^{-2} g/L, path length = 10 mm).

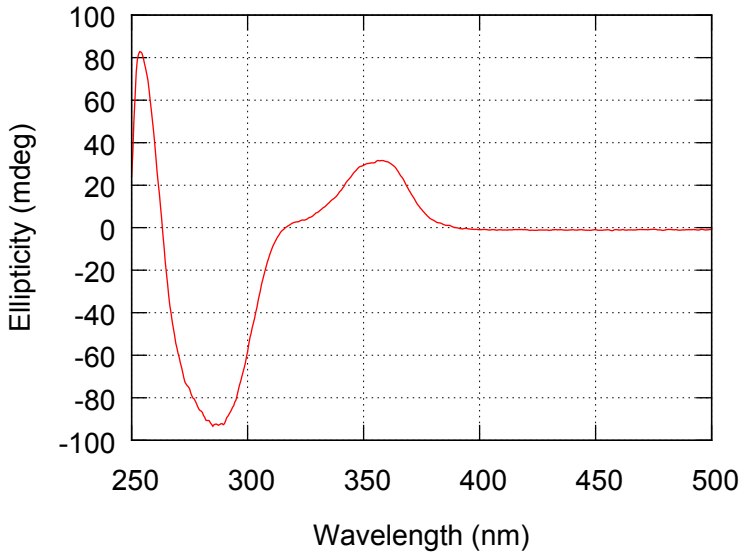

Figure S298. CD spectrum of **2(40)** in EtOAc (2.98×10^{-2} g/L, path length = 10 mm).

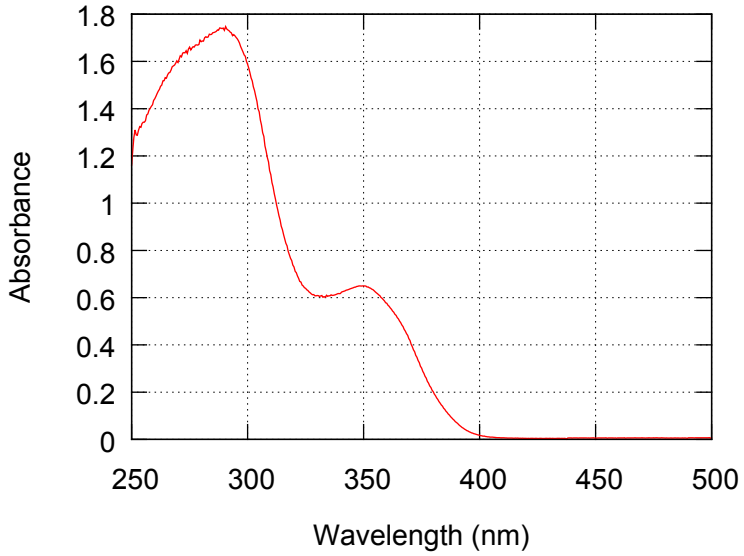

Figure S299. UV-vis absorption spectrum of **3(40)** in EtOAc (3.05×10^{-2} g/L, path length = 10 mm).

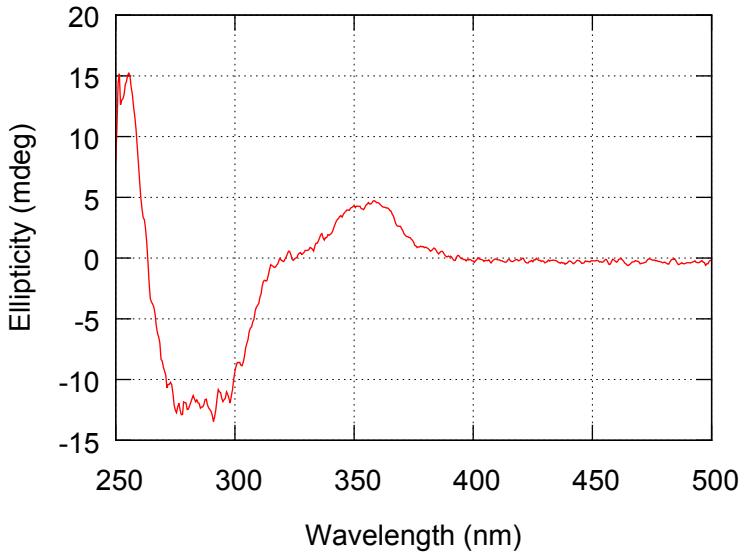

Figure S300. CD spectrum of **3(40)** in EtOAc (3.05×10^{-2} g/L, path length = 10 mm).

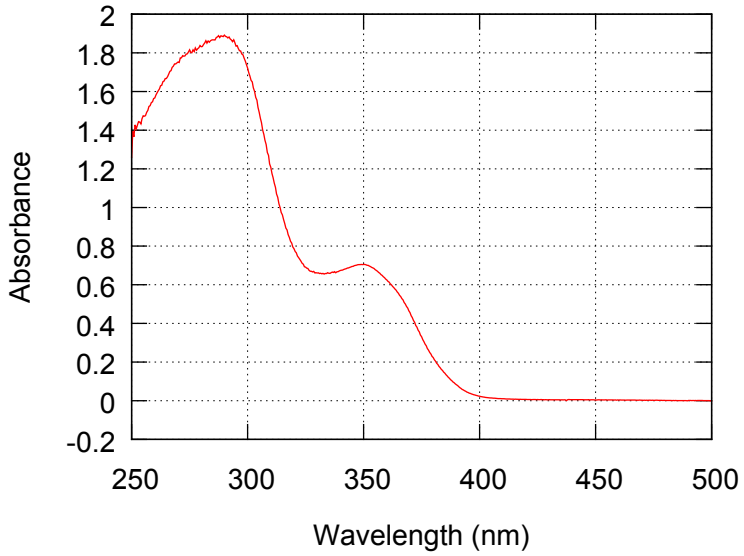

Figure S301. UV-vis absorption spectrum of **4(40)** in EtOAc (2.99×10^{-2} g/L, path length = 10 mm).

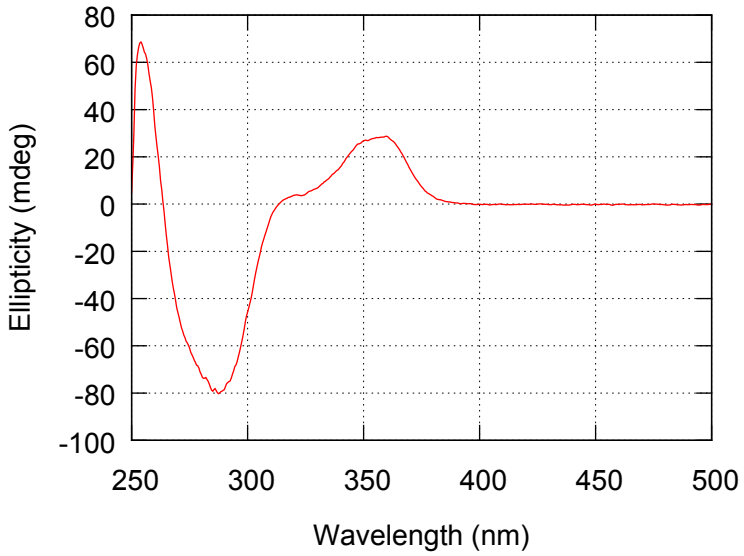

Figure S302. CD spectrum of **4(40)** in EtOAc (2.99×10^{-2} g/L, path length = 10 mm).

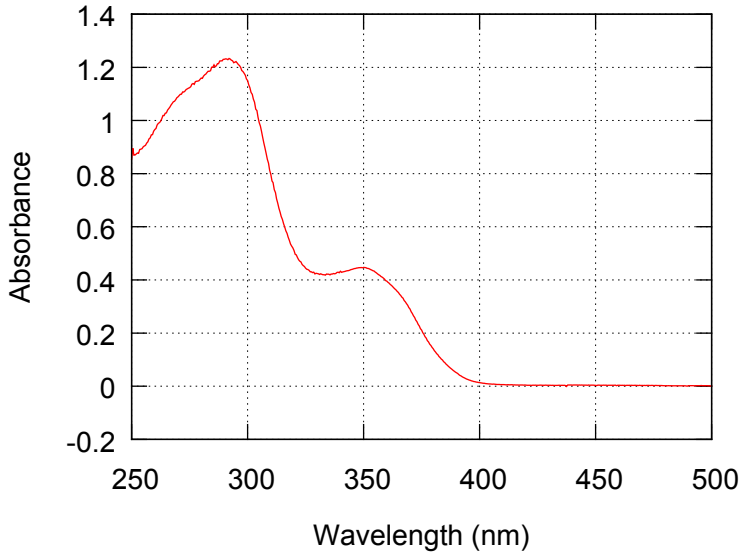

Figure S303. UV-vis absorption spectrum of **5(40)** in EtOAc (3×10^{-2} g/L, path length = 10 mm).

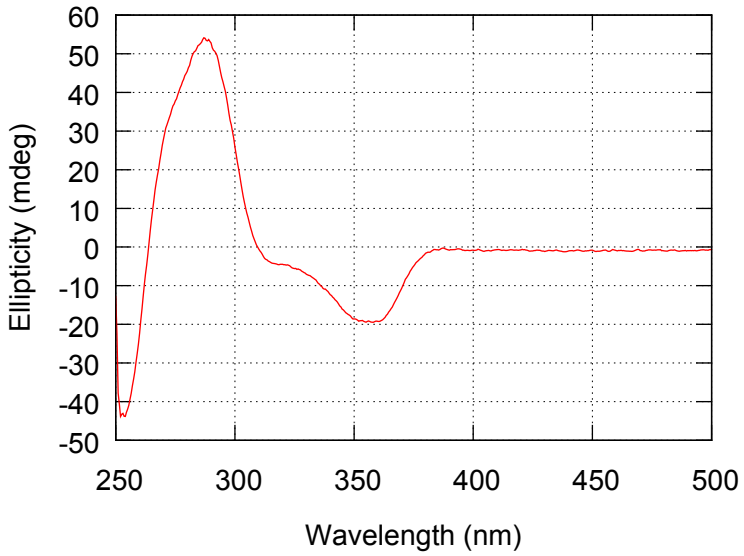

Figure S304. CD spectrum of **5(40)** in EtOAc (3×10^{-2} g/L, path length = 10 mm).

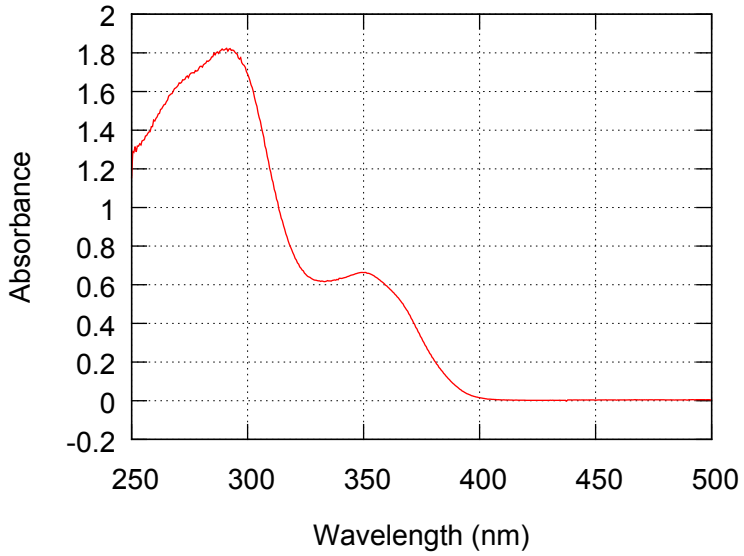

Figure S305. UV-vis absorption spectrum of **6(40)** in EtOAc (3.01×10^{-2} g/L, path length = 10 mm).

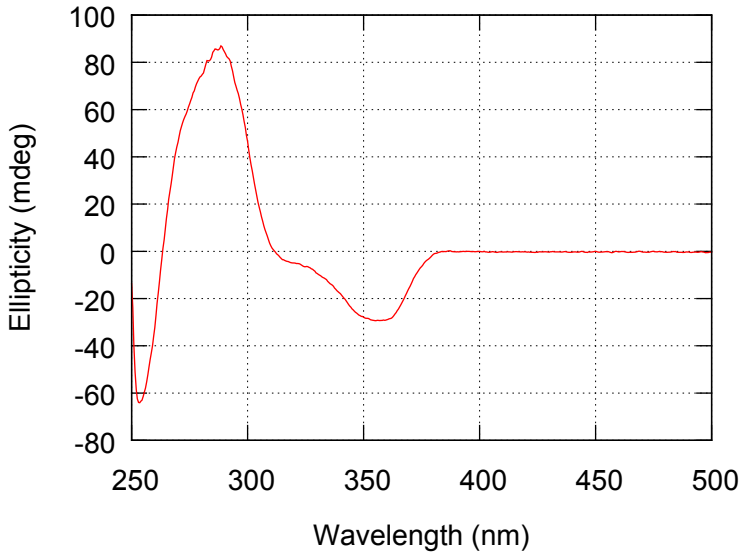

Figure S306. CD spectrum of **6(40)** in EtOAc (3.01×10^{-2} g/L, path length = 10 mm).

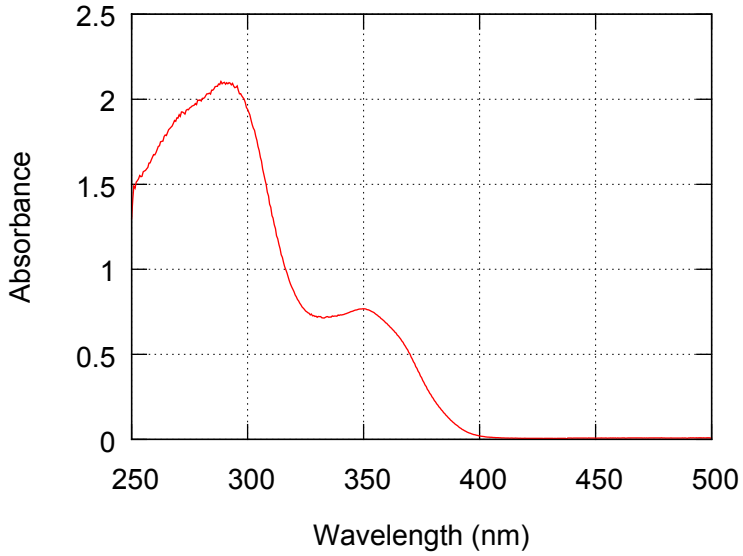

Figure S307. UV-vis absorption spectrum of **7(40)** in EtOAc (2.99×10^{-2} g/L, path length = 10 mm).

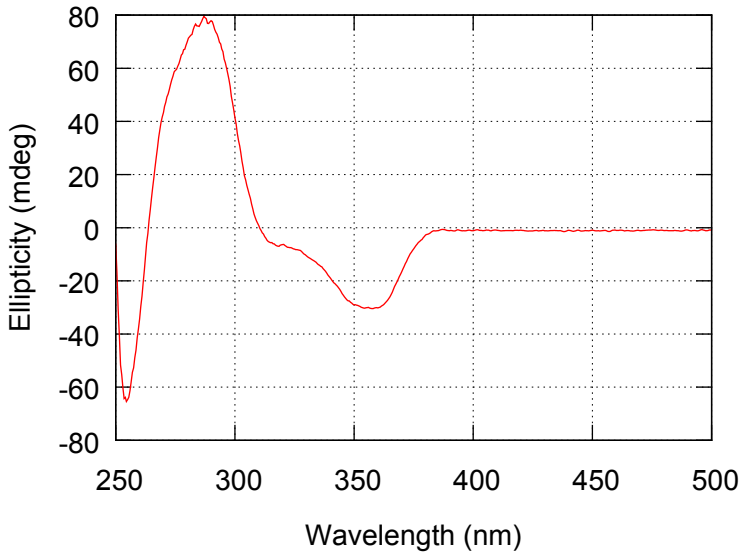

Figure S308. CD spectrum of **7(40)** in EtOAc (2.99×10^{-2} g/L, path length = 10 mm).

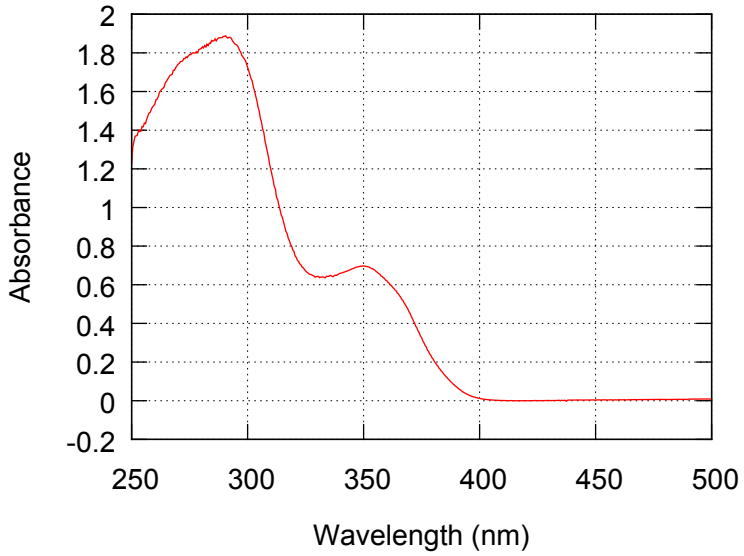

Figure S309. UV-vis absorption spectrum of **8(40)** in EtOAc (3.03×10^{-2} g/L, path length = 10 mm).

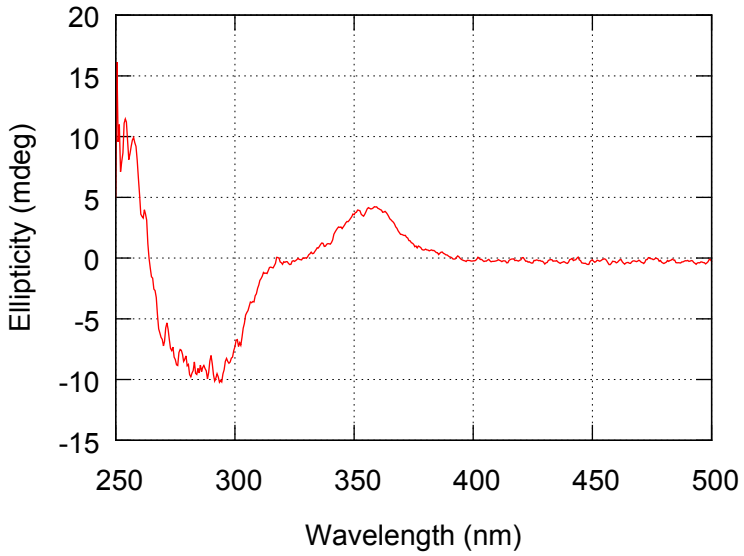

Figure S310. CD spectrum of **8(40)** in EtOAc (3.03×10^{-2} g/L, path length = 10 mm).

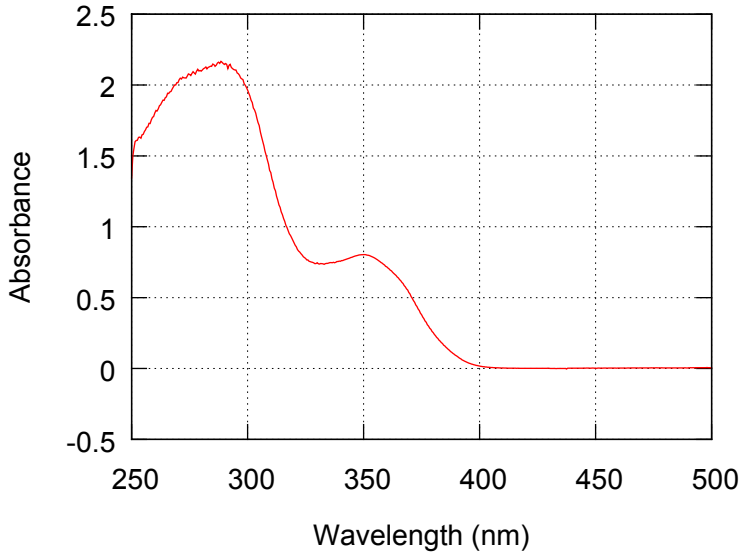

Figure S311. UV-vis absorption spectrum of **9(40)** in EtOAc (3.14×10^{-2} g/L, path length = 10 mm).

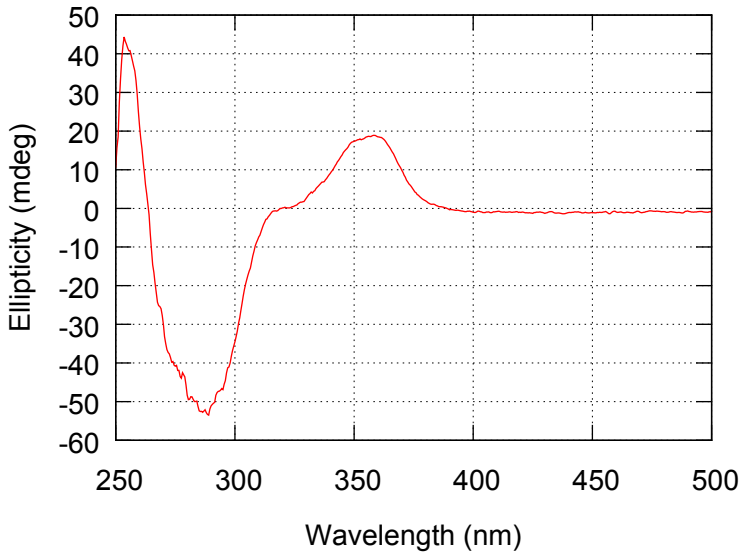

Figure S312. CD spectrum of **9(40)** in EtOAc (3.14×10^{-2} g/L, path length = 10 mm).

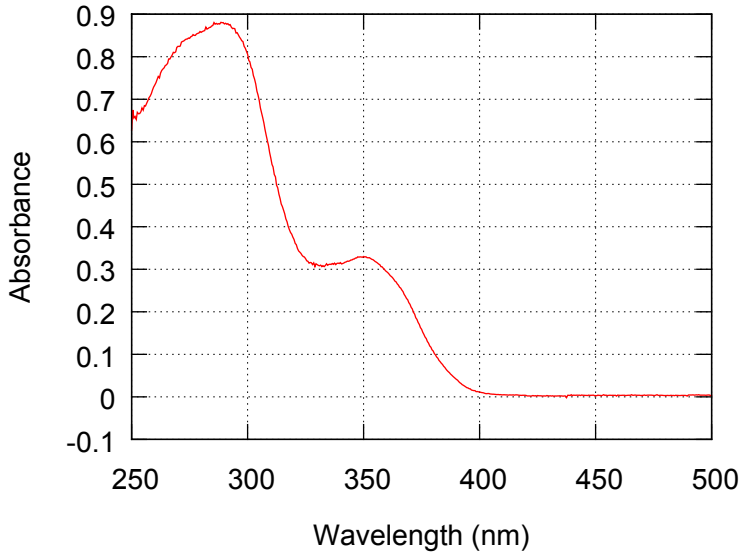

Figure S313. UV-vis absorption spectrum of **10(40)** in EtOAc (3.02×10^{-2} g/L, path length = 10 mm).

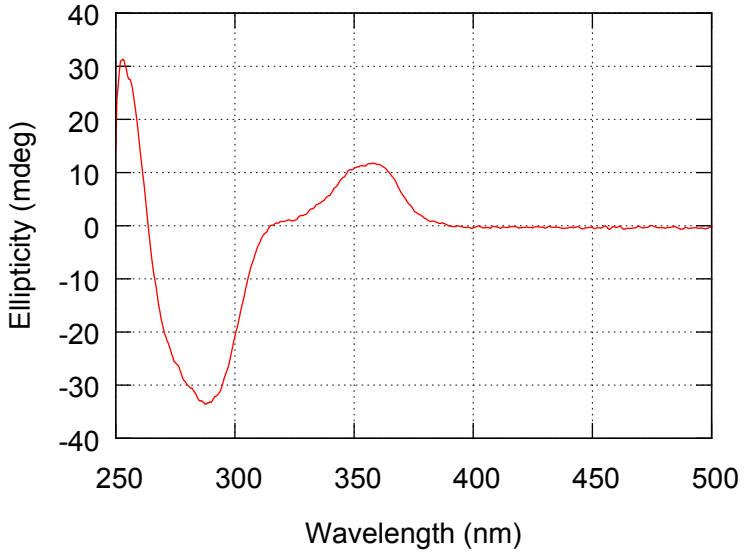

Figure S314. CD spectrum of **10(40)** in EtOAc (3.02×10^{-2} g/L, path length = 10 mm).